ADVERTIMENT. La consulta d'aquesta tesi queda condicionada a l'acceptació de les següents condicions d'ús: La difusió d'aquesta tesi per mitjà del servei TDX (www.tesisenxarxa.net) ha estat autoritzada pels titulars dels drets de propietat intel·lectual únicament per a usos privats emmarcats en activitats d'investigació i docència. No s'autoritza la seva reproducció amb finalitats de lucre ni la seva difusió i posada a disposició des d'un lloc aliè al servei TDX. No s'autoritza la presentació del seu contingut en una finestra o marc aliè a TDX (framing). Aquesta reserva de drets afecta tant al resum de presentació de la tesi com als seus continguts. En la utilització o cita de parts de la tesi és obligat indicar el nom de la persona autora.

ADVERTENCIA. La consulta de esta tesis queda condicionada a la aceptación de las siguientes condiciones de uso: La difusión de esta tesis por medio del servicio TDR (www.tesisenred.net) ha sido autorizada por los titulares de los derechos de propiedad intelectual únicamente para usos privados enmarcados en actividades de investigación y docencia. No se autoriza su reproducción con finalidades de lucro ni su difusión y puesta a disposición desde un sitio ajeno al servicio TDR. No se autoriza la presentación de su contenido en una ventana o marco ajeno a TDR (framing). Esta reserva de derechos afecta tanto al resumen de presentación de la tesis como a sus contenidos. En la utilización o cita de partes de la tesis es obligado indicar el nombre de la persona autora.

WARNING. On having consulted this thesis you're accepting the following use conditions: Spreading this thesis by the TDX (www.tesisenxarxa.net) service has been authorized by the titular of the intellectual property rights only for private uses placed in investigation and teaching activities. Reproduction with lucrative aims is not authorized neither its spreading and availability from a site foreign to the TDX service. Introducing its content in a window or frame foreign to the TDX service is not authorized (framing). This rights affect to the presentation summary of the thesis as well as to its contents. In the using or citation of parts of the thesis it's obliged to indicate the name of the author

Conceptual Design of Alternative Energy Systems from Biomass

Conceptual Design of Alternative Energy Systems from Biomass

María del Mar Pérez Fortes

Industrial Engineer

A Thesis presented for the degree of
Doctor of Philosophy

Directed by Prof. Dr. Luis Puigjaner Corbella and co-directed by Dr. Enrique Velo García

Escola Tècnica Superior d'Enginyeria Industrial de Barcelona
Universitat Politècnica de Catalunya

April 2011

Copyright © 2011 by María del Mar Pérez Fortes
The copyright of this thesis rest with the author. No quotations of it should be published without the author's prior consent and information derived from it should be acknowledged.

Trademarked names are used in this book without the inclusion of a trademark symbol. All the names of the different computer programs cited in this thesis (Aspen Hysys, Aspen Plus, MS Visual Basic, CPLEX, GAMS, MATLAB, etc.) are © of their owners.

To my mother and father.

One thing only I know, and that is that I know nothing.

Socrates (469 BC - 399 BC)

Summary

The energy sector is moving towards a new energy paradigm, which favours more efficient conversion processes, renewable sources and micro-generation. Bioenergy, or energy from biomass, is a promising solution for the future energy mix. This is an emerging area. To promote it, engineering consideration must be integrated together with economic, environmental and social aspects in bioenergy projects. Biomass properties enhancement is crucial. It concerns energy and matter densifications, to facilitate transportation and to stabilise moisture and dry matter losses or gains. Centralised and distributed energy systems (CES and DES, respectively) lead to different features and opportunities on the use of biomass. In the former case, biomass can be adequately co-used with fossil fuels. The latter case is exemplified by residential applications or rural electrification. To carry out the study of centralised and distributed energy systems in this field, tailor-made approaches are needed to exploit the characteristics of each potential system.

The objective of this thesis is to investigate the potential of the emerging bioenergy sector by studying the gasification of biomass using advanced process modelling techniques, and incorporating specific supply chain management strategies, in the framework of conceptual design for decision-making support towards enhanced final design. The studied energy systems are: (i) an integrated gasification combined cycle power plant combined with carbon capture and storage techniques (IGCC-CCS) for centralised energy systems; and (ii) a biomass gasifier combined with a gas engine (BG-GE) for distributed energy systems, being the nominal net power for each plant 285 MW_e and 14 kW_e, respectively. Detailed process system engineering modelling and optimisation techniques are integrated with supply chain management to analyse co-gasification and co-production of electricity and hydrogen alternatives in IGCC-CCS, and co-combustion of biomass and coal in pulverised coal power plants, for sustainable nets in the light of economic and environmental considerations. Process modelling is integrated with supply chain management optimisation for rural electrification by means of BG-GE systems, taking into account economic, environmental and social issues.

The conceived superstructure can be used for preliminary design of different process alternatives, retrofit of existing ones and to gain knowledge on process operating conditions of gasification plants. The resulting multi-objective optimisation problem evaluates the trade-off between techno-economic and environmental criteria of 25 scenarios, based on different feedstock mixtures and on topological changes. Those considerations comprise different coal, petcoke and biomass combinations and electricity generation from syngas, electricity generation from H_2 and purified H_2 production without and with PSA purge gas use in the combined cycle. The Pareto frontier analyses reveals that the scenario with petcoke as feedstock for H_2 production with PSA purge gas use is the best in terms of techno-economic optimisation. The scenario with residual biomass without PSA flue gas profit is the best in terms of environmental optimisation. CCS technology implementation leads to an efficiency penalty of 8.7% in net power terms if H_2 is used in the combined cycle. To maintain the same power level than that obtained with the combustion of syngas, the feedstock should be increased by 21% on a mass basis. The integrated nature of the IGCC-CCS plant limits co-production.

Supply chain case studies highlight, for Spain, a huge biomass waste potential that can be optimally used to produce electricity and H_2 by investing on new IGCC-CCS power plants, or to be co-combusted in the existing power plants. For the first case, the optimal NPV is around 230 M€ for a considered period of 25 years. The sensitivity of the optimal solutions to changes in prices is demonstrated, showing that the same network configuration can easily have positive or negative NPV's depending on the product price. For the second case, policy subsidies or alternatively price increases range from 5.84% to 20.25%, depending on the thermal share replacement. The investment is within 549 M€ and 1640 M€. A supply chain in a specific community from Ghana is proposed and optimised in the framework of rural electrification. The case study contemplates 9 communities and an overall electricity demand of 118 MWh/yr, to be satisfied by cassava peels and by means of BG-GE systems. The results reveal an unviable network, with a NPV of $-261212.6, an Impact 2002+ of 36.8 pts and a social parameter of 27, for each optimised point of view. From the resulting networks, distributed approaches need a certain level of centralisation to be feasible on time.

Bioenergy complies with the requirement of the emerging energy paradigm: it offers decisive advantages in terms of environmental and social impact. Its deployment is already straightforward with the support of current state-of-the-art technologies. Challenges concern the improvement of biomass pre-treatment processes and storage, to meet sustainable standards for energy generation. Despite all the striking advantages, biomass conversion, combined with carbon capture and storage needs political incentives to enter definitely and extensively the market, as would be the case for any energy conversion alternative.

Resumen

El sector energético se está dirigiendo hacia un nuevo paradigma, favoreciendo la aparición de procesos de conversión más eficientes, el uso de las fuentes de energía renovables y la micro-generación. La bioenergía, o energía de la biomasa, es una solución prometedora para la futura combinación de energías, siendo todavía un área emergente. Para promoverla, los conceptos de ingeniería deben de integrarse junto con los aspectos económicos, ambientales y sociales en el desarrollo de proyectos. La mejora de las propiedades de la biomasa es crucial para conseguir este objetivo: su densificación en términos de energía y materia es necesaria para facilitar el transporte y estabilizar las variaciones de humedad y de materia seca. Los sistemas de energía centralizados y distribuidos (CES y DES, respectivamente) conducen a diferentes características y con ello, a diferentes oportunidades en el uso de la biomasa. En el primer caso, la biomasa puede ser adecuadamente co-utilizada con combustibles fósiles. El segundo caso se ejemplifica en usos residenciales o de electrificación rural. Para llevar a cabo el estudio de sistemas de energía centralizados y distribuidos en este ámbito se necesitan enfoques a medida para explotar las características de cada posible sistema.

El objetivo de esta tesis es investigar el potencial del sector bioenergético, mediante el estudio de la gasificación de biomasa a través de técnicas avanzadas de modelización de procesos y de la incorporación de estrategias de gestión de la cadena de suministro, en el marco del diseño conceptual para la toma de decisiones. Los sistemas de energía estudiados son: (i) gasificación integrada con ciclo combinado y con métodos de captura y almacenamiento de CO_2 (IGCC-CCS) para los sistemas de energía centralizados, y (ii) un gasificador de biomasa combinada con un motor de gas (BG-GE) para los sistemas de energía distribuidos, siendo la potencia neta nominal de cada planta de 285 MW_e y de 14 kW_e, respectivamente. Las técnicas de modelado y optimización de ingeniería de procesos se han integrado con técnicas de gestión de la cadena de suministro para analizar las alternativas de co-gasificación y co-producción de electricidad e hidrógeno en plantas IGCC-CCS, y para la co-combustión de biomasa con carbón pulverizado en centrales de carbón, con el objetivo de diseñar redes sostenibles economica y ambientalmente. La simulación de procesos se ha integrado con la optimización de la gestión de la cadena de suministro en electrificación rural por medio de los sistemas de BG-GE, teniendo en cuenta cuestiones económicas, ambientales y sociales.

La superestructura puede ser utilizada en el diseño preliminar de alternativas para los diferentes procesos, para adaptar los ya existentes y para adquirir conocimiento sobre las condiciones de operación de plantas de gasificación. El problema de optimización multi-objetivo resultante evalúa el equilibrio entre los criterios técnico-económicos y ambientales de 25 escenarios, con diferentes materias primas y cambios topológicos. Se incluyen mezclas de carbón, coque y biomasa y la generación de electricidad a partir de gas de síntesis, la generación de electricidad a partir de H_2 y la producción de H_2 puro, considerando o no el uso del gas de purga del PSA en el ciclo combinado. El análisis de Pareto revela que el escenario que utiliza coque de petróleo como materia prima para producir H_2, con reciclo del gas de purga del PSA, es la mejor opción en términos de optimización técnico-económica. El escenario con biomasa residual sin reaprovechamiento del gas de purga del PSA es la mejor opción en términos de optimización medioambiental. La implementación de CCS conlleva una penalización en la eficiencia de un 8,7% en términos de potencia neta, si el H_2 se utiliza en el ciclo combinado. Para mantener el mismo nivel de potencia que la obtenida con la combustión de gas de síntesis, el flujo de materia prima debe aumentar en un 21%, en base másica. La naturaleza integrada de la planta IGCC-CCS limita las posibilidades de co-producción.

Los casos de estudio propuestos en gestión de cadenas de suministro de sistemas centralizados, señalan que España tiene un potencial considerable de biomasa residual, que puede ser utilizada para producir electricidad e hidrógeno, invirtiendo en nuevas centrales IGCC-CCS, o para producir electricidad mediante co-combustión en las centrales térmicas de carbón ya existentes. Para el primer caso, el valor actual neto óptimo es de alrededor de 230 millones de € para un periodo considerado de 25 años. Las configuraciones de cadenas de suministro óptimas son altamente sensibles, dejando de ser óptimas si el precio del producto varía, incluso llegando a valores de valor actual neto negativos. Para el segundo caso, se ha calculado que las políticas de subvención en este tipo de proyectos deben de tener en cuenta la sostenibilidad económica, cubriendo en un rango de 5,84% a 20,25% el aumento de los precios de la electricidad en función del porcentaje de substitución del potencial térmico del carbón de entrada a la planta. La inversión está en el intervalo comprendido entre 549 y 1640 millones de €. El caso de estudio propuesto y optimizado como ejemplo de un sistema distribuido tiene en cuenta una comunidad de Ghana en el marco de la electrificación rural. El caso de estudio contempla nueve comunidades y una demanda total de electricidad de 118 MWh/año, a abastecer con peladuras de yuca y mediante plantas BG-GE. Los resultados revelan una red inviable, con un valor actual neto de -261212,6$, un Impacto 2002+ de 36,8 pts y un parámetro social de 27, según cada punto de vista optimizado. De las cadenas de suministro óptimas se deduce que cierto nivel de centralización es necesario para que las propuestas sean sostenibles en el tiempo.

El sector de la bioenergía cumple con las exigencias del paradigma energético emergente, ofreciendo ventajas en términos de impacto ambiental y social. Su implementación es posible con el apoyo de las tecnologías actuales de conversión de energía. Los principales retos están en la mejora de los procesos de pretratamiento de la biomasa y en su almacenamiento, con el objetivo de adquirir las condiciones necesarias para la producción de energía. A pesar de todas las ventajas, la conversión de la biomasa, junto con los métodos de captura y almacenamiento de CO_2, necesitan de incentivos políticos para poder penetrar definitivamente en el mercado, como sería el caso de cualquier otra tecnología alternativa de conversión de energía.

Acknowledgments

Within a few years, when I see my thesis report, I will see a small sample of what has been four years and a half for me. In addition to the professional growth, from my time in CEPIMA and from my PhD period, I take with me all the special people I've met, their professionalism, good advice, smiles and endless happy memories that are already part of me. Thank you all. Thanks to my unconditional, my family, whom I admire for their humility and greatness, and my friends, who trust in me, from whom I'm still learning and know how to make me smile. Thanks to all who have made it possible for me to get here. Thanks to all who have helped me to choose my way. To you, since you are my light.

I would like to thank the financial support received from the "Generalitat de Catalunya" (Comissionat per a Universitats i Recerca del Departament d'Innovació, Universitats i Empresa) to carry out this thesis.

Agradecimientos

Dentro de unos años, cuando vuelva a ver mi informe de tesis, veré una pequeña muestra de lo que han sido estos cuatro años y medio para mí. Además del crecimiento profesional, de mi paso por CEPIMA y de mi etapa de doctorado, me llevo conmigo a la gente especial que he conocido, su profesionalidad, sus buenos consejos, sus sonrisas y los infinitos buenos recuerdos que ya forman parte de mí. Gracias a todos. Gracias a mis incondicionales, a mi familia, a quien admiro por su humildad y su grandeza, a mis amigos, que confían en mí, de los que sigo aprendiendo y que me saben sacar una sonrisa cuando no hay ganas de reír. Gracias a todos los que han hecho posible que yo llegue hasta aquí, y a los que me han ayudado a escoger mi camino. A vosotros, por ser mi luz.

Finalmente, quiero agradecer la financiación recibida de la "Generalitat de Catalunya" (Comissionat per a Universitats i Recerca del Departament d'Innovació, Universitats i Empresa) para la realización de esta tesis.

Contents

Part I Overview

Appendixes

List of Tables

List of Figures

Part I

Overview

Chapter 1

Introduction

The purpose of this chapter is to place the reader within the context of this thesis. It gives an overview briefly contemplating the roadmap of the work developed: revisiting the existing panorama, introducing the biomass and gasification interlinked perspective, presenting the challenges at urban and rural areas and large and small scale gasification through integrated gasification combined cycle - carbon capture and storage (IGCC-CCS) and biomass gasification - gas engine (BG-GE) for power generation. In addition to that, it introduces the techniques used: process modelling for optimal design and supply chain management (SCM). The chapter finishes with the general objectives and the outline of this thesis report.

1.1 Foreword and motivation

The development of a successful bioenergy sector in both developed or industrialised and developing countries will contribute to a long-term diversity, security and self-sufficiency of energy supply (Sims, 2004). Current challenges emerging in the worldwide energy sector can be summarised in three key topics: diminution of natural sources, climate change and technology development. It is in this context where bioenergy is seen as one of the most appreciated options to mitigate greenhouse gases (GHG) emissions by fossil fuels replacement and to be a sustainable source of energy in vehicles and in electric power generation, certainly by adequately exploiting the resources and the technology options (Faaij, 2006).

Bioenergy is an energy supply alternative which encompasses a broad range of sectors, which can be categorised in two big blocks: energy generation and biomass as a source. In this sense, Figure 1.1 compiles the major interlinked components identified. *Energy generation* has to deal with the different biomass conversion routes to increase the efficiency of the already existing processes and to expand and research new mature commercial technologies. To illustrate these points, co-combustion of biomass with coal in conventional pulverised coal (PC) power plants implies lower costs and higher efficiencies than other bioenergy options, taking advantage of the already existing

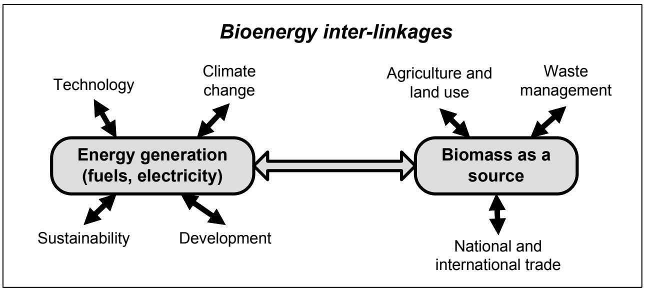

Figure 1.1: Bioenergy, and actuation and policy areas of concern.

plants, and avoiding emissions directly related with the diminution of the coal fraction in the boiler (Faaij, 2006). On the other hand, also as example, co-gasification of biomass with coal in integrated gasification combined cycle (IGCC) power plants is more efficient than in conventional PC plants (in terms of energy produced by inlet thermal power), and these plants are by now closing the demonstration phase leading to a fully commercial period.

Global trends are promoting the utilisation of renewable sources as alternative to fossil fuels to mitigate climate change and to alleviate peak oil effects. There exists a change of paradigm in this emerging energy sector: centralised versus distributed installations. Decentralisation ideally involves population implication, climate change mitigation and supply security. There will not be a unique technology or renewable resource massive implementation: the "solution" passes through a combination of various energy sources conversion technologies to meet the energy demand (Bouffard & Kirschen, 2008). The alternative to centralised and conventional sources of energy should be sustainable in the time, that means responsible resource exploitation, matching the source availability with the energy carrier demand, and therefore with the capacity of the plant.

Poverty, understood as the lack of socio-economic welfare, is linked to energy access; therefore electricity consumption and development are connected, as low values of gross domestic product (GDP) and human development index (HDI) demonstrate for 120 countries (Kanagawa & Nakata, 2008). In Kanagawa and Nakata (2008), energy access is defined as "the situation where people can secure the modern energy access at affordable prices". It is consequently important to promote energy access in poorer countries taking into account their economic possibilities. The International Energy Agency (IEA), through its World Energy Outlook (WEO) (2010), puts into relevance the link between energy and development, and promotes universal modern energy acces. As Urban *et al.* (2007) and Van Ruijven *et al.* (2008) point out, current energy models are biased towards industrialised countries. Accordingly, not only economical factors should be revised, but also demand characteristics, capability for operational and maintenance tasks and/or accessibility to the grid. The proposal aims at managing each project with its own reality, context and particularities, changing the mind from past experiences to the new energy paradigm.

Biomass as energy source is coupled with two main sectors of the economy: agriculture and waste management. On the one hand, agriculture can be used to produce food, feed, fibre of fuel (the so-called "4F's") leading to a certain controversy and competitiveness for the land use, and therefore, for water use. Land as a resource deals with the pressure of population growth, life styles variations and climate change consequences (Otto, 2009). On the other hand, residues management is also interlinked with other markets. Waste can be used as raw material in certain processes, as feed or as fertiliser, or in other industries that treat them to be further used in other processes. These lead to a complex competitive trade, where obviously prices are fixed by the demand (Faaij, 2006).

Biomass markets are changing from exclusively national and even local, to international markets: globalisation makes accessible a broad range of globally dispersed potential suppliers and consumers not equally distributed around the world. Some regions are foreseen to become net exporters, such as Eastern Europe, Russia, Oceania, Sub-Saharan Africa, East Asia and parts of Latin and North America. Some others are probable importers like several European Union (EU) member countries, or Japan as a large fossil fuels consumer (Uslu *et al.*, 2008). As the works by Janssen *et al.* (2009) and Madjera (2009) point out, developing countries, specifically Africa, have the potential to become significant producers and exporters of raw biomass while supplying basic needs. Seeing that, there exists the necessity of a global approach that should take into account the use and exploitation of the resources and their direct and indirect effects. In order to develop a stable market for biomass being a commodity, supply and demand should be secured in a sustainable way. Biomass, as a product, should accomplish technical standards for homogenisation and should overcome logistical barriers, being biomass densification crucial before transportation. Biomass market involves social and economic developments (Rosillo-Calle *et al.*, 2007).

The represented issues in Figure 1.1, should be accompanied by appropriated regulations, policies and standards to direct trade, deal with land controversies, and guide the development of the bioenergy sector. As Strachan and Dowlatabadi (2002) remarks, the government has a main responsibility in the world change of living due to the energy paradigm transformation, ensuring a sustainable biomass source exploitation. As example of developed directives worldwide: the EU has established a target of 20% share of renewable energy out of the total European energy consumption by 2020 (Capros *et al.*, 2010). The US, in its Energy Independence and Security Act (EISA) of 2007, states that advanced biofuels shall supply at least 21 billion gallons of US motor fuels by 2022. It is generally recognised that in order to achieve these targets, efficient networks to sustainable supply the amounts of biomass required, cost effective technologies to convert biomass, and improved distribution infrastructures to deliver the final product (i.e., energy or fuel) are to be developed (US, 2010). Moreover, the efficient integration of these three elements is equally relevant to reach the posed goals. Different organisation reports, from the IEA and the Electric Power Research Institute (EPRI) for instance, affirm that different countries need common strategies to mitigate GHG emissions and to secure the energy supply by lowering the dependence on fossil fuels. Furthermore, it is estimated that the energy demand will be doubled by 2030, then biomass exploitation becomes into a need.

Summing up, the bioenergy sector is nowadays accepted as having the potential to provide an important part of the projected renewable energy provisions of the future. Nevertheless, it has to overcome technological, economical and social barriers to obtain the needed political and social supports and to be attractive as an investment project (Bridgwater, 2003). Practitioners should dispose of tools to guide this energy sector transformation in industrialised and developing countries, thus, in different contexts. As a result, the efforts are concentrated on developing integrated frameworks to support the decision making process.

1.1.1 The *scale* of the problem

Biomass as energy source, in comparison with fossil fuels, has a low calorific value as well as intrinsic characteristics that derive into technological limitations. That is the reason why 100% biomass to energy projects typically employs small scale conversion systems, and furthermore, they are situated close to the biomass generation source as well as close to the demand points, in order to avoid high logistic and network infrastructure constraints (Strachan & Dowlatabadi, 2002; Caputo *et al.*, 2005; Gold & Seuring, 2011). Nevertheless, as Bouffard and Kirschen (2008) points out, the electricity generation sector of the future will have to combine the best attributes of both paradigms, the advantages of centralised and those of distributed energy systems. In this context, bioenergy should be equally present in big and small scale conversion systems, therefore co-using biomass with fossil fuels or using it alone, respectively.

According to Faaij (2006), *large gasification systems* are from 10 MW_{th}, and *small gasification systems* cover the range from less than 100 kW_{th} up to a few MW_{th}. In terms of electricity and in accordance with Siemons (2001), small scale gasification plants enclose plants with a power up to 200 kW_e. These ranges lead to significant value differences in terms of land use for the plant infrastructure, investment, operation and maintenance costs and plant dimensions. For example, the ELCOGAS IGCC power plant uses a land extension of 480000 m^2, while a small scale gasification plant can occupy around 25 m^2. *Centralised energy systems* (CES) consist in large power plants that export electricity to the grid and transport the raw material or energy source to the plant; *decentralised or distributed energy systems* (DES) entail localised electricity generation near the demand points and near the biomass generation places, being appropriate one or other option depending on the conditions of the area. There exists no agreement in the literature about the definition of distributed generation; nevertheless it is usually perceived as small scale electricity generation (Mitra *et al.*, 2008). The literature overviews from Bayod *et al.* (2005) and Mitra *et al.* (2008), point out that the term can be referred to (i) stand alone or autonomous applications, (ii) standby sources that supply power during grid outages, (iii) co-generation or waste heat recovery installations with power injection to the grid if the DES has a higher power production than the local demand, (iv) DES that support the grid by decreasing power losses and improving the system voltage profile and to (v) energy systems connected directly to the grid that sell the electricity produced. This thesis use the term DES as stand alone applications. See in Figure 1.2 an overview of centralised vs. distributed systems. CES involve the use of transmission and distribution lines, while DES may use microgrids to connect a limited number of consumers.

The possible location of the gasification plant, that determines its characteristics and dimension, is described in this work according to rural-urban areas and developing-developed countries "division". None of these classifications have well extended norms. One of the possible definitions for *rural area* uses a threshold of 150 inhabitants/km^2, including countryside, towns and small cities. Other definitions take into account towns and municipalities outside the urban centres, with population of 10000 or more; or population living outside regions with major urban settlements of 50000 or more people, dividing the areas into "metropolitan adjacent" or "not adjacent" categories

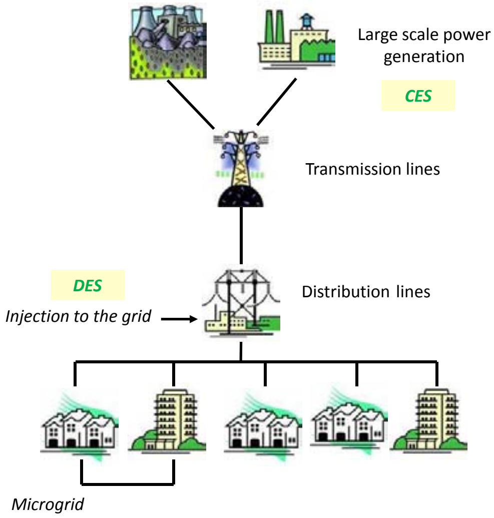

Figure 1.2: Conventional and decentralised based systems.

(du Plessis *et al.*, 2002). *Urban areas* include a central city and the surrounding dense areas that have together a population of 50000 or more, and a population density exceeding 1000 inhabitants/km^2, according to the US Census Bureau, (2008). The *developed-developing countries* division is controversial, since it is difficult to assess the standards of living for worldwide countries, and hence their level of development. For example, Kofi Annan, ex-secretary general of United Nations (UN), defined a developed country as "the one that allows all its citizens to enjoy a free and healthy life in a safe environment". Nevertheless, the World Bank (WB) classifies the countries according to their gross national income (GNI), being developing countries those ones with a GNI lower than US$3855 (2008). The UN has proposed the human development index (HDI) with the aim of characterising the growth of a country, involving a set of several indicators: life expectancy at birth, mean years of schooling, expected years of schooling and the GNI per capita. The WEO from IEA (2010) includes in the developing countries category Africa, Developing Asia, Latin America and Middle East regional grouping. The World Energy Assessment from the United Nations Development Program (UNDP) (2004) uses the term industrialised country to refer to high-income countries that belongs to the Organisation for Economic Co-operation and Development (OECD). Even if there are many transition economies with high degree of industrialisation, they are not considered here due to their specific requirements for development. In this way, developed countries are also called industrialised, as well as advanced, more developed or more economically developed countries. In this work either of the terms industrialised and developed countries are used.

See in Figure 1.3 a qualitative distribution of the areas according to the rural-urban and developed-developing divisions criteria, and the place of this thesis contributions. Large and small gasification scales can be implemented in developed and developing countries: the difference remains in CES vs. DES, thus somehow into urban vs. rural areas. Nevertheless, energy chains should be established according to each country/project context and taking into account economic, environmental and

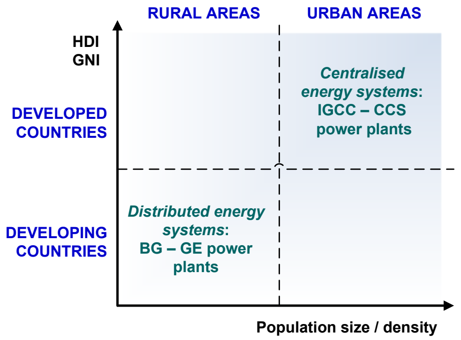

Figure 1.3: Contributions of this thesis in the social context.

social issues; as well as according to the lessons learnt concerning traditional fuels exploitation and climate change. Even if the technology to be implemented can be the same in developed and developing countries for CES and DES, the specifications of each project should be fixed according to features such as the sector financing, the existance of a grid, the grid distribution losses or the demand (Urban *et al.*, 2007).

Gasification principles for large and small scale gasification remain the same, but the type of reactor as well as the final syngas or producer gas composition and uses are habitually different. As shown in Figure 1.3, for this thesis approach, large scale gasification is represented by biomass-coal blends used in IGCC power plants, with carbon capture and storage (CCS) technology (IGCC-CCS). Small scale biomass gasification is represented by 100% biomass gasification with producer gas use in a gas engine (BG-GE). See in the following sections (i) the main characteristics of biomass as a resource, (ii) the available technologies to take profit of biomass and among them, (iii) gasification as the technology selected in this thesis, (iv) syngas cleaning as a key for the final syngas use, and (v) an overview of the techniques used to approach the biomass gasification design problem.

1.2 Biomass as a resource

Biomass, in terms of a renewable energy source, is defined as "all the organic matter contained in plant and animal based products, including organic wastes, that can be captured and used as a source of stored chemical energy" (Sims, 2004). Biomass can be classified into three big categories according to its origin (Sims, 2004; Faaij, 2006): primary, secondary and tertiary biomass in agreement with the process from which it results. See in Figure 1.4 this well extended biomass classification, by means of the sources and raw materials that each cathegory can include. According to Sims (2004), biomass contributes significantly to the world's primary energy supply, with 45 EJ/yr profited through traditional and modern techniques. Among this number, the traditional use of biomass is estimated to be 38 EJ/yr, since it is the first energy source in developing countries, which involves a 20%-35% of their national primary energy demand, while in developing countries its contribution is on a 3%. The traditional use of biomass implies cooking and heating in a non-sustainable and inefficient way, basically by means of direct firing. Although there is no global information about the

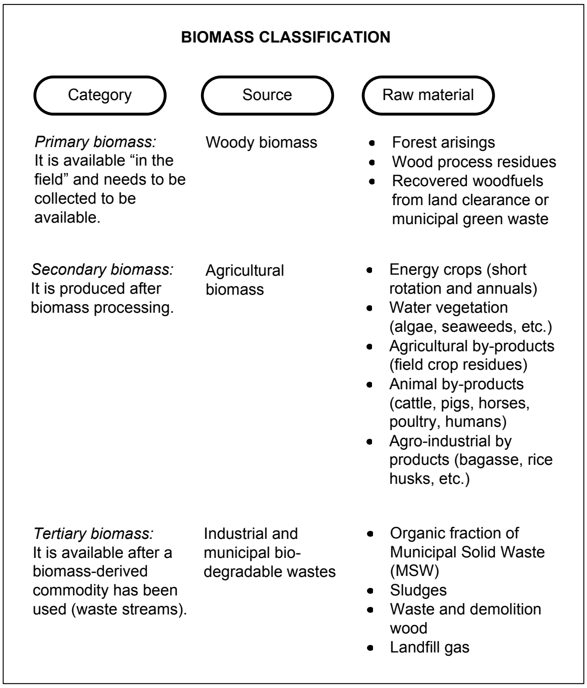

Figure 1.4: Biomass sources classification, based on Sims (2004) and Faaij (2006).

biomass market size, it is assumed that the non-conventional use of the biomass may be around 29 EJ/yr. As Silveira (2005) points out, "biomass is the fuel of the rural poor in developing countries".

The most relevant properties of biomass as energy carrier or chemical feedstock in thermochemical conversion processes (see Section 1.2.1 for processes classification) are, according to McKendry (2002a) and Reed (1981): proximate and ultimate analyses, moisture content (MC), lower and higher heating values (LHV and HHV), heats of formation, ashes content, biochemical composition (hemicellulose, cellulose, lignin and extractives), bulk density (BD) and grindability. Properties variability among biomass resources lead to distinct degrees of suitability to be converted by diverse technologies.

In Mathews (2008), it is said that the world is in a transition from an economy fuelled by carbon from the past ("petroeconomy"), to an economy fuelled by biomass ("bioeconomy"). According to Rosillo-Calle *et al.* (2007) and Mathews (2008), bioenergy is extensively considered as carbon neutral, since the carbon emitted replaces the carbon absorbed during the plant growing through photosynthesis. Nonetheless, each specific situation should be treated separately. For instance, the work of Tilman *et al.* (2006) demonstrates a negative carbon balance for low-input high-diversity grassland biomass.

Three situations can be identified concerning CO_2 emissions for fossil and biomass fuels, as represented in Figure 1.5. *Carbon positive* fuels represent the fossil fuels behaviour releasing CO_2 to the atmosphere. *Carbon neutral* fuels symbolise biomass resources, that absorb CO_2 from the atmosphere and release the absorbed CO_2 to it. Nevertheless, in practice, the CO_2 balance is positive due to the fossil fuels used

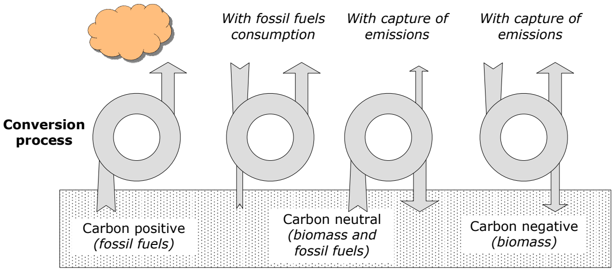

Figure 1.5: Biosources carbon balance, based on Mathews (2008).

mainly in production and logistics activities. *Carbon negative* fuels represent biomass resources absorbing CO_2 from the atmosphere, releasing less to it, and directing part of the captured emissions during growing to the soil, as biochar or through CCS. In this way, fossil fuels with CCS (see Section 1.4.1 for further detail) aim at a complete carbon neutrality, even if a small fraction of the CO_2 is not captured and hence it is discharged in the atmosphere.

1.2.1 Available technologies

An important portfolio of technologies allows for biomass energy production in forms of heat, electricity, co-generation or transport fuels and chemical feedstocks. The conversion technology that better match with a specific type of biomass, depends on the composition and amount of the resource, the desired final product, environmental standards and economic and project specific conditions (McKendry, 2002b; Faaij, 2006). As indicated by McKendry (2002b), the different conversion technologies can be grouped into two categories, according to the MC of the biomass feedstock. Thermochemical conversion processes are suitable for low MC biomass (less than 50%), while physico-chemical and biological ones fit with humid biomass. Figure 1.6 shows the different available technologies and products obtained. Gasification belongs to the thermochemical conversion category. A biorefinery (as defined in Section 1.4), aims at integrating different technologies to produce heat, electricity, fuels and chemicals, at the same facility.

1.3 Syngas generation: Gasification

Synthesis gas, called *syngas*, is a mixture of mainly H_2 and CO, with different proportions of H_2O and CO_2. Usually, the term *producer gas* is used to describe a syngas with H_2, CO and CH_4, coming from a low temperature gasification. Typically, low temperature gasification counts with air as gasifying agent. Thus, the producer gas normally has an important fraction of N_2. Syngas and/or producer gas is referred to as a medium energy gas, ranging from 4 to 18 MJ/m^3 of calorific value, depending on the gasifying agent (McKendry, 2002b).

Flexibility is one of the main characteristics of syngas, since it is not restricted to a single source of fuel; it can be obtained from natural gas, coal, petroleum refinery fractions, biomass and organic wastes. Traditionally, natural gas and petroleum fractions have been the largest syngas sources worldwide, due to the trade-off

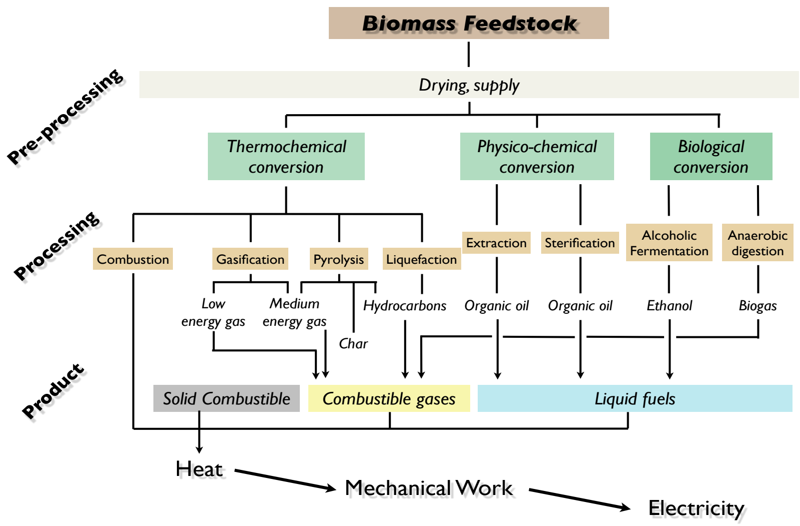

Figure 1.6: Main biomass conversion processes.

between costs and availability; however, because of global economic, energetic and environmental contexts, coal and biomass are of growing interest and use. Syngas is moreover the worldwide most used source of H_2 and CO. The proportion of H_2/CO depends on the source and on the syngas generation process and its performing parameters (Wender, 1996).

Two main routes are currently available for syngas generation, both of them traditionally and highly used for H_2 generation from fossil fuels, specifically from natural gas and coal. *Syngas from natural gas* mainly refers to partial oxidation with oxygen, oxidation with steam or oxidation with steam and oxygen; being the principal steam reforming. *Syngas from coal* involves gasification. After syngas generation, a second process is needed for further H_2 generation and purification: the so-called water-gas shift (WGS) reaction, in which the conversion of CO into CO_2 takes place.

Gasification can be defined as a partial combustion of an organic matter, producing as a result a combustible gas. Two types of gasification processes can be distinguished: indirectly heated or allothermal gasification and directly heated or authothermal gasification. In the first one, the necessary heat for the gasification reactions is provided by an external source. In the second one, the needed heat comes from internal partial combustion of the organic matter itself. Therefore, gasification can occurs with oxygen, air, hydrogen and/or steam as gasifying agents. The syngas generation method considered in this thesis is direct gasification. Less oxygen (air) is used than that required for the raw material complete combustion. Steam is normally used as the customary temperature moderator; however, CO_2 and N_2 can assume also this role. The usual gasification process refers to solid organic matter as feedstock, where gas-solid and gas phase reactions take place. Several applications demonstrate that gasification is also applicable to liquid and gas feedstocks, being called otherwise partial oxidation. A specific gaseous feedstock, natural gas, can produce syngas through a steam reforming (Highman & van der Burght, 2003). Figure 1.7 depicts a summary of the possible pathways to obtain syngas and highlights the pathway of concern in this

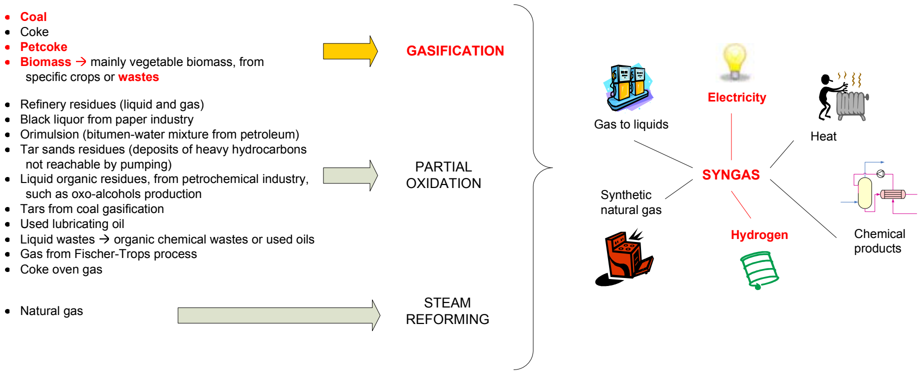

Figure 1.7: Syngas generation pathways, remarking coal, petcoke and biomass to produce electricity and hydrogen.

thesis. As solids, coal and petcoke (wastes from the refinery industry) are traditionally and widely used, while biomass is nowadays being considered with more interest as the main source (100% biomass) or in co-gasification with coal. Gasification takes place into three main types of reactors that differ on the type of bed. These are moving or fixed bed, fluidised bed and entrained bed gasifiers.

The most relevant gasification aspects for process design are (i) type of reactor and (ii) feedstock characteristics. A general gasification picture is given in NETL (2007), which provides gasification data for year 2007, revealing that the global marketplace has coal as dominant feedstock, and that Sasol Lurgi, General Electric energy and Shell are the main gasifier providers. It is important to mention that China is developing its own technology, as the current project Tianjin IGCC power plant exemplifies. Gasification plants are now operating over 27 countries, leaded by Asia/Australia region, due to the rapid growth of China. The preferred products are mainly chemicals (such as fertilisers). They are followed by Fischer-Tropsch (FT) liquids, power and gaseous fuels. See in Section 1.4 a summary of the different products that can be generated from syngas.

The use of gasification versus the use of combustion to take profit from the heating value of a solid combustible is favoured due to the higher efficiency of gasification, that produces less CO_2 emissions per unit of product. Moreover, gasification produces a versatile gas that can be used in a wider range of applications, rather than heating or electricity productions, as summarised in Figure 1.7. Regarding the production of electricity, the syngas allows its use in a combined cycle (also high efficient gas turbines), while a solid combustion can be only used to produce electricity by steam turbines. The efficiency difference can be of 6 points Highman and van der Burght (2003).

1.3.1 Biomass and gasification

When regarding to biomass gasification, it is inevitable to tackle with *tars*. As defined in Milne *et al.* (1998) "tars are the organics produced under thermal or partial oxidation regimes of any organic material and are generally assumed to be largely aromatics". Tars tolerance of gasifier downstream units is a matter of research. It is stated through the experience that tars constitute a problem when the syngas is not simply burnt in a combustor. Another drawback concerns their condensation before syngas usage: because of their carcinogenic effects they can cause health damage and generate environmental problems due to their disposal. An European tar protocol has been developed not only to assess a standard methodology for their measure, but also for characterising the quality of a clean syngas, and the determination of the degree of contamination of the gasifier downstream technology (van de Kamp *et al.*, 2005). Tars avoiding passes through two methodologies. Firstly, tar formation reduction in the gasifier itself. *Primary methods* include adequate selection of the main operating parameters, i.e. pressure and temperature, the use of a catalyst and specific design modifications, such as shape or dimensions. Note that tars are formed during the pyrolysis step. Secondly, tars removal from syngas. *Secondary methods* entail hot gas cleaning downstream the gasifier by means of thermal or catalytic tar cracking, as well as wet scrubbing or mechanical methods such as cyclones and filters. A challenge of the 100% biomass gasification pilot plants is to find an adequate gasifier design to produce a syngas free of tars, avoiding the syngas cleaning process before its final application, thus gaining compactness and saving in costs. Nevertheless, nowadays, the most used approach for tars avoiding is gasification with secondary methods.

The formation of carbonaceous materials, i.e. char, particle fines and tars, and inorganics release in form of fly ashes or slag, are strictly correlated to the fuel structure and composition. Due to the low melting point of the biomass ashes, an entrained bed gasifier looks very attractive to obtain a tar free syngas with less oxidant consumption. Nevertheless, due to the *aggressive behaviour of ashes*, a non-slagging process is recommended, except for the biomass mixed with high amounts of other feeds, such as coal or petcoke. In addition to that, entrained bed gasifiers require of small particle diameter, and there is no effective method for size reduction of fibrous biomass. Fixed beds, with no highly restrictive particles size, are extensively used for small scale gasification of biomass applied successfully in rural areas (Reed & Das, 1988). According to Mastellone *et al.* (2010), among all gasification technologies applied, fluidised beds are the most promising ones as a result of their operation flexibility for different oxidants, thus, for different fluidising agents, temperature and residence time ranges. They also allow for catalyst addition. According to Highman and van der Burght (2003), low rank coals and biomass are more suitable for fluidised beds owing to their ashes reactivity. See a summary of the typical working conditions for the different gasifiers in Table 2.1.

As has been described, tars formation and ashes reactivity are the main drawbacks in biomass gasification. The most extended bed used for large scale gasification is the fluidised one, while the most extended bed for small scale gasification is the fixed one. Entrained bed gasifiers are normally used for *co-gasification*. This is defined in Hernández *et al.* (2010) as "the joint conversion of two carbonaceous fuels (one of them of fossil origin) into a gas with a useable heating value". Renewable sources mixed with fossil fuels allow for reducing environmental and disposal costs, with no relevant efficiency reduction.

1.4 Syngas purification units and final applications

From a practical point of view, the syngas can be considered as an intermediate between an organic material and a wide range of end-use products, as depicted in

Figure 1.7. The term *polygeneration* may refer to one gasification plant that makes different products; when only two products are manufactured, the term used is *co-production*. The concept of polygeneration and co-gasification is the essence of the *biorefineries*, which aim at mimicking the energy efficiency of oil refineries through the production of fuels, power and chemicals from biomass and other organics. An integrated biorefinery optimises the biomass use to produce biofuels, bioenergy and biomaterials; the approach includes knowledge from plant genetics, biochemistry, biotechnology, biomass chemistry, separation and process engineering (Ragauskas *et al.*, 2006). There are four types of biorefineries, being one of them the biosyngas-based refinery. The other types are pyrolysis, hydrothermal and fermentation based (Demirbas, 2009).

The layout of the cleaning process, which aims at meeting the needed conditions of cleanliness and temperature before the syngas usage, is determined by the final syngas application(s) downstream the gasification process itself, the feedstock type and the syngas generation conditions, mainly pressure, temperature and oxygen purity (Wang *et al.*, 2008). Moreover, the train of cleaning units should work optimally in a wide range of syngas compositions, i.e. H_2/CO ratio, sulphur, nitrogen, chlorine and phosphorous proportions, and in a wide range of operating conditions, derived from the variability in the feedstock (Highman & van der Burght, 2003). Analogously to tar removal methods, syngas cleaning units can be divided into two types according to their place of action: during gasification, generally for solid removal, and after gasification, mainly for fluid pollutants removal, being called respectively *primary* and *secondary cleaning methods*. IGCC-CCS and BG-GE approaches have different needs of syngas cleanliness and temperature, as the final gas applications determine.

1.4.1 Carbon capture and storage

In a climate change constrained society and economy, CCS offers the opportunity to reduce carbon emissions and enable coal producing countries to consume their reserves in an environmental friendly way. IGCC-CCS plants allows for countries like China, with high reserves of coal and with a large increasing demand of electricity, to reduce notably its carbon footprint. CCS is not suitable for distributed implementation due to its cost and complexity (Bouffard & Kirschen, 2008).

CO_2 is considered one of the most important GHG. Many current industrial processes, not only for energy production, release CO_2; mainly refineries, iron and steel industries, oil and gas extraction, cement production and paper and mills. Moreover, virtually, all industries produce CO_2 emissions due to their electricity consumption. CCS aim at liquefying the CO_2 stream before its release into the atmosphere, and transport it to a final geological storage. In order to implement such a solution, it is necessary to have an integrated approach considering the whole supply chain. It means that a CCS process in a factory, which can be done with existing and well proved technology in the field of gas purification, should be directly linked to the localisation of a possible geological reservoir for the captured GHG. It also has to consider the different CO_2 transportation network possibilities, by pipelines or by boats, which are similar to the ones used for natural gas transportation. In power plants, the implementation of a carbon capture technology can penalise the global efficiency of the plant (IEA-GHG, 2008).

Besides the technical and logistic aspects, also public acceptance is important to be considered together with the requirements on legal and politic developments which altogether have a key role to implement CCS as a part of the climate change solution. The obligatory nature of the CO_2 capture measure and the purity of the CO_2 to be injected have to be extensively discussed and assessed from legal and technical points of view (IEA-GHG, 2008).

1.5 Decision making

Multiple criteria decision analyses (MCDA) comprise the methods for process optimisation-decision making through multiple objectives, thus diminishing risk. MCDA is applied in this thesis to two types of systems: process and supply chain systems. IGCC-CCS and BG-GE processes modelling represent the aspects of interest to gain knowledge about the system's performance in terms of thermodynamics, mass and energy flows. IGCC-CCS and BG-GE supply chains modelling enable the investigation of possible alternatives for supply chain management.

1.5.1 Process modelling

The aim of process design is to specify the most economical and effective practical procedures to transform raw materials to produce a new product, to manufacture an existing product by new means or to bring about some designated material transformation in a commercial scale, so as to satisfy a market need (Turton *et al.*, 1998, 3rd Edition 2009). The classical design procedure is seen as an iterative procedure to estimate in advance the resource implications. Most often, several alternatives process routes have to be explored and tested in some detail before it becomes clear which the most economic process synthesis is. To reduce uncertainty in the decision making task, for instance, in terms of dimensions, materials or type of units selection, the use of process simulation is a convenient strategy. *Process simulation* is understood as the use of computer software resources to perform mathematical models of process components for the construction of an accurate, representative model of the whole chemical process aiming at understanding its behaviour during regular plant operation. Depending on the degree of model accuracy, called granularity, the precision of process design cost estimates varies within a wide range. This work deals with *preliminary design*, where the precision of the cost has a margin of 10%-25%. The preliminary design step represents only the 0.4%-0.8% of the total project cost (Douglas, 1988). This pre-design level includes an optimisation approach to identify *the best design* according to selected custom criteria. *Optimal process design* can assess the performance of a process according to economic, technical, thermodynamic and/or environmental indicators. Process modelling coupled with life cycle assessment (LCA) envisaged to incorporate the environmental aspects, can guide the process design towards a widest point of view, rather than the plant as a unique entity.

1.5.2 Supply chain management

A *supply chain* (SC) is defined as "a set of three or more entities (organisations or individuals) directly involved in the upstream and downstream flows of products, services, finances and/or information from a source to a customer" (Mentzer *et al.*,

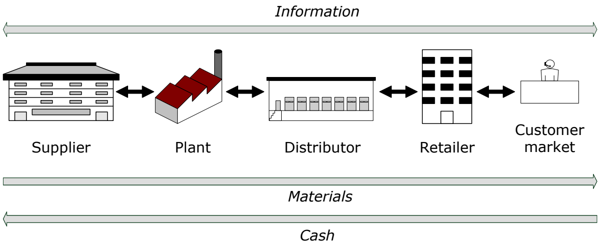

Figure 1.8: Supply chain network and related fluxes.

2001). Therefore, in a SC, it is possible to recognise processing sites, distributors, transporters, warehouses and raw material suppliers, as shown in Figure 1.8.

Supply chain management (SCM) can be defined as "the systemic and strategic coordination of the traditional business functions and tactics across these business functions within a particular company and across business within the SC, for the purposes of improving the long-term performance of the individual companies and the SC as a whole" (Mentzer *et al.*, 2001). Note that the different SC components can be geographically distributed. SCM copes with the SC flows, that are materials, cash and information (see Figure 1.8), in a coordinated way, along the different processes to deliver efficiently goods or services. This is especially important for biomass to energy projects which are highly geographically dependent and whose profitability can be strongly influenced by the location of the different processes and biomass sources, being the logistic variables of special complexity to manage (Caputo *et al.*, 2005). Commonly, biomass production and transportation account for a significant fraction of the whole bioenergy SC cost (Panichelli & Gnansounou, 2008). Therefore, a tool able to evaluate the possible trade-offs between different feedstock sources, each one with specific properties, i.e. MC, energy and bulk densities, and the location of processing and consumption sites, is a requisite to develop efficient bioenergy networks. This thesis tackles with the SCM problem that is, the strategic-tactical problem associated to the optimal design and operation of a *bio-based SC's* (BSC), with biomass as raw material, taking into account a variety of specific considerations depending on the case studies. Generally speaking, the SC strategic level determines the network through which production and distribution serves the marketplace. The intent of the SC network design problem is typically to determine the optimal sourcing, manufacturing and distribution network for the new and existing product lines of a company (e.g., expansion or contraction of the business, introduction of new products, new strategic suppliers). The most common approach, which is the one followed here, is to formulate a large-scale mixed integer linear program (MILP) that captures the relevant fixed and variable operating costs for each facility and each major product (Graves & Tomlin, 2003).

1.6 Research scope and objectives

The energy sector is changing towards more efficient processes and renewable sources. Bioenergy is seen as one of the most important renewable energy sources used in the world. Countries worldwide have become conscious of the biomass potential through modern processing methods to satisfy the energy needs, promote development and alleviate climate change. As a consequence, the energy paradigm is moving towards less fossil fuel dependants and more carbon innocuous centralised systems, as well as towards DES, aiming to profit the closest and renewable source of energy. Biomass sources can be of different origins, being wastes from forestry and agricultural activities of special concern thereby diminishing the land use controversy. There exist a need to secure the sustainability of the biomass as a resource, as well as there exist the need of standardising the biomass trade. All in all, the bioenergy sector should deal with environmental, social and economic issues and adopt decisions that take into account biomass intrinsic characteristics, availability and population demand.

The main objective of this thesis is to contribute in the emerging bioenergy sector by studying gasification of biomass using advanced process modelling techniques, and incorporating specific SCM strategies. This work distinguishes between centralised or large scale and distributed or small scale power generation layouts in different contexts. This general aim can be divided into three more specific objectives:

- To develop a process system engineering approach for IGCC-CCS modelling and optimisation.
- To propose working conditions guidelines in co-gasification and co-production of H_2 and electricity in IGCC-CCS plants.
- To apply existing models and tools in SCM to different bio-based supply chains, in scale and social/economical contexts, to be able to propose sustainable networks.

1.7 Thesis outline

The general context of this thesis carries out the main research lines described in the abovementioned objectives. Figure 1.9 represents schematically the outline of the document. The work is divided into three main blocks, being Part II the core of the thesis. This part contributes to design and planning CES and DES, in different contexts.

In addition to this introduction, Part I gives a more detailed overview of the thesis topics and approaches. Chapter 2 presents a state-of-the-art review that finishes with a SWOT (strengths, weaknesses, opportunities and threats) analysis that integrates the main concerning features, allowing for the identification of the most important trends and challenges of the bioenergy sector. Then, Chapter 3 revises the foundations of all the methods and tools that are used throughout this thesis.

The essence of this thesis is in Part II, focused on the one hand on CES, being the IGCC-CCS power plant the centralised system of concern. With the purpose of helping in decision-making on strategic and tactical levels of the project (also called "business" level), Chapters 4, 5 and 6 deal with process design, and Chapter 7 with SC design. Chapter 4 describes the gasifier modelling methodology and reports the model validation results. Chapter 5 acts in an analogous way for the syngas cleaning blocks, the carbon capture train of units and the combined cycle. Once the model is built-up and validated, hence it is assumed that the global model is able to reproduce reliable results, Chapter 6 profits the developed tool for sensitive analyses performance and multiobjective optimisation, giving as a result some guidelines in co-gasification and

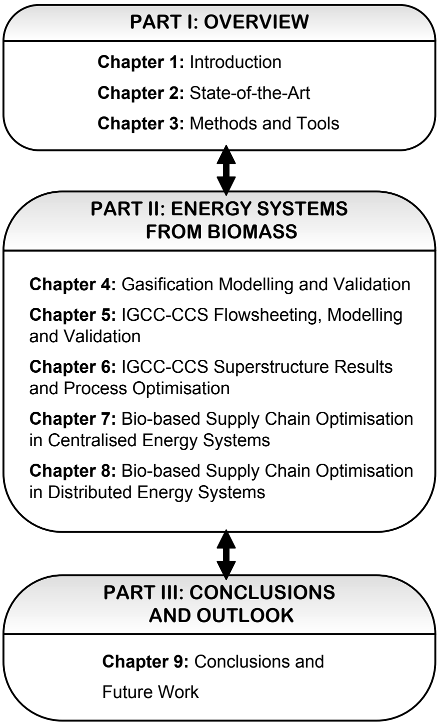

Figure 1.9: Thesis outline.

co-production processes. To finish with CES, Chapter 7 considers the optimisation of two supply chains located in Spain: the first one evaluates the possibility of 100% gasification plants locations to cover the demand of some located markets of electricity and hydrogen, and the second one evaluates the possibility of co-combustion of coal and biomass in already existing conventional thermal power plants aiming to obtain the best biomass distribution chain. Next, Chapter 8 is focused on DES: the BG-GE systems. It uses the developed modelling tool to look at the performances of such a system with the incorporation of waste heat recovery. Then, it concerns the optimisation of one SC located in Atebubu district, in Ghana, and evaluates the problem of sustainable rural electrification.

Finally, Chapter 9 summarises this thesis contributions, goes over the conclusions and suggests future work along the lines of research opened in this work.

Notation

Superscripts and subindices

e	electric
th	thermal

Acronyms

BD	bulk density
BG	biomass gasification

BSC	bio-based supply chain
CCS	carbon capture and storage
CES	centralised energy systems
DES	distributed energy systems
EISA	Energy Independence and Security Act
EPRI	Electric Power Research Institute
EU	European Union
FT	Fischer-Tropsch
GE	gas engine
GDP	gross domestic product
GHG	greenhouse gases
GNI	gross national income
HDI	human development index
HHV	higher heating value
IEA	International Energy Agency
IGCC	integrated gasification combined cycle
LCA	life cycle assessment
LHV	lower heating value
MC	moisture content
MCDA	multiple criteria decision analyses
MILP	mixed integer linear program
MSW	municipal solid waste
OECD	Organisation for Economic Co-operation and Development
PC	pulverised coal
SC	supply chain
SCM	supply chain management
SWOT	strengths, weaknesses, opportunities and threats
UN	United Nations
UNDP	United Nations Development Program
WB	World Bank
WEO	World Energy Outlook
WGS	water-gas shift

Chapter 2

State-of-the-Art

In Chapter 1, the need of decision-making tools in the bioenergy context is identified. Therefore, the purpose of this work is to use multiple criteria decision analyses (MCDA) methods for process and supply chain (SC) systems optimisation at the design level, of centralised and distributed biomass schemes (CES and DES). This chapter presents a literature review of the gasification plants main characteristics and components, the approaches used to optimise the preliminary plant design and the specific needs identified to achieve it.

2.1 Introduction

Generation and use of syngas or producer gas from biomass in centralised and distributed systems depends essentially on the characteristics of four major components: the percentage of biomass gasified, the type of gasifier, the specific final gas usage and the plant scale. Consequently, even if the raw material and the basics of gasification technology basically remain the same, the resulting plant design will be different in each particular case. Accordingly, the state-of-the-art has been organised around these main components.

The conceptual design (also called "preliminary") links the different issues treated on the thesis. It is the phase between the "laboratory scale" research and the detailed engineering design of the final plant. To this end, the concept of superstructure is used. The superstructure built supports process system modelling, process system alternatives and process system optimisation. Then, mathematical programming has been chosen for the representation and optimisation of the whole underlying SC. The referred papers in this chapter are focused on these methodologies, which are further described in Chapter 3.

The following sections present the state-of-the-art of the thesis topic at various levels of detail, from the modelling of individual plant's units until the aggregate modelling of the whole integrated SC of a CES. It is worth noting that the distinction between levels (CES and DES) tends to disappear when considering DES, where energy

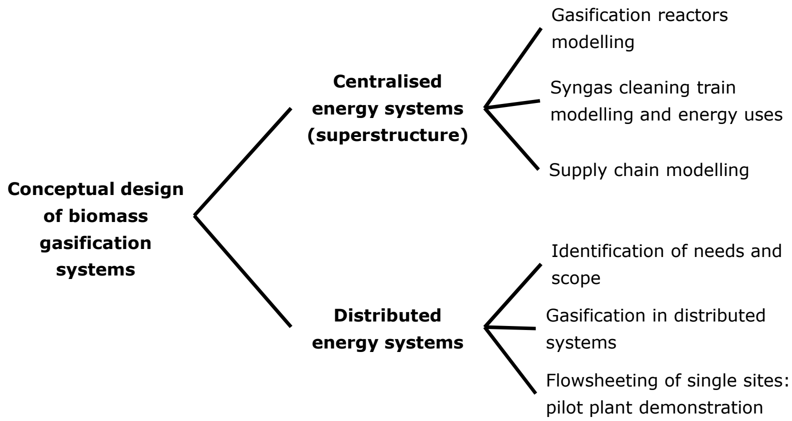

Figure 2.1: Scheme of the subjects developed in this chapter.

plants operate as "islands", being individually optimised and becoming eventually part of a grid. Consequently, in this latter case, the state-of-the-art description is organised following the inverse path: from the most general level to the particular level, to finally identify the challenges in plant operation. See in Figure 2.1 the outline of this chapter.

2.2 Centralised energy systems

Large scale gasification systems normally use entrained or fluidised beds for the production of syngas. Increasing the share of biomass in the energy supply would be associated with the reduction of GHG emissions and with the independence from imported and domestic fossil fuels. There exists an interest on the use of biomass and waste material as fuel, therefore, there is much effort devoted in enhancing their conditions for transport, handling and processing. Conceptual modelling should take into account the biomass properties to determine the feasibility in terms of efficiency and most appropriate mixtures of feedstocks and products mix.

2.2.1 Gasification reactors modelling

Types of gasifier

The gasification process can be carried out into three main types of gasifier that differ in the type of bed made-up by the raw material itself. These are moving or fixed bed, fluidised bed and entrained bed gasifiers. Only a few processes do not fit into these three categories, for instance in situ gasification of coal or underground gasification, molten iron bath gasification, plasma gasification or hydrogasification, as described in Highman and van der Burght (2003).

The *moving bed* or *fixed bed gasifier* is the most widely used reactor allowing the feed to have the largest particle size. The bed moves downward as the feedstock is consumed and the residence time can be in the order of hours. The feedstock is introduced at the top of the reactor and the gasifying agents can be introduced also at top, being called co-current or downdraft configuration, or at the bottom of the reactor, being in this case the counter-current or updraft configuration. Oxidant requirements are low and the gasification temperature is also relatively low if compared with the other types of beds (in the order of 600°C to 900°C). The main drawbacks are the amount of tars in the produced gas, pyrolysis products (such as hydrocarbons, CH_4) and fly ash resulting from an uncompleted slagging phenomenon. Reed and Das (1988) states that the downdraft configuration might achieve higher conversion rates with relatively low tar formation, thus it is the most widely applied configuration for power generation. Fixed beds are not suitable for large scale gasification due to scale-up problems caused by matter agglomeration. This effect avoids a uniform penetration of the gasifying agent and leads to mixing problems with the feed. The temperature profile along the bed shows a peak temperature at the combustion zone. Nowadays this is the most widely used gasifier for 100% biomass gasification. Consequently, fixed beds are mainly used for rural potential use involving distributed systems. For example, the papers by Sharma (2009) and Hiremath *et al.* (2009) report the Indian extended use of small scale-fixed bed gasifiers with special attention into the biomass supply and its matching with the energy needs of the area. It is possible to find in the market batch and continuous moving bed gasifiers. The batch mode the most usual one.

The *fluidised bed gasifier* is based on the principle of fluidisation that occurs when particles velocity and the mixture formed by the gasifying agent, moderator and other recirculation flows speeds are the same. This phenomenon drives the particles to an state of levitation. The fluidised bed offers a good mixing or contact between the feedstock and the gasifying agent, leading to better heat and mass transfer actions between gas and solid phases. It has a behaviour close to that from an ideal continuously stirred tank reactor (CSTR). The fluidisation phenomenon allows a stable temperature along the bed. As a difference from the previous bed, in which the temperature is limited by the bed itself moving downward during its consumption, the temperature is controlled to avoid ash slagging to do not interrupt the fluidisation phenomenon (Highman & van der Burght, 2003). The solid conversion is restricted as a result of this temperature limitation. As the particles become lighter during the conversion process, it is very common to entrain them out of the reactor. That is the reason why fluidised beds usually have a recirculation stream. The residence time ranges from seconds to minutes. They are well extended too for biomass as well as for coal gasification.

The *entrained bed gasifier* takes advantage of the particles entrainment property, with the gasifying agent and moderator agent flows in co-current way. The residence time is of several seconds. The particle size is the main restriction, since it should be in the range of microns to be transported with the gas phase. To assure the highest conversion of the solid, the reactor temperatures are larger if compared with the previous types of bed. As a consequence, ashes are converted into slag. As the slag should be liquid enough to do not block the gasifier operation it is usual to use an additive, such as limestone, to lower the ash melting point to an appropriate operating gasification temperature. For the aforementioned reasons, entrained bed gasifiers have the highest solid conversion. Therefore, it is usually assumed that the solid is completely converted and it can be considered that no tars are produced when gasifying biomass, due to the high temperatures that assure tars destruction by thermal cracking (Coca, 2003; Highman & van der Burght, 2003). IGCC power plants usually use entrained beds.

Even if the gasification mechanism principles are the same in each type of reactor,

Table 2.1: Comparison of the three types of gasifier by their most important characteristics.

	Moving bed[1]	Fluidised bed[2]	Entrained bed[3]
T (°C)	600-875	800-1,100	1,250-1,600
P (bar)	1	1	25
Particle size (mm)	6-50	6-10	<0.1
Moisture (%)	15-20	10	2
Feedstock	Wood	Biomass	Coal:petcoke
Oxidant	Air	Air	Oxygen
Ash slagging	No	No	Yes
Carbon conversion (%)	99	97	99
Syngas (% dry mole)			
CO	18	31	60
H_2	15	18.9	21
CO_2	10	6.7	4
CH_4	1.5	2.1	0

[1] Dogru *et al.* (2002), Jayah *et al.* (2003), Hsi *et al.* (2008).
[2] Highman and van der Burght (2003).
[3] Coca (2003).

a typical syngas composition can be suited for each type of gasifier through their most common conditions of pressure and temperature. See in Table 2.1 a summary of the main characteristics and their most common values. Note that the values from the table are tentative and only serve as a general overview: any type of bed can work at high or at low pressure, be fed by different feedstock sources and use different gasifying agents. Overall, the syngas composition on a dry molar basis ranges from 15% to 21% H_2 and 18% to 60% CO (Dogru *et al.*, 2002; Highman & van der Burght, 2003; Coca, 2003). At the end, the choice of the appropriate gasifier type and the appropriate working conditions depends on the feed extrinsic and intrinsic characteristics and the final use of the syngas.

Downstream the gasifier different processes can provide with electricity, heat, chemicals or liquid fuels. The *gasifier pressure* is usually given by the conditions of the final application. For example, in a combined cycle (CC), the gasifier pressure is set by the gas turbine (GT) pressure. In turn, the feedstock pressure is usually matched with the final application too since a solid compression consumes less energy than a gas compression. The *gasifier temperature* can be limited by the melting point of ashes.

Modelling the gasifier

Gasification modelling is still a subject of research even if significant approaches have been already built-up. The level of detail of the model essentially obeys the mode of operation of the plant: dynamic or steady-state. The different modelling approaches range from the macroscopic level, which encompasses *thermo-chemical equilibrium* approaches, to the microscopic level, which considers *chemical kinetics* and heat transfer detailed mechanism. The thermo-chemical equilibrium can be defined by the reactions or by the final chemical compounds. In both cases Gibb's free energy is minimised, but the difference remains in the number of reactions considered: in the former case the number of reactions is limited, while in the latter case all the reactions involving the final compounds can be taken into account. At the microscopic level, the boundary layer or pore diffusion is usually performed with kinetics. As a result, the most extended approach is the unreacted-core shrinking model (Wen & Chaung, 1973). In both levels, mass and energy balances must be accomplished. When a dynamic gasification process is of concern, the unique model to be used is the kinetic one given that equilibrium models cannot provide a time dependant response.

The *residence time* is the parameter that allows determining the suitability of the selected approach. For large residences times, the equilibrium model is preferably selected. It is worth mentioning that the kinetic approach is more reactor and feed-dependant than the equilibrium approach. The *gasification temperature* is usually considered as the gasifier outlet temperature, since it can be easily measured. Therefore, lumped parameters, consider this temperature value even if the gasifier does not have a unique temperature but a profile of temperatures that follow the deployment of the gasifier zones. The study by Reimert and Schaub (2003) adjusts the final modelled gas composition performing the equilibrium reactions at other temperature rather than the reactor outlet temperature.

Concerning model suitability, the study by Ruggiero and Manfrida (1999) states that even if the syngas composition is not accurately matched by an equilibrium approach, this is fast, robust and reliable enough to be used for outputs prediction when sensitivity analyses are performed. The papers by Usón *et al.* (2004) and Gautam *et al.* (2010) point out that at high temperatures (around 1200°C or more), the equilibrium approach fits with the experimental syngas compositions. In contrast, at low temperatures, the reaction rates are smaller and the residence time should be higher to reach the equilibrium. Then, the question is when the equilibrium is reached. The answer can be found by comparing the equilibrium model outputs with experimental or kinetic models results. Only two of the studies revised tackles with the formation of tars during biomass gasification: the papers by Di Blasi (2000) and Jand and Foscolo (2005).

Equilibrium and kinetic approaches have been implemented and validated for the three types of bed in the revised literature. Table 2.2 provides with a summary of a sample of papers concerning gasification modelling, taking into account pressure and temperature of gasification, type of feed, scale and state. It is noticeable that the studies using fixed bed gasifiers are mainly referred to biomass as raw material for small scale applications. In contrast, entrained bed gasifiers are used more with coal as feed and in large plants. In the middle, the fluidised bed works are referred to laboratory practices, and works with biomass as raw material.

Biomass *co-use* in large scale reactors

Co-firing can be defined as the simultaneous combustion of two or more fuels in the same combustion plant (Berndes *et al.*, 2010), using biomass along with a fossil fuel (Sami *et al.*, 2001). *Co-gasification* has been defined in Section 1.3.1, and in an analogous way as co-firing, concerns the use of biomass with a fossil fuel, in this case, in a gasifier.

The technologies summed up in Figure 1.6 include large and small scale biomass applications. Large scale systems to produce power and heat by means of a gas contemplate biogas production through anaerobic digestion, combustion or flue gas production through combustion and syngas generation through gasification. Combustion and gasification are the two conversion processes considered in this thesis. In turn, they offer five alternatives for biomass usage: combustion, co-combustion or co-firing, gasification, co-gasification and gasification for co-firing (Faaij, 2006). From the point of view of efficiency in CES, GHG emissions reduction and solution immediacy, co-firing and co-gasification are the chosen possibilities. These two options have in

Table 2.2: Gasifier modelling review.

Source	Raw material	Gasifier type	P(bar), T(°C)[1]	Scale[2]	Time dependence	Approach
Gautam *et al.* (2010)	Biomass	Fixed	1, 800	Pilot-Small	Steady	Equilibrium chemical reactions
Loeser and Redfern (2009)	Biomass	Fixed	1, n.s.[3]	Small	Steady	Equilibrium chemical compounds
Melgar *et al.* (2007)	Biomass	Fixed	1, 700	Pilot-Small	Steady	Equilibrium chemical reactions
Giltrap *et al.* (2003)	Biomass	Fixed	1, 927	Small	Steady	Kinetic model
Altafini *et al.* (2003)	Biomass	Fixed	1, 800	Pilot-Small	Steady	Equilibrium chemical compounds
Di Blasi (2000)	Biomass	Fixed	1, 850	Small	Dynamic	Kinetic model
Wang and Kinoshita (1993)	Biomass	Fixed	1, 800	Small	Dynamic Steady	Kinetic model
Nikoo and Mahinpey (2008)	Biomass	Fluidised	1, 800	Lab	Steady	Kinetic model for heterogeneous reactions, equilibrium chemical compounds for homogeneous reactions
Jand and Foscolo (2005)	Biomass	Fluidised	1, 675	Lab	Dynamic	Kinetic model
Ruggiero and Manfrida (1999)	Biomass	Fluidised Entrained	1 and pressurised; n.s.	Pilot-Large	Steady	Equilibrium chemical compounds
Emun *et al.* (2009)	Coal slurry	Entrained	8, 1250	Large	Steady	Equilibrium chemical compounds
Robinson and Luyben (2008)	Coal slurry	Entrained	55.17, 1370	Large	Dynamic Steady	Kinetic model
Nathen *et al.* (2008)	Coal	Entrained	n.s., 1500	Large	Steady	Equilibrium chemical compounds
Frey and Akunuri (2001)	Coal slurry	Entrained	42, 1260	Large	Steady	Equilibrium chemical compounds
Wen and Chaung (1973)	Coal slurry and liquefaction residues	Entrained	22, 1800	Large (pilot plant)	Dynamic Steady	Kinetic model
Govind and Shah (1984)	Coal slurry and liquefaction residues	Entrained	22, 1800	Large (pilot plant)	Dynamic Steady	Kinetic model
Reimert and Schaub (2003)	General	General	General	General	Steady	Equilibrium chemical reactions[4]

[1] The reported temperature is an average value (the most of the sources provide with a temperature interval).
[2] Large and small scales belong to industrial scale.
[3] n.s: non specified.
[4] Equilibrium constant for defined reactions are at a temperature other than that in the reactor.

common the range of power produced (hundreds of MW) and the use of already existing installations originally performed with 100% fossil fuels. Typical 100% biomass plants are smaller: combustion plants are around 20-50 MW_e and gasification plants are in the range of 10 MW_e (Rodrigues *et al.*, 2007). Co-firing and co-gasification permit the usage of local biomass sources, being of special interest for organic wastes management. CO_2, sulphur and nitrogen emissions reduction is a direct advantage derived from coal fraction substitution.

Co-firing is the cheapest method compared to other biomass uses and to other renewable sources. It can cost from 2 to 5 times less than other bioenergy alternative (Berndes *et al.*, 2010). According to Gómez *et al.* (2010b) the specific investment ranges from 100 €/kW to 880 €/kW, with kW of inlet thermal power, depending on the type of coal power plant and the selected co-firing system. Faaij (2006) states that this is the largest biomass conversion technology that is growing in the EU countries nowadays. Co-firing plants have relatively higher energy efficiency due to the already existing economies of scale in the thermal power plants, and lower investments by appropriately matching the biomass quality, the co-firing option and the coal percentage substitution than other bioenergy options.

The coal-fired power plants can be of different types according to the type of reactor: fluidised bed boilers, pulverised coal-fired boilers (PC) and grate-fired boilers. The *biomass quality* should mimic as far as possible the properties of a fossil fuel. These are low moisture content (MC), optimal grindability to be pulverised and high bulk and energey densities (BD and LHV, respectively). Biomass has all these drawbacks: high MC, due to its fibrous nature it is hard to be reduced into powder, and low BD and LHV. Those are the reasons why the quality of biomass should be improved to optimise its transport, handling and processing. Pre-treated biomass is needed to further develop the supply and use of it in CES. Pellets, torrefied biomass, torrefied pellets (TOP) and bio-oil (pyrolysis oil) are the state-of-the-art options currently proposed as "enhanced biomass", optimally used in co-firing, as well as in co-gasification, being torrefaction and fast pyrolysis in pre-commercial stage (Uslu *et al.*, 2008). From the cheapest to the most expensive technique, the *biomass co-firing options* include: (i) direct co-firing by blending biomass with coal or co-milling, or (ii) indirect co-firing by separate injection and parallel firing in separate boilers that are connected to a common steam turbine (ST). Indirect co-firing also contemplates advanced techniques such as gasification to burn the syngas (Tillman, 2000; Perry & Rosillo-Calle, 2008; Basu *et al.*, 2011).

The paper by Damen and Faaij (2006) identifies the main energy loss sources due to biomass co-firing. Those are increase of electricity internal use caused by the higher milling and drying needs, lower boiler efficiency and boiler de-rating as a consequence of the air consumption increase. In van Loo and Koppejan (2008) it is seen that the co-firing influence on the thermal efficiency of the boiler depends on the co-firing ratio and the MC of the biomass. Nonetheless, a range of 3%-5% of coal substitution has an insignificant effect on the efficiency. The studies by Perry and Rosillo-Calle (2008) and Berndes *et al.* (2010) point out that the biomass share should be limited due to corrosion, slagging and fouling problems. The paper by Baxter (2005) adds the formation of striated flows, fly ash utilisation and fuel conversion decrease. According to Chiaramonti *et al.* (2005), co-firing bio-oil with coal does not have technical problems, but the investment is high. A successful operation, after a proper boiler modification, is reported for a 5% substitution of coal on thermal basis. Faaij (2006) reports up to 10% of co-firing rates on thermal basis, with no important consequences in the boiler. The work by Damen and Faaij (2006) has found that the net energy penalty, that takes into account plant and biomass transportation consumptions, is not significant when co-firing up to 7% of biomass on a weight basis. In the range of 7% to 20% on a weight basis, an increase in the energy penalty is observed: an energy efficiency loss of 3% should be assumed for the overall combustion plant. Different experiences in UK demonstrate that biomass can be effectively co-fired up to 20% in weight basis, even if some technical problems have been encountered, i.e. corrosion and no space for biomass storage before burning (Perry & Rosillo-Calle, 2008). The paper by Gómez *et al.* (2010b) proposes a maximum coal fraction substitution of 10% on thermal basis, since higher fractions can decrease the boiler efficiency and cause corrosion problems. It also states that less than a 5% on thermal basis does not imply a valuable change in the plant performance. The affordable shares according to Berndes *et al.* (2010), at mid term and with no technical penalisations, are 15% for fluidised bed boilers and 10% for PC boilers and grate-fired boilers, in energy basis.

A conventional coal-fired power plant can have an *energy efficiency* of 30%-45% on a LHV basis, depending on the technology and the antiquity of the plant (Berndes *et al.*, 2010). The study by Van Den Broek *et al.* (1996) reports a range from 39% to 44% for co-firing PC power plants, up from 100 MW. Van Den Broek *et al.* (1996) have calculated the difference between biomass combusted alone in small scale plants and biomass co-combusted in larger plants, in efficiency terms. The value is of about 7 points, changing from 30% to 37%. The value of the efficiency reduction in a conventional power plant shifting to co-firing, is calculated by a quadratic equation that depends on the biomass percentage in Tillman (2000). This value is relatively small, till 1.9 points, in the range 5% to 20% of biomass use on a mass basis. The work by Gómez *et al.* (2010a) reports a value of 38% as co-firing efficiency.

The energy efficiency in the work by Sami *et al.* (2001) increases. It puts into relevance the synergetic effect between coal and biomass. Not only the efficiency is enhanced, but also NO_x, SO_x and CO_2 emissions are reduced. Similar results for NO_x and CO_2 emissions are reported by Basu *et al.* (2011) and Munir *et al.* (2011), respectively. Damen and Faaij (2006) and Perry and Rosillo-Calle (2008) put into relevance that the emissions from production, conversion and transportation of biomass, as well as land use change and displacement, should be taken into account in a co-firing project. The final balance shows net GHG emissions avoided.

While biomass co-fired at PC boilers in power plants have been highly reported, co-gasification using entrained flow gasifiers is still an emergent issue. It is due to the non-fully commercial status of the IGCC power plants: according to Koukouzas *et al.* (2008), co-gasification is affected by the typical features of a new technology, i.e. high capital costs and low reliability. Current trends on renewable energy and promotion of gasification, especially in emerging countries, may motivate the study of co-gasification. The most recent and relevant papers are Valero and Usón (2006), Koukouzas *et al.* (2008), Fermoso *et al.* (2009), Fermoso *et al.* (2010), Hernández *et al.* (2010) and Mastellone *et al.* (2010) these two last concerning fluidised beds. The first paper reports an entrained bed gasifier model for co-gasification of coal and petcoke with biomass up to 10% on a mass basis. This percentage is limited by a British Coal study, that has proved that this is the maximum proportion of sewage sludge and straw considered with no technical problems. Nevertheless, the net electrical efficiency decreases mainly due to a higher electricity consumption in the biomass pre-treatment system. In contrast, the Koukouzas *et al.* (2008) work counts with a gasifier that allows a 75:25 mixture of biomass pellets and lignite on a mass basis. In Fermoso *et al.* (2009), Fermoso *et al.* (2010) and Hernández *et al.* (2010), *synergic effects* are observed by biomass and fossil fuels co-feeding, leading to better feeding properties that derives into carbon losses reduction and into a syngas with higher LHV. Even if those effects are far from being well understood, they are found advantageous. Concretely, for pressurised entrained bed gasifiers, Fermoso *et al.* (2009) have encountered a synergic effect in ternary blends by coal, petcoke and biomass (almond shells, olive stones and eucalyptus), and in binary blends by coal and biomass, in which H_2/CO ratio decreases with the addition of biomass, while the carbon conversion and the cold gas efficiency (CGE) increase. The experimental work by Hernández *et al.* (2010) demonstrates that an increase in the biomass proportion of the blends formed by dealcoholised grape marc with coal:petcoke, results in a CGE increase. Mastellone *et al.* (2010) have performed co-gasification of coal, plastic and wood, with special concern in the appropriate proportions of raw materials to achieve the desired syngas composition. According to Kajitani *et al.* (2010) and Hernández *et al.* (2010) synergetic effects are observed at low temperature ranges. Hence, gasification reactors at more than around 850°C, do not manifest such a positive effects. Even more, Hernández *et al.* (2010) reported a maximum value for the H_2/CO ratio value, that started to decrease when increasing the temperature.

The study by Lapuerta *et al.* (2008) points out the need of an homogeneous biomass resource for co-gasification. This should come from different sources with different seasonal availabilities. This is focused on woody and herbaceous biomass types and puts into relevance the trade-off between type and fraction of biomass, gasification temperature and biomass/air ratio with the final gas composition. Synergetic effects are also observed, mainly in the CGE. The paper attributes the benefits to the catalytic effect of biomass ash.

The abovementioned studies stand for co-gasification of coal and biomass directly mixed in the feeding step. In contrast, Yuehong *et al.* (2006) and Baliban *et al.* (2010), in an analogous way as co-firing options, obtain syngas from different sources separately: from natural gas by reforming, and from biomass and coal gasification, or only from coal gasification like in the second work. The purpose is to optimise the different sources contributions depending on the final syngas usage.

Biomass waste use in co-firing and co-gasification is not only an option for wastes disposal but a renewable energy generation alternative that diminishes the consumption of fossil fuels, by taking advange of the already existent CES and the economies of scale. The main biomass drawbacks are high MC, low BD and low LHV. In order to be used as a sustainable commodity in large power plants, the biomass should be enhanced to ease its transport, handling and processing, and to be as far as possible homogeneous, independently of its origin. Biomass share limitation in co-use applications relies on technical constraints.

2.2.2 Syngas final applications and cleaning train units

Syngas requirements before the final application include *temperature*, *pressure*, *composition* and *pollutants level.* For instance, Knoef (2008) specifies that syngas cooling is required for combustion in gas engines, for filters having a maximum acceptable temperature and for an optimal syngas compression. The pressure level can be reached in the gasification reactor. In turn, gas purity, independently from the scale, ranges from pollutant levels of mg/m^3, passing through ppm, and reaching ppb: the syngas cleaning level is dictated by the flue gas emission requirements and the specific device conditions to work properly and during long time. Wet and dry, hot and cold cleaning systems have been developed and implemented.

High temperature and pressure are the most suitable conditions for a long range of syngas applications. The next characteristics can be described for each purpose depicted in the right side of Figure 1.7 (Wang *et al.*, 2008; Highman & van der Burght, 2003):

- *Electricity production.* It is generated through syngas combustion in a GT or in a CC. It is also produced through the H_2 transformation in a fuel cell (FC). Note that for small scale, the most extended use is a engine.
  - IGCC power plants: These are the specific combination of gasification with a CC. Most common plants use coal and other fuels from fossil origin, such as residues from oil industry. The matching between gasification and CC involves the adaptation of syngas temperature, directly entailing a loss of efficiency. This is due to the misuse of the high temperature stream obtained in the entrained bed gasifier, which is not profited for electricity generation. That is the reason why hot or warm syngas cleaning processes are of concern. Ideally, for power generation, pressure and temperature should be maintained along the layout as far as possible. IGCC power plants are far from this ideal situation. Usually cryogenic temperatures are needed in the Air Separation Unit (ASU), and syngas is cooled down before filtering and desulphurisation stages, to be heated once again in the combustor of the GT cycle. *Advanced cycles* deals with the enhancement of the CC efficiency through isothermal compression or through heat integration.
  - Fuel cells: There exist several types of FC's, i.e. solid oxide, molten carbonate, phosphoric acid, and proton exchange membranes (SOFC, MCFC, PAFC, and PEM, respectively). As discussed in Hernández-Pacheco *et al.* (2005), the solid oxide fuel cell (SOFC), which operates at high temperatures (600°C-1000°C), is the most extended type of FC to be integrated in a gasification plant for power production. The FC allows the use of different mixtures containing CH_4, CO and H_2. In fact, only H_2 is converted in the anode, but CH_4 and CO can be converted into H_2 inside the FC through a reforming process. The major research on this field is developed in small scale gasification, as further detailed in Section 2.3.2.
- *Heat.* The production of heat from syngas involves the combustion of it into a kiln to heat water. This application does not need exhaustive cleaning processes and no specific conditions of pressure and temperature, since the kiln as technology does not have special pollutant limitations and/or operation restrictions. Co-generation or waste heat recovery can be also included in this category.
- *Chemical products.* C1 chemistry is the chemistry involved in syngas processing, thus entailing CH_4 and CO_2, that shows the possible conversion routes to obtain industrial chemicals, i.e. ammonia, small organic compounds and oxo-alcohols. It states the formation mechanisms of multi-carbon molecules from one single carbon (Wender, 1996). Specifically, for each chemical:

- Ammonia: It is mainly obtained from the reforming of natural gas. Only a 10% of the world production is performed by coal or heavy oil gasification. It is produced from syngas through a catalysed process at high pressure. In this case, the N_2/H_2 ratio is the important syngas variable to be optimised.
- Small organic compounds: CO is the raw material used to synthesize organic chemicals like acetic acid, phosgene or formic acid. Due to its toxic nature, CO storage is dangerous and CO processing plants have to be close to the gasification plant. The syngas should be purer in CO (more than a 98.5% on a molar basis) to be used for this application. The final use of these small organic compounds can be the synthesis of plastics, adhesives, preservatives or paints.
- Oxo-alcohols: They are higher alcohols used as plasticisers and in the manufacture of synthetic detergents. These are obtained by reacting syngas with olefins, producing aldehydes which are then hydrogenated to produce the oxo-alcohol. The important syngas variable is the H_2/CO ratio, that should be close to 1.

- *Hydrogen production.* Pure H_2 can be produced from syngas to be sold on the market. The syngas cleaning untis are followed by water reforming of CH_4 (in the case that the level of CH_4 is high) and by a WGS process, that transforms CO into CO_2 and H_2. Then, a CO_2 removal process separates CO_2 from the main stream. For the WGS reactor, high pressure is needed. The fraction of H_2 or the H_2/CO ratio should be enhanced during the syngas obtaining.
- *Synthetic natural gas (SNG).* This is a natural gas that can be produced by syngas from any carbon based feedstock. CH_4 synthesis takes place after gas cleaning units, and considers a methanation reaction which transforms CO and H_2 into CH_4 and water, generally using supported nickel catalysts (Watson, 1980). Typical operating temperatures are 300°C-400°C and it is preferably to fulfill the reaction at high pressure. After this step, there is a CO_2 removal unit to purify the CH_4 stream (Gassner & Maréchal, 2009b).
- *Liquid fuels.* These are also called synfuels or gas-to-liquid (GTL) fuels.
  - Fischer-Tropsch (FT) fuels: Syngas can be used to produce hydrocarbons of variable chain length, alternative to conventional diesel, kerosene and gasoline. Usually H_2/CO ratio should be about 2 (sometimes a WGS reactor is needed to obtain the desired proportion). The advantage when comparing with traditional fuels is that FT fuels do not contain or contain little contaminants such as sulphur or aromatics.
  - Methanol and Dimethyl Ether (DME): These are alternatives to gasoline and diesel. Methanol can react with triacylglycerols to produce biodiesel. It can be obtained by CO and/or CO_2 hydrogenation. DME is obtained from methanol in a dehydration step. H_2/CO and CO_2/CO molar ratios should be optimised for each step.
  - Other liquid fuels are obtained by syngas fermentation, thus biologically converted into organic acids, alcohols and polyesters. A biological process uses lower temperature and pressure than a catalysed process. Syngas

fermentation has several barriers to be commercially extended such as its difficulty to maintain anaerobic conditions or product inhibition.

The criteria to *select gas cleaning units* that better suit with the final syngas application are summed up:

- Gas purity and composition. For instance, H_2/CO ratio should be adapted to its final application requirement.
- Selectivity. This is the ability to remove one component while others remain in the main flowrate. For example, in a GT application, it is necessary to remove acid compounds such as H_2S or COS, but CO_2 is not of concern since it contributes to the GT power increasing the flowrate that activates the turbine.
- Economic issues such as investment and maintenance costs. As example, in an absorption unit there exists a trade-off between investment and solvent regeneration.

Reimert and Schaub (2003) propose the following criteria: (i) the needed separation factor is stated, giving a quick idea about the necessary process to separate a mixture. Differences between components in terms of volatility, solubility, molecular size and shape are assessed. (ii) The ordinary or extreme conditions needed, such as high or low temperature, high or low pressure are stated, and (iii) the value of the specific substance to separate and the final desired value are set. That proportionate a range of types and alternatives to be used. (iv) Finally, the know-how from specific experiences is the best reference when facing a specific problem.

Summing up, the most used and efficient option in a gasification plant establishes the pressure in the gasifier itself and maintain it until the syngas usage. High temperature can be used in a downstream heat exchanger integrated with the heat exchangers network (HEN) of the plant. In general, final syngas uses require from specific H_2/CO ratios. Acid and basic pollutants should be removed. Gas purity and composition, selectivity and economical issues are of concern when choosing a cleaning method.

Types of syngas purification and concentration units

Syngas purification mainly includes solids, tars, heavy metals, halogens, alkalines, acid and basic species removal processes. Some of them are released as by-products. In turn, CO_2 absorption process has concentration as purpose, with H_2 as the desired product.

Heterogeneous and homogeneous mixtures require from different cleaning methods. For heterogeneous mixtures, i.e. a solid-gas mixture, *mechanical separation methods* such as filtration or water scrubbing are applied to separate the different phases. Mechanical methods are used to separate mainly fly ash and dust from the syngas stream. Cyclones are often used, but result ineffective for small size particles, in the order of sub-microns. Ceramic candles or sintered metal filters and wet scrubbers fit better for them. These last ones can operate close to 800°C. For homogeneous mixtures, i.e. in this case only the gas phase, *diffusion based separation processes* are suitable. They convert a feed mixture into two or more products that differ in composition. The most widely processes used in syngas cleaning are absorption and adsorption.

Absorption methods are divided into physical and chemical processes depending on the type of bond connexion between the selected species with the solvent: simple physical absorption or stronger chemical bond with the solvent. Physical and chemical absorptions are typically used for syngas purification. The absorption process counts with a regeneration step where the solvent is cleaned from pollutants and recycled to be used again in the absorber. In general they are formed by two columns, one for absorption and the other for solvent recovery, and a set of a heat exchangers and pumps that transform the solvent back to the absorber conditions (Reimert & Schaub, 2003). The loading capacity of the solvents or absorbents depend exclusively on the gas species solubility (generally modelled using Henry's law), and the chemical reactivity of the gas species with the solution media which could require of electrolytes formation, that are the result of the chemical reactions of the absorbed gases with the solvent. Gas species solubility is mainly influenced by the operating pressure and the composition of the syngas. The amount of solvent in the solution is a decision variable, which mainly depends on the gas species to be removed. Well known physical solvents are for example methanol and dimethyl ethers of polyethylene glycol (DMPEG), which work using common processes called Rectisol and Selexol, respectively. Water-based chemical solvents are for instance the amines. The MDEA (methyldiethanol amine) is the most widely used one due to its high selectivity.

Adsorption systems are normally formed by a solid bed able to capture selected species. This is a surface phenomenon. The bed has to be either periodically changed or regenerated in situ. This adsorption-desorption process involves changes in temperature and pressure: low T and high P for adsorption, while the contrary conditions (i.e. high T and low P), for desorption. For example, the Pressure Swing Adsorption (PSA) cycle operates at a constant T, and at high P for the adsorption, and at low P for desorption. This PSA unit is used for H_2 concentration and purification.

According to Sharma *et al.* (2008), a gas cleaning process can be operated at three temperature regimes as a consequence of the syngas final application in a gasification plant. Cold, warm and hot cleaning are distinguished: less than 25°C, less than 300°C and more than 300°C, respectively. Comparatively, all the commercially available processes operate using cold and warm syngas. It means that for gasification plants, where the syngas is obtained at high temperature, commercial choices involve a loss of energy and exergy efficiencies. Hot gas cleaning can diminish operational costs when final syngas applications need high temperature, for instance, for H_2 production by steam reforming and WGS, or co-generation in a FC. The study by Pisa *et al.* (1997) is focused on IGCC power plants alternative designs by different desulphurisation processes. A hot desulphurisation process with ferrite ($ZnFe_2SO_4$) is evaluated. This bed needs oxygen to convert H_2S and steam to proportionate the optimal humidity for operation. The results show that the highest the steam consumption, the highest the penalisation in power terms. Therefore, the steam consumption finally reduces the global efficiency of the plant. Absorption processes require temperatures around 200°C, while adsorption processes require nearly ambient temperatures. Syngas cooling has several problems inherent to ashes presence, due to their slagging condition at certain temperature ranges.

Brown *et al.* (2009) point out that tars cause environmental and operation trouble, being condensable tars the main problem since they can damage units from the whole flowsheet. In Chapter 1 was mentioned that there are two possibilities for tars removal: primary and secondary methods. Catalytic conversion as secondary method is an example of process intensification, allowing for tars and solids removal. It has been proven that particulates recirculation to the gasifier contributes to tar control (Arena

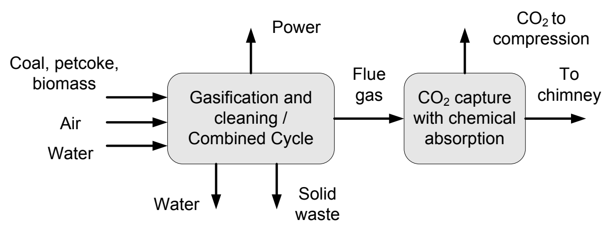

Figure 2.2: Post-combustion carbon capture configuration.

et al., 2010). For nitrogen, cyanide and halide species removal, a wet scrubbing process is well extended in cold and warm range of temperatures.

Due to the importance of CO_2 emissions in the context of energy production, the next section describes carbon capture as one feasible choice to be included in syngas cleaning.

Carbon capture and storage

The partial pressure of the CO_2 in the gas mixture represents the CO_2 concentration, and directly influences the CO_2 removal efficiency. It is easier to separate it as the partial pressure increases. In large gasification power plants, the difference between syngas CO_2 partial pressure before and after the GT is complex to assess. Higher partial pressures are found before the GT: even though CO_2 is generated during the combustion step, the flue gas is diluted with N_2 from the air. Moreover, the flue gas is expanded due to the inherent turbine expansion. Therefore, pre and post-combustion carbon capture techniques are inherently different. Other CO_2 capture method is based on oxy-combustion, metal oxidation and its capture using membranes. This last one is not described here, since it is not used in gasification plants (Metz *et al.*, 2005).

Chemical solvent processes are used for CO_2 partial pressures below 15 bar. Physical solvent processes are applicable to gas streams which have higher CO_2 partial pressure and/or a high total pressure. *Post-combustion* techniques are mainly based on chemical absorption, in which amines play an important role. The outlet CO_2 stream is thereafter treated, compressed and liquefied to be prepared for transportation to its final disposal. As shown in Figure 2.2, after the GT combustion, thus, after syngas production and use, the flue gas is processed.

Pre-combustion, as Figure 2.3 depicts, requires of a WGS reactor. The CO_2 produced is captured and then CO_2 and H_2 are separated. The relatively pure H_2 can be sent to the CC to produce power. Analogously to the post-combustion scenario, CO_2 is sent to a compression system to be liquefied before its transportation. A purer H_2 stream can be obtained through a PSA to be sold on the market. This pre-combustion technique counts with a physical solvent that absorbs acid compounds. Huang *et al.* (2008) have evaluated the same absorption process for both, CO_2 and H_2S abatement by means of process intensification. It is seen that sulphur penalises the WGS reactor performance.

For oxygen blown gasifiers at high operating pressures and relatively high CO_2 concentrations, the predominant choice is a physical solvent absorption system: according to Metz *et al.* (2005), the most extended technology to capture CO_2 before the GT combustion is the Selexol process. It uses dimethyl ether of polyethylene glycol

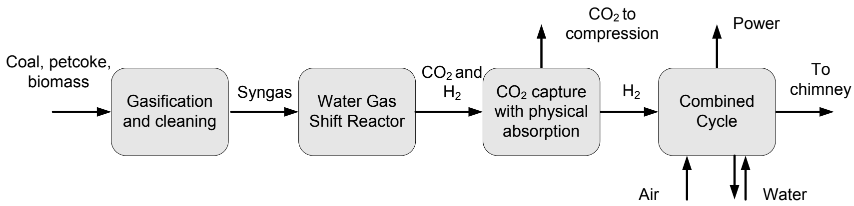

Figure 2.3: Pre-combustion carbon capture configuration.

(dimethyl ether of PEG) as solvent, achieving a CO_2 capture efficiency of more than 90%. The optimum pressure for H_2 purification is in the range of 15-30 bar. The H_2 concentration in the outlet stream of a modern PSA unit usually lies between 80% and 92% on a volume basis. There exists a gap between the extended knowledge of the mentioned processes and their integrated use in gasification or even in combustion plants.

Several works can be found in the field of carbon capture and storage (CCS) applied to power plants. Desideri and Paolucci (1999) is one of the first works developed in carbon capture topic concerning modelling. The authors reproduce, in Aspen Plus, a carbon capture technology in post-combustion configuration for conventional power plants. Their approach contemplates an exhaustive description of the system, model validation with literature data, whole plant performance evaluation and cost analysis. The developed approach allows for optimisation when changing input conditions. It is concluded that the 90% of CO_2 emissions can be reduced using this methodology, but capital costs are significant and penalise the final cost of energy (COE). The work by Hamelinck and Faaij (2002) is based on biomass gasification for methanol, hydrogen and electricity productions. This last is performed taking advantage of the remaining gases after methanol or hydrogen production units. Those products have a relatively low LHV if compared with fossil fuels, but they offer the possibility of being self-sustained in electricity consumption through the proposed configuration. The considered process involves pre-treatment, gasification, gas cleaning, reforming of higher hydrocarbons, a shift step to obtain a proper H_2/CO ratio and the final gas separation for H_2 production or methanol synthesis and purification. The software used is again Aspen Plus. The main purpose of the work is to identify biomass to methanol and H_2 conversion key points that may drive to higher efficiencies at lower costs. The study by Kanniche and Bouallou (2007) takes into account an IGCC power plant with CCS technology in pre-combustion configuration, fuelled by coal. An evaluation of scenarios considering different physical and chemical solvents, contrasting them by means of technical and economical parameters, is performed. Aspen Plus is again the chosen simulation tool. They aim at being as much conservative as possible, then avoiding big modifications to an already existing IGCC power plant. Consequently, the existing operating conditions without CCS technology are conserved as much as possible. The work carried out demonstrates that physical processes, Selexol and Rectisol, and activated amines have lower thermal consumption (mainly in the desorption column) than other commercial options. Capturing CO_2 leads to a 24% of efficiency reduction, thus penalising the power produced. Therefore, CCS units should be included carefully integrated in the already existing power plant.

The article by Descamps *et al.* (2008) describes a Rectisol process, with methanol as solvent, for CO_2 abatement in pre-combustion configuration for an IGCC power plant. Before the absorption process, a CO_2 production step is needed. In this case, the process counts with three WGS reactors to obtain a high CO conversion rate. The steam consumed is integrated in the CC steam network. The performed sensitivity analyses demonstrate that CO conversion depends on the amount of used water, concretely a H_2O/CO ratio of 1 in the first reactor optimises the conversion. The final conversion achieved is around 92% on a molar basis. The CO_2 absorption rate can vary between 77% and 98% on a molar basis. Higher rates imply a slight increase of GT power production and a slight decrease of ST power production. The work by Chen and Rubin (2009) develops an integrated platform to evaluate CCS costs and performance for IGCC power plants. Their base case counts with a Selexol system for CO_2 separation. All the rest of units that constitute the plant are based on commercial components. The WGS step has two stages (one for syngas steam consumption and the other one for external steam supply), and the Selexol unit includes two stages, one for sulphur and another one for carbon removal. It is observed that a redesign of the heat integration system of the plant is needed. A probabilistic uncertainty analysis is performed and shows that most of the uncertainty in costs estimation comes from the plant itself rather than from the carbon capture system. Design optimisation is studied by Biagini *et al.* (2010) for different biomass conversion processes to produce H_2: gasification and combustion, with pre and post-combustion configurations, at small scale. Sensitivity analyses are performed taken into account the amount of air and steam added to the gasifier and the moisture content (MC) of the biomass, which are the key variables.

Research in the field of CCS is mainly in a pre-design stage. As a consequence, few real experiences can be found, mainly due to the associated energy consumption. Therefore, it is deduced that the implementation of a carbon capture process should principally obey to environmental issues.

Summing up, syngas cleaning units are associated to well known processes. Nevertheless, new trends are observed in the field of processes intensification and hot gas cleaning, to allow a better profitability of the resources and of the high temperatures of the gas, respectively.

Superstructure approach

A *superstructure* for gasification processes is the workspace that facilitates the allocation of individual unit operations and their connectivity, thus representing the process operation. In Biegler *et al.* (1997) it is defined as the ensemble of all feasible flowsheets, combinations of equipment, raw materials and products. See Chapters 3 and 6 for further details about the superstructure as a methodology and this thesis specific superstructure, respectively.

In this thesis work, a superstructure has been created for IGCC power plants performance evaluation and optimisation, which can be applied to other gasification plant configurations. To set out the current available options representing real power plants, Table 2.3 provides with a summary of all the existing IGCC power plants at commercial scale. Gasification for electricity production in a CC is a process suggested approximately at the mid-term of the last century. That is the reason why only a limited number of plants are installed. All of them are considered as demonstration plants, defining the current lines for future generation of fully commercial IGCC power plants. R&D in the IGCC power plants field aims at improving the environmental

Table 2.3: Worldwide IGCC power plants (Council, 2008; Coca, 2003; Stahl & Neergaard, 1998).

Owner	Location	Start	Net output (MW_e)	Feed
Cool Water	USA	1984	120	Coal
Nuon	Buggenum, Netherlands	1994	250	Coal+Biomass
Wabash	Terre Haute, Indiana, USA	1995	260	Coal+Petcoke
Tampa Electric	Polk County, Florida, USA	1996	250	Coal+Petcoke
SUV	Vresova, Czech Republic	1996	350	Lignite
Schwarze Pumpe	Lausitz, Germany	1996	40	Lignite+Wastes
Texaco	El Dorado, Kansas, USA	1996	40	Petcoke
Sydkraft AB	Värnamo, Sweden	1996	6	Wood
Pernis Refinery	Rotterdam, Netherlands	1997	127	Visbreaker+Tar
Elcogas	Puertollano, Spain	1997	285	Coal+Petcoke
ISAB Energy	Sicily, Italy	1999	520	Asphalt
Motiva	Delaware, USA	2000	240	Petcoke
Exxon Mobil	Singapore	2000	180	Crude oil
Sarlux	Sardinia, Italy	2001	545	Visbreaker+Tar
Chawan IGCC	Jurong Island, Singapore	2001	160	Tar
API Energia	Falconara, Italy	2002	280	Visbreaker+Tar
Fife Energy	Scotland	2003	109	Coal+Wastes
Valero	Delaware, USA	2003	160	Petcoke
NPRC	Sekiyu, Japan	2003	342	Petroleum residues
Clean Coal Power	Nakoso, Japan	2006	250	Coal
CITGO	LA, USA	2006	570	Petcoke
IOC	Orissa, India	2006	180	Petcoke
Sulcis	Sardinia, Italy	2006	450	Coal
Eni Sannazzaro	Sannazzaro, Italy	2006	250	Oil Residues
Piñon Pine	Nevada, USA	-	100	Coal
Global Energy	Kentucky, USA	-	500	Coal+Wastes

performance, decrease marginal costs and investment and assure the technology availability/reliability (Council, 2008; Coca, 2003; Stahl & Neergaard, 1998). IGCC power plants are a current opportunity in the energy sector, as a lot of new projects envisaged around the world demonstrate, mainly based on coal and located, in order of starting projects, in USA, Canada, China, and Europe. New IGCC power plants with CO_2 capture technologies have been a reference for the conception of this thesis superstructure. The report by Metz *et al.* (2005) shows that research is done in this direction by Shell, Texaco and E-gas, demonstrating real and practical interest on IGCC-CCS. The most used technology is the Selexol capture system in pre-combustion configuration.

Looking at the construction of a gasification plant as an investment project, which has to be environmentally-friendly, it is necessary to know all the trade-offs and to find the optimal solution to be converted in a real project. Even if the gasification technology has been already extensively used, and all cleaning units have been widely applied too, the optimal combination of them is still a design challenge. Several works have already tried to measure the global performance of large scale gasification plants in a pre-design framework.

For instance, the work by Hamelinck and Faaij (2002) evaluates technical and economic parameters of gasification plants to produce methanol and hydrogen, taking into account future prospects. Even if they have not developed a superstructure understood as in this thesis work, they also use an Aspen Plus simulation to obtain energy and mass balances of interest for the economical evaluation of the proposed configurations. When large scale production is of concern, biomass supply is an important item influencing operation and maintenance costs, mainly when long distances should be covered. Hydrogen and methanol should be considered as conventional fuels alternatives; nevertheless the main bottleneck lies on the distribution infrastructure, mainly for hydrogen delivery. The work by Chiesa *et al.* (2005) considers the production of hydrogen and electricity from coal. Different scenarios, considering CO_2 venting or CO_2 capture, electricity production with conventional gas turbines or with turbines for burning specifically syngas or pure H_2, are evaluated. Process intensification for acid species is also included by removing CO_2 and sulphur acid species by the same unit operation. Different analyses are proposed considering performance and emissions through simulation of real commercial units. The economic analysis performed by Kreutz *et al.* (2005), shows that one of the barriers found for a wide H_2 economy is the lack of a cost effective method of storage and the lack of a large interested market on it. The CO_2 storage capacity and CO_2 transportation have to be addressed in an efficient way to promote such a solution.

CCS in different plant types is tackled by Rubin *et al.* (2007). Natural gas combined cycle plant (NGCC), IGCC plant and PC plant are considered. It takes into account different possibilities for final transportation and storage of CO_2: geologic, saline storage and enhanced oil recovery (EOR). They found, while comparing coal gasification and combustion with CCS, that costs are very sensitive to coal quality. Depending on it, PC plants or IGCC plants can be the cheapest options among the three possibilities considered, being IGCC plants the most penalised by the extra energy consumption from the CCS system. Chen and Rubin (2009) consider uncertainty in the cost of CCS in an IGCC power plant by taking into account coal quality and CCS removal efficiency.

2.2.3 Supply chain modelling

Producing energy from biomass conveys different steps: fuel supply, energy conversion, energy use and residue disposal or recycling (van Loo & Koppejan, 2008). The interest on biomass based SC, or bio-based SC (BSC) for different final purposes, ranging from energy to fuels production, has increased since the 90's as a consequence of the current energy paradigm. As has been introduced in previous sections, a BSC problem has special features that distinghish it from a conventional SC problem: the use of multiple biomass sources that can be from different locations, and the subsequent necessary pre-treatment to get it homogeneous in terms of mass and energy. These features imply the combination of different MC's, LHV's and BD's, that result on a "new" product, different from the original one(s). Biomass high MC, low BD, low LHV and fibrous nature, lead to a necessary biomass improvement in order to optimise its transport, handling and processing. These are the main reasons why a BSC should deal with changes on raw material properties. It should be noted that the biomass market is still an emergent market.

Several recent works can be cited in the framework of biomass as a feedstock. Gold and Seuring (2011) review supply chain management (SCM) and transportation matters, by taking into account the economic, ecological and social sustainability of the chain. The BSC echelons considered are four: (i) harvesting and collection, (ii) storage, (iii) transport and (iv) pre-treatment. The echelons contemplated by van Loo and Koppejan (2008) additionally include the growing biomass step, previous to harvest. Biomass as raw material in energy processes should comply with quality controls and

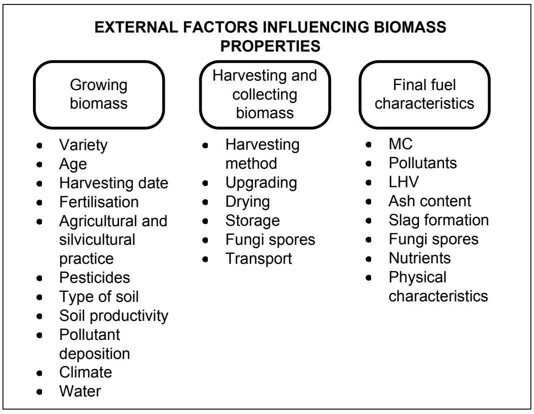

Figure 2.4: Factors that influence biomass characteristics depending on the echelon in the BSC. Based on van Loo and Koppejan (2008).

follow the stipulated standards to be optimally commercialised. Currently, regulations and standards, are still under development. As van Loo and Koppejan (2008) points out, the BSC steps are quality-influenced by several factors. It means that biomass changes its characteristics not only by the echelon purpose itself, for instance, due to an energy densification, or due to a shape homogenisation, but also by other external factors that modifies the biomass properties. See in Figure 2.4 a list of the most relevant external factors. The outline of a BSC to produce electricity is depicted in Figure 2.5.

Therefore, a BSC has five major steps before the final treatment. The sequence of pre-treatment, storage and transport in Figure 2.5 may change depending on the biomass type, the specific case study conditions and the supply strategy chosen. Nevertheless, it is more convenient to store and transport biomass in an upgraded state to avoid costs and non-desired effects, such as MC gaining. (i) *Biomass growing, harvesting and collecting* are involved in a biomass production category. This step aims at recovering biomass waste or at using energy crops. Usual processes at this stage are drying, i.e. natural drying in the land field, and baling or chipping, to diminish the volume and reduce the risk of deterioration. The study by Van Belle *et al.* (2003) presents a qualitative and quantitative study of this first BSC step, considering chipping, central storage of wood residues and intra-land transport. The harvesting or collection period depends on the *seasonality* of the resource, thus the amount of fuel can be discontinuous during the year. Moreover, different biomass sources can be mixed in a central gathering point, allowing for seasonality impact mitigation. The paper by Rentizelas *et al.* (2009b) exemplifies a BSC with multiple sources and multiple final products production, i.e. electricity, heat and cooling. The approach is applied for a specific region of Greece. The results provide with optimal locations and investment details for potential investors.

(ii) *Biomass pre-treatment* includes all the necessary steps to produce an upgraded fuel. The main objective is the reduction of costs for treatment, storage, transportation and handling activities, through an homogeneous fuel without impurities and denser in terms of matter and energy. Pre-treatment techniques can be briquetting, pelletisation, torrefaction and pyrolysis, being the last two still under development. The work by Uslu *et al.* (2008) states that only upgraded biomass can be used for international

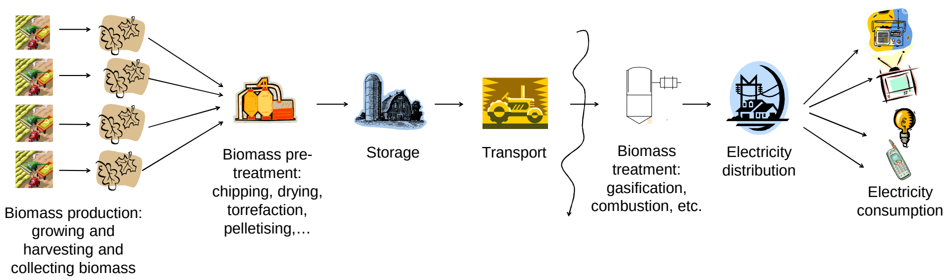

Figure 2.5: A BSC to produce and distribute electricity. Based on Gold and Seuring (2011).

trade. Torrefaction, pelletisation, TOP process and pyrolysis are evaluated in terms of mass yield, energy yield and process efficiency. Economies of scale are also analysed. In the line of biomass pre-treatments, Panichelli and Gnansounou (2008) contemplate forest wood residues from final cuttings to produce torrified wood that supplies a gasification unit to provide electricity. They allocate biomass quantities between predefined combinations of candidate sites to find the best set of locations for the energy units, in terms of costs minimisation. Magalhaes *et al.* (2009) are focused on biomass pre-treatment options, i.e. torrefaction and fast pyrolysis, evaluating prices, forest yield, transportation distances, investment and operating costs. The analysed case study is situated in The Netherlands, with importation of biomass. The best option found is TOP process. In turn, the pyrolysis as a pre-treatment is the cheapest option, while torrefaction has the lowest operational costs. The paper by Wu *et al.* (2010) evaluates the SC of bioslurry, which is a mixture formed by bio-oil and biochar, taking into account the trade-off between the chain cost increment due to the distributed pyrolysis units investment, and the chain cost reduction due to the diminution on transportation costs. It is demonstrated that the BSC, in order to be feasible with bioslurry, should count with central treatment plants larger than a certain capacity. That is the reason why co-firing bioslurry with fossil fuels is a reliable alternative.

(iii) *Storage* can be considered throughout the BSC. This is crucial when there is a time gap between production and consumption, thus when there exists a certain biomass seasonality. This stage is often used taking advantage of the drying phenomenon that takes place here, even if some dry matter loss occurs (Rentizelas *et al.*, 2009d). See in Figure 2.4 that storage is one of the factors that influences biomass properties. *Handling systems* are needed to transport the biomass from the point of delivery or storage to the next step. These techniques are for instance wheel loaders, cranes, belt conveyors, chain conveyors, screw conveyors, hydraulic piston feeders and bucket elevators (van Loo & Koppejan, 2008). Storage costs depend on its location and the type of storage, i.e. open air, roof covered, air fan, indoor storage; that in turn depends on the climate, shape and volume of biomass and time of storage (Gold & Seuring, 2011). The work by Rentizelas *et al.* (2009d) emphasizes the multi-biomass seasonal availability combined with the biomass storage problem, being the most exhaustive contribution on storage effects among the literature consulted. The stages considered before the conversion plant include harvesting and collection, handling in field and transportation, storage, loading and unloading, transport, and biomass pre-treatment. This last stage can be included in any of the abovementioned stages, and it can optimally precede the transportation stage. Storage can be equally located at biomass origin, in an intermediate step or at the power station site.

(iv) *Transportation* of biomass represents a relevant cost issue due to the low energy density of the energy carrier. Costs depend on travel-time, which is a function of distance, speed, tortuosity, hauliers capacity and amount to be transported. Moreover, operating costs such as driver remuneration or fuel costs, as well as social and environmental impacts should be evaluated (Gold & Seuring, 2011). The work by Forsberg (2000) sets out the transportation problem in terms of environmental viability and ecological sustainability, by trailer, truck, train, ship or pipeline, depending on the distance and the state of the feedstock. In the transportation echelon, optimisation passes through an appropriate match between the amount of disposable biomass near the plant and the plant size. The paper by Yu *et al.* (2009) evaluates a mallee residues SC focused on the transportation costs. It uses a discrete mathematical model for mallee production, harvest, on-farm transportation and road haulage modelling. Their case study reveals that on farm transportation for central biomass gathering during the first stage of the BSC, can be more expensive than biomass road transportation. The reason is the strong influence of feedstock collection area in costs. In turn, the studies by Pootakham and Kumar (2010a) and Pootakham and Kumar (2010b) compare transportation of bio-oil by pipeline and by truck through a life cycle assessment (LCA). The two works provide with specific energy consumptions, emissions and costs of each one of the alternatives. It is seen that the transportation media election depends on the distance to be displaced and the source of energy that is used to pump the bio-oil or to run the trucks.

(v) The final BSC echelon contemplates *biomass treatment* in the processing plant to produce electricity, as the alternative derived from Figure 2.5.

Several other works can be cited in the framework of the whole SC performance. Forsberg (2000) contemplates international biomass trade between countries that have more biomass residues available than the value they can use for their own benefit and countries that need them. This work, in terms of environmental issues, evaluates carbon, nitrogen and sulphur cycles: the effects of removing waste biomass from natural systems is evaluated in terms of removed nutrients from the soil. It is seen that ashes recycling after biomass processing can help to maintain a long term level of soil productivity, since the big majority of nutrients are found in the ash fraction of biomass. In the same field, the work by Hamelinck *et al.* (2005) considers an international BSC that takes into account biomass production and consumption in different regions, i.e. as energy import regions Western Europe and as production areas Scandinavia, Eastern Europe and Latin America. Biomass transformed into briquettes or pellets must be used to save transportation costs. Nevertheless, there exists a trade-off between type of transport, distance and biomass densification method, since the cost of biomass pre-treatments as a whole should not be higher than the compensated logistic costs. This is an important consideration to take into account when long distances should be covered. It is demonstrated that international bioenergy trade has a real potential; however, governments must stimulate the biomass market in terms of prices, policies and social acceptance. In turn, the study by Cherubini and Stromman (2011) is a review of all the papers performed in the field of LCA of bioenergy systems. The big majority of the studies found a reduction in GHG emissions and in fossil fuel energy consumption. Nevertheless, it is difficult to compare the different papers results since the elected functional units are not the same.

A mixed integer linear program (MILP) that determines the optimal sizes and locations of biomass-based gasification-to-methanol plants, or biofuel plants, is developed by Leduc *et al.* (2008). The objective function considers operating costs and the investment required to establish the BSC. The raw material is poplar coppice, which is an energy crop, and the demand is based on gasoline-methanol consumption for car usage. The possible consumer sites are the already existing gas stations in Austria. The evaluation of three scenarios, differing in methanol-gasoline blends, is performed. By-production of heat is also considered as a net economic revenue, and CO_2 emissions are accounted finally, but not introduced into the model as an environmental objective or as an environmental constraint. Ayoub *et al.* (2009) present a methodology for designing and evaluating biomass networks, aiming at producing different bio-products, from one or more biomass resources. The purpose of the methodology is to provide with a framework to create a superstructure that connects biomass resources to products, via current and possible future available processes; which can be used to develop an optimisation model. Their methodology is applied at a local level and proposes better biomass uses by means of costs and environmental impacts accounting. The environmental indicator used accounts for air emissions, water pollutants and solid wastes. More recently, Van Dyken *et al.* (2010) develop a linear optimisation model to plan capacity expansions in energy systems, where several alternatives for biomass and technologies are considered simultaneously. The main objective of the work is to present a generic model that includes different echelons such as sources, handling, processing, storage and final usage. LHV, MC and BD are the key biomass parameteres that change along the SC. The objectives to be optimised are operating costs and emissions of the whole SC.

There exists a wide range of objectives that authors/decision-makers want to optimise. They can be classified into economic, environmental and social concerns. Thus, the SC, should be sustainable in economic, ecological and social terms. For instance, Caputo *et al.* (2005) take into account the net present value (NPV) to evaluate 100% biomass gasification and combustion plants. It is concluded that transport constraints, in economic terms, turn into less restrictive constraints while the size of the plant increases, being scale effects important for economic and logistic performances. Damen and Faaij (2006) perform a life cycle inventory (LCI) of a BSC for co-firing compared to a 100% coal power plant; net avoided primary energy and GHG emissions are significantly reduced. In turn, Perry and Rosillo-Calle (2008) are focused on CO_2 emissions along the whole SC, from production, conversion, transportation and land use displacement caused by the modification of the biomass use, as well as the manufacture of the substitute product. In terms of transportation, shipping has lesser emissions than any other way of transport, thus reducing the negative effect of biomass long distances displacement. Iakovou *et al.* (2010) describe BSC specific strategic, tactical and operational decisions that should be overcome. These are summed up in Figure 2.6. Only few papers tackle with BSC sustainable design in economic and environmental terms at the same time and in a systematic way. Again, storage and transport are revealed as key activities that need from optimisation.

This literature review shows that the BSC should be taken into account when considering the implementation of a biomass processing plant, or when considering the utilisation of biomass in an already existing plant as a part of the feedstock mix. Seasonality and heterogeneity, in terms of properties and sources, should be

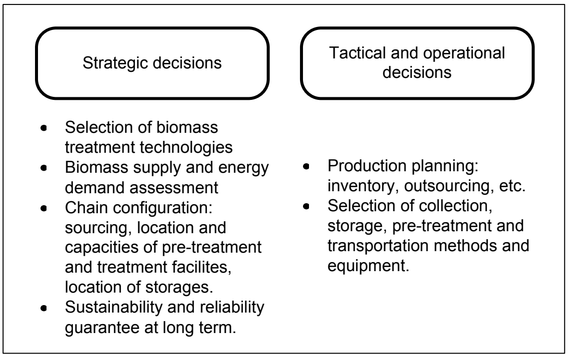

Figure 2.6: Decision making strategy for BSC. Based on Iakovou *et al.* (2010).

overcome for each specific type of raw material. Logistic costs and environmental concerns should be assessed carefully. As a renewable fund, the use of conventional resources to provide energy along the BSC should be minimised. Overall, traditional techniques of mathematical programming for SC modelling have a new challenge in terms of biomass properties simulation along the chain.

2.3 Distributed energy systems

Gasification at small scale uses fixed beds or fluidised bed gasifiers. Small scale systems are employed to meet with the requirements of DES using locally available biomass at or near the point of use. The main characteristics of a DES are source sustainability and no need of grid support, high efficiency, demand accomplishment, consumer's implication and fossil fuels independence. There is not a unique choice for biomass systems, but a tailor-made solution for specific case studies comprising different ranges of scale and different technological choices, depending on the available biomass. Rural areas and rural areas from developing countries in particular, require from new approaches for optimisation, different from those that have been considered so far, as well as proven and reliable technology.

2.3.1 Identification of needs and scope

Rural electrification takes advantage from biomass residues which are nearby the treatment plant. All the echelons described for CES are analogous for DES. Nevertheless, transportation is not the bottleneck here. However, if considering surplus biomass trade, transportation becomes of higher importance. The objectives considered for optimisation in small scale gasification in rural areas, are somewhat different from those considered for a large scale plant optimisation.

The study by Silva and Nakata (2009) remarks that one of the main reasons why renewable energy technologies in modular configuration have not been highly extended in rural areas is the lack of an integrated approach in rural electrification planning. Integrated approaches should include economic, environmental and social criteria, according to each specific case study context. Silva and Nakata (2009) are focused on a specific case study situated in a remote area in Colombia. It evaluates two possible options for energy access: electrification by diesel or renewable sources. The paper uses goal programming to assess a qualitative response in terms of electricity generation cost (\$/kWh), employment generation (jobs/kWh), avoided emissions (kgCO_2/kWh) and land use (m^2/kWh per year) in terms of interference with land use for agriculture or habitat conservation caused by the plant and place of storage extensions. In a previous work, Silva and Nakata (2008) use linear programming (LP) to deal with the energy planning model. The considered case study is the same rural region from Colombia. The authors demonstrate that such rural electrification projects can be financially sustainable, if taken into account the appropriate data concerning reliable geographical location of sources and clients, income levels and energy demand. The mathematical problem deals with an objective function based on the minimisation of subsidised costs. The mix of possible biomass processing technologies considers electricity generation by diesel engines, biomass boilers, gasification-gas engines and fast-pyrolysis matched with diesel engines. As a result, the technology that minimises costs is the combustion of biomass. The adequate performances of gasification and pyrolysis are penalised by their prices. It suggests that the proliferation of advanced techniques will be derived from environmental policies that should motivate their specific implementation by more environmentally restricted systems. Kanase-Patil *et al.* (2010) uses LP formulation to assure a reliable integrated renewable energy system, by evaluating the COE, the costumer interruption costs, and the expected energy not supplied. The renewable mix of technologies takes into account biomass, solar, hydrological and wind resources. Then, four scenarios are considered to meet with the energy demand in domestic, agricultural, community and rural industry areas of an specific zone from India, based on combinations of the abovementioned sources. LINGO and HOMER softwares, which are specific tools for renewable energy mix determination, are used to verify the results of the developed model. The system that combines micro-hydrological power, biomass gasification, biogas production, wind and solar photovoltaic is the best one in terms of reliability and costs.

The work by Kanagawa and Nakata (2008) is also focused on India, and aims at finding quantitative relations between social and economic development by evaluating the literacy rate versus the electrification rate. The paper by Hiremath *et al.* (2009) takes into account a high number of state-of-the-art evaluating parameters used for decentralised energy planning. Goal programming is the chosen methodology to take advantage from its level of subjectivity. The selected objective functions are cost, system efficiency, petroleum products usage, locally available resources, employing generation, emissions (CO_2, NO_x and SO_x) and reliability on renewable energy systems, subjected to demand and supply constraints. The results show that, in the considered context, biomass-based systems have the potential to meet with rural needs, offering reliability, promoting local participation, local control and creation of skills. Cherni *et al.* (2007) and Brent and Kruger (2009) develop, describe and use a multi-criteria decision tool called SURE, that aims at choosing the appropriate energy mix of technologies to match with the energy demand of a rural area, reducing poverty at the same time. The tool combines quantitative and qualitative parameters, and allows for changes on the priorities according to the decision-maker criteria. The model analyses the strengths and weaknesses of a community according to five resources: physical, financial, natural, social and human. Then, it tries to find compromise solutions to supply the energy demand. Behind the software, a local survey has been drawn to state the baseline of a rural community in Colombia, to identify its energy needs and the growing tendency. In Brent and Kruger (2009), the Delphi research methodology is used with experienced individuals in the field of energy and poverty. SURE and the developed tool by the Intermediate Technology Development Group (ITDG) are integrated, and compared with the results from the experts panel. It is put into relevance that technology assessment methods should be further developed to formulate more appropriated implementation strategies. The paper by Ferrer-Martí *et al.* (2009) is an example of modular renewable energy source implementation, concretely wind, that uses MILP to assess the optimal location of wind generators and the appropriate micro-grid extension in a specific community from Perú, by minimising the initial investment.

Janssen *et al.* (2009) promotes the sustainable use of the African land to produce bioenergy, stating that the country has an important extension of marginal and degraded land that can be suitable for a socio-economic development based on biomass trade and use. The study assesses the suitable areas for bioenergy, excluding all regions used for food and with severe water, terrain or soil constraints. This land use needs from appropriated policies and development plans, dealing at the same time with rural development, sustainable production, community participation in the projects, modernisation of agricultural policies, creation of standards and fuel-food conflicts avoiding. Hamimu (2009) promotes biomass trade from biomass waste in Sub-Saharan countries. Biomass should be used not only for exportation, but also for own consumption, to assure independence from fossil fuels. This work reveals the land tenure issue in some countries from Africa, where they cannot be property of the farmers. Therefore, governments should avoid speculation with this matter and promote fair partnership between local farmers and foreign investors. Otto (2009) distinguishes between biofuels production for exportation and biofuels production for local use through advanced uses of biomass to promote the emergent business models in the sector, dealing with the connection among the two markets.

Summing up, LP and goal programming are well extended approaches for solutions selection in DES problems, but they do not take into account allocation. New trends such as biomass sharing between communities and bioenergy trade need from the allocation problem resolution. There is a lack of systematic energy models that promote biomass trade and use in developing or rural areas. Those new approaches should take into account a wide range of issues, i.e. economic, environmental and social.

2.3.2 Gasification at small scale

Gasification at small scale is in the range of less than 10 MW_{th} and less than 200 kW_e (see Section 1.1.1 for more details). Even if it is not a "new" process, research is still needed due to the low commercialisation level achieved by small gasifiers, thus involving a not extended know-how. Small scale gasification has been characterised by a discontinuous technology development, changeable government interests and a pioneering role from research and non-governmental organisations (NGO's). Concerning technical aspects, there has been a low deployment of research results but at the same time a progressive development exists guided by the demand, specially on producer gas quality. Investment costs are in general still high (Knoef, 2000).

The first experiences with gasification are from XVIII century in England and France, with coal gasification used to light the city. At the beginning of the XIX

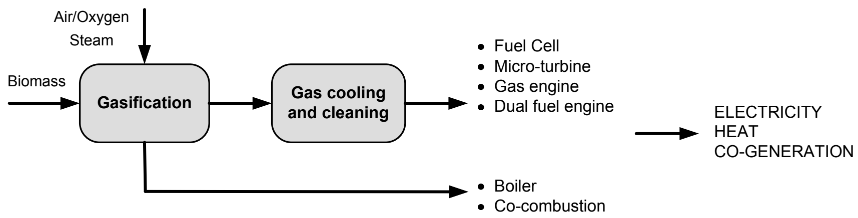

Figure 2.7: Most extended uses of producer gas from small scale gasification. Based on Bridgwater *et al.* (2002) and Karellas *et al.* (2008).

century, "gasworks" using mainly coal and coke were employed to produce gas for lighting and cooking in some American countries. Then, during the two World Wars, this technology was further used for fuel supply in transport vehicles. At this time, wood gasifiers were used as mobile sources of gas to power cars. Finally, cheap prices of fossil fuels determined the end of a high extended use of gasification (Reed & Das, 1988; Highman & van der Burght, 2003). During the nineties, small scale biomass gasification was again encouraged by the new restrictive environmental laws and the aiming to be independent from fossil fuels.

The producer gas generated in a gasifier can be used in the applications listed in Figure 2.7, ordered from the smallest to the largest scale in power terms. They offer the possibility to produce electricity, heat or co-generation of the both of them. The producer gas quality depends on its final application. The less restrictive is the boiler option, while FC's are the most special alternative. According to Lapuerta *et al.* (2008), gasification-gas engine presents more advantages than gasification-gas turbine, i.e. higher efficiency in terms of electricity generation and the possibility of integrating thermal applications.

The paper review by Dong *et al.* (2009) reveals co-generation at small scale as a major alternative to traditional systems for energy savings and environmental damage mitigation. Gasification combined with internal combustion engines (ICE's), micro-turbines, GT's and/or FC's are among the emerging possibilities; having higher efficiency than combustion-based co-generation options. Research is still needed to improve their efficiency. Moreover, fully automatic operated plants are needed at a minimum level of pollutants. The Indian perspective described on Buragohain *et al.* (2010) aims at supplying present and future thermal and electrical needs through decentralised generation, concretely through gasification at small scale, coupled with ICE's, boiler-steam turbines and in bigger scales with combined cycles. The load factor of the plant is revealed as a crucial decision parameter since rural demand is relatively low and changeable during the day.

The paper by Dornburg and Faaij (2001) presents the duality large-small scale biomass gasification and combustion as competing alternatives, regarding the trade-off between transportation cost, economies of scale and easiness for heat utilisation. From the studied gasification and combustion plants, with heat, power and combined heat and power options between 0.03-300 $MW_{th-input}$, the relative primary energy consumed improves with the scale. Gasification is better in energetic performances terms than combustion. It is not the case for economic parameters, in which combustion is better. Husain *et al.* (2003) have performed a case study in Malaysia that use palm oil mills residues to produce heat and power by means of boiler-turbines

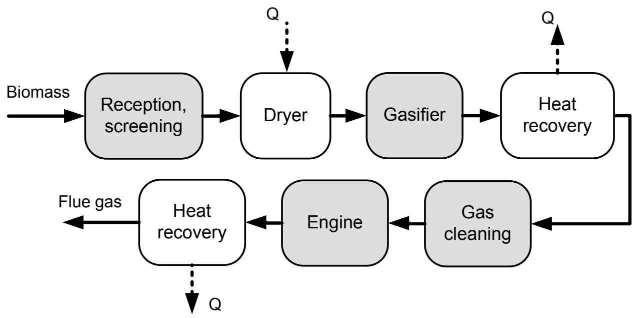

Figure 2.8: Potential producers and consumers of heat in a BG-GE system (in white). Based on Brammer and Bridgwater (2002).

installations. This is an example of local wastes used to generate inputs for the palm oil industry itself. The installations have low thermal efficiencies due to the heterogeneity of the residues; moreover, more advances technologies are advised.

Brammer and Bridgwater (2002) evaluate gasification with co-generation performance, with a gas engine in the range of 500-3000 kW_e connected to the electricity distribution grid and the district heating net. MC of biomass should be controlled. The drying level is evaluated in terms of energy needed and in terms of installation performance. The excess of heat from the process can be used for district heating and/or biomass drying. This is evaluated in terms of COE and overall efficiency, which takes into account the net electricity and the exported heat. The biomass gasifier combined with a gas engine (BG-GE) installation may improve its global efficiency from 20% to 80% with heat recovery options.

Dual diesel engines can be operated with producer gas and with bio-oil from fast pyrolysis. The scenario studied by Bridgwater *et al.* (2002) considers a centralised fast pyrolysis installation to supply specific located diesel engines. This is somehow competing with BG-GE systems. Fast pyrolysis is regarded as a biomass pre-treatment option or as a treatment itself. As Demirbas (2009) points out, biorenewable liquids are the main fossil fuels substitutive in ICE's. Nevertheless, the study by Brammer and Bridgwater (2002) found that at the considered conditions for European countries, bio-oil application to produce heat is the most economically competitive alternative, followed by co-generation. In contrast, only electricity production emerges as an uncompetitive option.

The most important barrier towards the commercial stage of small scale biomass gasifiers are still the high investment cost and the already small amount of experts in the field. The increase in process efficiency by means of co-generation does not seem enough to reach the combustion technology status. Even if it is not a fully commercial choice, a wide range of gasification successful and failed case studies to produce power and/or heat exists, as described in the next section.

Case studies

All case studies found in the bibliography are installed in Africa, Asia and Latin America. As already mentioned in Chapter 1, even if it is a technology traditionally used in developing countries, the potential is not restricted to those areas. The study by Stassen (1995) is an exhaustive review of small scale biomass gasification for power or heat. It provides with homogeneous data about installed gasifiers performance, economics, safety and public acceptability, while detailing ranges of application, implementation conditions and environmental damages. The monitored plants are 15 commercial gasifiers, 12 of them for electricity production for community, industrial or irrigation uses, and the rest for heating in industrial applications. They range between 15 kW_e to 160 kW_e, and 600 kW_{th} to 4060 kW_{th}, respectively. Malfunction reasons are incompatibility between the gasifier operating conditions and the raw material characteristics, equipment performance different from what the manufacturer specified and the lack of expertise. Moreover, low demand in developing areas causes small load factors and de-rating phenomena in the gas engine. Behind these reasons there is a market for small scale gasifiers that has never been large enough to develop a feasible technology. Other causes concern economics: subsidies to cover the investment, people not paying for the services and current low prices of fossil fuels. Stassen (1995) reveals that biomass gasification is a feasible and sustainable alternative to fossil fuels if biomass supply is constant, there exists a market for technology and consumables, as well as people capable to work on the project. In turn, Han *et al.* (2008) define five types of failings: institutional, political, technical, financial and social, involving failures on strategy, commercial activities and public support.

More recent case studies are compiled and discussed in Blunck and Dimpl (2010). Fifteen years after the work by Stassen (1995), this report discloses that among the current worldwide providers, it does not exist a reliable technology readily available. Moreover, the health threat due to carcinogenic wastes is still there. Only autonomous units for heat production in industrial applications have proliferated. Not only Africa, Asia and Latin America are implementing this technology, but also Scandinavian countries are becoming users of biomass gasification mainly for heating purposes. In turn, modular gasification power plants should be adapted to local conditions. At this moment, those projects are profitable only by means of government subsidies. The conclusion drawn from the German situation is that due to the low efficiency, a 20% if power production is of concern using an ICE, the only way to be sustainable is through co-generation. The conclusion by Blunck and Dimpl (2010) is clear: at the moment, small scale biomass gasification is not an appropriate technology for decentralised power production in remote areas. Therefore, the situation has not changed too much in fifteen years.

In spite of all the drawbacks or challenges that this technology has to overcome, the literature shows succesful case studies that reports the benefits of modular gasification in real case studies. Thus, they demonstrate that this is an option for rural electrification that has been used and still remains in the range of possibilities. The study by Senelwa and Sims (1999) evaluates the renewable potential in Kenya, with biomass as the main alternative due to the big amount of biomass waste they have. The population consumes biomass by traditional ways. Hence, more advanced techniques to profit it are needed. The interest is on biomass gasification by, in spite of importing the technology and the know-how, promoting local manufacturing and encouraging reliability through local pilot projects. A project developed in Cambodia (Abe *et al.*, 2007) reveals the importance of the matching between technology and electricity demand along with the capacity to pay. Gasification remains the alternative to biomass combustion. The latter is recommended for electricity demands higher than 1 MW_e, which is far from the real need of rural population. Rice husks, cashew nut shells, bagasse, peanut shells, old rubber trees and natural forest residues are the studied energy sources. In addition to the this volume of residues, the potential of abandoned lands to be harvested with crops dedicated to electricity production for international trade is also evaluated. Comparing BG-GE with diesel installations, it is seen that even if the gasification installation is more expensive in investment terms, operational costs compensate the initial effort. China is a large agricultural country. The paper by Zeng *et al.* (2007) describes that the country abuses of combustion for biomass waste destruction and energy generation. Straw is the main source and the alternatives go beyond gasification and production of briquettes for further commercialisation. So that they are looking for solutions in a context characterised by a quick population grow and non-exploited biomass waste. As a difference from the previous works, this study proposes the biomass gasification usage for centralised projects, due to the huge amount of biomass. Pakistan is an example of a country that has realised the potential of its own biomass waste generation, mainly bagasse, and is looking for alternatives. They need the know-how to take advantage of its potential and disseminate it, and a well management plan for research and development, which are lacking now (Mirza *et al.*, 2008). The case from Melani village in South Africa (Mamphweli & Meyer, 2009) reports a successful gasification power plant of around 120 kW_e that utilises pine wood waste and saw mill as raw materials. The plant has replaced a combustion installation, and has generated benefits such as job creation and electricity guarantee. The implementation of this plant follows a detailed business plan. The study by Chauhan (2010) is focused on biomass resources from India. The big amount of surplus biomass, mainly husk and stalk, has lead to an important biomass commerce through both, formal and informal channels. Briquetting is gaining force in biomass commercialisation and the industrial interest is posed on biomass usage for co-generation.

Overall, the observed trends in those case studies reflect that biomass as a commodity in the energy sector has a huge potential. It is specially true for countries where biomass wastes are not exploited or are unefficiently profited and land is misused. Gasification, despite of the reported difficulties, is a current choice for biomass profit that produces a versatile gas that can be applied in a wide range of efficient alternatives. Heating purposes have been revealed as the most extended practice in small scale. Gasification projects needs from detailed business plans, far from purely cooperation projects.

Advanced options

The last biomass gasification systems contemplate the use of the producer gas in a FC. Most work found in this subject concerns modelling rather than experimental installations, since it is far from a commercial status. At the moment, those installations require from high investments. Depending on the type of FC to be used, the optimal inlet conditions of the producer gas, are different in terms of H_2/CO ratio, CO_2 and temperature.

The study by McIlveen-Wright *et al.* (2000) reports that the use of FC's can cover a range from 20 to 500 kW_e. If compared to BG-GE installations, BG-FC plants increase the electrical efficiency from 13%-17% to 25%-28%. In an analogous way as in a large scale gasification plant, methane reformers, shift reactors and PSA adsorbers are needed to produce H_2. The author contemplates the use of MCFC and PAFC: the MCFC can tolerate CO_2, can use H_2 and CO as fuel, and has an operating temperature around 650°C that provides with low temperature waste heat for heating purposes. In contrast, the PAFC can tolerate acid compounds, requires from a shifter to convert CO into H_2 and operates at around 200°C. The best performances were demonstrated for BG, using wood, combined with MCFC's. BG-PAFC shows similar performances in terms of CO_2 emissions and electrical efficiency than BG-GE. In a second study by McIlveen-Wright and Guiney (2002), the co-generation option is evaluated for an isolated community: the integration comes from the usage of waste heat from the FC to pre-dry the wood as well as for heating water. At the same time, the producer gas from the gasifier preheats the used air in the FC. The simulation results show better performances than combustion and gasification but at higher prices. Moreover, FC's require from specialised people. The study by Jurado (2005) revises the application of a MCFC combined with a microturbine to combined heat and power. This configuration can reach 85% of overall efficiency at near zero emissions. Microturbines can be used in a range of 25-200 kW_e. The MCFC can reach an electricity efficiency of 60% (while that value for PAFCs is around 40%). The focus of the paper is on the control scheme of the hybrid system, by transient state modelling. Iaquaniello and Mangiapane (2006) integrates BG with a MCFC. In this case, the use of an allothermal gasifier, with dry cleaning gas and an operating pressure around 3-4 bar, are contemplated to optimise the producer gas H_2/CO ratio. A major investment item is allocated in the compression stages. In turn, the works by Karellas *et al.* (2008) and Sadhukhan *et al.* (2010) proves BG integration with SOFCs in isolated communities and buildings. In the former, and analogously to the work from Jurado (2005), the performance is studied in combination with a microturbine. This type of FC operates at high temperatures, around 900°C. The highly integrated systems BG-SOFC provide with net efficiencies of 45% when only electricity is considered, and of 85% if also heating purposes are taken into account. Sadhukhan *et al.* (2010) exposes the same range of efficiencies. In this case the working pressure is around 8 bar and the chosen gasifier contemplates allothermal gasification with a fluidised bed reactor. Integrations come from a GT with a SOFC, which in turn is integrated with a heat pump. From this work thermodynamic feasibility through heat integration should be established by means of conceptual modelling to demonstrate increasing efficiencies. The paper by Toonssen *et al.* (2009) is focused on decentralised electricity generation using biomass gasification through a fluidised bed combined with a PEM. This most advanced option proposes a central gasification plant that produces H_2 distributed by a grid, to feed PEMs for heat and power generation. The PEM operates at low temperatures, around 80°C. It makes them suitable for domestic application. The authors analyse the behaviour in terms of energy and exergy efficiencies.

Summing up, one of the emerging technologies in the field of small scale gasification contemplates the use of FC's. The gasifiers tend to be allothermal and to work at pressure. The results report high efficiencies through expensive plants that require highly specialised people. One of the main advantage-disadvantage is the high level of integration of those systems, which leads to a loss in flexibility.

2.3.3 Flowsheeting of single sites: pilot plant demonstration

To go forward in modular biomass gasification, operating conditions should be improved in terms of reliability and sustainability, feedstock flexibility and generated gas cleanliness. The research objectives are focused on biomass feeding and gasification,

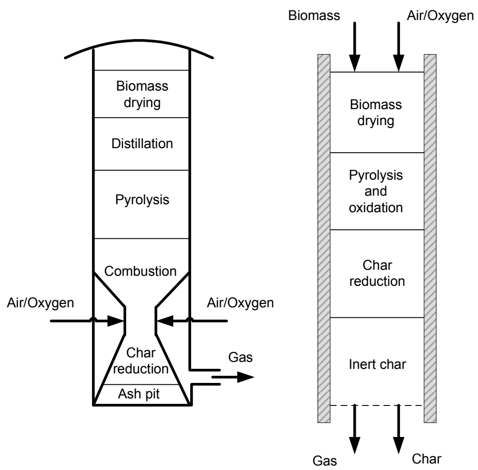

Figure 2.9: Imbert downdraft gasifier (left side) and stratified downdraft gasifier (righ side). Based on Reed and Das (1988).

producer gas cleaning and engine operation. The following papers put into relevance the type of technical work that is developed in BG-GE installations to overcome with operational problems from past experiences.

According to Reed and Das (1988), gasifier design improvement passes through a better understanding of basics, improved monitoring of the performance and a better adaptation of the biomass features. Reed and Das (1988) disclose that downdraft gasifiers are the most suitable reactors for small scale applications due to their relatively little amount of produced tars. The Imbert downdraft gasifier and the stratified downdraft gasifier are the two most extended designs. The latter is also called open-core, open-top or topless gasifier. See in Figure 2.9 a diagram that depicts and compares the main zones from both systems. Between them, the Imbert gasifier configuration is the most extended one. Its main characteristics concern the air entrance, though a set of radial nozzles, and the throated combustion zone, with a diameter difference between pyrolysis and gasification or reduction zones. Air can have a double entrance, entering also at the top of the reactor, going through the body of the gasifier to be finally released at the throat (Sharma, 2009). In contrast, the stratified downdraft biomass gasifier has a constant diameter throughout the reactor and the gasifying agent is introduced at the top of the gasifier. Due to the throat constriction, Imbert gasifiers are more feeding size restricted than stratified beds. The throat angle has as main purpose the cracking of tars facilitation (Hsi *et al.*, 2008).

The experimental work consulted, puts into relevance that there is no standard limit concerning the MC of the feedstock, even if the type of gasifier is the same. It ranges from a minimum value of 7% in Sheth and Babu (2009) to a maximum of 25% in Dogru *et al.* (2002). The *equivalence ratio* (ER) or the air-to-biomass ratio, is a working parameter defined differently depending on the source. For instance, in Reed and Das (1988) it is defined as the ratio between the oxygen or the air used, related to the amount of oxygen or air required for a complete combustion, both of them on a mass or mole basis. Using ER oxygen-based, gasification ranges between 0.25 and nearly 0.9. In Sheth and Babu (2009) it is defined in an analogous way but with the air flowrate in volume. Zainal *et al.* (2002) defines it as the ratio between the flowrate of air on volume basis and the flowrate of feed on a mass basis. MC and the amount of air/oxygen to the gasifier are the most important parameters that affect the producer gas quality; Zainal *et al.* (2002), Hsi *et al.* (2008) and Sheth and Babu (2009) reveal an optimal value for the ER that leads to a maximum LHV in the producer gas.

The most extended *feedstock* used in small scale gasification is chips of wood, followed by specific types of shells and bagasse. In Imbert gasifiers, different authors identify the relationship between the throat diameter and the biomass size, and between the throat volume with the performance of the reduction zone (Zainal *et al.*, 2002; Jayah *et al.*, 2003; Panwar *et al.*, 2009). The calorific value of the produced gas obtained in such pilot plants is between 4.2 MJ/m^3_N for acacia and bagasse (Sharma, 2009) and 6.3 MJ/m^3_N for wood from carpentry industry (Sheth & Babu, 2009). The papers by Zainal *et al.* (2002) and Hsi *et al.* (2008) treat uncertainty on their equipments for measure.

The system *pressure* is near atmospheric in all the cases. In fact, in the reported flowsheets by Dogru *et al.* (2002), Sharma (2009), Panwar *et al.* (2009) and Elrich and Fransson (2011), a blower embedded in the producer gas trajectory to the flare or to the engine is in charge of the producer gas movement.

The most common plant layout counts with a cyclone, a wet scrubber and several filters to clean the gas from tars and particulate matter. The gas after the gasifier, according to Dogru *et al.* (2002) and Sharma (2009) is about 300°C. In contrast, Hasler and Nussbaumer (1999) and Ramadhas *et al.* (2008) report a value of around 500°C. In Reed and Das (1988) this temperature is around 700°C. The temperatures profile of the gasifier, to better understand the gasification process, is usually measured and somehow controlled in the consulted bibliography. The syngas composition at different times and sample points along the turn and the flowsheet is also commonly studied through gas chromatography. The producer gas flowrate, as well as the fuel conversion rate, liquid condensates rate and ash production rate are also estimated. It is perceived that all the reactors operate in batch mode, therefore the reported flowrates usually correspond to the amount of fuel fed into the reactor divided by the total operation time during steady operation. Each experimental installation has its own method to start the gasification operation, for instance through igniters, or by means of charcoal produced in previous gasification operation combusted with diesel (Hsi *et al.*, 2008; Sheth & Babu, 2009).

In Zainal *et al.* (2002) the air flowrate enters the throat by means of a pipe that crosses the length of the gasifier. It is observed by temperature registration, that the combustion zone is affected by bridging. The final results for their pilot plant of 80 kW_{th} are 80% as CGE, 10-11% of efficiency of the global process matched with an ICE. The experimental study by Dogru *et al.* (2002) monitors too the pressure drops along the flowsheet for a pilot plant of 5 kW_e, which is crucial to assure the proper work of the purification units. Jayah *et al.* (2003), Pathak *et al.* (2008) and Panwar *et al.* (2009) consider the performance of the gasifiers only for thermal applications. In the first case it is used to produce hot air to dry tea, by means of rubberwood chips gasification. Operation and design parameters performance are studied. They demonstrate that air inlet temperature to the gasifier is not a key parameter on the gasifier operation. In contrast, the MC is of special concern if considering the heat losses in the gasifier. Moreover, it is seen that the length of the gasification zone is a critical design parameter. The paper by Panwar *et al.* (2009) replaces the operation of liquefy petroleum gas by wood gasification for food processing industry, presenting encouraging results. The challenges presented in Hsi *et al.* (2008) mention tar removal and an automated operation. The plant of concern has 8.2 kg/h of inlet biomass. It is seen that the air flowrate is the most important factor in the gasifier performance. Again, it is observed that air pre-heating has marginal effects on the overall plant running. The work by Sharma (2009) reports the results of a 75 kW_{th} plant. Here, the polluted water from spray towers is filtered and recycled. Cooling after the gasifier can be run by means of wet cleaning, or by means of a heat exchanger, when dry cleaning is considered. The measure mechanism used for the gasifier temperatures profile is a pipe with branched thermocouples. It is observed that this mechanism influence the flow of feedstock inside the reactor. The paper by Elrich and Fransson (2011) is the first experimental work that evaluates the use of pellets instead of chips: the quality of pellets from wood is not the same than the quality of pellets from agricultural residues. The char bed porosity in the gasifier, that depends on the type of feedstock, is the most important factor for pressure drop calculation.

According to Hasler and Nussbaumer (1999), tars and particles should be removed before the ICE to avoid damages or inappropriate maintenance tasks: less than 50 mg/m^3_N for particles in the order of microns, and less than 100 mg/m^3_N for tars, are recommended values. Those numbers imply high removal efficiencies: higher than 90% for particles, and around 90% for tars removal. Contaminants elimination also comprises water and condensates elimination. Condensates are produced as a consequence of cold temperature needed before the engine, to maximise as much as possible the volume of combustible gas. The paper evaluates different cleaning units for particles and tars, as secondary methods: sand bed filter, wash tower, venturi scrubber, rotational atomiser, wet electrostatic precipitator, fabric filter, rotational particle separator, fixed bed tar adsorber and catalytic tar cracker. The most effective unit for particles removal is the wet electrostatic precipitator, followed by the rotational atomiser. In turn, the most effective unit for tars removal is the catalytic tar cracker, followed by the sand (activated carbon) bed filter and the venturi scrubber. Wet gas cleaning systems are the most selected removal methods for tars.

Concerning the tars issue, Sutton *et al.* (2001) review the use of dolomite, alkali metals and nickel as catalysts in primary methods, showing their suitability for hydrocarbons removal or for production reduction, through experimental analyses. Arena *et al.* (2010) demonstrate experimentally that olivine is a good candidate for catalysed gasification. In this case, tar amount is highly decreased for plastic wastes. An example of current research work in the field is driven by the Energy research Center of the Netherlands (ECN), with the OLGA (OiL GAs scrubber) technology, which contemplates the use of special scrubbing oils to remove tars from syngas. The challenge of a lot of actual small gasification pilot plants, that use biomass waste from rural areas, is not to remove tars efficiently, but to find an adequate design to produce a syngas free of tars, avoiding the syngas cleaning process before the final application. According to Sheth and Babu (2009) a tars cracking process occurs in the combustion zone, thus in the throat of the downdraft gasifier: tars from the pyrolysed gas mixture cracks into water and non-condensable gases. This process, added to the fact that tars and particles are dependant on the fuel structure and composition, supports the basis that optimal conditions in the gasifier, with cleaning primary methods and with appropriate feedstock, can certainly minimise tars production.

ICE's can be of two types, compression-ignition and spark-ignition engines. The

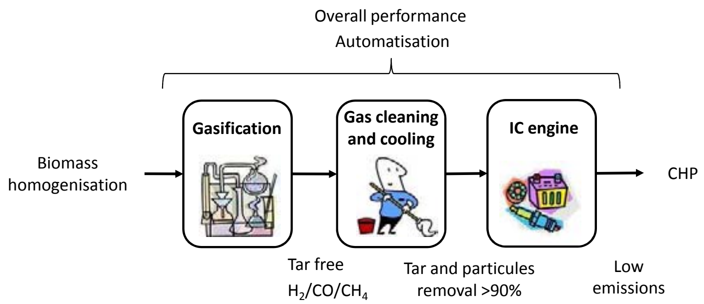

Figure 2.10: Small scale gasification research lines.

former corresponds to diesel engines, while the latter corresponds to Otto engines. Both of them can work with gas, being converted into dual-fuel engines and gas engines, respectively. Diesel engines can work in both modes of operation, in which diesel starts the ignition of the producer gas. The conversion from conventional engines to gas fuelled engines is relatively easy and cheap (Reed & Das, 1988). Sahoo *et al.* (2009) state that more research is needed to understand the ignition capacity of the producer gas. Muñoz *et al.* (2000) have observed a minimal loss of power when substituting gasoline by gas. The temperature of the exhaust gases is around 100°C. No special anomalies are detected, except for the impossibility of an appropriate cold start. Moreover, long term operation should be studied in terms of corrosion or soot accumulations. The study by Sridhar *et al.* (2001) puts into relevance one of the most important drawbacks in an engine adapted to gas: the de-rating phenomena, in which the maximum power to be supplied is lower than the nominal maximum power due to the maximum load that the engine is able to handle. The maximum de-rating detected in power is 16%, being the gas engine efficiency in the range of 32%. Uma *et al.* (2004) have matched engine load with diesel replacement. Finally, the substitution rate proved is 67-86%, in a load condition of 80%. Concerning emissions, CO_2 increases, but NO_x and SO_2 decrease, compared to 100% diesel performance. In Ramadhas *et al.* (2008), it is concluded that the capacity of the dual engine selected to supply a specific demand should be higher than the required one, since the engine can run at maximum 60% of the maximum load condition. Analogously to the previous work, CO_2 emissions are observed to decrease. Nevertheless, the sulphur and nitrogen emissions are similar in dual than in 100% diesel mode.

Overall, it is important to remark that experimental experiences from one source to another are not normalised then, the results are relatively comparable. Therefore, a normalisation of the way of operation should be necessary. Moreover, it has been observed that the most research works on modular gasification are in India, which is an important user of this technology. From the abovementioned pilot plant experiences, several research focuses can be extracted as depicted in Figure 2.10. These are raw material characterisation and homogenisation, better operation results from the gasifier (concerning generation of tars and producer gas composition), more efficient cleaning units (mainly in terms of tars) and an overall optimal performance of the BG-GE plant, to guarantee an efficient and sustainable process, at a minimum cost. Moreover, the plant should be as far as possible automatic.

2.4 Trends and challenges

In Sections 2.2 and 2.3, a literature survey has been conducted for CES and DES that use biomass gasification to produce energy.

In the case of *large scale biomass plants*, the interest is on the co-use of biomass with fossil fuels, i.e. co-gasification and co-firing, to alleviate fossil fuels dependency, exploit and take profit of biomass waste and take advantage of the already developed technology and know-how in large scale gasification and PC power plants. It is therefore the cheapest biomass use among the technological possibilities in bioenergy. A superstructure development approach is a recognised technique for the assessment of optimal solutions in a chemical process. In this situation, the interest is on the election of the appropriate share of biomass to be used in the feedstock mixture, the most advantageous gas cleaning processes and the consideration of polygeneration. IGCC power plants are the state-of-the-art alternative to combustion power plants in the field of biomass use at a large scale. Gasification has been modelled through kinetic and equilibrium approaches, but its modelling is sensitive to the feedstock used, the reactor type and operational conditions. Gas cleaning units comprise well known processes, but the combination of them with the current trends is an issue of research. In this line, CCS is an emerging technique in the field of GHG emissions control, for CO_2 alleviation in power plants and industries. Therefore, gasification combined with syngas cleaning and CCS is a current research line in the field of bioenergy uses. The employ of biomass for large scale electricity and/or heat production is limited by the intrinsic properties of the biomass matched with the limitations of the known technologies. These drawbacks are mainly due to the lignocellulosic nature of biomass, high MC, low LHV and production of tars. As a result, 100% utilisation of biomass, reduces the scale of the plant profitable use to tens of MW's. In turn, biomass can be a mix of raw materials from different nature with different seasonality. *Biomass supply* should be reliable in terms of sustainability, costs and homogeneous properties as a plant feedstock. The SC study is needed to overcome the drawbacks of biomass in terms of "inappropriate" properties and transportation costs, as well as to assess the impact of re-use of biomass waste in activities that once were not affected. IGCC-CCS offers technological, feedstock and product share challenges.

For *small scale biomass plants* in rural areas the most extended tendency is to match local resources with local energy needs, not taking into account the combination of resources and consumers from different sites. Today's needs make necessary the possibility of complementing local resources and needs with external needs and resources, at national and international scales. To carry out this scenario in a sustainable manner, energy models must take into account the specific economic and social context of each case study "tailored". Biomass must be regulated in terms of raw material properties in order to promote international trade. In rural areas, it is very common to burn biomass wastes. Thus, the alternative to be promoted is biomass gasification, as a more efficient and environmental friendly option. A large number of case studies highlights that although not being yet a fully developed technology, gasification of biomass is a preferential option for the future. The significant deficits in gasification projects for small scale energy production reflect a lack of appropriate tactics: donor projects that did not take into account the financial sustainability of the plant, biomass fuel that does not comply with operational conditions of the gasifier, impaired automatic processes, unskilled people to work on it, wet cleaning of gases, ash and tar problem, poor quality of installation and larger plants that does not match low local demand. Therefore, operational conditions of a BG-GE plant should be improved, to be as much as possible useful for a great range of biomass materials, to enhance the overall efficiency of the plant, i.e. with waste heat use, and to reduce tars and contaminants. In turn, the strategic and tactical conditions should be also improved, to assure BSC sustainability in terms of costs and environmental matters.

With all the information presented in this chapter, it is possible to develop a SWOT analysis in the *field of biomass gasification* for both scales and within the scope of this thesis. Since, as already revealed, the two scales have essentially the same trends and challenges, but adapted to each specific framework.

- *Strenghts*
  - Biomass is a renewable source of energy, if sustainably exploited. Even more, gasification can be considered as an option for wastes disposal.
  - There exists several techniques to enhance the properties of the biomass as raw material, such as pelletisation, torrefaction or fast-pyrolysis.
  - Gasification can be more efficient than combustion thus, leading to less consumption of fuel per MW produced, and leading to less GHG's emissions.
  - Biomass co-use till certain percentages does not have a remarkable effect in the loss of the plant efficiency. It allows to be co-used with minor changes in a plant that usually works with coal.
  - The syngas, or producer gas, is very versatile and can be profited to produce several final products: electricity, heat, chemicals, synthetic natural gas and liquid fuels. The biorefinery concept aims at producing more than one product at the same plant.
  - IGCC power plants are near commercial status. Cleaning gas technologies are well known processes.
  - CCS can be easily inserted in an IGCC power plant to produce H_2 to be burnt in the CC, or to produce H_2 to be sold on the market. The latter option allows for CO_2 storage.
  - BG-GE is used in a lot of case studies to produce electricity at a local level. It stimulates social benefits such as employ generation. It does not need special capabilities to be operated.
  - BG-GE can improve its performance taking into account co-generation. BG produces a versatile gas that can be utilised in emerging renewable technologies such as FC's.
- *Weaknesses*
  - Biomass as raw material can be heterogeneous, seasonal, can have high MC, low LHV and BD, depending on the type of biomass, geographical location and climate. It leads to high transportation costs.
  - Biomass pre-treatment techniques, such as torrefaction or fast-pyrolysis are still under development.
  - Biomass gasification is susceptible to produce ashes and tars. Those contaminants have carcinogenic effects and makes mandatory to deal with by-products disposal.

  - Biomass gasification, and the subsequent producer gas use, suffer from de-rating, thus being impossible to use the final application unit as its maximum capacity.
  - Operational conditions of biomass gasification are dependant on the type of biomass used.
  - Gasification projects have not fully demonstrated their sustainability in economic terms.

- *Opportunities*
  - The energy situation is undergoing a fundamental change: limited fossil fuel reserves, climate change and mitigating GHG emissions. The energy paradigm is moving towards micro-generation.
  - IGCC-CCS experiences worldwide are limited.
  - BG-GE pilot plant experiences are not widely found in the bibliography.
  - The legislation framework in most of the countries favours the use of renewable sources.
  - International, national and local biomass trade need from standards to regulate it.
  - The Millenium Development Goals, and other policies for poverty mitigation, count with energy access policies.
  - Rural areas, and specially, rural areas from developing countries, are rich on biomass waste.
  - In rural areas from developing countries there exist land that is not used for food, susceptible to be used for energy crops. Developed countries need biomass that cannot be produced on their lands, therefore being an opportunity for international trade.

- *Threats*
  - The low cost of fossil fuels.
  - The competition with other renewable fuels.
  - Other uses of biomass wastes.
  - Land controversy when using specific energy crops, between food and fuel. Moreover, there is the possibility of scarcity of water as a resource.
  - The development prospect of future policies that may not favour the development of the bioenergy sector.
  - The bioenergy sector, as an emerging sector, has a lack of standards, for instance, in biomass trade.
  - Rural areas has low and dynamic power demands. It is therefore difficult to match an appropriate efficiency for the power plant during all the working hours.

From the previous analysis, the bioenergy field, as well as the energy sector in general, is very much influenced by government policies. From matching internal and external analyses, it is shown that the greatest opportunities come from the emerging nature of IGCC-CCS systems and BG-GE projects, as well as the need for research on their technology, supply chain and the potential of biomass as a resource. The context of those options is favourable due to the change of energy paradigm. However, the use of land for energy crops should be carefully evaluated to avoid further problems.

Contrasting strengths and weaknesses in this framework, decision tools are needed to evaluate the trade-off. Therefore, this thesis contribution is on the development of *decision making tools* for the biomass use at large and small scale, in different contexts in a sustainable way. It pursues to offer a systematic and consistent approach in biomass gasification projects. The final contributions aim at elucidating the kind, scale and location of the gasification plants. The objectives of this thesis, already mentioned in Chapter 1 are:

- To develop a process system engineering approach for IGCC-CCS modelling and optimisation.
- To propose working conditions guidelines in co-gasification and co-production of H_2 and electricity in IGCC-CCS plants.
- To apply existing models and tools in SCM to different BSC, in scale and social/economical contexts, to be able to propose sustainable networks.

Notation

Latin letters

P	pressure
T	temperature

Superscripts and subindices

e	electric
th	thermal

Acronyms

ASU	air separation unit
BSC	bio-based supply chain
BD	bulk density
BG	biomass gasification
CC	combined cycle
CCS	carbon capture and storage
CES	centralized energy systems
CGE	cold gas efficiency
COE	cost of energy
CSTR	continuously stirred tank reactor
DES	distributed energy systems
DME	dimethyl eter
DMPEG	dimethyl ethers of polyethylene glycol
ECN	Energy research Center of the Netherlands
EOR	enhanced oil recovery
ER	equivalence ratio
EU	European Union
FC	fuel cell

FT	Fischer-Tropsch
GE	gas engine
GHG	greenhouse gases
GT	gas turbine
GTL	gas-to-liquid
HEN	heat exchangers network
ICE	internal combustion engine
IGCC	integrated gasification combined cycle
ITDG	Intermediate Technology Development Group
LCA	life cycle assessment
LCI	life cycle inventory
LHV	lower heating value
LP	linear programming
MC	moisture content
MCDA	multiple criteria decision analysis
MCFC	molten carbonate fuel cell
MDEA	methyldiethanol amine
MILP	mixed integer linear program
NGCC	natural gas combined cycle
NGO	non-governmental organisation
NPV	net present value
OLGA	oil gas scrubber
PAFC	phosphoric acid fuel cell
PC	pulverised coal
PEG	polyethylene glycol
PEM	proton exchange membrane
PSA	pressure swing adsorption
R&D	research and development
SC	supply chain
SCM	supply chain management
SNG	synthetic natural gas
SOFC	solid oxide fuel cell
ST	steam turbine
SWOT	strengths, weaknesses, opportunities and threats analysis
TOP	torrefied pellets
WGS	water gas shift

Chapter 3

Methods and Tools

This chapter summarises the main methods and tools used throughout this thesis. The key issue that encompasses all the subjects of endeavour in the work done is *conceptual design*. Therefore, the final results must not only elucidate about the ways to achieve the objectives described in Chapter 1, but must also provide with a specific tool to support decision making in gasification of biomass, for future developments in different contexts.

3.1 Introduction

The thesis objectives, as described in Chapter 1, are:

- To develop a process system engineering approach for IGCC-CCS modelling and optimisation.
- To propose working conditions guidelines in co-gasification and co-production of H_2 and electricity in IGCC-CCS plants.
- To apply existing models and tools in supply chain management (SCM) to different bio-based supply chains (BSC), in scale and social/economical contexts, to be able to propose sustainable networks.

The methodology to attain the proposed objectives is conceptual design using modelling and simulation techniques. Within the bounds of conceptual design, simulation and multiple-criteria decision analysis (MCDA) are used to implement the proposed tool to support decision-making in gasification of biomass framework. Figure 3.1 shows the outline of the methodology employed.

Design of chemical processes comprises grassroots design, in which a completely new process is conceived, and retrofit design, where the purpose is to enhance an already existing process. Design at any level is a creative process that has to be effective, therefore aware with mechanical, technical and economic limitations (Biegler

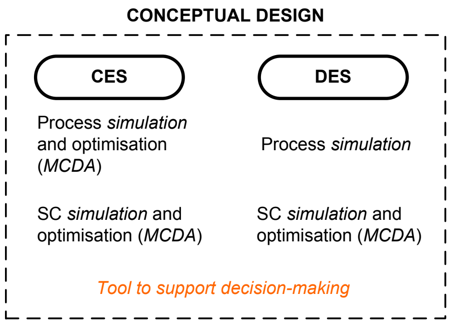

Figure 3.1: Key components in the methodology followed in this thesis.

et al., 1997). In turn, *operations research* (OR) and *management science* (MS), aims at scientifically deciding how to best design and operate person-machine systems, usually under conditions that require the allocation of scarce resources (Ravindran, 2008). As can be deduced, techniques traditionally applied to OR-MS can be applied to the design of chemical processes for the best candidate selection taking into account certain limitations. In fact, the OR-MS techniques and applications continue to grow in a big number of decision-making areas. Multi-disciplinary teams are needed to deal with all the requirements and points of view that this preliminary step should embrace. In this thesis, conceptual design, implying simulation and optimisation, is applied to specific energy systems and their SCM.

3.2 Conceptual design

The term *conceptual design* can be understood as the phase from product design cycle where the basic solution is established through the formulation of abstract ideas with approximate concrete representations. Moreover, those ideas are evaluated with different selected criteria. This stage starts with "high-level" requirements descriptions and continues with "high-level" solutions descriptions. By the end of the conceptual design phase, a decision concerning the process system must be taken (Wang *et al.*, 2002). According to Douglas (1988), conceptual design in chemical processes implies to find the best process flowsheet, i.e. selection of process units and connections among them, and estimate the optimal operating conditions from the most significant parameters. It is often referred as a *pre-design stage*. At a higher level of decision-making, and extrapolating both previous definitions, conceptual design can be applied not only to processes development, but also to the development of the whole supply chain (SC), as performed here.

In Biegler *et al.* (1997), at this preliminary stage, a *flowsheet synthesis* activity is crucial to develop the different process alternatives and to choose the most appropriate one. The synthesis procedure can be described by five main steps. It starts by (i) gathering information and generating the conceptual layout that manifests the user needs. Then, the approach continues with (ii) the representation of the process alternatives and (iii) evaluation of their behaviour, i.e. mass and energy balances, (iv) criteria selection for assessing the preliminary designs and (v) generation, search and election of the "best" flowsheet among the alternatives, through comparison

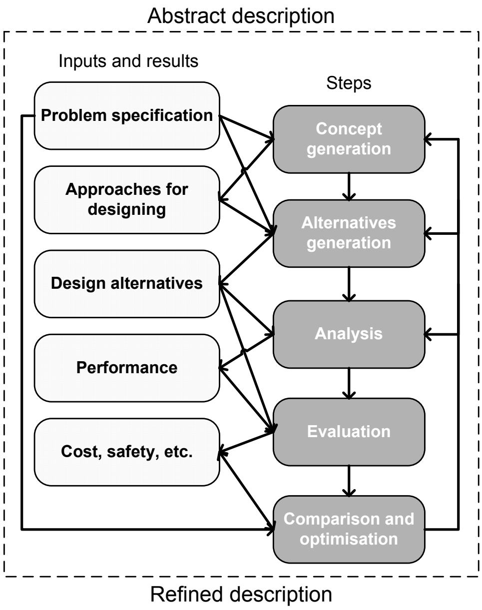

Figure 3.2: Phases of the design synthesis work at the preliminary stage.

and optimisation. Usually the evaluation criteria contains an economic analysis, being necessary to determine equipment sizes, capacities, and finally investment and operation costs. See in Figure 3.2 a scheme of the synthesis activity. As a result, a refined or concise description of the process is obtained. One of the main issues in the field is to develop a *systematic approach* to generate and search process alternatives. The following possibilities can be cited. (i) Total enumeration of an explicit space, which is the most intuitive. The engineer generates, evaluates and compares the designs. This option is only feasible if the total number of options is small. (ii) Tree search in the space of design decisions is a more methodical approach in which at every mode on the tree the taken decisions are recorded. (iii) The next method, a step forward systematic approach, counts with the generation of a *base case*. From this scenario, the other designs are obtained by evaluating changes in the original flowsheet. Those changes can be automated. A *superstructure* of decisions contains all the flowsheet alternatives to attain a design objective, being possible to automate the generation of alternatives. Establishing targets for the design, specifically in HEN and reactors, and problem abstraction at the beginning of the process, are necessary to take several basic decisions that will affect the range of alternatives created. The first optimised conceptual flowsheet is needed at an early stage, to serve as a base for all more detail engineering. Two possibilities are available to find alternative flowsheets, through the manipulation of the decision variables: (i) trial and error, by means of case studies or scenarios, and (ii) mathematical programming, which is the most systematic and efficient way to obtain the alternatives.

Turton *et al.* (1998, 3rd Edition 2009) named as parametric and topological the two types of decision variables that can be optimised in the pre-design stage. *Topological optimisation* deals with equipment's arrangement, therefore with products and by-products generation. In turn, *parametric optimisation* implies finding the most appropriate operating conditions, i.e. temperature, pressure and concentrations. It is crucial to be able to identify the key decision variables of the process, to reach the user commitments, and to optimise the efficiency of the optimisation process. Turton *et al.* (1998, 3rd Edition 2009) describes the framework to generate alternative flowsheets as follows. First of all, it is necessary to create the block flow diagram (BFD) from the generic idea about the final objective, applying heuristics or short-cut methods to conceive the first layout of the process. Then, a base case process flow diagram (PFD) should be drawn: determination of reaction kinetics and physical property data, as well as the development of mass and energy balances. At this preliminary stage, the PFD should be elaborated bearing in mind to look at the big picture, without excessive details. Once the PFD is calculated, the next step is optimisation, having the base case as starting point. In fact, the level of detail of the PFD should coincide with the type of data needed in the objective(s) function(s) (OF's). After the optimal design election, the attention is on an integrated and efficient HEN design. It can be developed through pinch analysis and exergy concepts. All other integration issues can be proposed at this stage.

A step further in design, therefore, beyond the scope of conceptual design, implies the detailed elaboration of the PFD: process topology, stream information and equipment information should appear on it. For the preliminary design level, equipment information concerning detailed sizes is omitted. For costs calculation those are necessary. They can be calculated using heuristics or short-cut methods. The piping and instrumentation diagram (P&ID) is a further step to start with the construction of the plant. It provides information about the piping, instrumentation and utilities connection. Operating conditions, stream flows, equipment locations, pipe routing, i.e. lengths and fittings, as well as supports, structures and foundations are not included. The elaboration of the PFC and P&ID should follow several conventions.

Douglas (1988) is the first reference work about conceptual design. Here, a *hierarchical approach* is depicted to simplify the design problem. See in Figure 3.3 (left side) the main questions that should be answered to conceive the first definitive and optimised layout of the plant at this conceptual stage. Different decisions are derived from each level, from the subsequent addition of layers of detail. In conceptual design it is important to discriminate between important information and details. Again, the importance of the problem remains in a complete base case, from which the alternatives are generated. Douglas (1988) defines optimal design conditions among a set of case studies. In this book, as well as in all the books of design, an important issue to be optimised are costs. See in Figure 3.3 (right side) the levels of engineering design, according to the accuracy of the costs estimates. For candidate flowsheet screening and preliminary design an order of magnitude is enough.

According to Ulrich and Vasudevan (2004) and Turton *et al.* (1998, 3rd Edition 2009), other important subjects that should be considered apart from economic aspects are safety, environment, ethics and professionalism. Therefore, multiple objective optimisation (MOO) is needed to overcome with a broader picture of the biomass gasification conceptual design problem.

Summing up, for CES and DES, at this conceptual design or preliminary design stage, the objective is to obtain a "high level description" of the gasification system and to depict several guidelines for the selection of the best designs according to multiple criteria. The methodology to deal with the design problem aims at being systematic,

HIERARCHY OF DECISIONS

1. Batch vs. continuous
2. Input-output structure of the flowsheet
3. Recycle structure of the flowsheet
4. General structure of the separation system
    a. Vapour recovery system
    b. Liquid recovery system
5. HEN

TYPES OF DESIGN ESTIMATES

1. Order of magnitude estimate based on similar previous cost data; accuracy exceeds **+/- 40%**
2. Study estimate based on major equipment items; accuracy up to **+/- 25%**
3. Preliminary estimate based on specific data to allow the budgeting; accuracy between **+/- 12%**
4. Definitive estimate based on almost complete data, before specifications; accuracy between **+/- 6%**
5. Detailed estimate based on complete engineering specifications; accuracy between **+/- 3%**

Figure 3.3: Hierarchy of decisions (left side) and levels of engineering design (right side), based on Douglas (1988).

being crucial to do not miss important topological and parametric design variables. In this sense, well known tools for optimisation should be applied to find the solution to the problem.

3.2.1 Optimisation

Optimisation is the process of improving an existing situation, device or system (Turton *et al.*, 1998, 3rd Edition 2009). In Biegler *et al.* (1997), a process or system is optimised by giving the best solution within constraints. Since the purpose of optimisation is to improve a process, it is necessary to start from a defined scenario that is the so-called base case. The concept of *best solution* is applied when there exist more than one optimisation criteria and the individual optimal solution for each one of them may not correspond to the same alternative.

In order to be able to find the best solution, it should be possible to quantify it. The optimisation problem is defined by one or more objective functions that should be maximised, or minimised. These are determined by decision variables that represent degrees of freedom in the optimisation procedure. Those variables should be adjusted to satisfy the problem constraints. Dependent variables can be solved from the constraints. From the conceptual design point of view, the distinction among variables is crucial to set out the base case and the required results.

In lots of cases, the task of finding the optimal flowsheet is developed by trial and error or case studies development. This is called here *scenario based optimisation*. This approach is used for CES optimisation. In contrast, Ravindran (2008), Turton *et al.* (1998, 3rd Edition 2009) or Puigjaner *et al.* (2006) among others, describes optimisation as an area directly related with mathematical programming and OR. In this sense, mathematical programming allows for a systematic approach to the problem and coverage of the total range of possibilities, in parametric and topological optimisations. Depending on the properties of the objective functions and the constraints, the optimisation problem can be linear, non-linear, mixed integer linear or mixed integer nonlinear. This line of attack is used for the BSC's optimisation, that use the mixed integer linear programming (MILP) developed in Laínez-Aguirre (2010).

This optimisation step is usually related to *decision support systems*. Those systems, coupled with the intelligence of individuals and the capabilities of the

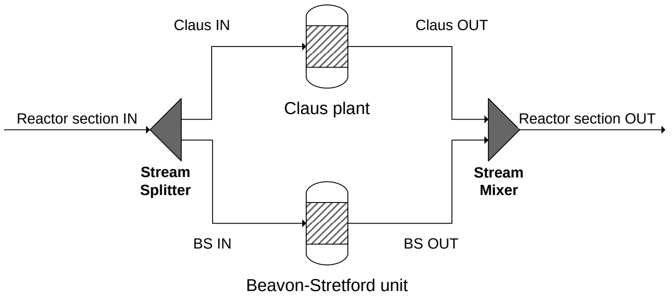

Figure 3.4: Representation of the superstructure capability to allow for topological changes in simulators.

computers, aims at improving the quality of decisions (Turban *et al.*, 2005).

3.2.2 Superstructure

As was previously mentioned in Chapter 2 and according to Biegler *et al.* (1997), a superstructure is a design space able to compile all the feasible options for topological changes of a determined flowsheet, embracing equipment combinations that affects the final results or products and by-products characteristics. The superstructure representation involves the appearance of units that develop the same role in the flowsheet. Therefore, if using process simulators, those options can be considered by adding *splitters* and *mixers* according to the process layout. The optimisation procedure in this case should be able to select the optimal split fractions, for instance in a case of co-production, or the discrete binary selection of values if one unit should be used instead of another. For example, see in Figure 3.4 the sulphur recovery task that can be developed by a Claus plant or a Beavon-Stretford unit. Therefore, the optimisation algorithm will maximise or minimise the OF by varying the stream splitter among 0 or 1.

In this thesis, the superstructure conceived is beyond the boundaries of the IGCC-CCS plant, referring to production of only electricity, hydrogen or co-production. As depicted in Figure 6.2 and strictly speaking, as the SC design allows to chose among a list of available pre-treatment methods, these are also part of the superstructure.

3.3 Multiple-criteria decision analysis

OR-MS methodologies applications are growing in the field of decision-making. Decision analysis refers to the methodological process of identifying, modelling, assessing and determining a suitable way of action for a given decision problem. Decision problems usually present multiple and conflicting criteria to evaluate alternatives. It is then necessary to make compromises or trade-offs regarding the results of the different possible choices. In MCDA context, the term *objective* is used to designate a path to be followed for improvement as perceived by the decision-maker. In contrast, the concept *goal* is a specifc target of an objective, attained by the best choice. A multiple-criteria decision-making (MCDM) problem can be represented as described in Ravindran (2008):

$$\text{Maximise or minimise} \quad \underset{a \in A}{[O_1(a), O_2(a), \ldots, O_k(a)]} \tag{3.1}$$

Where, a is one of the possible alternatives, A is the feasible region constituted by all the alternatives and O_k are the objectives. The different methods to solve a MCDM problem can be classified in two big groups: multiple-criteria methods for finite alternatives (MCMFA) and multiple-criteria mathematical programming (MCMP). The former is used to select the preferred alternative from a finite set of choices; while in the latter there are an infinite number of them, or those are not known a priori. MCMFA and MCMP problems are solved by different methods, as listed in Figure 3.5.

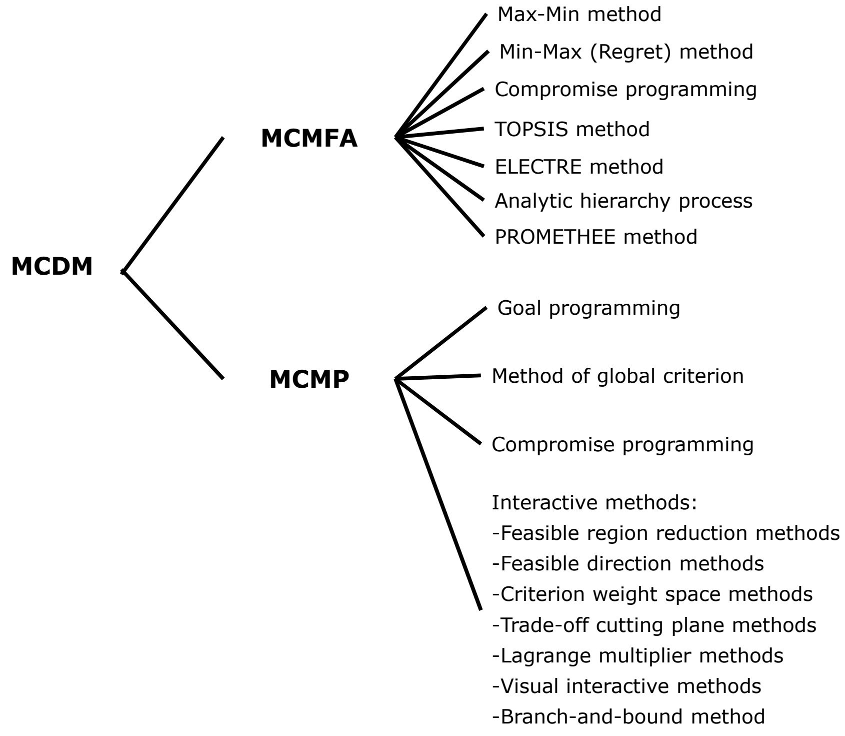

Figure 3.5: Classification of the MCDM methods according to Ravindran (2008), for finite and infinite (or not known) number of alternatives, MCMFA and MCMP, respectively.

The solution is given by a ranking of alternatives from the best to the worst one, or by an alternative selection. This last selection can be referred as the best, preferred or satisfying solution: the chosen alternative meets or surpasses the decision-maker criteria. But, if the criteria of the decision-maker is not specific or concise, i.e. no prioritisation of the OFs, instead of giving one specific solution, a set of feasible solutions may be possible, the so-called *Pareto optimal solutions*. These are also called the *Pareto frontier* (PF). A Pareto optimal solution is also called a *non-dominated solution* or *efficient solution*, and this is an alternative that is not dominated by any other feasible solution. Therefore, for a Pareto solution, an increase or improvement in the value of a criterion implies at least one decrease or decline in the value of any other decisive factor (Turban *et al.*, 2005).

Specifically, for MCMP problems, the feasible alternatives are represented by a collection of mathematical constraints. Eq. (3.1) can be rewritten as in Eq. (3.2) to better represent a MCMP problem.

$$\begin{aligned} \text{Maximise or minimise} \qquad & \mathrm{F}(x) = \{f_1(x), f_2(x), \ldots, f_k(x)\} \\ & \text{subject to } g_j(x) \leq 0 \text{ for } j = 1, \ldots, m \end{aligned} \tag{3.2}$$

Where, x is a n-vector of decision variables and f_k are the objective functions. Being S the decision space and Z the objective space:

$$S = \{x/g_j(x) \leq 0, \text{ for all } j\} \tag{3.3}$$

$$Z = \{z/F(x) = z \text{ for some } x \in S\} \tag{3.4}$$

The solution to a MCMP problem is called *superior solution*: it is feasible and satisfies all the OFs. Nevertheless, as previously commented, one unique solution is difficult to find, as the objective functions deal with conflicting criteria. Therefore, Pareto solutions appear more appropriate.

The MCMP methods to choose the best configuration(s) (Figure 3.5), are classified according to the decision-maker preference criteria. Goal programming is used when the preferences of the decision-maker are completely known. In contrast, method of global criterion and compromise programming are used when no information is known about the decision-maker preferences. In the middle, interactive methods are used when partial information about the decision-maker preferences is reachable progressively during the resolution of the problem. In this thesis, it is assumed that the decision-maker has no specific goals values, and the extremes of the PF are found by optimising each objective. Those approaches used in this work, assume that the decision-making task is made under certainty, in respect to data used. Other approaches also consider decision-making under uncertainty and risk. In this thesis, and going back to Figure 3.5, the TOPSIS method is used, which tries to choose the best choice among a finite number of alternatives. TOPSIS (technique for order preference by similarity to ideal solution) methodology is based on the principle that the satisfying solution should be simultaneously closest to the ideal solution, *utopian*, and farthest from the negative-ideal solution, *nadir*. Ideal and negative-ideal solutions are found by selecting the best and worst OFs solutions from the PF scenarios. These solutions are not necessarily one feasible alternative.

Summing up, the superstructure for IGCC-CCS is used to generate a finite number of scenarios analysed through MCMFA: the PFs are found for the selected objective functions, and then TOPSIS methodology allows choosing the best scenario. In SCM for CES and DES, by means of MCMP, a MILP formulation is used to find the PF's extremes for the BSC's. See Laínez-Aguirre (2010) for more details.

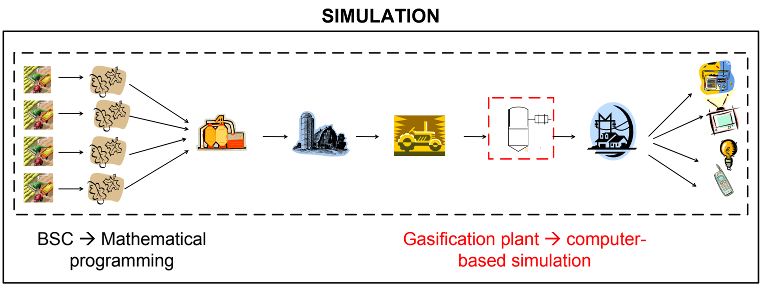

Figure 3.6: The boundaries of the simulations performed in this thesis.

3.4 Simulation

The calculation of mass and energy balances to evaluate the different alternatives in the IGCC-CCS system and to perform the BG-GE process, as well as the SC unit's performances, are carried out through *simulation* (see Figure 3.6). According to Ravindran (2008), simulation comprises different actions: laboratory plants, pilot plants and simulation softwares. This thesis is focused on *computer-based simulation* that intends to model an existing or proposed system, capturing the most influencing parameters on the overall system operation. In this case, the systems modelled are two gasification plants and two supply chains, and the simulation outputs reproduce the real plant/SC behaviour and allow predicting alternative designs, meeting improved specified objectives.

To evaluate the conceptual flowsheet developed at this pre-design stage, mass and energy balances are calculated in a rigorous way through process simulators. Those simulators work with a set of non-linear equations representing the connectivity of the units, the specific model equations of each unit, transport and thermodynamic properties. The system of equations can be solved in two ways: *sequential modular* (SM) and *equation-oriented* (EO) (Biegler *et al.*, 1997; Turton *et al.*, 1998, 3rd Edition 2009; Puigjaner *et al.*, 2006). The essence of the resolution techniques is different for both approaches, as depicted in Figure 3.7. SM mode is solved hierarchically. Note that the three stages are fed forward and back, but they are solved individually. Flowsheet topology sequences the unit modules, initialises the flowsheet and identifies loops and tear streams. Then, the unit models output streams are calculated from the input streams and the design parameters. The procedures are solved following the flowsheet topology. The units belong to a library of units, each one of them solved with specific equations, for separators, reactors and transfer units. The last level deals with physical and thermodynamic property models. In contrast, in the EO mode, the equations of the flowsheet topology and unit models are combined in the same set of equations. This structure permits much more flexibility when choosing the degrees of freedom. Both modes deal with the resolution of systems of non-linear equations. Each solving methodology has advantages for different types of flowsheeting problems.

This thesis uses Aspen Plus and Aspen Hysys as simulation tools. Both of them are SM. Aspen Plus requires the use of design specifications, which are coded in FORTRAN, to fix output values, while Aspen Hysys allows to solve a unit operation not only by taking into account input variables. It allows the simulator to solve it if a certain number of degrees of freedom are set to find a solution with the available

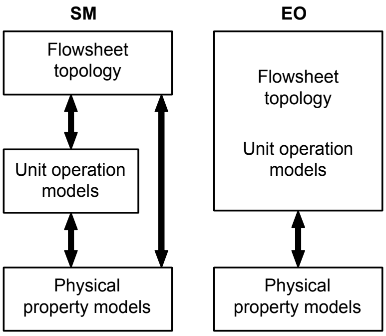

Figure 3.7: Configuration of SM and EO modes, based on Biegler *et al.* (1997).

equations (AspenTech, 2010). The superstructure is actually developed in Aspen Plus. Nevertheless, as a prior step to this final model, an Aspen Hysys-Aspen Plus superstructure was developed to profit the easiness from Aspen Hysys to handle with non-conventional compounds and with custom models. This first superstructure has been used to evaluate exhaustive kinetics models, as further explained in Chapters 4 and 5. See in Figure 3.8 the interaction among interfaces of Aspen Hysys. Custom models, i.e. unit operation extensions and kinetic reaction extensions, are programmed using MS Visual Basic, given the capability of Aspen Hysys to accept COM objects (the so-called extensions). Unit operation extensions correspond to metamodels, artificial neural networks (ANN), see Section 3.4.1 for further explanation, trained with Aspen Plus data. This incorporation counts with cleaning units involving electrolytes. The development of this first superstructure follows mainly a modelling approach contribution combining simulation softwares, in collaboration with Bojarski (2010).

The final superstructure is based solely on Aspen Plus models: the use of just one simulation tool increases the calculation speed to find compromise solutions and is more robust. Therefore, in this second approach, the attention is more on the case study rather than on the conception of the tool. Aspen Plus allows for user models, coded in FORTRAN, which are directly linked to its model library. In this case, the use of ANN's is not needed, since all the units are modelled in the same software.

According to Turton *et al.* (1998, 3rd Edition 2009) and Puigjaner *et al.* (2006), Figure 3.9 is a scheme of the main concepts involving a simulation problem and its linkages with the main process simulator components. An important issue in process simulation is the election of the proper thermodynamic package: it should be chosen according to the type of process and species involved on it. Those thermodynamic packages can belong to ideal, predictive models, activity coefficient estimation models, water/vapour, equations of state, correlations and special model families. A flowsheet builder provides the needed environment to connect streams and units, following the base case layout. The evaluation of the OFs is done processing output data from the simulation. MS Excel spreadsheets and MATLAB are used to graphically perform sensitivity analyses and PFs.

GAMS (generic algebraic modelling system) is the modelling framework for mathematical programming problems, used in SCM optimisation. It has specific solvers to deal with the different types of mathematical problems. For further details, see Laínez-Aguirre (2010).

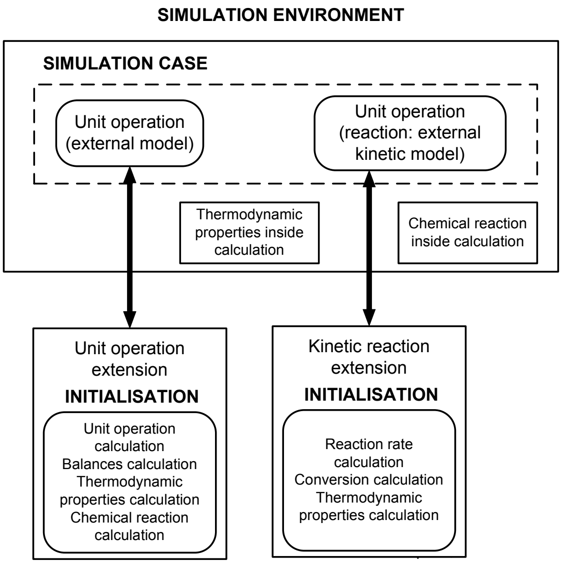

Figure 3.8: Custom models in Aspen Hysys.

3.4.1 Metamodels

A *metamodel* or *surrogate model* is a mathematical function, cheaper from a computational point of view than the actual model, that approximates the behaviour of the pre-existing model over the domain of variation of its inputs. This is particularly useful when performing sensitivity analyses in SM mode. Different standard functions are available for metamodels. The most used are polynomials and splines. Kriging, ANN's and other methodologies coming from design of experiments and response surface techniques, are also utilised (Fang *et al.*, 2006).

The metamodels used in this thesis serve to perform distillation columns. In the initial superstructure built, metamodels are used to embed Aspen Plus simulated units into the Aspen Hysys main flowsheet. The data fitting to the ANN is done using MATLAB toolbox for ANN's. The whole process implementation has three main stages: (i) generation of representative data in Aspen Plus by characteristic sensitivity analyses, (ii) ANN training, through MATLAB and (iii) ANN use in Aspen Hysys. This last step uses the Aspen Hysys operation extension.

In the final superstructure, RadFrac columns and empirical correlations are substituted by component splitter models. This model divides the input flows into the user's predefined products according to the species distribution. This action implies a thermodynamic package change, from electrolytes formation combined with non-random two liquid (ELECNRTL) to Peng-Robinson equation of state (PR) (see Chapter 5 for further description).

3.5 Key performance indicators

Key performance indicators (KPI's) are the metrics used for optimisation. They allow quantifying the performance of each alternative, and therefore they allow choosing

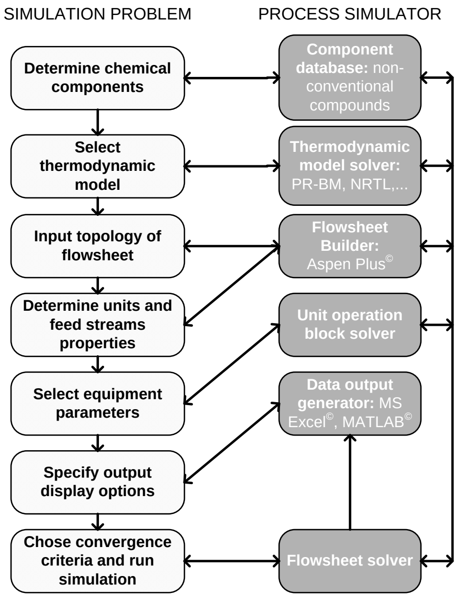

Figure 3.9: Relationship between the simulation problem input data and the main process simulator components, for the final superstructure, based on Turton *et al.* (1998, 3rd Edition 2009).

the best scenario. In other terms, these KPIs correspond to the different OFs in the decision-making task under multiple objectives. The selected metrics should be relevant, robust, understandable, reproducible and unbiased (Turban *et al.*, 2005). The chosen metrics used as KPI should represent the decision-maker interests and reflect different aspects of the process. As has been already commented, the economic parameters are very common to evaluate a project. The different indicators should be normalised to a unique measure of performance to make them comparable. In MCDA techniques to choose the best design alternative, the different OF values are usually normalised in order to be weighted.

The metrics considered in this thesis include plant performance, economic and environmental points of view. In the first metric, the different relevant efficiencies derived from the performance of the IGCC-CCS plant are used. BG-GE efficiencies calculation is analogous. In the second metric, the cost of energy (COE) and the net present value (NPV) are of concern. In the third one, the environmental point of view is evaluated through a life cycle assessment (LCA). These three metrics are described in the following paragraphs. The trade-off among them is evaluated graphically, by means of PF technique, which does not need normalisation. A fourth criterion, concerning a social point of view, is used for DES. This is further detailed in Chapter 8.

3.5.1 Plant engineering point of view

To deal with the varying performance of various design alternatives, different efficiency parameters are evaluated according to the final product of the IGCC plant. The parameters are defined as follows:

- Cold gas efficiency (CGE) (Usón *et al.*, 2004) is defined as the ratio between the chemical energy contained in the raw gas (rg), i.e. the syngas coming out the gasifier, and the total chemical energy contained in the fuel. Both of these values are measured using their LHV (Eq. 3.5). In the case of fuel blends, the LHV$_{fuel}$ is calculated from the contribution of each i-th fuel on a mass basis (w_i), as in Eq. (3.6).

$$\text{CGE} = \frac{m_{rg} \cdot \text{LHV}_{rg}}{m_{feed} \cdot \text{LHV}_{feed}} \% \tag{3.5}$$

$$\text{LHV}_{fuel} = \sum w_i \text{LHV}_i \tag{3.6}$$

- The energy efficiency of the combined cycle (CC) (Eff_{CC}) is defined as the ratio between the net power of the CC, considering the energy consumed by the compressor, and the total chemical energy contained in the clean gas (cg) which is fed to the gas turbine, as in Eq. (3.7). Concerning co-production options, this "clean gas" can be hydrogen or PSA purge gas.

$$Eff_{CC} = \frac{Power_{net}}{m_{cg} \cdot \text{LHV}_{cg}} \% \tag{3.7}$$

- By considering the plant as a whole, the total profitable energy that enters the system is related with the final electricity that goes to the grid. This energy efficiency (Eff_{global}) is calculated as in Eq. (3.8).

$$Eff_{global} = \frac{Power_{net}}{m_{feed} \cdot \text{LHV}_{feed}} \% \tag{3.8}$$

- Similarly, in the case of H_2 production, the global efficiency is calculated as in Eq. (3.10). In the same way as in the case of CC, the partial efficiency of the carbon capture process can be calculated as in Eq. (3.9).

$$Eff_{CCapture} = \frac{m_{H_2} \cdot \text{LHV}_{H_2}}{m_{cg} \cdot \text{LHV}_{cg}} \% \tag{3.9}$$

$$Eff_{global_{H_2}} = \frac{m_{H_2} \cdot \text{LHV}_{H_2}}{m_{feed} \cdot \text{LHV}_{feed}} \% \tag{3.10}$$

- Eqs. (3.5) and (3.7) evaluate the performance of the gasifier and of the CC separately, while Eff_{global} provides a metric for the overall installation. To relate the former definitions, the efficiency associated with the gas cleaning operations (Eff_{cl}) can be defined as in Eq. (3.11), in which m_{rg} and m_{cg} refer to the mass flows of raw and clean gas obtained.

$$Eff_{cl} = \frac{m_{rg} \cdot LHV_{rg}}{m_{cg} \cdot \text{LHV}_{cg}} \tag{3.11}$$

  Consequently, Eff_{global} can be calculated from the partial efficiencies as in Eq. (3.12).

$$Eff_{global} = Eff_{CC} \cdot Eff_{cl} \cdot \text{CGE} \tag{3.12}$$

  The same reasoning can be applied to the H_2 production, resulting in Eq. (3.13)

$$Eff_{global_{H_2}} = Eff_{CCapture} \cdot Eff_{cl} \cdot \text{CGE} \tag{3.13}$$

- In the case that syngas is used for co-production, i.e. the production of hydrogen and electricity simultaneously, the efficiency calculation should combine the efficiencies related to both electricity (Eff_{global}) and hydrogen ($Eff_{global_{H_2}}$) production. Thus, the final global efficiency, called the total efficiency, is defined as in Eq.(3.14).

$$Eff_{total} = \frac{Power_{net} + m_{H_2} \cdot \mathrm{LHV}_{H_2}}{m_{feed} \cdot \mathrm{LHV}_{feed}} \tag{3.14}$$

3.5.2 Economic point of view

The gasification projects presented in this thesis should be treated as long term financial projects. Therefore, the interest is on seeing the value of them as investment projects. From a business point of view, it implies a strategic level decision. When regarding to a long term financial project, implicitly, the cost of the project is deferred in time. In terms of monetary flows, it means an initial expense to obtain a future sequence of benefits. The basic elements that have to be evaluated for an investment project are (Santandreu & Santandreu, 2000):

- The project life. Project profitability and risk depend on the time horizon estimated for the "commercial life" of the product.
- Size of the project. This is the value of the project in monetary terms.
- Cash-flow. Its usual calculation in a simplified way entails net profit plus depreciation of fixed assets.

Three main issues are always included to analyse a long term project: (i) profitability, (ii) liquidity and (iii) risk. The criteria used to evaluate those projects should take into account the three abovementioned items. Two types of criteria can be cited to help in the decision-making task: static and dynamic criteria. The first one does not take into account the chronologic factor. Even if this is a "mistake", the advantage is on its simplicity, and therefore, on its readiness to show some preliminary results. The most used static criteria are the static cash-flow method, the pay-back method and the accounting rate of return method.

Dynamic criteria take into account the monetary aspect as well as the moment where the resources input or output takes place. The homogenisation of monetary fluxes is done through capitalisation of costs and benefits to a future year, or discounting costs and benefits to measure them as current costs and benefits. The most important dynamic criteria used are the NPV, the internal rate of return and the dynamic pay-back.

The NPV is the criterion used for the BSC's optimisation. This is calculated as in Eq. (3.15).

$$\mathrm{NPV} = \left(\frac{C_1}{1+i_r} + \frac{C_2}{(1+i_r)^2} + \frac{C_3}{(1+i_r)^3} + \ldots + \frac{C_n}{(1+i)^n} \right) - C_0 \tag{3.15}$$

Where, C_0, ..., C_n are the cash-flows in each period; i_r is the interest rate and n is the project life in years. C_0 corresponds to the investment made to start the project.

The COE is used for scenarios-based optimisation. This metric is calculated as in Eq. (3.16) and determines the price of the energy to guarantee the pay-back of the plant investment and the plant maintenance and operation costs coverage. The numerator corresponds to the outcomes and the denominator to the incomes. The revenues are due to electricity and hydrogen sales; the subscript equivalent, *eq*, refers to power and H_2 considered at the same time) (Ordorica-Garcia *et al.*, 2006; Koukouzas *et al.*, 2008). The COE is evaluated in €/kWh$_{eq}$.

$$\mathrm{COE} = \frac{\mathrm{TCR} + \sum_n \mathrm{TOC}_n/(1+i_r)^n}{\sum_n (\mathrm{E}_n + \mathrm{H}_{2n})/(1+i_r)^n} \tag{3.16}$$

Where, TCR is the total capital requirement, and TOC_n are the total operating costs per year. In turn, E_n and H_{2n} are the correspondent electricity and hydrogen produced in kWh per year.

The i_r can be estimated through different methodologies, being its inference crucial for the project evaluation. The most usual criteria adopted are: (i) i_r takes the value of the discount rate of the long term financial markets, such as the public debt; (ii) it takes a typical value used for the enterprises from the sector; (iii) it can adopt the rate of the enterprise debt and (iv) can take into account the opportunity cost (Santandreu & Santandreu, 2000).

For the case studies considering co-production, the *revenue* is calculated in a simple way that only takes into account the variation in raw material costs and the profit obtained by selling all of the electricity and hydrogen produced. Therefore, for comparison purposes, the investment in the plant and its operation and maintenance costs are the same for all case studies (see Chapter 6). The actualisation factors are from the journal called *Chemical Engineering*, Section *Economic Indicators*.

Investment and operating costs estimation

The TCR and TOC, as well as the cash-flows, are calculated taken into account two approaches. The first one follows the work by Frey (1991) and Frey and Akunuri (2001). Probabilistic expressions with their range of application are reported, based on real IGCC power plants. Additionally, the general methodology described in Ulrich and Vasudevan (2004) for costs estimation, is used for the IGCC-CCS units that are not described in the former sources. The dimensions variability is reflected in the costs expressions by means of the sizing variable that depends on the plant dimension. Thus, it depends on the flowrates estimated for each scenario. Those flowrates are obtained from the simulation. See in Table 3.1 the items included in TCR and TOC, as calculated for the performance evaluation when using the Aspen Hysys-Aspen Plus superstructure.

The second approach follows the papers by Hamelinck and Faaij (2002) and van Vliet *et al.* (2009), and is based on economies of scale. It is used for scenarios-based optimisation using Aspen Plus superstructure, gaining simplicity and reducing time calculation from the previous method. The total annualised costs do not include feedstock costs. The main items are (i) TCR; (ii) annual costs (AC), which are TOC minus fuel costs; (iii) feedstock costs (FdC) and (iv) electricity and H_2 supplies.

CO_2 metrics

For Chapter 6 scenarios evaluation, specific metrics related to the CCS train of units should be taken into account. Those are the cost of CO_2 avoided and the cost of CO_2

Table 3.1: Costs breakdown for the Aspen Hysys-Aspen Plus superstructure.

TCR (€)	Total direct costs	Equipment and general facilities
	Total indirect costs	Indirect construction costs, sales tax, fees, permits
	Contingencies	Process and project contingencies
	Others	Royalties, inventories, initial chemicals charge, land
TOC (€/yr)	Fixed operating costs	Operating work
		Maintenance work
		Maintenance material
		Administrative and support work
	Variable operating costs	Total fuel cost
		Total consumable cost
		Ash disposal
		By-product credit (sulphur and slag)

captured (Metz *et al.*, 2005). They are defined as in Eqs. (3.18) and (3.19) respectively, and the COE is evaluated by taking into account the production of electricity exclusively. The cost of CO_2 avoided reflects the average cost of the reduction on CO_2 emissions. The total mass of CO_2 emitted, in tonnes, is used for the calculation, by comparing the IGCC plant with and without CCS technology, maintaining the same dimensions. *bc* concerns the base case in topological configuration. The cost of CO_2 captured reflects the economic viability of a CO_2 capture system by stipulating the appropriate price for the CO_2 in the market or, from another point of view, the appropriate subsidy. This cost should compensate the investment on the CCS train of units. For clarification purposes, Eq. (3.17) depicts the CO_2 mass balance. The cost of avoiding CO_2 emissions includes the costs associated to transportation and pumping to final disposal.

$$\mathrm{CO}_{2,captured} = \mathrm{CO}_{2,emitted}^{bc} - \mathrm{CO}_{2,emitted}^{CCS} \tag{3.17}$$

$$\text{Cost of } \mathrm{CO}_{2,avoided}[€/t\mathrm{CO}_2] = \frac{\mathrm{COE}_{CCS} - \mathrm{COE}_{bc}}{(\mathrm{CO}_{2,emitted}/\mathrm{kWh})_{bc} - (\mathrm{CO}_{2,emitted}/\mathrm{kWh})_{CCS}} \tag{3.18}$$

$$\text{Cost of } \mathrm{CO}_{2,captured}[€/tCO_2] = \frac{\mathrm{COE}_{CCS} - \mathrm{COE}_{bc}}{(\mathrm{CO}_{2,captured}/\mathrm{kWh})_{CCS}} \tag{3.19}$$

3.5.3 Environmental point of view

Any industrial process is compromised with the environment in two aspects: raw materials consumption and emissions. In this thesis, two environmental approaches are followed: evaluation of only CO_2 emissions, and evaluation of the overall impact through a LCA approach. This framework can include the entire life cycle of the process from raw material obtaining since final disposal (from cradle to grave). Impact 2002+ is the chosen environmental metric. To evaluate it, it is necessary to know all the environmental interventions, i.e. inputs and outputs through the system boundaries. The input data are extracted from the base case requirements and the calibration parameters. The output data are gathered from the superstructure results. LCA methodology is based on ISO documents (ISO14040). This methodology is based on four main steps, as depicted in Figure 3.10:

- Goal definition and scope. The boundaries of the system and the functional unit (FU) are chosen. In the case of power plants, electricity can be used in many different ways, being a difficult task to evaluate and model appropriately the use of it. Therefore, the most common boundaries are drawn from cradle to gate. The FU is usually the main output, in this case evaluated as MJ produced in the considered time horizon.

- Life cycle inventory (LCI) requires the evaluation of raw material and utilities consumptions, as well as by-products flows and emissions, including transportation. At the end of this stage, the impacts are inferred. This step is the most time consuming action in a LCA. LCI databases are used to make the predictions.

- Life cycle impact assessment (LCIA) step interprets the LCI data, by means of environmental metrics, in this case, Impact 2002+. Different metrics diverge in their location along the environmental damage chain. LCI are translated into mid-points and end-points metrics by means of characterisation factors. Impact 2002+ links LCI results, by means of 15 mid-point impacts, i.e. human toxicity, respiratory effects, ionising radiation, ozone layer depletion, photochemical oxidation, aquatic ecotoxicity, terrestrial ecotoxicity, terrestrial acidification/nitrification, aquatic acidification, aquatic eutrophication, land occupation, global warming, non-renewable energy and mineral extraction, to 4 end-point categories or areas of protection, that are human health, ecosystem quality, climate change-global warming potential and resources.

- Results interpretation deals with the user's analysis evaluation, through graphical representations and comparison with other projects. This is the most subjective step in this methodology.

As a matter of example, a detailed LCA is applied to two IGCC configurations, that work with solid raw material or with natural gas. Other metrics apart from Impact 2002+ are also calculated in Chapter 6. The methodology is further described and used for other case studies in Bojarski (2010).

Summing up, Figure 3.11 shows the information workflow of the process analysis. After the configuration of the superstructure, the main input data are introduced into the flowsheet, including equipment selection. Simulation results are extracted, in order to estimate investment and operating costs, as well as process efficiencies and environmental impacts. MS Excel files are used to calculate the selected KPI's.

3.6 Final remarks

This thesis uses the ELCOGAS IGCC power plant layout as base case. For CES, Chapters 4, 5 and 6 uses the methodology described for conceptual design: process modelling and validation, and superstructure building-up for alternatives evaluation (process synthesis). The MCDA followed contemplates a scenario-based optimisation, taking into account technical, economic and environmental criteria. Several sensitivity analyses are performed to validate the models, and to understand the behaviour of the plant, when varying the most influencing parameters. In this line, mainly the gasification variables and the split fractions, which are responsible of the topological

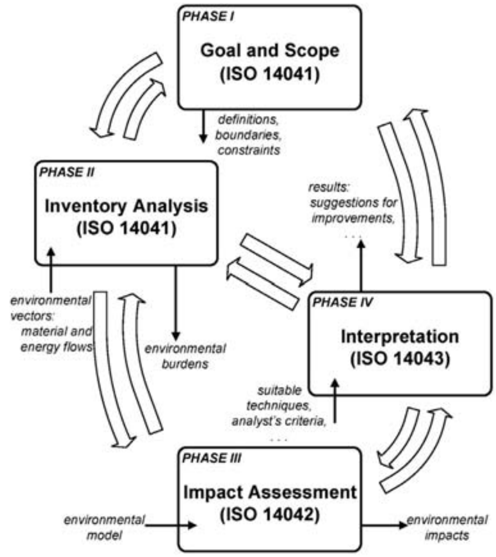

Figure 3.10: LCA steps, by Puigjaner and Guillén (2008).

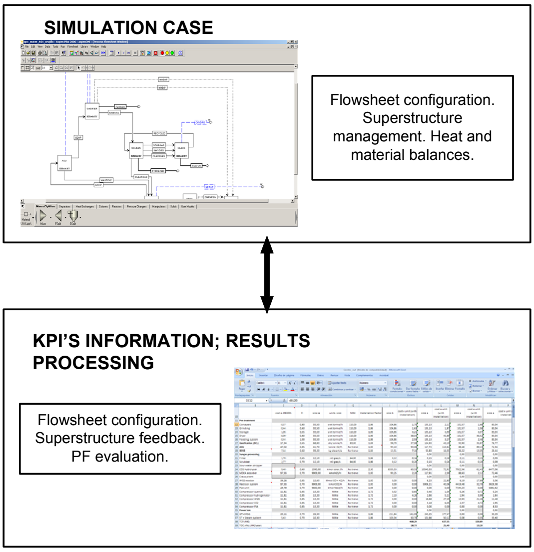

Figure 3.11: Flowsheet analysis workflow.

changes, are studied. Pareto curves, to find the PF's, are used to infer the best choices in co-gasification and co-production analyses. The TOPSIS methodology is utilised to choose the best scenario. The final Aspen Plus superstructure is a versatile and flexible simulator for preliminary design of different process alternatives, retrofit of existing ones, and serves to improve process operating conditions of actual IGCC-CCS plants. For DES, the developed superstructure for the previous approach is used to unfold the main parameters of a BG-GE plant.

The BSC of centralised and distributed energy systems based on gasification are optimised by means of MILP formulation. Each approach is studied for real case studies in Spain and Ghana, respectively, trying to capture the main issues of each context. The OFs count with NPV and LCA optimisation. DES also use a social criterion. These case studies are detailed in Chapters 7 and 8.

Notation

Latin letters

a	process alternative
A	feasible region constituted by all process alternatives
C_n	cash flow during period n
Eff	efficiency
E_n	produced electricity
F	set of objective functions
f_k	objective function
g_i	constraint
i_r	interest rate
m_i	mass flow rate of component i
O_k	objective
S	decision space
w_i	mass fraction of component i
x	n-vector of decision variables
Z	objective space

Superscripts and subindices

bc	base case
CC	combined cycle
CCS	carbon capture and storage
cg	clean gas
cl	gas cleaning operations
eq	equivalent; when adding power and H_2 calorific value in co-production case studies
$feed$	solid feedstock
$global$	considering the plant as a whole, when only electricity is produced
H_2	produced hydrogen
n	project life in years
rg	raw gas
$total$	considering the plant as a whole in co-production scenarios

Acronyms

AC	annual costs
ANN	artificial neural network

BFD	block flow diagram
BG	biomass gasification
BSC	bio-based supply chain
CC	combined cycle
CCS	carbon capture and storage
CES	centralised energy systems
CGE	cold gas efficiency
COE	cost of energy
DES	distributed energy systems
ELECNRTL	electrolytes formation combined with NRTL property method
EO	equation-oriented
FdC	feedstock costs
FU	functional unit
GAMS	generic algebraic modelling system
GE	gas engine
HEN	heat exchangers network
IGCC	integrated gasification combined cycle
KPI	key performance indicator
LCA	life cycle assessment
LCI	life cycle inventory
LCIA	life cycle impact assessment
MCDA	multiple criteria decision analyses
MCDM	multiple criteria decision making
MCMFA	multiple criteria methods for finite alternatives
MCMP	multiple criteria mathematical programming
MILP	mixed integer linear programming
MS	management science
MOO	multiple objective optimisation
NPV	net present value
NRTL	non-random two liquid
OF	objective function
OR	operations research
PF	Pareto frontier
PFD	process flow diagram
P&ID	piping and instrumentation diagram
PR	Peng-Robinson equation of state
SC	supply chain
SCM	supply chain management
SM	sequential modular
TCR	total capital requirement
TOC	total operating costs
TOPSIS	technique for order preference by similarity to ideal solution

Part II

Energy Systems from Biomass

Chapter 4

Gasification Modelling and Validation

Syngas or producer gas generation through gasification consists in the production of a gas from a solid, mainly formed by CO, H_2 and CH_4 in different proportions according to the reactor configuration, the feedstock composition and the operation conditions. This chapter describes two gasification modelling approaches: kinetics and equilibrium based. The thermo-chemical equilibrium model is presented as the model used in the gasification plants conceptual design. The influence of feedstock composition and gasifying agents, reactor temperature and pressure in the final gas composition are evaluated through sensitivity analyses. The major hypotheses of this syngas generation step are enumerated. Thereafter, those hypotheses are applied in the modelling and optimisation of the entire gasification plant. ELCOGAS IGCC plant located in Puertollano (Spain), which has 335 MW_e of nominal gross output, is the reference to develop and validate the model built in this chapter and in Chapter 5.

4.1 Introduction

Expanding economies and climate change are challenging issues that require cleaner and more efficient power production plants. Gasification has been used commercially around the world for more than 50 years, in chemical, refining and fertiliser industries, and for 35 years by the electric power industry. More than 420 gasifiers are currently in use worldwide (Council, 2008). IGCC power plants are versatile for two reasons: a wide range of carbon-based inputs can be fed into the gasifier; and different products can be obtained from the syngas that is produced, i.e. electricity, heat, chemicals, synthetic natural gas, liquid fuels or H_2, depending on the layout of the gasification plant, as further described in Chapter 2. According to NETL (2007), coal is the main feedstock for IGCC power plants followed by petroleum refinery by-products, natural gas, petcoke and biomass. Despite this trend, renewable energy sources will play an important role in the future of the energy generation sector. Biomass is seen as an important resource in terms of supply prediction. It is the largest, most diverse and readily exploitable source of renewable energy (Ravindranath *et al.*, 2004). Differences between combustion and gasification are mainly due to the oxidation level. Moreover, gasification is not a final process itself, but a process for solid conversion to obtain a valuable gas. Comparatively, gasification-with-syngas-use process offers a higher efficiency and lower environmental impact, in terms of GHG emissions, than combustion. The amount of syngas produced in a gasification process is lower than the flue gas produced in a combustion process on a volume basis. Therefore, cleaning syngas is cheaper, easier and more effective than cleaning combustion gases (McKendry, 2002b).

Two reactor models are discussed in this chapter; the first one divides the gasification process into several stages, studies gas-particle interaction and simulates the final gas phase equilibrium. Thus, this model considers char formation depending on the reactor conditions and chemical kinetics are of concern. The second one considers the total conversion of the fuel and the final gas equilibrium through the minimisation of Gibb's free energy at the gasifier temperature and restricted to a set of chemical compounds. The temperature in this case is determined by the heat of formation of the raw material and the cooling of ashes. The residence time of particles is calculated for this specific thesis gasifier case study to infer how close to equilibrium the system is. The implementation of kinetic and equilibrium models using different process simulation environments is discussed in the next sections. Model calibration and validation contrasted with power or pilot plant data, as well as results generation by means of sensitivity analyses are described.

As mentioned in Chapter 3, the final superstructure has been developed in Aspen Plus. Nevertheless, as a prior step to this final model, an Aspen Hysys-Aspen Plus superstructure was developed to benefit from the easiness from Aspen Hysys to handle non-conventional compounds and custom models. Therefore, the kinetic model of the gasifier is developed in Aspen Hysys, and the equilibrium model is developed in Aspen Plus.

4.2 Physicochemical representation of the system

One important aspect in modelling coal, petcoke and biomass is the difficulty to find appropriate models to represent and estimate their physicochemical behaviour. Most simulation environments provide the possibility of representing non-conventional chemical compounds, understood as those that do not have an integer molecular representation. Typically any of the abovementioned raw materials can be represented with a molecular formula such as $C_aH_b\ O_cN_dS_e(H_2O)_wA$, while any treated raw material would be converted into $C_\alpha H_\beta O_\gamma N_\delta S_\epsilon A$. In both cases A represents the ashes content of the material(s).

The materials enthalpy and density can be extrapolated from the ultimate and proximate analyses. ULTANAL and PROXANAL properties, available in Aspen Plus, allow to define a non-conventional compound. Regarding the behaviour of the gas phase, an equation of state (EOS) is selected from the wide variety of EOS within the Aspen Plus software package. This selection is mainly driven by the possibility of estimating properties accurately near critical points. The Peng-Robinson EOS is accepted for hydrocarbons and light gases.

In Aspen Hysys, the components of the solid (C, H, O, N, S) and ashes are introduced as Hypo-Components, specifying their molecular weight, density, critical properties, normal boiling point and heat of formation. The heterogeneous kinetic reactions are introduced into Aspen Hysys as a custom model, through a kinetic reaction extension that depends on the composition of the solid. The pyrolysis step has been modelled as a complete unit operation extension. The Peng-Robinson EOS is also used.

4.3 Chemical kinetics approach

This approach is similar to that developed by Wen and Chaung (1973) and Govind and Shah (1984) for coal gasification. Aspen Hysys is the software selected for modelling. The proposed gasifier model encompasses a sequence of four main steps: (i) pyrolysis and volatiles combustion, (ii) oxidation, (iii) gasification and (iv) gas equilibrium. The main assumptions are:

- Steady state and one dimension.
- Oxidation and gasification zones have uniform temperatures with adiabatic behaviour; consequently the considered overall reactor is a non-isothermal reactor.
- The fuel particle level is of concern. The *unreacted-core-shrinking model* describes the solid-gas reactions. Chemical reactions occur on a spherical surface and are considered to proceed from the surface till the particle's core, without any release of mineral matter, which is considered inert. The transportation considerations comprise the chemical reaction itself, ashes layer diffusion and surface convection, from the inner to the outside face of the particle. Kinetic constants for solid-gas reactions are as follows:

$$\frac{1}{k_t} = \frac{1}{h_{gas}} + \frac{Y-1}{Y} \cdot \frac{1}{k_{ash}} + \frac{1}{Y^2 k_q} \tag{4.1}$$

  Where, k_t is the specific reaction rate; h_{gas} is the external convection coefficient; k_{ash} is the specific rate of gas diffusion through the ash layer, and k_q is the chemical rate constant (that follows the Arrhenius law). Y is the ratio between the particle and the core radius's.

- Particles interactions are not considered.
- The temperature within the particle is uniform.
- Solid and gas phases are assumed to be completely inter-mixed. Consequently, the approach considers the simulation of each reactor section using continuous stirred tank reactors (CSTR) in series, one tank for each step: volatiles combustion, oxidation, gasification and gas equilibrium. In turn, the pyrolisys step is modelled through a unit operation extension.

(i) *Pyrolysis* is the decomposition of the feedstock into solid (char) and volatiles, in the absence of oxygen and due to the effect of temperature. The raw material and char are represented with their molecular formulas as previously described, $\mathrm{C}_a\mathrm{H}_b\mathrm{O}_c\mathrm{N}_d\mathrm{S}_e(\mathrm{H_2O})_w\mathrm{A}$ and $\mathrm{C}_\alpha\mathrm{H}_\beta\mathrm{O}_\gamma\mathrm{N}_\delta\mathrm{S}_\epsilon\mathrm{A}$, respectively. In both cases, A represents the ash content. For instance, the mixture of coal and petcoke from ELCOGAS power plant is $\mathrm{CH_{0.5681}O_{0.0419}N_{0.0197}S_{0.0203}(H_20)_{0.1111}Z}$ in ar basis (from Table 4.4). Eq. (4.2) represents the pyrolysis step in general terms.

$$\mathrm{C}_a\mathrm{H}_b\mathrm{O}_c\mathrm{N}_d\mathrm{S}_e(\mathrm{H_2O})_w\mathrm{A} \quad \longrightarrow \quad \mathrm{C}_\alpha\mathrm{H}_\beta\mathrm{O}_\gamma\mathrm{N}_\delta\mathrm{S}_\epsilon\mathrm{A} + \mathrm{volatiles} + w\mathrm{H_2O} \tag{4.2}$$

Raw material and char are modelled in the software as Hypo-Components, since the default options in Aspen Hysys do not allow to handle with solids with such complex stoichiometry. Both, raw material and char, are introduced as different proportions of C, H, O, N, S and A. The molecular formula of char is calculated based on experimental correlations from Badzioch and Hawsley (1970), which state the total amount of volatiles released based on the reactor temperature and raw material volatile matter, from the proximate analysis. According to the authors, coal devolatilisation corresponds to a first order kinetic process. Eq. (4.3) calculates the amount of volatiles released, that is the amount of raw material converted into volatiles. The parameter ξ_V adapts the percentage of volatiles from the proximate analysis, i.e. V_{PA} in daf basis, to the percentage of volatiles that are really released (V_r), at atmospheric pressure. Eqs. from (4.4) to (4.8) are used to calculate ξ_V, which is based on experimental data. ξ_R and ξ_Q corresponds to the amount of volatile matter that remains in char and the losses of dry matter due to volatilisation, respectively.

$$\begin{aligned} V_r &= \xi_V \cdot V_{PA} && (4.3) \\ \xi_V &= \xi_Q \cdot (1 - \xi_R) && (4.4) \\ \xi_R &= e^{-\xi_1 \cdot (T - \xi_2)} && (4.5) \end{aligned}$$

$$\begin{aligned} \xi_1 &= 6.56 - 0.23 \cdot \mathrm{C_o} + 2.79 \cdot 10^{-3} \cdot \mathrm{C_o}^2 - 1.1 \cdot 10^{-5} \cdot \mathrm{C_o}^3 && (4.6) \\ \xi_2 &= 521210 - 20120 \cdot \mathrm{C_o} + 254.95 \cdot \mathrm{C_o}^2 - 1.1 \cdot \mathrm{C_o}^3 && (4.7) \end{aligned}$$

$$\xi_Q = -1.52 + 0.04 \cdot \mathrm{C_o} \qquad (4.8)$$

Where, T is the assumed pyrolysis temperature in K and C_o is the amount of carbon in the raw material on daf mass percentage. The experimental sample analysed has a carbon value between 80% and 92%.

As the gasification process considered takes place in a pressurised entrained flow bed gasifier (PRENFLO), the V_r value is corrected by Eq. (4.9) (Anthony & Howard, 1976). This expression adds the effect of the pressure in the pyrolysis step. P is in atm. The range covered through the performed experimental analysis is from 0.1 atm to 50 atm.

$$V_r* = V_r \cdot (1 - 0.066 \cdot \ln P) \qquad (4.9)$$

Loison and Chauvin (1964) define volatiles composition (distribution of mainly C, H, O) based on experimental knowledge. To facilitate its estimation and simplify the model, tars formation is considered as only C_6H_6 production. However, other approaches could supply a set of typical aromatic compounds to be produced if data become available. Volatiles should be in the range of 10% to 40%. The components result is given in volume percentages on a daf basis of the final mixture composed by tars, water and gases species (V_{tar}, $V_{\mathrm{H_2O}}$ and V_{gas}). See the detailed expressions in Eqs. (4.10) to (4.17). Eqs. from (4.13) to (4.17) represent the percentages of volume of each element inside the gas phase.

$$
\begin{aligned}
V_{tar} &= -20.6 + 2.6 \cdot V_{PA} - 0.04 \cdot V_{PA}^2 && (4.10)\\
V_{\mathrm{H_2O}} &= 1.32 \cdot e^{(0.03 \cdot V_{PA})} && (4.11)\\
V_{gas} &= V_r * -V_{tar} - V_{\mathrm{H_2O}} && (4.12)\\
\%\mathrm{H_2} &= 60.21 + 0.89 \cdot V_{PA} - 0.03 \cdot V_{PA}^2 && (4.13)\\
\%\mathrm{CH_4} &= 57.37 - 0.78 \cdot V_{PA} - \frac{415.92}{V_{PA}} && (4.14)\\
\%\mathrm{CO} &= -31.52 + 1.05 \cdot V_{PA} - \frac{315.42}{V_{PA}} && (4.15)\\
\%\mathrm{CO_2} &= -5.35 + 0.23 \cdot V_{PA} + \frac{53.16}{V_{PA}} && (4.16)\\
\%\mathrm{HCN} &= 100 - (\%\mathrm{H_2} + \%\mathrm{CH_4} + \%\mathrm{CO} + \%\mathrm{CO_2}) && (4.17)
\end{aligned}
$$

The generation of the acid and basic species from N, S, combined with C, H, O (NH_3, HCN, H_2S and COS) is crucial in the considered approach, since the purpose of cleaning units is to release separately solids, acid and basic compounds. Their presence is calculated through experimental correlations deduced from the data from Kambara and Takarada (1993) and García-Labiano and Adánez (1996). See the related expressions in Eqs. (4.18), (4.19) and (4.20). C_o, N_o and S_o are those constituents proportion in raw material on daf mass percentage and on dry mass percentage for the latter. The final percentages obtained correspond to the percentages of inlet N_o and S_o, that are transformed into the named components, on a mass basis. T is the assumed pyrolysis temperature in K. The remaining N and S stay in the char. HCl is directly formed from the Cl fraction present at the inlet flow.

$$
\begin{aligned}
\%\mathrm{NH_3} &= 0.05 \cdot \left(\frac{\mathrm{N}_o}{\mathrm{C}_o}\right)^3 - 0.17 \cdot \left(\frac{\mathrm{N}_o}{\mathrm{C}_o}\right)^2 - 0.74 \cdot \frac{\mathrm{N}_o}{C_o} + 0.77 && (4.18)\\
\%\mathrm{H_2S} &= 0.41 \cdot S_o \cdot [80.8 + 0.007 \cdot (T - 1073)] && (4.19)\\
\%\mathrm{COS} &= 0.41 \cdot S_o \cdot [10.8 + 0.002 \cdot (T - 1073)] && (4.20)
\end{aligned}
$$

The volatile species at the end of this step are CO, H_2, CH_4, CO_2, C_6H_6, H_2S, COS, NH_3 and HCN. The larger fractions are from hydrogen, methane and tars. The model allows for changes in the raw material composition, the volatile fraction in dry basis and the average mass of ashes, assumed of 56 kg/mol in this case study, following ELCOGAS data. The abovementioned system of equations (from Eq.4.3 to Eq. 4.20) have been introduced in Aspen Hysys by means of a unit operation extension coded in MS Visual Basic.

Volatiles combustion occurs when the volatiles released in the pyrolysis step are in presence of oxygen. The complete transformation of volatiles compounds into CO_2 and H_2O is assumed. Eqs. (4.21) to (4.24) represent the main volatiles combustion reactions. These reactions are introduced in Aspen Hysys through a conversion reactor, in which the limiting reactants are CO, H_2, CH_4 and C_6H_6.

$$\mathrm{CO} + 0.5\mathrm{O_2} \longrightarrow \mathrm{CO_2} \quad (4.21)$$

$$\mathrm{H_2} + 0.5\mathrm{O_2} \longrightarrow \mathrm{H_2O} \quad (4.22)$$

$$\mathrm{CH_4} + 2\mathrm{O_2} \longrightarrow \mathrm{CO_2} + 2\mathrm{H_2O} \quad (4.23)$$

$$\mathrm{C_6H_6} + 7.5\mathrm{O_2} \longrightarrow 6\mathrm{CO_2} + 3\mathrm{H_2O} \quad (4.24)$$

(ii) *Oxidation* or *combustion* refers to char combustion and it is assumed to occur after the combustion of volatiles compounds. It comprises Eq. (4.25) which is a heterogeneous (solid-gas, SG) and exothermal reaction. This step is considered complete when all the remaining oxygen is consumed.

$$\begin{aligned} &\mathrm{C}_\alpha\mathrm{H}_\beta\mathrm{O}_\gamma\mathrm{N}_\delta\mathrm{S}_\epsilon\mathrm{A} + (\alpha/2 - \gamma/2 + \beta/4 - \epsilon/2)\mathrm{O}_2 \\ &\qquad \longrightarrow \alpha\mathrm{CO} + (\beta/2 - \epsilon)\mathrm{H}_2\mathrm{O} + \epsilon\mathrm{H}_2\mathrm{S} + \delta/2\mathrm{N}_2 + \mathrm{A} \end{aligned} \tag{4.25}$$

(iii) *Gasification* follows the oxidation step and it is assumed to start with the depletion of oxygen. Nevertheless, Eqs. (4.26) and (4.27) can start during the combustion stage. It is assumed that all SG and endothermic reactions occur in this step. The main gasification reaction is Eq. (4.28), in which the produced H_2 reacts with char. This step is assumed to be finished when all char is consumed, since a PRENFLO gasifier has a very low amount of char. Otherwise, it can take into account the procedure kinetics. The proportion of char that reacts into each equation is equally distributed.

$$\begin{aligned} &\mathrm{C}_\alpha\mathrm{H}_\beta\mathrm{O}_\gamma\mathrm{N}_\delta\mathrm{S}_\epsilon\mathrm{A} + (\alpha - \gamma)\mathrm{H}_2\mathrm{O} \\ &\qquad \longrightarrow \alpha\mathrm{CO} + (\alpha - \gamma + \beta/2 - \epsilon)\mathrm{H}_2 + \epsilon\mathrm{H}_2\mathrm{S} + \delta/2\mathrm{N}_2 + \mathrm{A} \end{aligned} \tag{4.26}$$

$$\begin{aligned} &\mathrm{C}_\alpha\mathrm{H}_\beta\mathrm{O}_\gamma\mathrm{N}_\delta\mathrm{S}_\epsilon\mathrm{A} + \alpha\mathrm{CO}_2 \\ &\qquad \longrightarrow 2\alpha\mathrm{CO} + \gamma\mathrm{H}_2\mathrm{O} + (\beta/2 - \epsilon - \gamma)\mathrm{H}_2 + \epsilon\mathrm{H}_2\mathrm{S} + \delta/2\mathrm{N}_2 + \mathrm{A} \end{aligned} \tag{4.27}$$

$$\begin{aligned} &\mathrm{C}_\alpha\mathrm{H}_\beta\mathrm{O}_\gamma\mathrm{N}_\delta\mathrm{S}_\epsilon\mathrm{A} + (2\alpha + \gamma + \epsilon - \beta/2)\mathrm{H}_2 \\ &\qquad \longrightarrow \alpha\mathrm{CH}_4 + (\gamma)\mathrm{H}_2\mathrm{O} + \epsilon\mathrm{H}_2\mathrm{S} + \delta/2\mathrm{N}_2 + \mathrm{A} \end{aligned} \tag{4.28}$$

Eqs. (4.29) to (4.46) are implemented using chemical extensions written in MS Visual Basic. k_t, each specific reaction rate, is calculated through Eq. (4.1). The expressions needed to completely define the kinetics from the abovementioned equations (Wen & Chaung, 1973; Govind & Shah, 1984; Usón, 2001) are as follows, and for Eqs. (4.25), (4.26), (4.27) and (4.28), respectively:

$$k_q = 8710 \cdot e^{(-17967/T_s)} \tag{4.29}$$

$$h_{gas} = \frac{0.292 \cdot \phi \cdot \left(\frac{4.26}{T_g}\right)\left(\frac{T_g}{1800}\right)^{1.75}}{P_{gasif} \cdot d_p} \tag{4.30}$$

$$k_{ash} = h_{gas} \cdot \varepsilon_p^{2.5} \tag{4.31}$$

$$r = k_t \cdot p_{\mathrm{O}_2} \tag{4.32}$$

$$k_q = 247 \cdot e^{(-21060/T_s)} \tag{4.33}$$

$$h_{gas} = \frac{10 \cdot 10^{-4} \cdot \left(\frac{T_g}{2000}\right)^{0.75}}{P_{gasif} \cdot d_p} \tag{4.34}$$

$$k_{ash} = h_{gas} \cdot \varepsilon_p^{2.5} \tag{4.35}$$

$$r = k_t \cdot \left(p_{\mathrm{H_2O}} - \frac{p_{\mathrm{H}_2} - p_{\mathrm{CO}}}{K_{\mathrm{H_2O}}}\right) \tag{4.36}$$

$$K_{\mathrm{H_2O}} = e^{(17.644 - \frac{30260}{1.8T_s})} \tag{4.37}$$

$$k_q = 247 \cdot e^{(-21060/T_s)} \tag{4.38}$$
$$h_{gas} = \frac{7.45 \cdot 10^{-4} \cdot \left(\frac{T_g}{2000}\right)^{0.75}}{P_{gasif} \cdot d_p} \tag{4.39}$$
$$k_{ash} = h_{gas} \cdot \varepsilon_p^{2.5} \tag{4.40}$$
$$r = k_t \cdot p_{\mathrm{CO_2}} \tag{4.41}$$

$$k_q = 0.12 \cdot e^{(-17921/T_s)} \tag{4.42}$$
$$h_{gas} = \frac{1.33 \cdot 10^{-3} \cdot \left(\frac{T_g}{2000}\right)^{0.75}}{P_{gasif} \cdot d_p} \tag{4.43}$$
$$k_{ash} = h_{gas} \cdot \varepsilon_p^{2.5} \tag{4.44}$$
$$r = k_t \cdot (p_{\mathrm{H_2}} - \sqrt{p_{\mathrm{CH_4}}/K_{\mathrm{H_2}}}) \tag{4.45}$$
$$K_{\mathrm{H_2}} = \frac{0.175}{34713} e^{\left(\frac{18400}{1.8 T_s}\right)} \tag{4.46}$$

In the abovementioned equations, r is the reaction rate and k's and rates are given in $\mathrm{g/cm^2 s \cdot atm}$. Temperatures are in K. T_s is the temperature of the solid or particle, while T_g is the temperature of the gas. P_{gasif} is the pressure in the gasifier in atm and d_p is the diameter of the particle. ε_p is the internal porosity of the ash layer, assumed to be 0.5. In r's calculation, p_i are partial pressures. ϕ is a parameter that depends on the mechanism that has a value of 2, according to Wen and Chaung (1973). The particle is assumed to be 55 μm and the overall surface of reaction results in $5 \cdot 10^5 \mathrm{m}^2$, taking into account a porosity of 0.1, 5.6 m of diameter and 15 m of height, as in the gasification reactor of ELCOGAS.

(iv) As last stage, the final produced gas from the SG reactions enters into an equilibrium reactor. This *gas equilibrium* is performed with three main reactions, Eqs. (4.47), (4.48) and (4.49). The equilibrium constants are extracted from Aspen Hysys library.

$$\mathrm{CO + H_2O \longleftrightarrow CO_2 + H_2} \tag{4.47}$$
$$\mathrm{CH_4 + H_2O \longleftrightarrow CO + 3H_2} \tag{4.48}$$
$$\mathrm{COS + H_2O \longleftrightarrow H_2S + CO_2} \tag{4.49}$$

Summing up, one isothermal zone comprises volatiles and char combustion. The other one is for gasification. As an adiabatic reactor is considered for this autothermal gasification process, all the heat released in the combustion is used for the gasification step. Figure 4.1 depicts a scheme of the modelled steps and the heat integration consideration. All heat streams are included in a balance unit. Thus, allowing for heat distribution from exothermic to endothermic reactors.

Before leaving the gasification reactor, the syngas is sent to an ashes distribution model that splits the solid stream into slag and fly ashes, based on industrial data. This component splitter takes into account a base ashes composition built on the same industrial data from ELCOGAS power plant. It has been considered that ashes

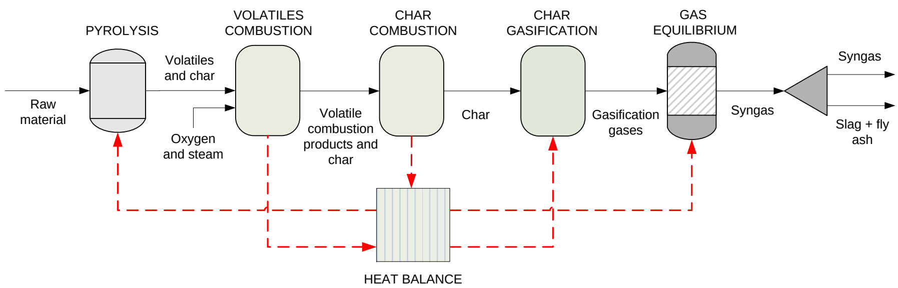

Figure 4.1: Modelling blocks for the proposed chemical kinetics approach.

are composed by metal oxide and heavy metals present at very low concentrations and as pure compounds. The mixture of components in the characterised ashes are represented by a limited number of constituents which are, in a coal:petcoke blend, Al_2O_3, SiO_2, As, Cd, Cr, Cu, Hg, Ni, Pb, Zn, Se and B. The metals taken into account are those that legislation enforces the control. The selected oxides are those present at larger proportions. This model is introduced in Aspen Hysys as a unit operation extension, and the data comes from the work developed in Jaume Almera Institute (CSIC, Barcelona). Table 4.1 lists the split fractions attributed to each element on a mass basis.

Table 4.1: Ash components distribution into slag and fly ash after gasification, on a mass percentage.

Ash component	Slag	Fly ash
Al_2O_3	0.9	0.1
SiO_2	0.9	0.1
As	0.1	0.9
Cd	0.1	0.9
Cr	0.8	0.2
Cu	0.5	0.5
Hg	0.0	1.0
Ni	0.7	0.3
Pb	0.0	1.0
Zn	0.0	1.0
Se	0.2	0.8
B	0.3	0.7

4.4 Equilibrium approach

A thermo-chemical equilibrium is a stable state that can be determined by thermodynamic methods, not being necessary a detailed knowledge of the reaction mechanisms (Borel & Favrat, 2010). One of the most extended approaches to model a gasification process consider the thermochemical equilibrium and minimise Gibbs free energy, by taking into account the final species composition (see Section 2.2.1).

The equilibrium constant K_{eq} is given by the following expression, for a generic reaction and assuming an ideal gas behaviour:

$$aA + bB \longleftrightarrow cC + dD \tag{4.50}$$

$$K_{eq} = \frac{p_C^c \cdot p_D^d}{p_A^a \cdot p_B^b} = \frac{x_C^c \cdot x_D^d}{x_A^a \cdot x_B^b} \cdot p^{(c+d-a-b)} \tag{4.51}$$

$$f(T) = \log(K_{eq}) = k_1 + k_2 T^{-1} + k_3 \cdot \log T + k_4 \cdot T + k_5 \cdot T^2 \tag{4.52}$$

For the case of a reaction like Eq. (4.50), K_{eq} can be expressed as a function of partial pressures as shown in Eq. (4.51), where P is the pressure at which the reaction takes place and T is the temperature. Typically K_{eq} can be calculated as in Eq. (4.52) as a function of the absolute temperature in K. k_n are particular constants for each reaction.

Eq. (4.51) expresses the equilibrium composition dependence on the system's pressure, reactants and products mole number. If the numbers of moles on the products side is identical to the number of moles on the reactants side, the total pressure does not have influence on the final composition; the *Le Châtelier's principle* provides with a general overview of the gasification reactions as equilibrium reactions. In the equilibrium state, if one of the factor of the system changes its value, i.e. pressure, temperature, volume or partial pressures, the system reacts to counteract the change and equilibrium is restored to new conditions. For instance, if the temperature increases in an endothermic reaction, the reaction will tend to react to the products side. Otherwise, if the total pressure increases, the partial pressure of the individual gas species increases as well. Then, the global system tends to shift the reaction to the side with less number of moles.

Gasification reactions can be described by many different equations, but they may be limited to a certain number of representative expressions since the reaction enthalpy of some of them can be derived by combining those representative ones. To calculate the associated heat streams, that is the integration between endothermic and exothermic reactions; a limitation to certain characteristic reaction groups is enough, because the reaction enthalpy of all other reactions can be derived by combining these elementary reactions. The most characteristic gasification reactions are given by Eqs. (4.53) to (4.62), and correspond to reactions with O_2, H_2O, CO_2 and H_2. For each reaction, the gas mole difference between products and reactants is indicated. Although the solid raw material composition is based on C, H, O, N and S, the main reactions only involve C as reactant (in contrast to the previous approach). Eqs. (4.53) to (4.55) correspond to combustion. Eq. (4.56) is the Boudouard reaction. Eq. (4.57) is the primary water-gas shift and Eq. (4.58) is the secondary water-gas shift. Eq. (4.59) is the water-gas shift reaction with gas species only, and Eq. (4.60) is the methanation reaction. Eqs. (4.61) and (4.62) correspond to methane steam and dry reforming. As reactions with oxygen are complete under gasification conditions, the main final composition influence come from Eqs. (4.56) to (4.60) in terms of equilibrium (Highman & van der Burght, 2003; Fermoso *et al.*, 2009).

Table 4.2: Equilibrium constants for the gasification equations at different temperatures (AspenTech, 2010).

Eq. #	K_{eq} units	800°C	1000°C	1200°C	1400°C	1600°C	1800°C
(4.53)	$bar^{0.5}$	$1.057 \cdot 10^{10}$	$1.339 \cdot 10^{9}$	$2.799 \cdot 10^{8}$	$8.019 \cdot 10^{7}$	$2.838 \cdot 10^{7}$	$1.164 \cdot 10^{7}$
(4.54)	$bar^{-0.5}$	$1.643 \cdot 10^{9}$	$1.147 \cdot 10^{7}$	$3.118 \cdot 10^{5}$	$2.027 \cdot 10^{4}$	$2.382 \cdot 10^{3}$	$4.261 \cdot 10^{2}$
(4.55)	$bar^{-0.5}$	$1.512 \cdot 10^{9}$	$1.893 \cdot 10^{7}$	$7.693 \cdot 10^{5}$	$6.676 \cdot 10^{4}$	$9.725 \cdot 10^{3}$	$2.050 \cdot 10^{3}$
(4.56)	bar	6.430	$1.168 \cdot 10^{2}$	$8.976 \cdot 10^{2}$	$3.956 \cdot 10^{3}$	$1.191 \cdot 10^{4}$	$2.732 \cdot 10^{4}$
(4.57)	bar	6.986	$7.074 \cdot 10^{1}$	$3.638 \cdot 10^{2}$	$1.201 \cdot 10^{3}$	$2.918 \cdot 10^{3}$	$5.679 \cdot 10^{3}$
(4.58)	bar	7.591	$4.285 \cdot 10^{1}$	$1.474 \cdot 10^{2}$	$3.647 \cdot 10^{2}$	$7.147 \cdot 10^{2}$	$1.181 \cdot 10^{3}$
(4.59)	-	1.087	$6.057 \cdot 10^{-1}$	$4.053 \cdot 10^{-1}$	$3.036 \cdot 10^{-1}$	$2.449 \cdot 10^{-1}$	$2.079 \cdot 10^{-1}$
(4.60)	bar^{-1}	$4.248 \cdot 10^{-2}$	$8.027 \cdot 10^{-3}$	$2.263 \cdot 10^{-3}$	$8.252 \cdot 10^{-4}$	$3.583 \cdot 10^{-4}$	$1.759 \cdot 10^{-4}$
(4.61)	bar^{2}	$1.645 \cdot 10^{2}$	$8.813 \cdot 10^{3}$	$1.608 \cdot 10^{5}$	$1.455 \cdot 10^{6}$	$8.143 \cdot 10^{6}$	$3.229 \cdot 10^{7}$
(4.62)	bar^{2}	$1.513 \cdot 10^{2}$	$1.455 \cdot 10^{4}$	$3.967 \cdot 10^{5}$	$4.794 \cdot 10^{6}$	$3.325 \cdot 10^{7}$	$1.554 \cdot 10^{8}$

$$C + 0.5O_2 \longleftrightarrow CO \qquad \Delta n = 0.5 \tag{4.53}$$

$$CO + 0.5O_2 \longleftrightarrow CO_2 \qquad \Delta n = -0.5 \tag{4.54}$$

$$H_2 + 0.5O_2 \longleftrightarrow H_2O \qquad \Delta n = -0.5 \tag{4.55}$$

$$C + CO_2 \longleftrightarrow 2CO \qquad \Delta n = 1 \tag{4.56}$$

$$C + H_2O \longleftrightarrow CO + H_2 \qquad \Delta n = 1 \tag{4.57}$$

$$C + 2H_2O \longleftrightarrow CO_2 + 2H_2 \qquad \Delta n = 1 \tag{4.58}$$

$$CO + H_2O \longleftrightarrow CO_2 + H_2 \qquad \Delta n = 0 \tag{4.59}$$

$$C + 2H_2 \longleftrightarrow CH_4 \qquad \Delta n = -1 \tag{4.60}$$

$$CH_4 + H_2O \longleftrightarrow CO + 3H_2 \qquad \Delta n = 2 \tag{4.61}$$

$$CH_4 + CO_2 \longleftrightarrow CO + 2H_2 \qquad \Delta n = 2 \tag{4.62}$$

Table 4.2 provides with a compilation of the equilibrium constant values and its temperature dependence for the above reactions at 25 bar. Gasification temperature range is estimated between 800°C and 1800°C, based on the characteristics described in Chapters 1 and 2. The K_{eq} values are extracted from Aspen Plus by means of a REquil reactor. The feedstock used is coal:petcoke at 50:50 in weight, with oxygen as the gasifying agent. This follows the ELCOGAS configuration.

Eqs. (4.53), (4.54) and (4.55) have oxygen as reactant, therefore they are exothermic. Also Eqs. (4.59) and (4.60) are exothermic. According to *Le Châtelier's principle*, K_{eq} decreases since the reaction tends to move to the reactants side. The opposite behaviour is seen in the endothermic reactions. As the temperature increases they tend to move towards the product side, thus increasing K_{eq}. High values of K_{eq} describe a reaction that is further displaced to the reactants side. In contrast, low K_{eq} values represent a reaction further displaced to the products side.

4.4.1 Residence time considerations

An important assumption to model gasification with an equilibrium reactor is that the residence time should be high enough to reach the equilibrium state, allowing for the highest solid conversion. If the residence time is not enough to reach the highest conversion rate, it can be compensated by an increase of temperature.

Table 4.3: Input data to calculate the residence time and the reactor pressure drop. Specific data is from ELCOGAS.

d_p (m)	$5.5{\cdot}10^{-5}$
D (m)	3.8
L (m)	60
U_g (m/s)[1]	8
Particles inlet mass flow (kg/s)	21.15
ρ_p (kg/m^3)[1]	1200
ρ_f (kg/m^3)[1]	1.2
Inlet gas P (N/m^2)	$3.33{\cdot}10^6$
μ_f (Pa·s)[1]	$1{\cdot}10^{-5}$

[1]Values from Kunzing (1981).

In order to estimate the gasifier reactor residence time, the SG pneumatic transfer by Kunzing (1981) is used. The residence time t_r calculation is the result of a particle force balance that considers the effect of weight (gravity force, g), the drag force (the drag component is the aerodynamic force component parallel to the gas flow) and the solid friction loss. In vertical transport of solids, like in an entrained bed gasifier, the gas velocity is reduced to the transport of solids velocity, thus decreasing the pressure drop. The overall pressure drop is calculated as the contribution of the static, frictional and acceleration phenomena. The particle velocity U_p is of concern. It is calculated as the difference between the velocity of the transport fluid without particles, U_g, and the terminal velocity, U_t (see Eq. 4.64). This last is defined as the velocity reached when the drag force is equal to the particle weight minus the buoyant force (see Eq. 4.63). The residence time is the fraction of the length of the reactor L between U_p (see Eq. 4.65). The necessary inputs for the calculation are shown in Table 4.3, where ρ_p and ρ_f are the solid and the fluid densities, d_p is the particle diameter and μ_f is the fluid dynamic viscosity. A superficial gas velocity of 8 m/s implies a dilute phase regime. For the sake of simplicity, the solid is considered as coal and the fluid as air. The calculated residence time is 7.7 s.

$$U_t = \frac{0.153 \cdot g^{0.71} \cdot d_p^{1.14} \cdot (\rho_p - \rho_f)^{0.71}}{\rho_f^{0.29} \cdot \mu_f^{0.43}} \tag{4.63}$$

$$U_p = U_t - U_g \tag{4.64}$$

$$t_r = \frac{L}{U_p} k_{ash} = h_{gas} \cdot \varepsilon_p^{2.5} \tag{4.65}$$

The reactor pressure drop is evaluated as well. Voidage, solid and gas friction factors are of concern (Kunzing, 1981). It results a pressure drop of 10^{-2} bar, practically negligible. In Section 4.5.1, the residence time is verified regarding if it is enough to reach the equilibrium status.

4.5 PRENFLO gasifier model

The *superstructure* construction starts with the gasifier reactor and the associated feedstock preparation system. The modelled gasifier is a PRENFLO gasifier. This is the most frequent reactor used in IGCC plants (Highman & van der Burght, 2003). In such gasifiers ashes melt into slag. Consequently, they produce syngas with notably low emission of fly ashes, while the char conversion, hence the process efficiency, is higher than for other types of gasifier (Section 2.2.1). In this modelling approach, the syngas is mainly used to produce electricity in an IGCC plant. The *gasification block* comprises the gasifier itself and the waste heat boiler (WHB). This last uses waste heat from the process of cooling down the syngas before it enters the cleaning units to produce steam for the combined cycle (CC). Before the gasification process itself, the feedstock must be conditioned to the gasifier requirements, in terms of moisture content (MC) and particle size. Entrained flow gasifiers require the fuel to be converted into small particles (in the order of μm), which calls for a previous milling step. Moreover, they usually use oxygen-enriched air (around 85% on a molar basis) and steam as gasification and moderator agents. The EOS recommended to model gas phase systems at high to medium pressure is the Peng-Robinson EOS with the Boston-Mathias alpha function (PR-BM). The following assumptions are considered:

- The gasifier is performed by means of an equilibrium approach minimising Gibb's free energy.
- The result syngas has no char.
- Tars and synergetic effects between biomass and fossil fuels are not considered.
- If processing biomass, no technological limits exist due to its fibrous nature. It is therefore assumed that any type of biomass that goes into the system has the appropriate characteristics to be pre-processed like coal.

The *feedstock dust preparation* step includes the feedstock dust preparation itself, the drying, the pressurisation and the gasifier feeding. Other pre-treatment options account for raw material properties enhancement, such as pyrolysis and torrefaction that improve the LHV of the mixture, which are disregarded here. The composition of the *base case* coincides with the base composition of ELCOGAS for validation purposes. It corresponds to a 50:50 mixture of coal and petcoke on a mass basis. The coal comes from the local ENCASUR mines and is sub-bituminous with high ash content. The petroleum coke or petcoke has high sulphur content and comes from the Puertollano REPSOL refinery, where it is obtained as a by-product. The residual biomass used as feasible waste for the co-gasification analyses in the IGCC power plant is olive pomace or orujillo, which is the solid residue that remains after pressing olives. Table 4.4 shows the main data for the feedstock composition. The HHV of the three fuels is taken into account when the data are introduced into the simulator. In addition, limestone is fed into the gasifier as an additive to reduce the ash fusion temperature. The limestone contains 95% $CaCO_3$ and 5% ashes. It is roughly 2-3% in weight of the total feedstock introduced into the system, which is fixed regardless of the blend used.

The model allows for mass composition changes in the coal, petcoke, and orujillo blend using a FORTRAN code introduced by means of a calculator block, to calculate the ultimate and proximate analyses and the HHV of the blend, on the basis of each fuel flow. The maximum feedstock flow is 2600 t/day, which corresponds to 100% of the gasifier/plant load. The FORTRAN code also takes into account the plant load. The *dust preparation* takes place in a crusher unit so that the inlet fineness can be changed from about 100 mm to 50-60 μm. Additional information to be introduced is the mixture's grindability, characterised by the Bond work index[1]. This is calculated in a

[1] This is defined as the energy required to grind a specific material, being the most common measure of grindability.

Table 4.4: Ultimate and proximate analyses of raw materials (Coca, 2003; ECN-Biomass, 2010).

% mass basis (dry)	Coal	Petcoke	Orujillo
Ultimate analysis			
C	41.07	88.40	50.00
H	2.81	3.34	6.50
O	7.51	0.02	36.30
N	0.92	2.04	0.80
S	1.05	5.91	0.10
Cl	0.04	0.00	0.20
Proximate analysis			
Moisture	11.80	7.00	7.60
Ashes	46.60	0.28	6.30
Fixed carbon	32.05	85.74	21.3
Volatiles	21.35	13.98	72.4
HHV_{dry} (MJ/kg)	13.58	32.65	20.38

calculator block using a FORTRAN code and taking into account the mass proportion of each component. The Bond index values are 73.80 kWh/t for petcoke and 11.37 kWh/t for coal. The orujillo is taken to have the same value as the coal. Since limestone is not in the consulted database, the Bond work index for dolomite is used, which is 11.31 kWh/t (Perry & Green, 1997). The *fuel drying* step involves two reactors: a combustion chamber, in which hot gases are generated, and the dryer itself, in which the feedstock stream is dried by SG contact. A Gibbs reactor model is used for the combustion chamber, in which natural gas is burnt with an excess of air. The excess of air is established using a calculator block. The air needed for feedstock drying is at 1.2 times the required stoichiometric oxygen. The stoichiometric value of air is calculated using the property set COMB-O2 from Aspen Plus. This reactor operates at 0.93 bar and the temperature is estimated as a fraction of the flame temperature. The dryer is modelled using a stoichiometric reactor with the feed stream as the limiting reactant, to achieve a final moisture content of 2% on a mass basis, as stipulated in a calculator block. Before the powdered fuel enters the gasifier, it is separated from the inert gas in *bag filters*. These are simulated with a flash separator. Before the feed enters the gasifier, it is pressurised at 30 bar inside a *lock hopper* system. This system is simulated in a simplified way as a mixer, taking into consideration the pure N_2 stream. Finally, the mixture is conducted to the gasifier. The three main stages in the feedstock dust preparation block, i.e. dust preparation, drying and conditioning, are summarised in Figure 4.2.

The *gasifier* is based on the Krupp-Koppers gasifier from ELCOGAS power plant. Its input and output data have been used to calibrate the model. The main gasifier operation conditions, pressure and temperature (P_{gasif} and T_{gasif}), are driven by the gas turbine (GT) working pressure and ash melting point, respectively. Thus, the GT pressure sets the gasifier pressure at 25 bar. The gasification temperature is specified to ensure the separation of ashes into molten slag. According to Song *et al.* (2009), this temperature lies between 1400°C and 1500°C for coal, depending on the limestone content. In the model, this temperature interval is established as a condition in gasification when the raw material composition is changed. Specifically, a temperature of 1450°C is fixed as a design specification in Aspen Plus.

The feedstock from the feedstock dust preparation step is a non-conventional stream. Consequently, before it is introduced into the Gibbs reactor it should be

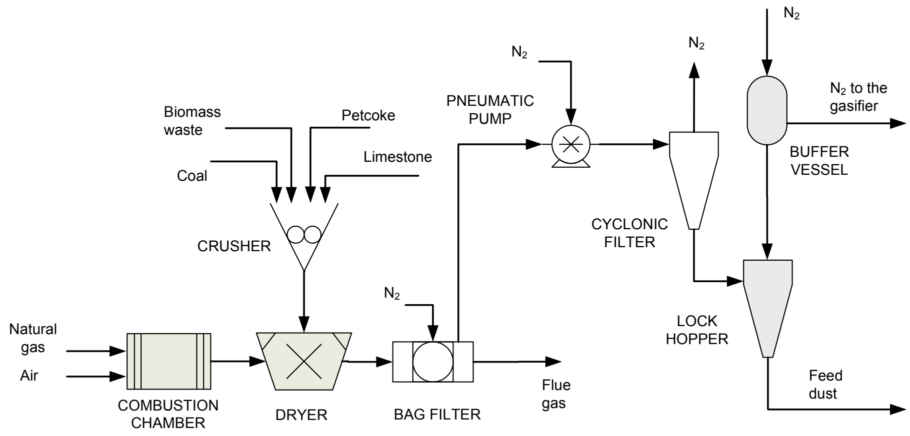

Figure 4.2: Feedstock conditioning step.

divided into its elements, since there is no Gibbs energy information for a non-conventional component. Therefore, before the gasifier itself, a yield reactor is used to decompose the raw material into $C_{graphite}$, H_2, O_2, N_2, S, Cl_2, H_2O and ashes, according to its ultimate analysis and the MC from the proximate analysis. T_{gasif} is estimated by introducing into the Gibbs reactor the heat of reaction associated with the feedstock stream decomposition ($QReaction$) and the heat released into a component separator that separates the raw syngas from the slag, formed by ashes and limestone, ($QSlag$). The diagram of the model is shown in Figure 4.3.

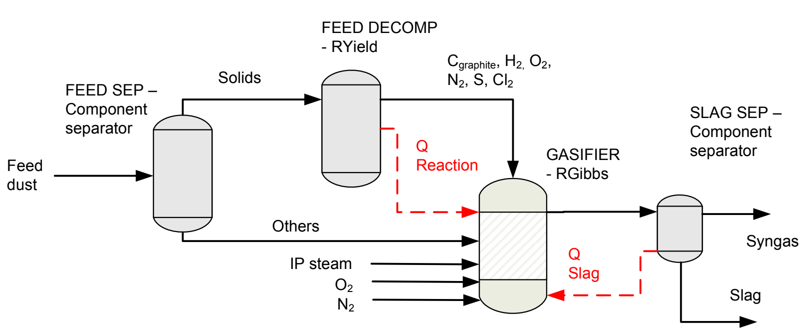

Figure 4.3: Gasifier modelling for the equilibrium approach.

Oxygen from the air separation unit (ASU), which is the main gasifier agent, intermediate pressure (IP) steam and N_2, which mainly act as temperature moderators, are also introduced into the Gibbs reactor. Oxygen and steam flowrates are estimated by specific ratios that depend on the raw material composition, according to its ultimate analysis characteristics. The oxygen ratio is defined as the ratio between the oxygen flowrate and the raw material mixture's stoichiometric oxygen, after decomposition into its components on a molar basis. This quotient is the equivalence ratio (ER). The steam ratio is defined on a mass basis and has the mass flow of

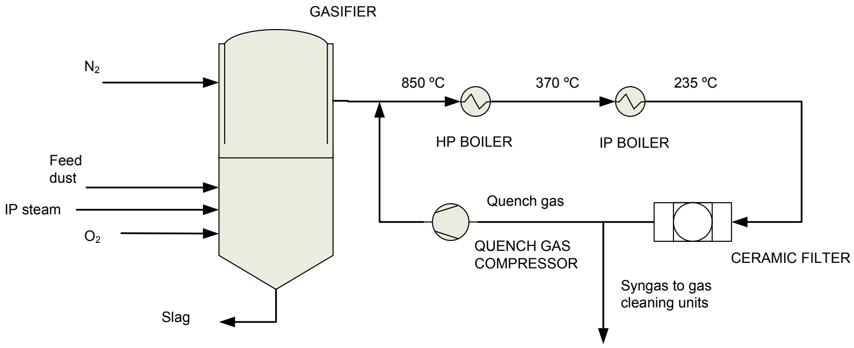

Figure 4.4: Gasifier and WHB.

$C_{graphite}$ as a denominator. The values of these ratios are 0.42 and 0.16, respectively, for the base case. They have been estimated by adjusting the gasification temperature to 1450°C and using the ELCOGAS input conditions, respectively.

The *waste heat boiler* (WHB) is placed after the production of syngas. This HEN uses the heat from cooling the syngas before it enters the gas cleaning units. Syngas cooling takes place in two steps: firstly, the temperature of gasification gases is reduced when they are mixed with the *quench gas*, which is a fraction of the cooled syngas itself that is recycled for this purpose, at around 235°C. In this step, the gases are cooled to 850°C which is close to the heat exchanger's material temperature limits (Coca, 2003). Secondly, in the WHB, the gas heat is recovered in a high pressure (HP) heat exchanger, so that the gas is cooled to 370°C and HP steam is generated. Finally, the gas is moved to an IP heat exchanger that cools it to 235°C and generates IP steam. After this last step, the quench gas is recycled to be mixed at the gasifier outlet. The recycled mass flow is determined by a design specification block, in which the temperature of 850°C is attained by modifying the quench gas flowrate. Gasification and syngas cooling are schematically represented in Fig. 4.4.

4.5.1 Calibration and validation

Gasifier model *calibration*, as well as superstructure calibration, is performed using real ELCOGAS plant working conditions. The purpose is to achieve the best agreement between model predictions and real data while maintaining certain model independence from the ELCOGAS conditions; i.e. keeping the sensitivity to raw material and operating conditions modifications. The model variables which are suitable for calibration are raw material types, feedstock mixtures, proximate and ultimate analyses, HHV, grindability and solid particle size distribution (PSD). In the feedstock dryer, the required natural gas and air are settled as constant values depending on the gasifier load and as 1.2 times the necessary stoichiometric oxygen, respectively. Global mass flowrate, gasifier load and limestone proportion can be changed freely in a calculator block. The ER and the steam ratio can be adapted to different specific feedstock requirements. Throughout all the cases proposed and studied along this thesis, the gasifier operating temperature is maintained constant.

In the *validation* step the model's performance is compared with available plant data and pilot plant data from literature. Firstly, the PRENFLO gasifier from

ELCOGAS produces a syngas that mainly consists of 21% H_2, 60% CO, 4% CO_2, 3.5 H_2O, 1% H_2S, 10% N_2 and COS, on a molar basis in the aforementioned conditions (Coca, 2003). The modelled syngas flow contains 20% H_2, 58% CO, 4.5% CO_2, 5% H_2O, 1% H_2S, 11% N_2 and COS on a molar basis. Traces of NH_3, HCN and HCl, are also obtained. It can be stated that the equilibrium model closely predicts the plant composition. Therefore, 7.7 s of residence time for a PRENFLO gasifier at these specific operation conditions, ensures a syngas composition close to equilibrium.

Secondly, the results by Fermoso *et al.* (2009) and Hernández *et al.* (2010) are used to validate the Gibbs equilibrium approach. The former is used to validate the gasifier behaviour while changing T_{gasif}, oxygen and steam streams to the gasifier. The latter is employed to evaluate the effect of biomass addition to the blend from the base case.

To validate with the work by Fermoso *et al.* (2009), the model has been adapted to the paper conditions by changing the raw material by only coal, P_{gasif}, the proportions of oxygen and steam and allowing the external heating of the gasifier. See the model and paper results in Figure 4.5. Analogous trends are found but, the values for syngas species do not match, because the reactor temperatures reported are not high enough to reach the equilibrium. Regarding T_{gasif} effects in syngas composition, H_2 and CO formation are favoured when the temperature increases, while CH_4 remains quite constant and CO_2 concentration decreases. The former syngas behaviour is the result of a combination of exothermic and endothermic reactions displacement. An increase in T_{gasif} leads to a decrease of K_{eq} in all exothermic reactions (diminishing the fraction of CO_2) while endothermic reactions are promoted (increasing the fraction of H_2 and CO). At constant temperature, an increase in oxygen ratio leads to a decrease in H_2 and CO formations and to an increase in CO_2 formation (as the oxidation reactions are shifted towards products). In the same way, as the steam ratio increases, H_2 formation is enhanced (according to Eq. 4.57) as well as CO_2 production, while the opposite holds for CO formation. The most sensitive equation is therefore Eq. (4.58).

Figure 4.5 shows that at low values of T_{gasif}, the rate of gasification reactions is too slow, since endothermic reactions move to the products side with little practical value, since high CO and H_2 proportions are preferred to optimise syngas usage. Nevertheless, for power production purposes, CH_4 is interesting since it offers a higher calorific value. Higher values of CH_4 are found at low T_{gasif}. Reforming reactions (Eqs. 4.61 and 4.62) take place at relatively low temperatures, even lower than the temperatures depicted in Figure 4.5, in which CH_4 is the most stable component.

The addition of biomass to the base case, whilst the proportion of coal and petcoke is maintained, has been carried out following the study by Hernández *et al.* (2010), and it is shown in Figure 4.6. The study evaluates the effect of biomass content on the syngas composition ratios H_2/CO, CH_4/H_2, H_2/CO_2 and CO/CO_2, as well as on H_2 and CO contents and the CGE (see Eq. 3.5). The equilibrium model results are obtained at higher temperatures than those reached in Hernández *et al.* (2010). Different trends and absolute values, except for H_2 composition are observed. The main reason for the discrepancies may be the fact that biomass synergies are not appreciated in the model, apart from that syngas compositions reported in the aforementioned work might not reach the chemical equilibrium. To sum up, the addition of biomass enhances the production of H_2, but leads to lower CGE, i.e. the LHV contained in the syngas decrease with the proportion of biomass. Regarding the syngas composition, the biomass increase entails less CO and more CO_2.

This calibration and validation procedure shows that an equilibrium reactor is a

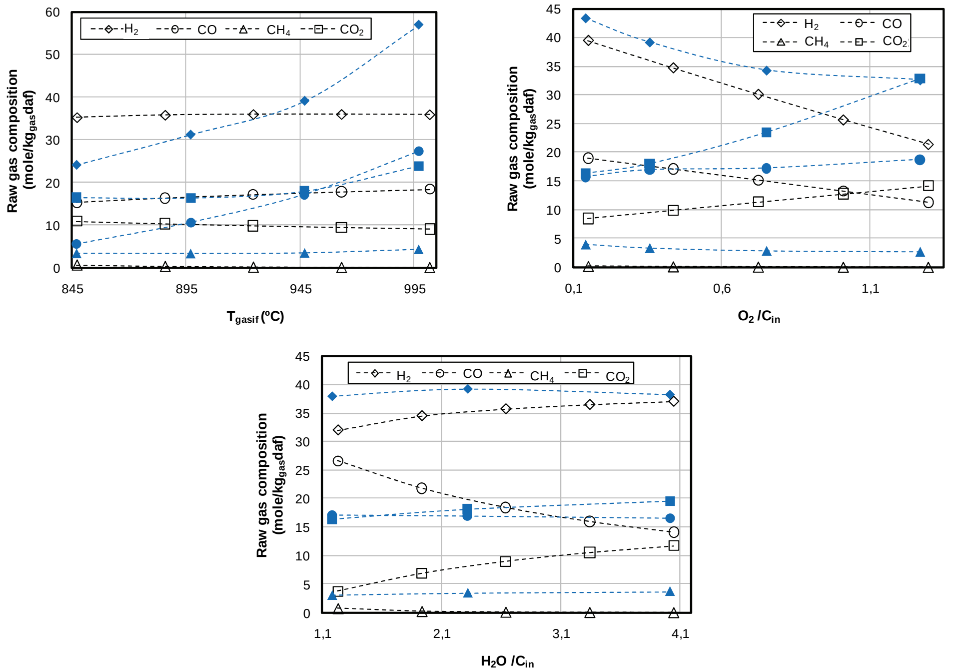

Figure 4.5: Effect of T_{gasif}, O_2/C_{in}, H_2O/C_{in} in the syngas composition (mole/mass). Blue lines are the experimental data from Fermoso *et al.* (2009).

suitable approximation for a PRENFLO gasifier under certain working conditions. The residence time and/or the temperature should allow the equilibrium. Moreover, co-gasification is a not well understood phenomena, and synergetic effects may induce behaviours others than the reactions stoichiometry can predict. In any case, the syngas equilibrium composition represents an extreme gasification result. Therefore, an equilibrium approach gives the most favourable situation for an IGCC power plant, with 100% feedstock consumption and 0% tars generation.

4.5.2 Preliminary results

The purpose of this section is to characterise the behaviour of the equilibrium approach while changing key inputs in the reactor. Different sensitivity analyses (SA) that take into account variations in T_{gasif}, P_{gasif}, ER, steam ratio and feedstock composition are carried out. Base case conditions are maintained for the gasifier parameters and characteristics that are not changed. The plotted results are syngas composition, H_2/CO ratio and CGE. The estimation of the LHV's is performed in Aspen Plus using the QVALNET property set.

SA1: T_{gasif} variation

SA1 is shown in Figure 4.7. T_{gasif} is varied along all the gasification temperature range, approximately between 800°C-1800°C. The left graph, shows that the syngas species presence vary considerably up to 1000°C. Then, at higher temperatures, the

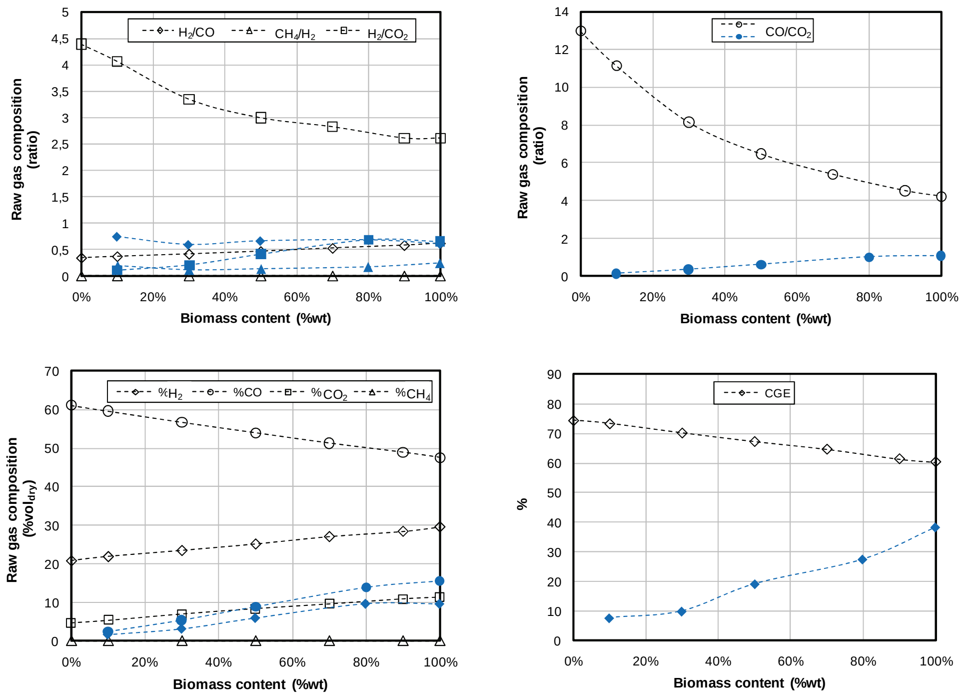

Figure 4.6: Effect of biomass addition in the syngas composition and CGE. Blue lines are the experimental data from Hernández *et al.* (2010).

proportions of H_2, CO, CH_4 and CO_2 are noticeably constant. However, CO_2 and CO show the higher variability in this stationary range, the former decreasing and the latter increasing. As seen in the right graph, H_2/CO ratio decreases with the temperature, after reaching a maximum value around 1000°C. CGE shows a general positive trend, from 68% to 74%, therefore, the syngas LHV increases with the temperature. Consequently, the proportion of CO is more significant for the LHV than the proportion of H_2.

SA2: P_{gasif} variation

This variation affects minimally T_{gasif}; it fluctuates by 2°C (from 1489°C at the lowest pressure considered, 1 bar, to 1487°C at the highest pressure taken into account, 55 bar). The range of pressure values considered is based on literature gasification plants, independently of the type of reactor, which in turn depends on requirements of the process downstream the gasifier. As demonstrated in Figure 4.8, the effect of pressure is negligible. Only Eq. (4.59) has a zero mole increment. However, it is possible to say that in the pressure range considered, the pressure effect is not noticeable for all the reactions, even if they have a mole increment different from zero.

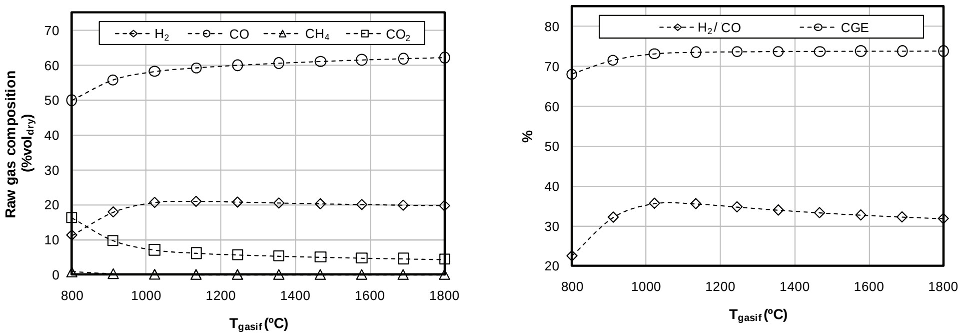

Figure 4.7: SA1: Effects of T_{gasif} variation.

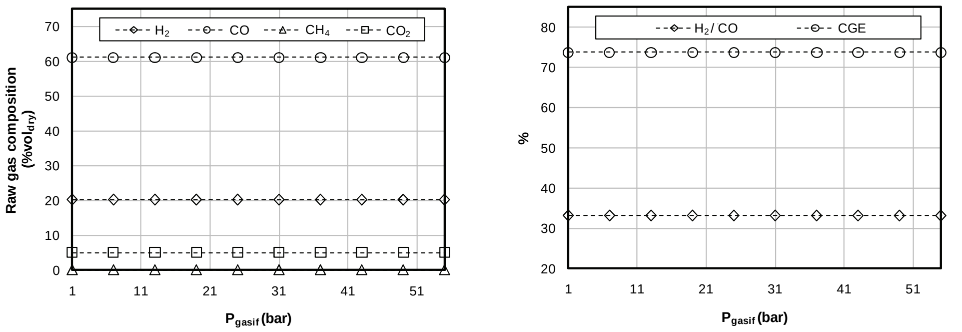

Figure 4.8: SA2: Effects of P_{gasif} variation.

SA3: ER variation

The ER variation range has been defined by varying the value determined for the base case. This scenario has an ER of 0.42 and it varies of +/- 30%. From this performance (see Figure 4.9, top-left graph) it is possible to delimit the ER variation to the *gasification zone*. This zone is comprised between the decrease in CH_4 production and the increase in CO_2 production, as well as the appearance of sulphur oxides (delimiting pyrolytic and combustion zones, respectively). Therefore, and matching with the above performed T_{gasif} zone, the ER range is limited to 0.4-0.55. Figure 4.9, top-right and bottom-left graphs, show a maximum in the production of H_2 at around ER=0.46. The CO_2 generation tends to increase while increasing the inlet oxygen as a consequence of Eqs. (4.50), (4.51) and (4.52). As in the previous SA's, CH_4 is fairly constant. CGE tends to decrease as the ER increases, due to the CO_2 increase and the CO decrease.

SA4: Steam ratio variation

The steam ratio varies between 0.15 and 0.4, according to ELCOGAS performance. Figure 4.10, bottom graph, illustrates that the gasification temperature diminishes as

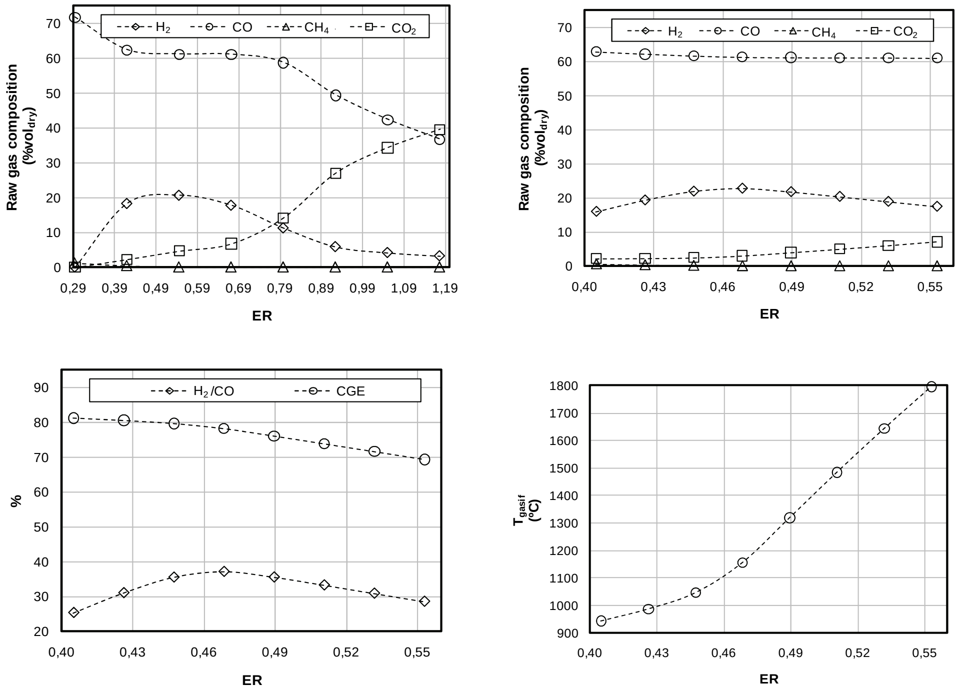

Figure 4.9: SA3: Effects of ER variation.

the steam ratio increases. According to Figure 4.10, upper graphs, CO diminishes and CO_2 and H_2 increase, whilst T_{gasif} decreases. CGE is quite constant while H_2/CO ratio increases. On exothermic reactions, Eq. (4.59), as the temperature decreases, the reaction is displaced to the products side. Steam in this range acts as a temperature moderator and to a lower extent, as a gasifying agent, since exothermic reactions are motivated rather than endothermic reactions.

SA5: Feedstock variation

Figure 4.11 depicts the addition of petcoke to the coal. The bottom-left graph shows that as the proportion of petcoke increases (since its LHV is higher than the LHV of coal - see Table 4.4), T_{gasif} increases. According to upper graphs, higher proportions of petcoke yield higher LHV_{rg} (since CO increases), therefore CGE increases. CO fraction exhibits the most important tendency change. It increases by 20% in the studied interval. H_2 decreases, as well as CO_2. In the bottom-right graph, O/C and H/O ratios are derived from the feedstock inlet composition. Higher values of C (lower O/C), imply higher values of calorific power. The same occurs as H/O increases.

To describe the effects of C, H, O inlet composition into the equilibrium syngas composition, the reactor is fed by individual streams of carbon, hydrogen and oxygen, by changing accordingly the overall ultimate analysis composition and assuming a 10% of ashes. The purpose here is to identify the effect of raw material elements in $\mathrm{LHV_{rg}}$, H_2 and ER variation to reach the specified T_{gasif} of 1450°C. The x axis

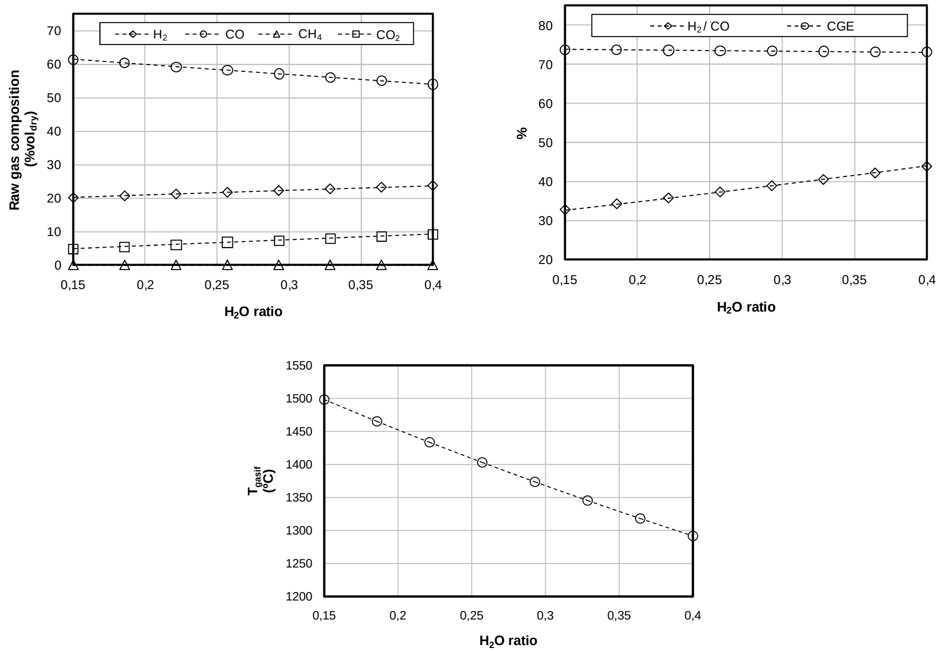

Figure 4.10: SA4: Effects of steam ratio variation.

reflects the analysed percentage of each element, i.e. C, H and O. The remaining inlet composition is deduced assuming a 50:50 fraction on a mass basis for the other two species. Figure 4.12, top-left and top-right graphs, show that higher fractions of H in the inlet mixture lead to better performance in LHV terms and to a higher proportion of outlet H_2. The opposite behaviour is observed for C and O, remarking that increases of O in raw material penalises the most the final LHV_{rg}. The bottom graph reflects the penalisation of higher O fractions concerning the necessity of higher ER fractions, therefore, higher O_2 consumptions. According to the parameters analysed, a high H inlet percentage is favourable.

The results highlight a minimal influence of P_{gasif} in the gasification performance. By adding more oxygen, H_2 tends to decrease, while CO_2 tends to increase. A steam ratio increase leads to a gasification temperature decrease, favouring H_2/CO. The final gas composition depends on the relations between C, H and O from the feedstock composition: more hydrogen in the inlet mixture favours the gasification performance. Therefore, a trade-off exists between directly heated-indirectly heated gasification processes and gasifying agent-raw material composition, being necessary to optimise the amounts of oxygen, steam or hydrogen, according to the feedstock characteristics and the syngas application.

4.5.3 ELCOGAS gasifier performance: Operation maps

An example of industrial application of gasifier modelling retrofitted with real power plant data are the *operation maps* used in ELCOGAS plant. In this thesis, operation maps have been used to validate the model by calculating an average

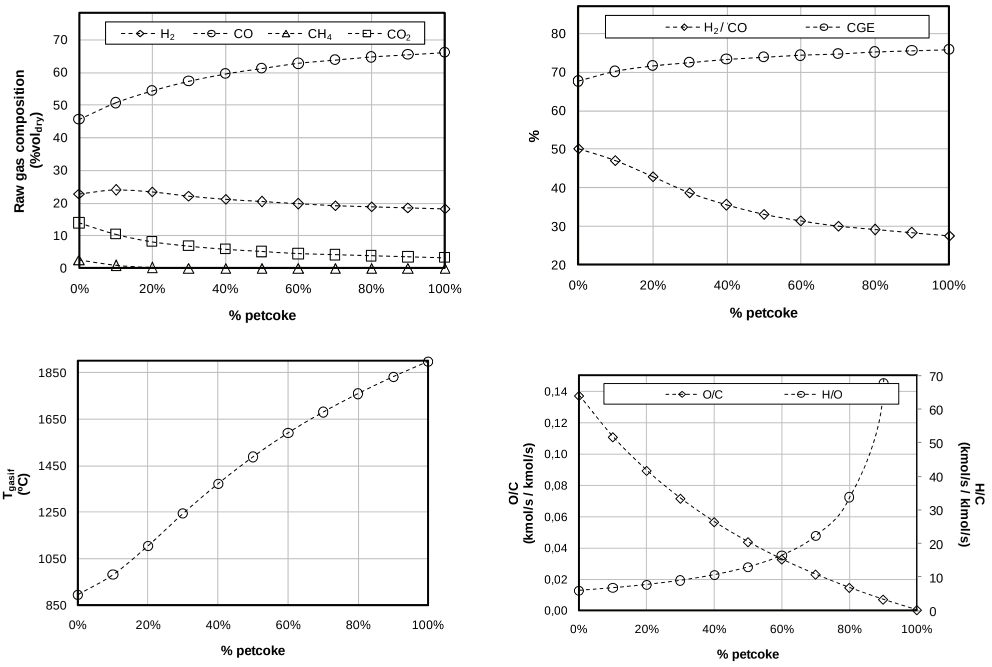

Figure 4.11: SA5: Effects of feedstock composition variation.

syngas composition at the considered operating conditions. An operation map is a two dimensional graph that assists the quotidian operation of the gasifier: it shows how varying steam and oxygen ratios, the values of CGE, T_{gasif} and syngas composition in terms of H_2, CO and CO_2 are modified. Different operation maps result when the pack of data (i) ashes percentage, (ii) oxygen purity, (iii) gasifier load and (iv) quench gas compressor connected or not, have certain specific and discrete values. Therefore, different operation maps are built-up according to those four data combinations. See in Figure 4.13 an example of operation map from ELCOGAS. In Figure 4.14 there is a plot of the concerned data (in red and green). Green values provides from direct monitoring in the plant. In contrast, red values are calculated with a gasifier model similar to that described in Section 4.3 (Usón *et al.*, 2004).

The data base of the plant performance is formed by stationary period's compilation. The information is provided by TDG (thermo-economic diagnosis) system that is connected with the plant information collection system. A comparison between the operations from years 2000-2002 and from years 2002-2009 (with more than 9000 steady states) has been performed. It is appreciated that the gasifier results (CGE and syngas composition) maintain the same trend, even if the absolute values have changed.

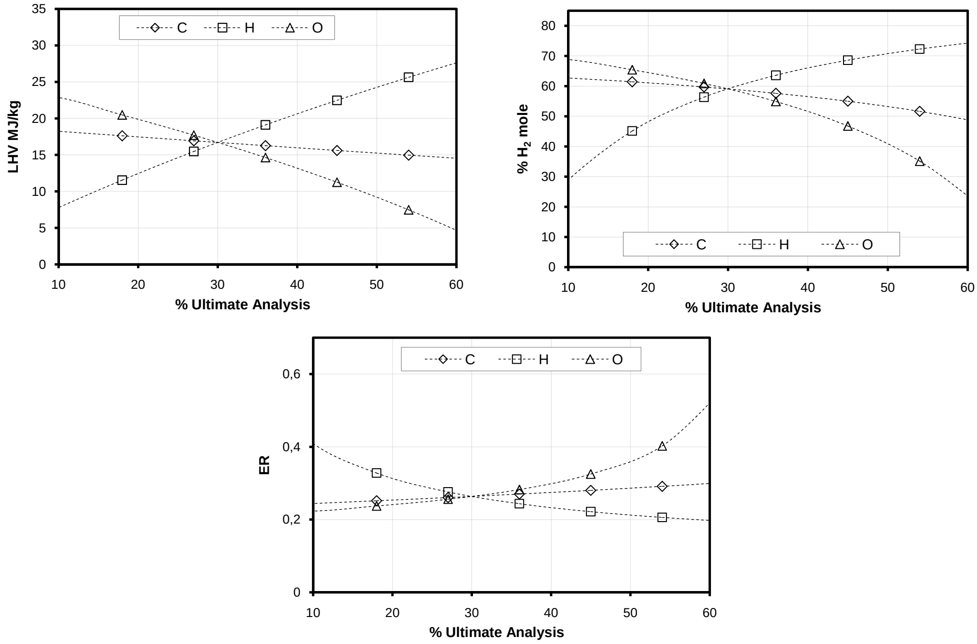

Figure 4.12: SA5: Effects of C, H, O elements variation.

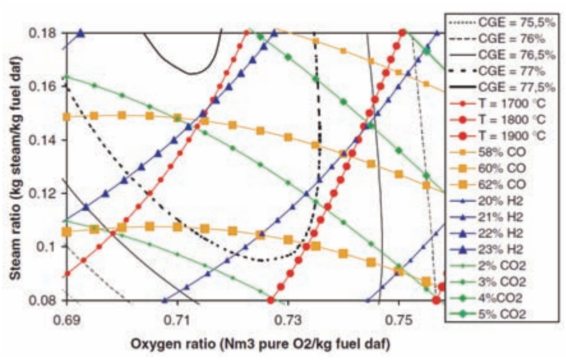

Figure 4.13: Operation map from ELCOGAS. Source: Valero and Usón (2006)

4.6 Final considerations

In this chapter, the equilibrium model minimising Gibbs free energy is used to simulate the performance of a PRENFLO gasifier with T_{gasif} 1450°C, P_{gasif} 25 bar and residence time 7.7 s. The model has been validated with ELCOGAS plant data, showing acceptable agreement. Chapter 2 has proposed the equilibrium model to describe entrained bed and fixed bed gasifiers. This chapter highlights that the model fitting is highly dependant on the specific gasification conditions, better at higher temperatures and/or longer residence times, as well as dependant on the raw materials

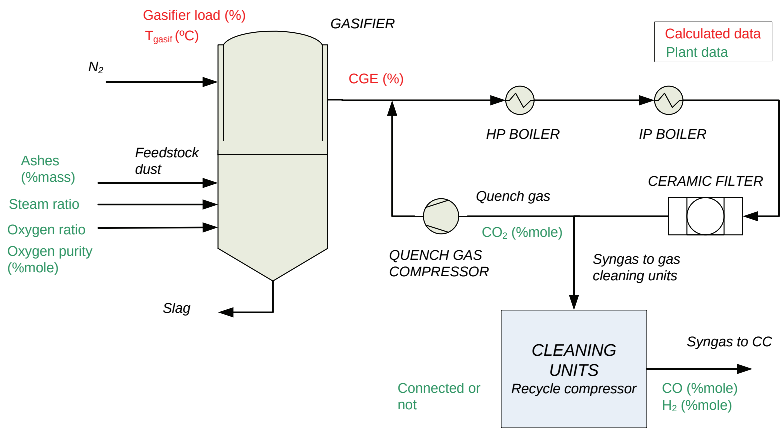

Figure 4.14: Considered data for the elaboration of the gasifier operation maps.

introduced in the reactor. In this view, if co-gasification with biomass is of concern, tars and synergetic effect should be known to adequately represent the gasification behaviour.

The effects of the temperature, pressure, ER, steam ratio and feedstock composition have been studied. Feedstock composition is an important variable to be considered and to be matched with the appropriate gasification agent/amount. In contrast, temperature and pressure are somehow pre-fixed by the ashes melting point and the final syngas applications. In the last section the retrofitting activity between modelling and real plant monitoring is exemplified by means of the operation maps of the gasifier in ELCOGAS plant.

Notation

Latin letters

a, b, c, d, e	molar composition of raw material
C_O, N_O, S_O	percentages of carbon, nitrogen and sulphur in raw material on a daf basis
d_p	particle diameter
D	diameter
g	gravity force
h_{gas}	external convection coefficient
k_{gas}	specific rate of gas diffusion
k_n	constant for K_{eq} calculation
k_q	chemical rate constant
k_t	specific reaction rate
K_{eq}	equilibrium constant
$K_{\mathrm{H_2}}$, $K_{\mathrm{H_2O}}$	intermediate equilibrium constants in the kinetics approach
L	length
P	pressure
p_i	partial pressure of species i
Q	heat

r	reaction rate
T	temperature
t_r	residence time
U	velocity
V_r	percentage of volatiles released on a volume basis
V_{r*}	percentage of volatiles released on a volume basis in a pressurised reactor
V_{tar}, V_{H_2O}, V_{gas}	percentage of tars, water and gases after the pyrolysis step on a volume basis
V_{PA}	percentage of volatiles in proximate analysis
Y	particle and core radius ratio

Greek symbols

α, β, γ, δ, ϵ	molar composition of char
ε_p	internal porosity
ε_1, ε_2	intermediate volatiles release parameter
μ	dynamic viscosity
ϕ	mechanism parameter
ρ	density
ξ_Q	dry matter lost by volatilisation
ξ_R	remaining volatile matter
ξ_V	parameter for volatiles release, based on experimental data

Superscripts and subindices

rg	raw gas
g	gas
f	fluid
$gasif$	gasification
p	particle
s	solid
t	terminal

Acronyms

ar	as received basis
ASU	air separation unit
CC	combined cycle
CCS	carbon capture and storage
CGE	cold gas efficiency
C_{in}	kg of inlet carbon
CSIC	Spanish National Research Council
CSTR	continuous stirred tank reactor
daf	dry and ash free basis
dry	dry basis
EOS	equation of state
ER	equivalence ratio
GHG	greenhouse gases
GT	gas turbine
HEN	heat exchangers network
HHV	higher heating value
HP	high pressure
IGCC	Integrated Gasification Combined Cycle
IP	intermediate pressure
LHV	lower heating value

MC	moisture content
PR-BM	Peng-Robinson equation of state with the Boston-Mathias alpha function
PRENFLO	pressurised entrained flow
PSD	particle size distribution
SA	sensitivity analysis
SG	solid-gas
TDG	thermo-economic diagnosis
WHB	waste heat boiler

Chapter 5

IGCC-CCS Flowsheeting, Modelling and Validation

Syngas cleaning, CO_2 capture, H_2 purification, combined cycle (CC), heat recovery steam generator (HRSG) and air separation unit (ASU) are the remaining stages configuring the IGCC-CCS power plant superstructure. The purpose of this chapter is the description of these units modelling approach. Next, for calibration and validation purposes, the model outputs are compared with real plant and data from literature. Additionally, validation of the superstructure and its required versatility towards plant conceptual design is carried out by sensitivity analyses, taking into account the main input and output streams. The developed superstructure allows for the addition of novel units and for changes in unit parameters, as required to each specific process design.

5.1 Introduction

Three key issues have motivated the creation of the modelling superstructure, i.e. (i) co-gasification, (ii) carbon capture and storage (CCS) and electricity-hydrogen production, and (iii) the integrated nature of the IGCC plant.

Co-gasification with biomass presents advantages with respect to conventional coal gasification, such as enhanced sustainability, if accurately exploited. Biomass presents some drawbacks in terms of density, grindability and LHV, which might release higher CO_2 and SO_x production per MW produced, if considering the whole supply network. Consequently, there is a trade-off in the amount of biomass that can be co-gasified in an IGCC plant, due to the emissions released during pre-treatment and transportation and the emissions saved due to co-gasification. Some studies have tackled co-gasification (Zhao *et al.*, 2006; Koukouzas *et al.*, 2008), with encouraging results. A study by Valero and Usón (2006) refers to the oxy-co-gasification of coal, petcoke and biomass in an IGCC power plant with oxygen-blown gasification. The study by Baliban *et al.* (2010) introduces a mixture of coal, biomass and natural gas into the liquid gasification process. Their results showed that this hybrid option could satisfy the entire US transport demand with very low environmental damage.

For an IGCC power plant, the *carbon removal* technique (CCS) requires the use of a pre-combustion capture technique, in which the high pressure that is maintained throughout the gas cleaning process is used to separate CO_2 by means of a physical absorption technique (Kanniche *et al.*, 2010). The H_2 obtained by the gasification of solid organic matter is produced first in the gasifier itself, and secondly in a WGS reactor in which CO reacts with H_2O to produce H_2 and CO_2. The production of H_2 inherently involves the production of CO_2. Thus, final CO_2 disposal solutions need to be researched.

IGCC plants have inherent implementation problems due to their *integrated nature* (Maurstad, 2005; Ansolabehere *et al.*, 2007). Several authors have discussed the possibility of integrating (i) the air separation unit (ASU) with the gas turbine (GT) streams and the (ii) production of steam from several hot streams sources along the flowsheet, by means of a heat recovery steam generation (HRSG) system. Two aspects of ASU-GT integration are considered: (i) the use of the GT compressor instead of an independent ASU compressor to supply the high pressure (HP) air required in the ASU and (ii) the reinjection of waste N_2 from the ASU into the GT combustor for flame temperature control and for flowrate increase. All authors agree that the use of waste N_2 from the ASU in the GT combustor leads to higher electricity production and less nitrogen oxides emissions, and that the use of the GT compressor instead of an independent ASU one leads to power consumption savings (Frey & Zhu, 2006; Wang *et al.*, 2010; Emun *et al.*, 2009). Several authors have applied mathematical optimisation tools and heat integration heuristics (pinch analysis) to provide insights into the required HEN, regarding the HRSG system in particular, or the heat and power integration of the entire plant in general terms, as well as the number and levels of pressure in the steam turbine (ST) cycles (Bassily, 2005; Gassner & Maréchal, 2009a; Elia *et al.*, 2010). There is no one optimal response for all cases.

This chapter presents the modelling approach and provides details of each modelled unit, i.e. gas cleaning, CCS, HRSG, ASU and combined cycle (CC) units, which are then validated. In the results section, the alternative designs generated by the superstructure are studied and compared, and the performance of the entire system is evaluated in each case.

5.2 IGCC with carbon capture units: base case description

The main stages in an IGCC process with carbon capture units can be grouped into *five blocks* that pursue the common purpose of transforming a solid fuel into a valuable gas that can be burnt, cooled down and expanded in a CC, or transformed and sold as pure H_2, as depicted in Figure 5.1. The model is calibrated using data from the ELCOGAS power plant and from studies by Desideri and Paolucci (1999), Hamelinck and Faaij (2002), Chiesa *et al.* (2005) and Descamps *et al.* (2008). Three of the five abovementioned blocks are described here, while the first two, feedstock dust preparation and gasification and waste heat boiler (WHB), have been further described in previous Chapter 4.

- *Syngas cleaning.* Syngas must be cleaned and conditioned to meet the end-user requirements, which may range from chemical or fuel production to power and/or heat generation. In the IGCC configuration, the objective is to clean the gas

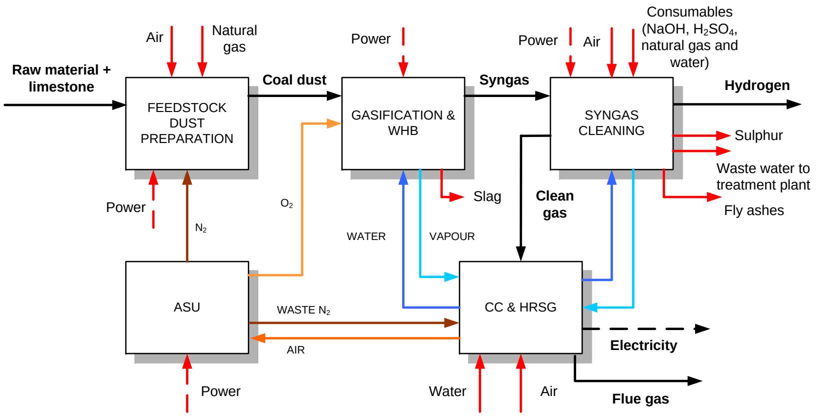

Figure 5.1: IGCC power plant layout. The main mass flows and IGCC operations interconnectivity are indicated. Inlet and outlet streams are marked in red. Main streams and final products, are marked in bold. The different integration systems are marked with different colours.

before it is combusted in the GT combustor to avoid, as far as possible, nitrogen and sulphur oxide emissions to the atmosphere and GT damages. In the case of H_2 generation, the objective is to separate CO_2 from H_2. The high H_2 content stream is further purified and sold as pure H_2 on the market. In the first step of both configurations, solids are removed from the gas in a ceramic filter. Secondly, the syngas is placed in a venturi scrubber in contact with water that removes cyanide, halide, acid (mainly H_2S) and basic (mainly NH_3) species. Thirdly, before its combustion or H_2 purification, the gas goes through an acid species removal step that involves a COS hydrolysis reactor and an MDEA absorber. The polluted water from the venturi scrubber is pre-treated in a sour water stripper before its transportation to a waste water treatment plant. The sulphur that is present as H_2S in the syngas is recovered as liquid sulphur in a Claus plant. The syngas cleaning layout follows the configuration of the ELCOGAS plant (Coca, 2003). In the case of H_2 generation application, the syngas cleaning block includes the carbon capture block. In its pre-combustion configuration, it requires a WGS reactor that produces H_2 and CO_2, followed by a process for CO_2 capture to separate CO_2 from H_2. Here, CO_2 removal is simulated using physical absorption through a Rectisol process that employs pure methanol as a solvent. The H_2 is then further purified by means of a pressure swing adsorption (PSA) system. Finally, the CO_2 stream is sent to a compression system to be liquefied for transport.

- *CC and HRSG.* The CC combines Brayton and Rankine cycles to produce electricity. The steam cycle uses the waste heat from the system to produce steam at different working pressures (high pressure, intermediate pressure and low pressure -HP, IP and LP-). Specifically, the HRSG is a HEN that uses waste heat from the flue gas from the GT to produce steam. The GT and ST are connected through this flue gas, which needs to be cooled down before it is released into the atmosphere. Thus, the processes can be integrated.

- *ASU.* The ASU unit produces oxygen at the required purity to be sent to the gasifier as a gasifying agent. Pure N_2 and waste N_2 are also obtained and are mainly used for raw material transportation, inertization, temperature moderation, pressurisation and nitrogen emission reduction, respectively.

To sum up, the five blocks in the gasification plant are connected as shown in Figure 5.1): the raw material that enters the system is firstly dried and crushed. The obtained feedstock dust is then transformed into syngas in a PRENFLO gasifier. The syngas is cooled down in a WHB that allows the heat to be used in the ST prior entrance in the gas purification block. Next, the syngas is cleaned by removing solids. Basic and acid trace components are eliminated by means of absorption cleaning processes. The clean gas is finally sent to a CC. Liquid sulphur is obtained as a by-product.

This type of plant has higher overall efficiency when its underlying blocks are integrated. The *integrated flows* considered in the present approach are shown in Figure 5.1 and described as follows:

- All the oxygen that the gasifier requires comes from the ASU, which uses compressed air from the CC compressor, rather than independent compression.

- After the ASU process, two N_2 streams are obtained: a relatively pure one, and waste nitrogen. The pure N_2 stream is used for transportation and pressurisation in the feedstock dust preparation block, and for temperature moderation in the gasifier. In turn, the residual N_2 from the ASU is used to control NO_x formation in the GT combustion chamber. In plants such as ELCOGAS, the N_2 network is not only used as a service, but also as a working tool for pneumatic pumps, fly ash discharge, filter cleaning or slag transportation. These applications have not been considered since they involve relatively small fluxes, which are of no concern in this preliminary design approach.

- In the steam network, the ST cycle provides steam for clean gas saturation before combustion in the GT, and for the gasification process. It also provides water for the venturi scrubber and steam for the WGS reactor. The so-called proportional parameters are fixed during the calibration step. In turn, heat from syngas cooling, in the WHB and the HRSG is used to produce steam in the CC.

Figure 5.1 shows the overall mass balance of the plant. The main consumers of the net power production are GT cycle compression, the ASU operation, CO_2 compression in the Rectisol process and CO_2 compression for liquefaction. The main technical data considered in the model are summarised in Table 5.1. More details for each one of the considered units are provided through the modelling strategy, in Section 5.3.

5.2.1 Modelling assumptions

The steam and N_2 networks are taken into account focusing on the main streams. The IGCC modelling approach does not consider the slag cooling and collection system or an exhaustive model for the cooling tower. The design of the waste water treatment plant is also outside of the scope of this thesis. The ELCOGAS power plant employs a CC from Siemens. Its output data, as well as input and output data from their gas cleaning units with no carbon capture, are used to calibrate the model. As a general physical property method to calculate the thermodynamic and transport properties

Table 5.1: Main technical data for the IGCC plant model.

Operating conditions	
Gasifier	
Feedstock	2600 t/day
Crusher fineness	50-60 μm
Feedstock MC	2%
P of lock hoppers	30 bar
T_{gasif}	1400-1500°C
P_{gasif}	25 bar
O_2/O_2 stoich (mole basis)	Raw material dependant, to control T_{gasif}
H_2O/C_{in} (mass basis)	0.16
T before the WHB	850°C
T before gas cleaning	235°C
Combined Cycle	
Air_{in}	Adjusted to regulate T_{gasif} and TOT
HP/IP/LP	127/35/6.5 bar
HP/IP/LP T before ST	510/520/265°C
Compressor P_r	15.7
T_{cg} before combustor	300°C
TOT	540°C
P saturation column	20.8 bar
T flue gas	100°C
T air to ASU	130°C
Consumables	
NaOH (15 mass%)	Proportional to syngas and cleaning water flows
H_2SO_4 (96 mass%)	Proportional to cleaning water flow
Natural gas	Proportional to feedstock flow
H_2O	Proportional to syngas and raw material flows
Air Separation Unit	
Oxygen purity	85 mole%
Radiation losses	2% adiabatic reactor
T_o	15°C
P_o	0.93 bar

of streams, the Peng-Robinson equation of state (EOS) and Boston-Mathias alpha function (PR-BM) is chosen. This EOS is recommended to model gas phase systems at IP to HP. NBS/NRC Steam Tables (for vapour and liquid states) are used for the ST with water as a working fluid, which are implemented in the software like any other EOS (AspenTech, 2010). The LHV's are estimated using Aspen Plus property sets (QVALNET). The stoichiometric value of air was calculated using the COMB-O2 property set from Aspen Plus (AspenTech, 2010).

Going deeply inside *absorption processes*, due to the non-ideal behaviour of the liquid phase owing to the occurrence of pH changes related to the speciation of dissolved gases in water or other solvents, the physical property method chosen to calculate thermodynamic and transport properties of the streams should be based on an activity coefficient model. Several different possibilities are available such as Wilson, UNIQUAC or NRTL (non-random two liquid) (Prausnitz *et al.*, 1986). Because of the consideration of gas species solvation and subsequent electrolytes formation, an extension of the NRTL model called ELECNRTL is suitable. This thermodynamic model allows modelling unit operations in which ions are present. The ions formed can be estimated by Aspen Plus using the Electrolytes Wizard command in the selection of components section. This command also generates the appropriate chemical equilibrium reactions for electrolyte appearance. Separation of vapour and liquid phases during equilibrium (VLE) is considered here as the main separation approach for absorption processes, therefore the *Henry's law* is used in combination with ELECNRTL and NRTL property methods. NRTL model can describe VLE and liquid-liquid equilibrium (LLE) of non-ideal solutions. Chemical absorption processes use ELECNRTL, while physical absorption processes use NRTL.

The Henry's law states that the partial pressure of species i in a volume of gas in equilibrium with a liquid, is directly proportional to the species mole fraction in the liquid phase at a constant temperature. See in Eq. (5.1) an ideal behaviour for a specific solvent; left hand side of the equation corresponds to gas phase. Thus, the right hand side corresponds to the liquid phase.

$$p_i = y_i \cdot P = x_i \cdot H_i(T) \tag{5.1}$$

Where, p_i is the partial pressure of i in the gas phase; y_i is the mole fraction of i in the gas phase; P is the total pressure; x_i is the mole fraction of i in the liquid phase and $H_i(T)$ is the Henry's law constant for i. The Henry's law constant expressed like in Eq. (5.1) has units of pressure. If a non-ideal behaviour is considered, the fugacity f_i is used to describe the partial pressure of the gas species. This factor is experimentally determined. The P term in Eq. (5.1) is substituted by f_i and ϕ_i, which is the fugacity coefficient, as in Eq. (5.2). In turn, for the liquid phase, this non-ideal behaviour is reflected by the activity a_i. In an analogous way as in the gas phase, in Eq. (5.3), γ_i is the activity coefficient, and relates the activity with the mole fraction.

$$p_i = y_i \cdot \frac{f_i}{\phi_i} = x_i \cdot H_i(T) \tag{5.2}$$

$$p_i = y_i \cdot \frac{f_i}{\phi_i} = \frac{a_i}{\gamma_i} \cdot H_i(T) \tag{5.3}$$

Aspen Plus uses Eq. (5.3) for each binary interaction between species and solvent. Henry's law constants are available from Aspen Plus Property System databank. $H_i(T)$ is calculated as in Eq. (5.4). Henry's coefficients for a specific solvent $(b_i, c_i, d_i, e_i, f_i)$ are explicit for each pair component-solvent. In this modelling approach, water and methanol are used as solvents. See the Henry's constants values summarised in Table 5.2. Those constants are suitable for a specific range of temperatures, T_{lower} (T_L) and T_{upper} (T_U) (AspenTech, 2010).

$$\ln H_i(T) = b_i + \frac{c_i}{T} + d_i \cdot \ln T + e_i \cdot T + \frac{f_i}{T^2} \tag{5.4}$$

The RadFrac model from Aspen Plus is used for all the absorption units in the IGCC flowsheet: venturi scrubber, sour water stripper, MDEA absorber and Rectisol process. The Radfrac model selected here uses the Henry's law together with ELECNRTL or NRTL to estimate the species separation among the liquid and gas phases, for each stage. The main separating agents are water and methanol; in turn, in the reboiler, heat is the separating agent that acts to recirculate the bottoms of the column. Liquid saturation is the equilibrium attribute that limit the capacity of the receiving phase.

For chemical absorption processes, the ionic dissociation is represented by an *equilibrium process*. Eq. (5.5) expresses the equilibrium constant K_{eq} as a function of the temperature, with specific coefficients (B, C, D, E). Thus, as the column has a specific temperature profile, K_{eq} is different for each reaction and for each stage.

$$\ln K_{eq} = B + \frac{C}{T} + D \cdot \ln T + E \cdot T \tag{5.5}$$

Table 5.2: Henry's coefficients (Eq. 5.4) for each binary mixture, with water and methanol as solvents, in N/m^2. Temperature in K (AspenTech, 2010).

	b_i	c_i	d_i	e_i	f_i	T_L	T_U
Solvent: H_2O							
H_2	152.2	-5312.5	-20.3	$1.3 \cdot 10^{-2}$	0.0	273.2	344.9
CO	568.8	-17742.0	-91.8	$1.2 \cdot 10^{-1}$	0.0	273.2	333.2
CO_2	192.7	-8982.0	-25.8	$1.2 \cdot 10^{-1}$	0.0	273.2	347.9
H_2S	143.9	-8281.7	-16.5	$-1.4 \cdot 10^{-1}$	0.0	273.2	333.2
COS	232.7	-12025.0	-30.4	0.0	0.0	273.0	303.0
NH_3	93.3	-1096.8	-16.56	$0.6 \cdot 10^{-1}$	0.0	273.0	373.0
HCN	53.8	-8136.8	0.0	$4.5 \cdot 10^{-2}$	0.0	283.0	383.0
HCl	-36.0	1215.0	8.4	$-9.6 \cdot 10^{-3}$	0.0	253.2	293.2
Solvent: CH_3OH							
H_2	-49.9	1867.4	12.6	$-2.7 \cdot 10^{-2}$	0.0	213.2	343.0
CO	15.7	1144.4	0.0	0.0	0.0	293.2	298.2
CO_2	27.0	-3426.7	1.5	$-2.5 \cdot 10^{-2}$	0.0	273.2	293.2
H_2S	22.0	-2050.8	0.0	0.0	0.0	263.2	298.2
COS	323.7	-12025.0	-30.4	0.0	0.0	273.0	303.0
NH_3	18.5	-1669.4	0.0	0.0	0.0	273.2	301.6
HCl	-36.0	1643.8	7.6	0.0	0.0	275.3	307.4

Those units using NRTL method are replaced in the flowsheet by meta-models, component splitter models in this case, which are calculated from the exhaustive models, due to the excessive time required for their resolution in sensitivity analyses (SA) or variables optimisation calculations.

The exhaustive kinetic equations for the COS hydrolyser and the Claus plant have been introduced in Aspen Hysys, and established in Aspen Plus by means of the limiting reactant fractional conversion.

Cleaning units remarks

In order to understand the results of a chemical plant section or unit, the metrics used should represent the overall behaviour. These metrics can range from simple mass flows to complex relationships between species concentrations in different streams. Normally, when the stream is treated or transformed it is useful to check the relation of concentrations among the inlet and outlet streams or the ratio of moles of specific species. In general, for a given block with A as inlet, and B and C as outlet streams, the following relations can be used (Eqs. 5.6 and 5.7) can be calculated:

$$\text{split}_i = \frac{m_i^B}{m_i^A} \tag{5.6}$$

$$\text{recovery}_i = \frac{m_i^B - m_i^C}{m_i^A} \tag{5.7}$$

Where m_i^X represents the mass or molar flow of component i in stream X. These recovery fraction and split fraction are used to calibrate and validate the models.

5.3 IGCC power plant modelling

5.3.1 Syngas cleaning

The aim of this block is to obtain a clean gas before combustion in a CC. In addition, CO_2 may be separated from H_2 to further purify the H_2 stream and thus produce pure H_2 to be sold. The basic cleaning process for both final applications is made up by cleaning units that work at high pressure, over 20 bar. The syngas is cleaned in the venturi scrubber and the COS hydrolyser-MDEA absorber. By-product streams are cleaned in the sour water stripper and in the Claus plant. The layout of the cleaning units is depicted in Figure 5.2. In the same figure, the superstructure arrangement is shown by means of splitters: clean gas can be used to directly produce power in the CC or it can be further cleaned by separating CO_2, which is liquefied and sent to its disposal. The relatively pure H_2 can be used in the CC or can be additionally purified in the PSA system. Looking at the splitters, several decisions should be taken concerning the separation factors. Therefore, co-generation of power and H_2 is one of the multiple possibilities of the syngas. Further extensions, for instance, unit replacement or additional novel units of the superstructure created can be easily implemented following the same guidelines. Note that the base case produces only power.

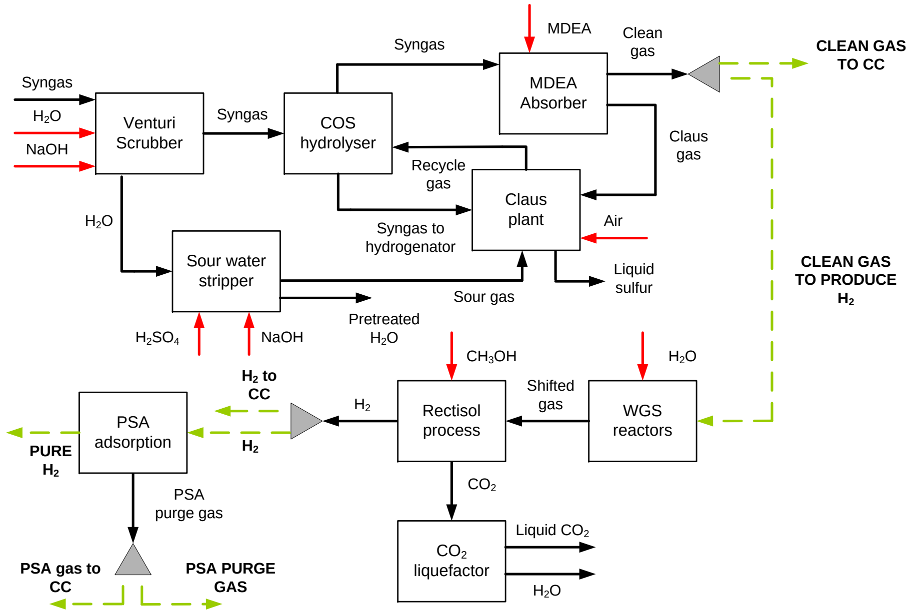

Figure 5.2: Cleaning units layout indicating main mass flows. Electricity and H_2 productions are also represented. Note that the inlet flowrates are marked in red. Superstructure choices are marked with dotted and green lines.

Table 5.3: Equilibrium constants for Eqs. (5.8) to (5.14) and Eq. (5.21), on a mole fraction basis. K_{eq} units depend on the stoichiometry of the reaction (AspenTech, 2010).

Eq. #	B	C	D	E
(5.8)	132.9	-13445.9	-22.5	0.0
(5.9)	-1.3	-3335.7	1.5	$-3.7 \cdot 10^{-3}$
(5.10)	231.5	-12092.1	-36.8	0.0
(5.11)	216.1	-12431.7	-35.5	0.0
(5.12)	214.6	-12995.4	-33.6	0.0
(5.13)	-9.8	-8585.5	0.0	0.0
(5.14)	22.9	-9945.5	0.0	$-5 \cdot 10^{-2}$
(5.21)	-9.4	-4235	0.0	0.0

Venturi scrubber

This unit is placed after the gasifier and after the removal of solids; all the solids in syngas after gasification are simply separated. Its main objective is to abate ammonia, cyanide and halide species. Some H_2S is also absorbed, although this is not the main purpose of the scrubber. This process unit allows contact between water and syngas. Thus, species transfer occurs according to the VLE, following Henry's law and considering the electrolyte reactions that take place in the liquid phase (see Section 5.2.1). It uses a 15% solution of NaOH by weight that acts as an acid capturer. The main Henry components are NH_3, CO_2 and H_2S (see in Table 5.2 the Henry's coefficients for each component and water). Indeed, the ionisation reactions are represented in Eqs. (5.8) to (5.14). Eq. (5.15) and Eq. (5.16) correspond to the dissociation of HCl and NaOH. Table 5.3 compiles the K_{eq} coefficients values (Eq. 5.5) for those ionisation equations.

$$2H_2O \longleftrightarrow H_3O^+ + OH^- \tag{5.8}$$

$$NH_3 + H_2O \longleftrightarrow {NH_4}^+ + OH^- \tag{5.9}$$

$$CO_2 + 2H_2O \longleftrightarrow H_3O^+ + {HCO_3}^- \tag{5.10}$$

$${HCO_3}^- + H_2O \longleftrightarrow H_3O^+ + CO_3^{2-} \tag{5.11}$$

$$H_2S + H_2O \longleftrightarrow H_3O^+ + HS^- \tag{5.12}$$

$$HS^- + H_2O \longleftrightarrow H_3O^+ + S^{2-} \tag{5.13}$$

$$HCN + H_2O \longleftrightarrow H_3O^+ + CN^- \tag{5.14}$$

$$HCl + H_2O \longrightarrow H_3O^+ + Cl^- \tag{5.15}$$

$$NaOH \longrightarrow Na^+ + OH^- \tag{5.16}$$

The venturi scrubber is modelled using a RadFrac column with a constant pressure of 23.6 bar. Water and NaOH consumption are proportional to the syngas flowrate that enters the venturi scrubber: 9% and 0.12% of the raw gas flowrate have been determined respectively. The proportionality factors are introduced into the model through two FORTRAN codes, by means of two calculator blocks. Polluted water goes to a sour water stripping system to be pre-treated before the final water disposal process. This system works at nearly atmospheric pressure (1.5 bar). Hence, water is depressurised in a flash vessel before it enters the first column. The flash vessel has been modelled as a two-phase flash reactor that operates at 1.5 bar and 53°C. The clean syngas obtained after the venturi scrubber is cooled to around 140°C before the COS hydrolyser. See the layout of the venturi scrubber-water stripping system performed with Aspen Plus units in Figure 5.3, where only the main streams are represented.

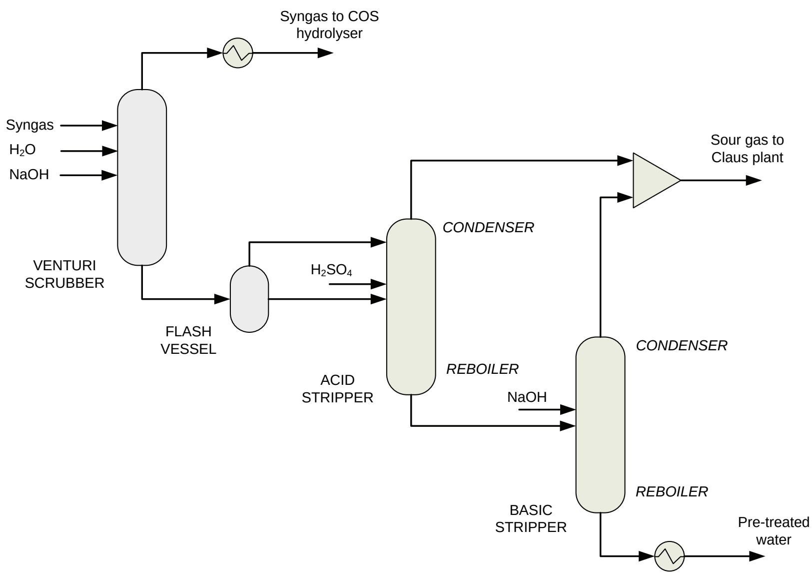

Figure 5.3: Venturi scrubber and sour water stripper.

Sour water stripping system

The main purpose of this system is to pre-treat the used water in the venturi scrubber by desorbing acid and basic species. It consists of two main units: (i) an acid stripper that abates acid species and (ii) a basic stripper that abates basic species. This system is modelled using electrolytes and considering the VLE by applying Henry's law. Again, Henry's law constants can be calculated from Table 5.2). The desorbing columns are pH regulated by adding acid and basic solutions: H_2SO_4 and NaOH with a purity of 96% and 15% by weight, respectively. The ionisation equations present in this unit are Eqs. (5.8) to (5.18).

$$H_2SO_4 + H_2O \longrightarrow H_3O^+ + HSO_4{}^- \tag{5.17}$$

$$HSO_4{}^- + H_2O \longrightarrow H_3O^+ + SO_4{}^{2-} \tag{5.18}$$

The solution flowrates depend on the water flowrate from the venturi scrubber. The relationships are introduced into the model through FORTRAN calculator blocks: the acid solution is 0.3% of the overall water mass flowrate that needs to be treated. Similarly, the basic solution corresponds to 1.2% of the mass flowrate that needs to be treated. The strippers are modelled with RadFrac columns with condenser and reboiler units. A sour gas stream is obtained after the stripping process. It is directed to the Claus plant for sulphur recovery. The final water temperature is around 40°C and the sour gas outlet temperature is about 105°C. See in Figure 5.3 the layout of the process as modelled in Aspen Plus.

COS hydrolyser and MDEA absorber

The purpose of these systems is to remove syngas sulphur compounds. The COS transformation into H_2S is modelled in Aspen Plus using a stoichiometric reactor with

COS fractional conversion of 0.99, based on a kinetic model performance modelled in Aspen Hysys. A pressure drop of 1.6 bar is assumed along the reactor. PR EOS is used here.

COS (carbonyl sulphide) needs to be transformed since the amines processes are effective for H_2S removal. The hydrolysis reaction (Eq. 5.19) uses alumina as catalyst. It is assumed that this reaction follows a first-order kinetic reaction for COS and a zero-order kinetic behaviour for H_2O (Rhodes *et al.*, 2000; Huang *et al.*, 2005). The reaction rate constant follows an Arrhenius relation as shown in Eq. (5.20), where Ak_{COS} is the pre-exponential factor, E_a is the activation energy and ρ_{cat} is the bulk density of the catalyst, given in $\mathrm{kg}_{cat}/\mathrm{m}^3$. R is the gas constant.

$$\mathrm{COS} + \mathrm{H_2O} \longrightarrow \mathrm{H_2S} + \mathrm{CO_2} \tag{5.19}$$

$$r = A_{\mathrm{COS}} e^{-\frac{E_a}{RT}} \rho_{cat} X_{\mathrm{COS}} \tag{5.20}$$

Information from Fiedorow *et al.* (1984); Huang *et al.* (2006) has been used to find the kinetic parameters for Eq. (5.20). The values obtained are $\mathrm{A_{COS}} = 1.7083 \cdot 10^8$ $\mathrm{m}^3/\mathrm{g}_{cat}\mathrm{h}$ and $E_a = 94733.9$ J/gmol. Finally, the rate r results in mol/m^{3}h. The reactor is modelled in Aspen Hysys by a plug flow reactor (PFR). X_{COS} is the molar concentration. The kinetics within the PFR are modelled by a custom-made kinetic reaction extension.

The MDEA (methyldiethanol amine, $C_5H_{13}O_2N$)-water solution acts as a chemical absorber for H_2S at high pressure and low temperature, 22 bar and 33°C. Absorption and desorption columns are simulated with the subsequent MDEA lean stream recirculation. The MDEA solvent is a 50% water solution on a mass basis. The amount of MDEA solution that is recycled is calculated by a sensitivity analysis for the base case, using ELCOGAS data. Due to the MDEA losses, the net consumption of MDEA is around 3 kg/h. The absorption-desorption columns are modelled using RadFrac models. The desorber works at 1.5 bar and relies on a condenser and a reboiler. As it is recycled, it must be recompressed. The temperature is conditioned before expansion-compression. The MDEA system considers the presence of electrolytes. The ionic dissociation reactions, the equilibrium expressions and the Henry's coefficients, are the same than in the previous units, the venturi scrubber and the sour water stripping system. Moreover, Eq. (5.21) is added to the list formed by Eqs. (5.8) to (5.14). See Tables 5.2 and 5.3 for coefficient values.

$$\mathrm{MDEA}^+ + \mathrm{H_2O} \longleftrightarrow \mathrm{MDEA} + \mathrm{H_3O}^+ \tag{5.21}$$

The absorption and desorption columns are modelled with RadFrac units. No pressure drop is considered. Two streams result from the process: the clean gas from the absorber that goes to the GT and the Claus gas from the desorber that goes to the Claus plant. The clean gas has about 60°C and it is heated to 150°C before the CC. It benefits from the excess heat from the cooling of the COS outlet stream, assuming a 0.7 bar of pressure loss. A recycle stream comes from the Claus plant process and it is added to the clean gas that goes out the MDEA absorber. Between the COS hydrolyser and the absorber a small fraction of clean gas goes to a hydrogenation reactor in the Claus plant. Figure 5.4 depicts the process layout modelled in Aspen Plus.

Claus plant

The aim of this plant is to recover sulphur through H_2S conversion into elemental sulphur. A secondary aim is to convert NH_3 and HCN into N_2. The Claus plant works

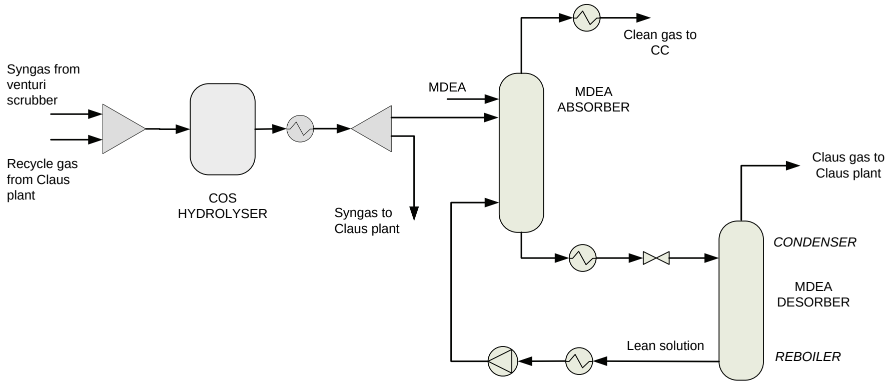

Figure 5.4: COS hydrolyser and MDEA absorption plant layout.

with two polluted streams: Claus gas from the MDEA absorber and sour gas from the sour water stripping process. Both gas streams are at 1.5 bar, and the process takes place at atmospheric pressure, 0.93 bar. The procedure relies on two parallel kilns and two series reactors that are catalysed by alumina. The Claus plant process finishes with a catalysed hydrogenator that is used to increase the overall sulphur removal efficiency through residual gas recycling. Thus, providing with another opportunity to remove the remaining sulphur from the gas. The kinetics model of the Claus plant comprises Eqs. (5.22) to (5.28) for the Claus kilns, and Eqs. (5.29) to (5.30) and catalysed Eq. (5.23) for the catalytic stage. In turn, Eqs. (5.31) and (5.32) correspond to hydrogenation, which is assumed to be in equilibrium. The Claus units are implemented in Aspen Hysys using continous stirred tank reactors (CSTR). The corresponding kinetic expressions and parameters, taken from Hawboldt (1998) and Monnery *et al.* (2000), are summarised in Eqs. (5.33) to (5.47) and in Table 5.4. The subindex f and r represent forward and reverse reactions, respectively. tg is the total concentration of gases.

The thermal and catalytic stages are modelled in Aspen Plus with stoichiometric reactors. The modelling approach in the superstructure considers the thermal stage in only one reactor and it is described by Eqs. (5.22), (5.23) and (5.25), according to the results obtained in the kinetic model. Concerning Eq. (5.23), the production of liquid sulphur is represented as the production of monomolecular S. The subsequent catalytic stage involves Eq. (5.23) at two different temperatures, 270°C and 210°C. There are two streams for air in the Claus kiln; 33% of the stoichiometric oxygen that is needed to combust the H_2S present in the gas and the stoichiometric air that is required to combust the rest of the gas components, since the gas stream is divided into H_2S and the rest of the species for modelling purposes, as depicted in Figure 5.5. The combustion of this last stream is simulated in a Gibbs reactor at 1000°C. The fraction of the stoichiometric air that is required to burn the quantity of H_2S present in the gas mixture is set in the simulation by means of a calculator block, using the property set COMB-O2 (AspenTech, 2010).

$$\mathrm{H_2S + 1.5O_2} \longrightarrow \mathrm{SO_2 + H_2O} \tag{5.22}$$

$$\mathrm{2H_2S + SO_2} \longrightarrow \mathrm{1.5S_2 + 2H_2O} \tag{5.23}$$

$$\mathrm{H_2S} \longrightarrow \mathrm{0.5S_2 + H_2} \tag{5.24}$$

$$2NH_3 \longrightarrow N_2 + 3H_2 \tag{5.25}$$
$$2NH_3 + 1.5O_2 \longrightarrow N_2 + 3H_2O \tag{5.26}$$
$$2CO + S_2 \longrightarrow 2COS \tag{5.27}$$
$$CH_4 + 2S_2 \longrightarrow CS_2 + 2H_2S \tag{5.28}$$
$$COS + H_2O \longrightarrow CO_2 + H_2S \tag{5.29}$$
$$CS_2 + H_2O \longrightarrow COS + H_2S \tag{5.30}$$
$$S_2 + 2H_2 \longleftrightarrow 2H_2S \tag{5.31}$$
$$SO_2 + 3H_2 \longleftrightarrow H_2S + 2H_2O \tag{5.32}$$

$$r_{Eq.(5.22)} = Ae^{-\frac{E_a}{RT}} p_{\mathrm{H_2S}} p_{\mathrm{O_2}}^{1.5} \tag{5.33}$$

$$r_{Eq.(5.23)} = A_f e^{-\frac{E_{a_f}}{RT}} p_{\mathrm{H_2S}} p_{\mathrm{SO_2}}^{0.5} - A_r e^{-\frac{E_{a_r}}{RT}} p_{\mathrm{H_2O}} p_{\mathrm{S_2}}^{0.75} \tag{5.34}$$

$$r_{Eq.(5.24)} = A_f e^{-\frac{E_{a_f}}{RT}} p_{\mathrm{H_2S}} p_{\mathrm{S_2}}^{0.5} - A_r e^{-\frac{E_{a_r}}{RT}} p_{\mathrm{H_2}} p_{\mathrm{S_2}} \tag{5.35}$$

$$r_{Eq.(5.25)} = Ae^{-\frac{E_a}{RT}} p_{\mathrm{NH_3}}^{1.25} \tag{5.36}$$

$$r_{Eq.(5.26)} = Ae^{-\frac{E_a}{RT}} p_{\mathrm{NH_3}} p_{\mathrm{O_2}}^{0.75} \tag{5.37}$$

$$r_{Eq.(5.27)} = A_f e^{-\frac{E_{a_f}}{RT}} X_{\mathrm{CO}} X_{\mathrm{S_2}} - 2A_r e^{-\frac{E_{a_r}}{RT}} X_{\mathrm{COS}} X_{tg} \tag{5.38}$$

$$r_{Eq.(5.28)} = Ae^{-\frac{E_a}{RT}} X_{\mathrm{CH_4}} X_{\mathrm{S_2}} \tag{5.39}$$

$$r_{Eq.(5.23_{cat})} = 1.663 \cdot 10^{-4} e^{-\frac{-30,780}{RT}} \frac{p_{\mathrm{H_2S}} \sqrt{p_{\mathrm{SO_2}}} - \dfrac{p_{\mathrm{H_2O}} p_{\mathrm{S_2}}^{0.1875}}{\sqrt{K}}}{(1 + 1.125 \cdot 10^{-5} e^{-\frac{-2,510}{RT}} p_{\mathrm{H_2O}})^2} \tag{5.40}$$

$$r_{Eq.(5.29)} = \frac{k_1 K_3 p_{\mathrm{COS}} p_{\mathrm{H_2O}}}{1 + K_3 P_{\mathrm{H_2O}}} \tag{5.41}$$

$$r_{Eq.(5.30)} = \frac{k_r K_w p_{\mathrm{CS_2}} p_{\mathrm{H_2O}}}{1 + K_w P_{\mathrm{H_2O}}} \tag{5.42}$$

$$K = \frac{p_{\mathrm{H_2O}} p_{\mathrm{S_2}}^{0.1875}}{p_{\mathrm{H_2S}}} \sqrt{p_{\mathrm{SO_2}}} \tag{5.43}$$

$$k_1 = 2.778 \cdot 10^{-4} e^{0.835 - \frac{-3,039}{T}} \tag{5.44}$$

Table 5.4: Kinetic parameters for the Claus plant (Hawboldt, 1998; Monnery *et al.*, 2000).

Eq. #	Parameters
(5.22)	A = 13.6 mole cm^{-3}s^{-1}atm$^{-1.5}$ E_a = 11 kcal mole^{-1}
(5.23)	A_f = 15762 mole cm^{-3}s^{-1}atm$^{-1.5}$ E_{af} = 49 kcal mole^{-1} A_r = 506 mole cm^{-3}s^{-1}atm$^{-1.75}$ E_{ar} = 44.9 kcal mole^{-1}
(5.24)	A_f = 5263 mole cm^{-3}s^{-1}atm$^{-1.5}$ E_{af} = 45 kcal mole^{-1} A_r = 13.6 mole cm^{-3}s^{-1}atm^{-2} E_{ar} = 23.4 kcal mole^{-1}
(5.25)	A = 0.00421 mole cm^{-3}s^{-1}atm$^{-1.25}$ E_a = 16.5 kcal mole^{-1}
(5.26)	A = 4430 mole cm^{-3}s^{-1}atm$^{-1.75}$ E_a = 40 kcal mole^{-1}
(5.27)	A_f = 3.18·10^5 m^{3}kmole^{-1}s^{-1} E_{af}/R= 6700 K A_r = 2.18·10^9 m^{3}kmole^{-1}s^{-1} E_{ar}/R= 21630 K
(5.28)	A = 5.53·10^{10}m^{3}kmole^{-1}s^{-1} E_a/R = 19320 K
(5.23$_{cat}$)	See Eq. (5.43) P in Pa r in mole s^{-1}kg$_{cat}^{-1}$
(5.28)	See Eq. (5.44) See Eq. (5.45) P in Pa r in mole s^{-1}kg$_{cat}^{-1}$
(5.29)	See Eq. (5.46) See Eq. (5.47) P in Pa r in mole s^{-1}kg$_{cat}^{-1}$

$$K_3 = 1 \cdot 10^{-3} e^{-15.89+\frac{10,010}{T}} \tag{5.45}$$

$$k_r = 2.778 \cdot 10^{-4} e^{2.983+\frac{4,860}{T}} \tag{5.46}$$

$$K_w = 1 \cdot 10^{-3} e^{-19.49+\frac{11,800}{T}} \tag{5.47}$$

According to the Aspen Hysys model results, the degrees of advance of the different chemical reactions are: total conversion of the O_2 from Eq. (5.22), and 0.96 of NH_3 conversion in Eq. (5.25). In the case of Eq. (5.23) the H_2S conversion is considered to be 0.5, while in the case of the two catalytic stages, a conversion of 0.8 and 0.6 is proposed for the SO_2. Finally, the hydrogenator consumes 0.5% of clean syngas to transform unrecovered S and untransformed SO_2 into H_2S, which then returns to the gas cleaning process. The recycle stream is compressed to 23.6 bar and heated to 141°C. The hydrogenator has been simulated with a Gibbs reactor. After each thermal and catalytic step, S is recovered by flash vessels that cool the stream flow to collect the liquid sulphur produced. Figure 5.5 shows the implementation layout of the Claus plant in Aspen Plus.

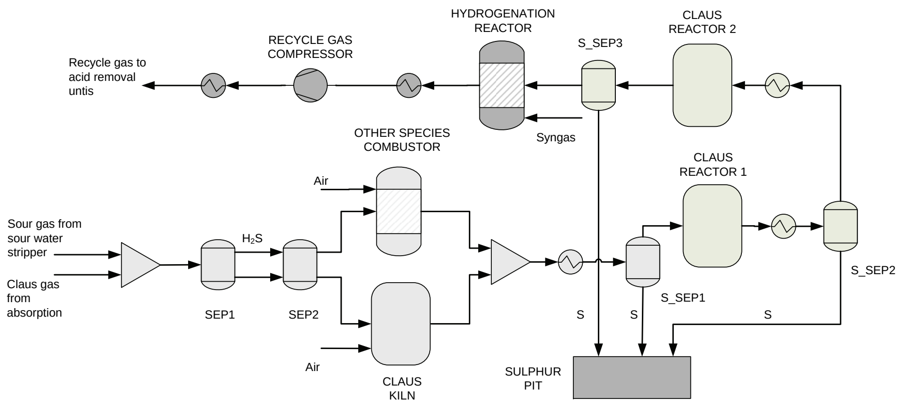

Figure 5.5: Claus plant layout.

WGS and CO_2 capture

This configuration follows a pre-combustion scheme. Figure 5.6 describes the carbon capture scheme as introduced in Aspen Plus, for the WGS and Rectisol processes.

- The first step before CO_2 capture is the conversion of CO into H_2 and CO_2 in the WGS reactors. This step is modelled following the configuration described in Chiesa *et al.* (2005). The shifting transformation takes place in two adiabatic reactors with the WGS reaction in equilibrium at two different temperatures: 400°C and 210°C. Downstream from the first reactor, the gas stream is cooled to meet the conditions of the second reactor. Downstream from the second reactor, the gas stream is cooled from 320°C to 200°C to assure the CO_2 removal unit conditions. Note that the WGS reaction is exothermic. The first reactor consumes IP steam to reach the high temperatures that are required. The β parameter, which is defined as the steam-to-CO ratio on a molar basis and is set to a value of 1.25, determines the amount of inlet steam, according to Descamps *et al.* (2008). This step is modelled in Aspen Plus with two equilibrium reactors.

- A Rectisol process, with methanol as the absorption solvent, removes CO_2. Table 5.2 provides the Henry's law parameters to evaluate the solubility of syngas species in methanol. The solvent expansion between columns takes place by means of three pressure drums, modelled as three flash vessels in Aspen Plus, which recover the CO_2 and allow for solvent recycling. These three units have been established to obtain the desired methanol purity. The higher H_2 concentration stream is obtained at the top of the absorption column. The purity is 80% on a molar basis. The final CO_2 stream comes from the decompression step and from the top of the desorption column. The purity is 70% on a molar basis. The final pressure of the H_2 stream is 21.7 bar, whilst that of CO_2 is 10 bar. The absorption column operates at low temperatures of around -30°C. The desorption column operates at 1.2 bar (note that the final CO_2 stream is compressed to the abovementioned 10 bar), and includes a condenser and a reboiler. The required amount of methanol is proportional to the mass flowrate of CO_2 contained in the WGS product stream: it is 4.5 times the CO_2 mass flowrate that needs to be treated. This value is introduced into the model through a calculator block. The parameters for the Rectisol unit are extracted from Hamelinck and Faaij (2002) and Descamps *et al.* (2008). The two main final streams contain other species that should be mentioned: the H_2 stream has a fraction of N_2, around 15% on a molar basis, and the CO_2 stream has a small fraction of syngas compounds. The methanol flowrate and the number of plates in the RadFrac models are fixed, but the N_2 stream can limit the Rectisol process. This is because the partial pressure of the CO_2 stream can be limited by an increase in the N_2 fraction, which is not large enough to displace the VLE and to be absorbed. On the H_2 side, the presence of more N_2, which flows together with the H_2 stream, reduces the stream purity and thus means that further treatment is required in the PSA system.

- After the Rectisol unit, the H_2 can either be further purified or be used to feed an ideal CC that works with hydrogen as a combustible (see Figure 5.2). The stream should be heated in both applications: up to 40°C to meet the PSA requirements, or up to 150°C to meet the syngas conditions that are required after the MDEA absorber and before entry to the CC. The configuration and parameter values for the PSA system for further H_2 purification are from Hamelinck and Faaij (2002). The system is based on two reactors that use two different solid beds: activated carbon and a zeolite molecular sieve. The trade-off in these systems is the number of reactors vs. the flue gas recycling stream to enhance H_2 recovery. After this process, the purge gas can be released to the atmosphere or compressed and used in the CC (see Figure 5.2). Its LHV is around 8 MJ/kg. Each PSA unit is modelled with a component separator: the first one assumes that all the CO_2 and all the H_2O are released from the main H_2 stream, and in the second one the remaining H_2 corresponds to 84% of the total H_2 flow. The final H_2 pressure is around 0.95 bar, with a purity of 99.99% on a molar basis.

- The CO_2 stream needs a liquefaction step to facilitate transportation and for geological storage. The liquefaction system follows that proposed by Desideri and Paolucci (1999). The operating pressure is assumed to be 150 bar. The compressor has an isentropic efficiency of 82% and an outlet temperature of 35°C before pipeline transportation. Prior compression, the water fraction of the CO_2 stream is separated from the main stream with a flash vessel to avoid problems in the pipeline. In this view, the 10 bar stream is cooled from 183°C to 25°C after the desorption column from the Rectisol system. The final purity of the CO_2 stream is 95.5% on a molar basis.

5.3.2 CC and HRSG

The global energy balance in syngas production for CC application considers the energy that enters via feedstock (LHV) and the energy obtained at the output of the CC. The net power production comprises as main consumers the GT cycle compression and the ASU operation. In terms of heat, all steam cycles supply all the steam consumed in the plant, at the expense of the ST power. As mentioned before, O_2 and N_2 flows are integrated within the system formed by the CC-ASU-gasifier: (i) air to the ASU is fed from the GT compressor; (ii) waste N_2 produced in the ASU is sent

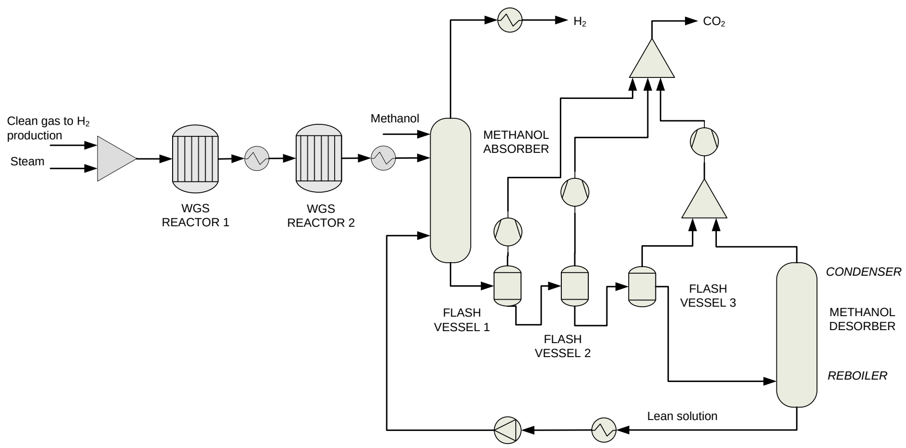

Figure 5.6: WGS reactors and carbon capture with Rectisol process layout.

to the GT to control the flame temperature, in the view of lower NO_x emissions, and (iii) the remaining N_2 stream is used in the feeding system of the gasifier.

The overall CC modelling strategy follows the approach by Zhu (2004) and Ongiro *et al.* (1995). The *GT cycle* comprises a compressor-combustion chamber-turbine system that uses clean gas. A saturation column before the clean gas combustion process saturates the stream with vapour and nitrogen. A simplified flowsheet of the process is shown in Fig. 5.7. Turbine and compressor stages are modelled with turbine and compressor units from the Aspen Plus library. Several mechanical and operating limitations are neglected such as choking and surging in the compressor (Giampaolo, 2006) or the GT inlet temperature (TIT), which has been considered free and not subjected to design limitations. The saturation column is a two-phase flash model in which water is added until the relative syngas humidity reaches 100% (Coca, 2003). This is modelled using a design specification. Turbine air cooling is modelled by taking into consideration a 4-stage GT. Thus, the compressor is also modelled as a 4-step process. Each corresponding stage n has the same pressure loss or gain ratio according to Eq. (5.48). This is implemented into the model by FORTRAN code using a calculator block, in which P_r is the pressure ratio of the turbine or compressor, P_{in} is the inlet pressure, and n_{st} is the total number of stages.

$$P_{i_{loss}} = P_{in} \cdot P_r^{\frac{n}{n_{st}}}\% \tag{5.48}$$

The combustor is modelled by a Gibbs reactor, and mainly N_2, H_2O, CO_2 and NO are released. Turbine outlet temperature (TOT) is a critical value since it influences the amount of heat recovered in the HRSG. It is controlled by the air mole flowrate of entry into the combustor by using a design specification. As in the gasifier, the design specification sets the air mole rate as the proportional stream of the stoichiometric air that is needed to burn the clean gas mixture and obtain the desired TOT, which is fixed at 540°C. In the base case, the proportional factor value is 2.45. However, this is modified by the syngas composition and the flowrate variations. The temperature in the combustor is 98% of the adiabatic one. Cooling air fractions are established by optimising the GT block in the range of 10 to 20% of the stage inlet gas.

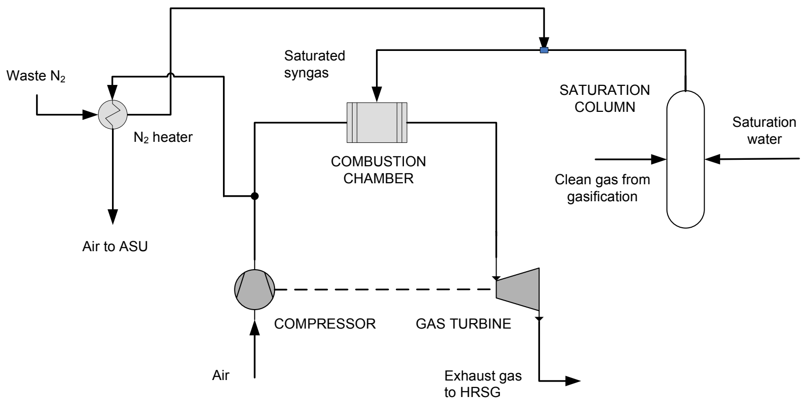

Figure 5.7: Simplified flowsheet of the GT cycle.

The HRSG is a complex HEN that considers various stream temperatures, and combines heat exchangers to produce steam at different temperatures and degrees of superheating. This conceptual design considers a simpler approach. The heat transfer area and heat transfer coefficients are neglected in the calculation of the heat produced by the flue gas temperature variations. To avoid inconsistent temperature crossing, the outlet gas temperature must be higher than the temperature of the steam to produce. The HRSG takes advantage of the syngas temperature drop from 540°C to 100°C. Thus, four heat exchangers have been considered to generate HP, IP and LP steam and to condensate water that then returns to the feed water tank. To maximise the power generated in the ST, the outlet temperatures for the HP, IP and LP steam sides heat exchangers have been estimated and set at 300°C, 180°C and 170°C, respectively.

Three cycles are considered in the *ST section*. They are composed of a water pump, economiser, evaporator, superheater and turbine, using analogous units from Aspen Plus (see a general flowsheet in Fig. 5.8).

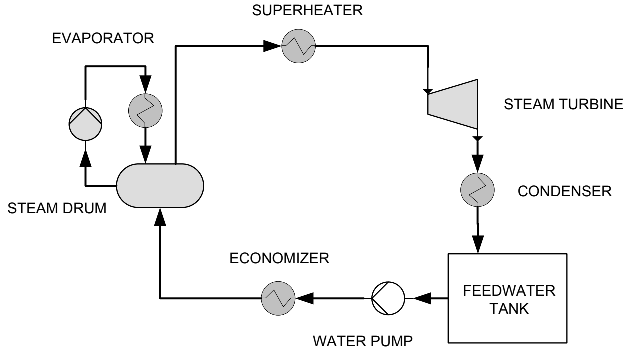

Figure 5.8: Simplified flowsheet of a ST cycle.

Steam is available at different pressures and it flows from its corresponding cycle, HP or IP, down to the LP cycle. Therefore, the LP turbine produces the highest amount of power, due to the large amount of steam that is depressurised. Water mass flows for each pressure cycle are calculated by considering the total heat that is recovered from the WHB and the HRSG, as well as the final estimated temperature before each turbine decompression. A calculator block is used for these values assignments. Table 5.1 provides the stream's temperatures. There is a net water consumption in the plant regarding (i) the steam fed to the gasifier, (ii) the steam consumed in the venturi scrubber to clean the syngas, (iii) the steam flow used in the saturator to saturate the clean gas before its combustion in the GT, and (iv) the water consumption needed in the WGS unit to produce H_2 and CO_2 from CO. The consumption of these streams penalises the heat flow from WHB and HRSG to the ST cycle. Finally, the net CC power is obtained by considering the gross power resulting from the ST and the GT (taking into account the air compressor consumption) and subtracting the power consumption of the ASU, the crusher, and the compressors and pumps from syngas cleaning unit blocks, including the power of the CO_2 capture system when co-production is considered.

5.3.3 ASU

This unit produces enriched air by separating oxygen and nitrogen to meet the requirements of the gasification and CC blocks. In this case, the outcome of the unit is an oxygen stream with 85% purity on a molar basis. The ASU product streams are enriched O_2, pure N_2 and waste N_2. These streams are pressurised externally to adapt them to the plant conditions, since the pressures in the ASU process are governed by the cryogenic and distillation conditions of the air. This procedure involves several steps, which are modelled in a simplified way with a component separator, compressors and heating units:

- Air pre-cooling. Air is taken to the purification unit temperature. Generally, this is carried out by a refrigeration fluid.
- Air purification and distillation. The main objective in the purification step is to remove impurities, such as water, from the air inlet stream. This is based on solid-gas (SG) absorption. As the pressure is determined by the GT compressor, the air pre-cooler is crucial to obtain the desired efficiency. Then, the distillation stage is a cryogenic process in which nitrogen and oxygen can be separated through a distillation column. This occurs at about 13 bar and -165°C. Oxygen is released as a liquid and nitrogen as a gas. The purity of waste N_2 is approximately 98% on a molar basis, and that of pure N_2 is about 99.9% on a molar basis. A component separator block is used here.
- Gas supply. The outlet streams need to be adapted to the desired conditions of pressure and temperature for the gasifier and the CC. These are 30 bar for the O_2, 20 bar for the waste N_2, and 50 bar for the IP N_2. The isentropic efficiencies of the compressors are assumed to be 0.72.

5.4 Calibration and validation

ELCOGAS power plant data, the works by Chiesa *et al.* (2005), Descamps *et al.* (2008) and exhaustive kinetic models from Aspen Hysys, are combined to adjust the

Table 5.5: Calibration parameters in the different syngas cleaning units.

Unit	Variable	Basis	Reference	Parameter
Venturi	H_2O consumption	mass	Syngas flowrate	9%
	NaOH consumption	mass	Syngas flowrate	0.12%
	Stages	number	-	10
Stripper	H_2SO_4 consumption	mass	H_2O flowrate	0.3%
	Acid stripper stages	number	-	5
	NaOH consumption	mass	H_2O flowrate	1.2%
	Basic stripper stages	number	-	8
Hydrolyser	COS	conversion	Eq. (5.19)	0.99
Absorber	MDEA solution flow	mass	-	118000 kg/h
	Absorber stages	number	-	5
	Desorber stages	number	-	12
	Desorber reflux ratio	mass	-	1.9
	Desorber boilup ratio	mass	-	0.3
Claus plant				
Kiln	O_2	conversion	Eq. (5.22)	1
	NH_3	conversion	Eq. (5.25)	0.96
	H_2S	conversion	Eq. (5.23)	0.50
	Air consumption	mole	H_2S flowrate	0.33·stoich.
Claus 1	SO_2	conversion	Eq. (5.23_{cat})	0.80
Claus 2	SO_2	conversion	Eq. (5.23_{cat})	0.60
WGS reactor	β	mole	-	1.25
Rectisol process	Methanol flow	mass	CO_2 flowrate	4.5
	Absorber stages	number	-	8
	Flash vessel 1	pressure	-	10 bar
	Flash vessel 2	pressure	-	2.7 bar
	Flash vessel 3	pressure	-	1.4 bar
	Desorber stages	number	-	15
	Desorber reflux ratio	mass	-	5
	Desorber boilup ratio	mass	-	0.3
PSA				
Bed 1	CO_2 and H_2O flows	separation	H_2 flow	0·H_2 flow
Bed 2	H_2 flow	separation	H_2 flow	0.84·H_2 flow

parameters of syngas cleaning units. These parameters have been described throughout the text and are summarised in Table 5.5. They are suitable for changes required in adapting to each specific case study as well as for optimisation purposes.

Validation of results consider the base case. For the gas cleaning process without H_2 purification, Figure 5.9 compares industrial information on the clean syngas composition and the composition of the Claus gas with the simulated compositions for both cases. Both streams are the outlet streams of the MDEA absorption-desorption process, which is the last cleaning step applied to the main gas stream before the CC. The measured and predicted values are on the x and y axes, respectively. Therefore, the points that are represented reflect the comparison between these values. The points closest to the quadrant division line are the most precise. If the IGCC power plant is considered as a whole, with no carbon capture units, the accuracy of the model in terms of the net power, by-products and clean gas characteristics can be validated, as shown in Table 5.6.

For the feedstock dust preparation, gasification and clean gas blocks together, the clean gas and Claus gas composition comparison is within an error margin of 10%. The comparison of results in Table 5.6 indicate that the largest discrepancy concerns the estimation of the LHV of the clean gas and the amount of sulphur recovery, which is overestimated. This suggests that a higher CC efficiency compensates for the underestimation of the LHV of the clean gas. In addition, auxiliary consumption

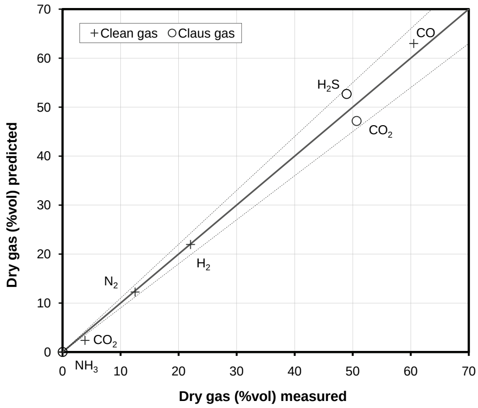

Figure 5.9: Comparison of components of clean gas and Claus gas between values calculated (predicted) by the model and the actually measured data from industry. The error bars correspond to 10% deviation.

Table 5.6: Overall IGCC plant validation data.

	Measured	Model	Error %
Raw gas flow (t/h)	202.5	192.3	-5.05
LHV clean gas (MJ/kg)	9.911	9.547	-3.68
Gross Power (MW)	308	315	2.27
ASU consumption (MW)	29	27.4	-5.52
Net Power (MW)	283	285	0.71
Sulphur (t/h)	3.11	3.32	6.59

is higher than in the real plant. The PSA unit has been directly validated by comparing the model results with the data from Chiesa *et al.* (2005) and Descamps *et al.* (2008). The CO conversion rate is 91%, in contrast to the 92% rate found in the study by Descamps *et al.* (2008). Concerning the Rectisol system, a CO_2 absorption rate of 95% is referred to in the literature, while a value of 99% is obtained in the simulation due to the modelling assumptions.

The results show that in a conceptual stage this modelling approach represents an approximation of sufficient accuracy of an IGCC power plant with CO_2 capture, with a maximum error of 10%. This is well within the error range of a preliminary design stage, which spans from 15% to 20% (Wells & Rose, 1986).

Once the accuracy of the model is checked, Table 5.7 summarises the split fractions of the main syngas components. The split fractions are defined according to Section 5.2.1, taking into account the syngas inlet and outlet streams of each individual block. Those units involving absorption procedures are substituted by component splitters as meta-models. In the first unit described, NH_3 and HCl are fairly depleted from the gas stream. The stripper cleans water from acid species in an efficient way. In contrast, its efficiency is not high for basic species. After the MDEA absorption process, half of the CO_2 amount remains in the syngas. In the Claus plant, nearly all the sulphur is recovered. The remaining NH_3 is recycled. The Rectisol process recovers all the H_2 and almost all the CO_2 present in the shifted stream.

Table 5.7: Split fractions for the main components in the different syngas cleaning units.

Unit	Component	Split fraction
Venturi	NH_3	0.207
	HCl	0
	CO_2	0.999
	H_2S	0.998
	HCN	0.977
Stripper	NH_3	0.188
	HCl	0
	CO_2	1
	H_2S	1
	HCN	1
Absorber	NH_3	0.999
	CO_2	0.503
	H_2S	0.997
	HCN	0.924
Claus plant	NH_3	0.318
	CO_2	1.120
	H_2S	0.029
	HCN	0
Rectisol process	H_2	0.996
	CO_2	0.999

As well as for the previous chapter, the influence of process variables on trends in model output variables is evaluated. Therefore, the results obtained from the SAs by varying the two gasifier ratios are represented in two-dimensional graphs, in which the axes correspond to the input variables and the output variable changes are plotted using contour lines. Blue points on the graphs are the discrete values obtained with the SAs, while the red star point is the highest value, of the output variable in the SA. The base case SA considers an oxygen ratio variation from 0.3 to 0.55.

Figure 5.10 reports the variation observed for T_{gasif}, TOT and the LHV_{rg}. The steam's role as a moderator in the gasifier is clearly shown, since more steam leads to lower temperatures. In addition, more inlet oxygen is associated with higher temperatures. The SA shows gasification temperatures in the range of 800°C to 2400°C, even when the *gasification zone* is in the middle of the temperature range, and limited by CH_4 and sulphur oxide production. The TOT is between 550°C and 490°C. In the modelled installation, temperatures below 540°C are not feasible in operating regions of the HRSG, due to the steam temperature requirements. Lower H_2O ratio combined with the lower equivalence ratio (ER), yields the highest LHV_{rg} values.

Syngas compositions (H_2, CO, CO_2, CH_4) are represented in Figure 5.11. The presence of CH_4 is mainly driven by the O_2 amount coupled with high gasifier temperatures (see Figure 5.10 left and Figure 5.11 bottom right). Non-linear shapes are found for H_2, CO and CO_2. The highest H_2 production is found for an ER close to 0.4 and for the highest ratio of steam that is fed into the gasifier. The relationship between CO_2 and H_2 is evident, but the highest values of CO_2 are observed for the maximum amount of O_2 and steam. As expected, the CO behaviour is the opposite of the CO_2 behaviour.

Figures 5.12 and 5.13 are highly interrelated. Firstly, steam and gas turbine powers are plotted. The amount of power produced by the GT reaches a maximum when the ER and the steam ratio are at their lowest levels. In contrast, ST production is greater at higher oxygen ratios but lower steam ratios. In both cases, the O_2 ratio has larger influence than the steam ratio.

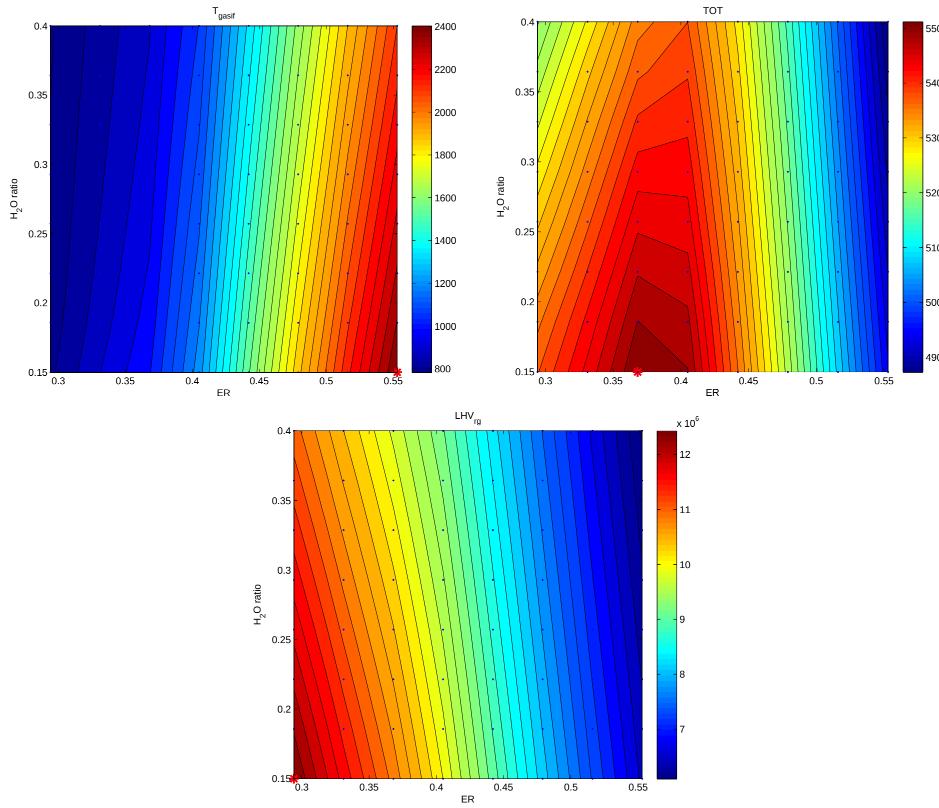

Figure 5.10: Iso-lines for T_{gasif}, TOT, and LHV_{rg} in °C and J/kg respectively, for the base case.

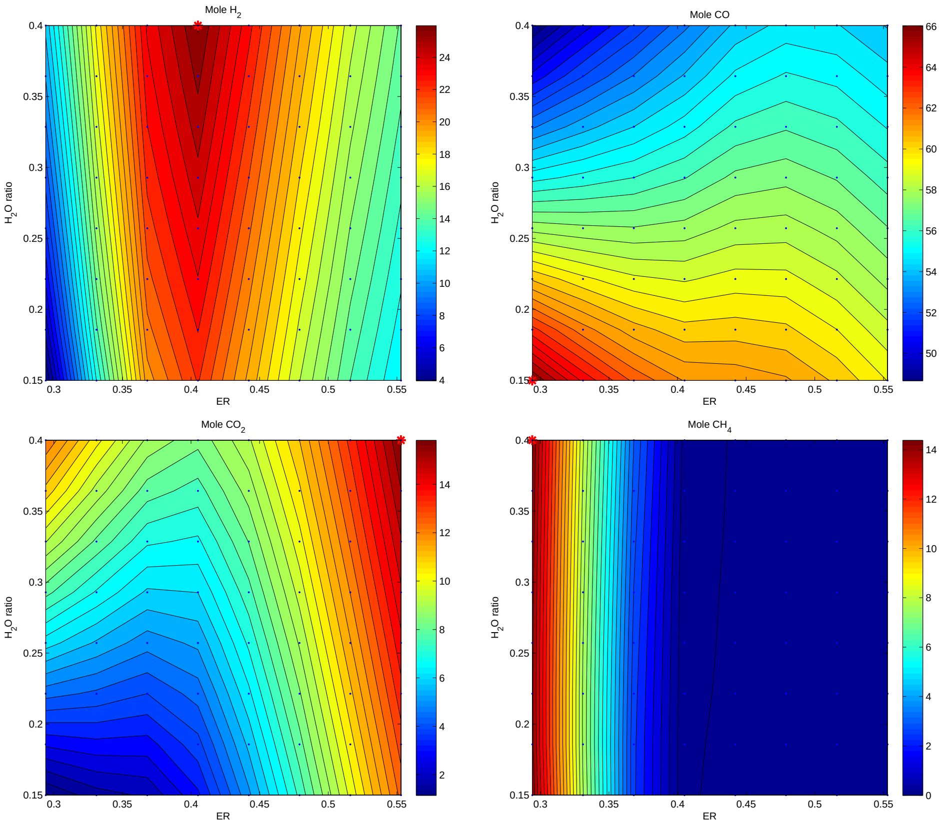

Figure 5.11: Iso-lines representing the mole fraction (%) of raw gas components in dry basis for the base case.

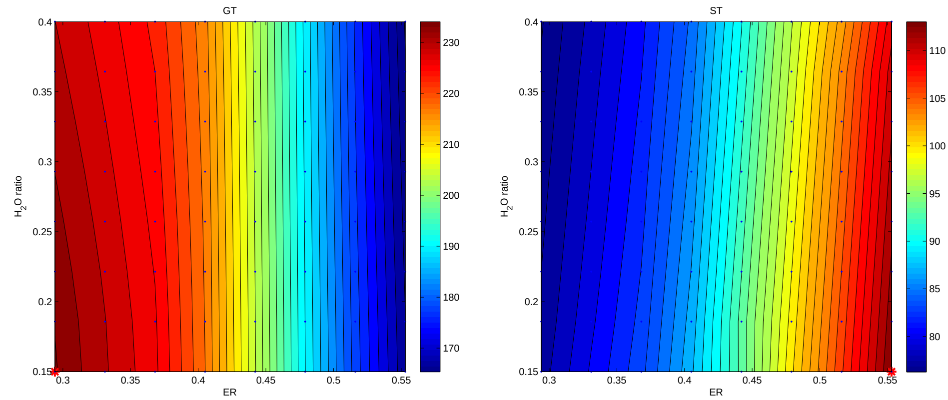

Figure 5.12: Iso-lines for gas and steam cycles power production (MW) for the base case.

As shown in Figure 5.13 (top left), the highest value of the cold gas efficiency (CGE) (defined in Eq. 3.6) coincides with that obtained for the maximum GT power production. This is in accordance with the higher LHV$_{rg}$ values found in Figure 5.10, given that the fuel LHV remains constant. The Eff_{global} (see Eq. 3.8) shows the same behaviour because most of the power comes from the GT and the fuel LHV remains constant. The highest value for Eff_{CC} (see Eq. 3.7) coincides with the highest ST power production and therefore with the highest gasification temperatures, at which the WHB recovers more heat for steam production.

The ER has a greater influence on the plant performance than the steam ratio. CGE is the main parameter that influences the final global efficiency of the plant when operated at IGCC mode, rather than Eff_{CC} since it is the GT that produces more power.

This calibration and validation step demonstrates the suitability of the present modelling approach for conceptual IGCC-CCS plant analysis.

5.4.1 Aspen Hysys-Aspen Plus superstructure validation

The Aspen Hysys-Aspen Plus superstructure has been also validated. See in Figure 5.14 the validation strategy followed here. Two sets of data are used:(i) final syngas compositions for each cleaning unit using the base case, and (ii) different coal:petcoke mixtures. Those mixtures are detailed in Table 5.8. C8 is a mixture of coal, petcoke and orujillo. The compositions reported in the table correspond to those values found after the drying step, considering a 2% of moisture. Plant inlet conditions are the same for all case studies.

For Figure 5.14 left graph, shows that the venturi scrubber model predicts quite accurate values for all the components, while the sour water stripper unit model produces values slightly higher than the industrial data for CO_2 and H_2S and lower for NH_3. The sour water stripper is the unit which has the higher discrepancies, when comparing to plant measurements. The main difference between the predicted and industrial composition in the Claus plant model is in CO gas composition, while the amount of liquid sulphur removed is quite similar for both, real and predicted values, i.e. 3113 and 2810 kg/h, respectively. The results error ranges in +/- 18%. In Figure

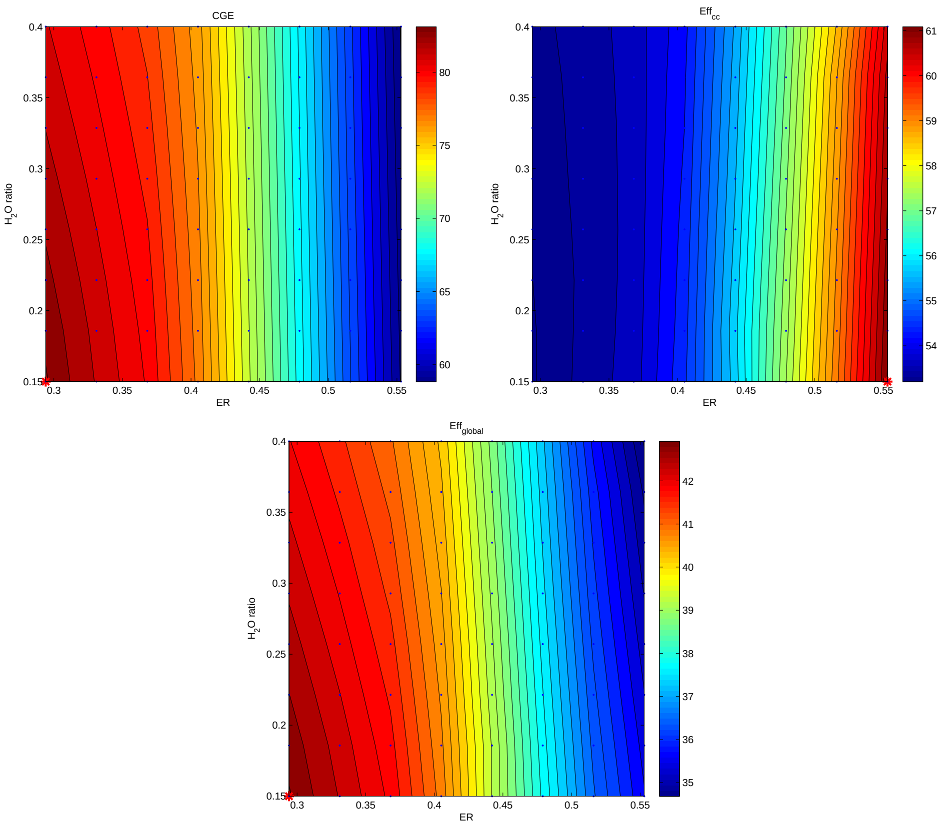

Figure 5.13: Iso-lines for CGE (Eq. 3.5), Eff_{CC} (Eq. 3.7) and Eff_{global} (Eq. 3.8) in % for the base case.

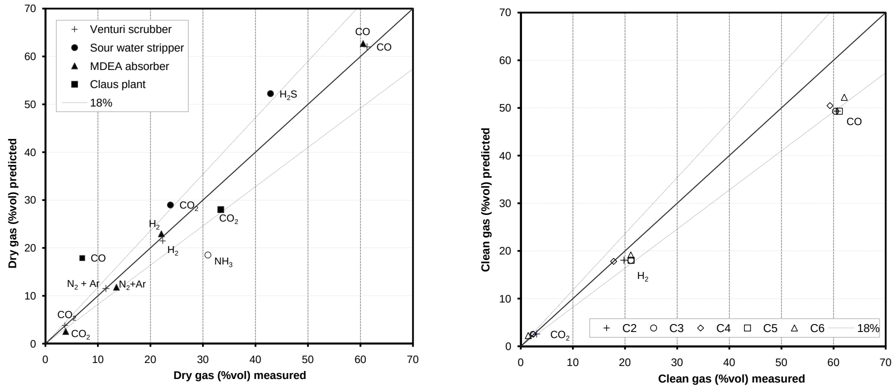

Figure 5.14: Comparison of predicted and measured values from the individual cleaning units (left side). Overall plant validation with different feedstock mixtures (right side).

Table 5.8: Feedstocks share used to validate the Aspen Hysys-Aspen Plus superstructure.

	C1	C2	C3	C4	C5	C6	C7	C8
Feedstock share								
Coal (%)	100	58	54	50	45	39	0	50
Petcoke (%)	0	42	46	50	55	61	100	40
Orujiilo (%)	0	0	0	0	0	0	0	10
Ultimate analysis (ar)								
C	40.30	59.76	61.61	63.46	65.78	68.56	86.63	59.70
H	2.76	2.97	3.00	3.02	3.04	3.07	3.28	3.32
O	7.36	4.28	3.98	3.69	3.32	2.88	0.02	7.24
N	0.90	1.36	1.41	1.45	1.51	1.57	2.00	1.33
S	1.03	3.03	3.22	3.41	3.65	3.94	5.80	2.84
Proximate analysis (ar)								
Moisture	2.00	2.00	2.00	2.00	2.00	2.00	2.00	2.00
Ashes	45.67	26.60	24.78	22.97	20.70	17.97	0.27	23.56
Fixed carbon	52.33	71.40	73.22	75.03	77.30	80.03	97.73	74.44
Volatiles	19.60	17.67	17.48	17.30	17.07	16.79	15.00	23.04
LHV_{dry} (MJ/kg)	15.75	23.10	23.80	24.51	25.38	26.43	33.26	23.10

5.14 right graph, the final clean gas composition that results from the model, are contrasted. The model predicts lower than measured gas concentrations for the main components H_2 and CO. The latter is the component with the largest discrepancy, within a maximum error of 18%. This modelling approach is also within the range 15-20% of accuracy in a conceptual level (Wells & Rose, 1986).

5.5 Preliminary results

Different products are obtained when topological changes are introduced in the modelled flowsheet by means of the superstructure built, in terms of the fraction of syngas that enters the CC or the CO_2 removal process: (i) all the syngas is used in the CC; (ii) co-production of power and H_2, (iii) production of H_2 only; (iv) production of H_2 only, with PSA purge gas recycling to be used in the CC, and (v) the H_2 stream that is separated after the Rectisol system is used in the CC. The superstructure has a set of splitters that allows the aforementioned processes to be carried out, as was represented in Figure 5.2.

The final gas streams are syngas, pure H_2, CO_2 and a purge gas that comes from the PSA unit. The latter mainly contains CO_2, H_2O and traces of CO and H_2. The LHV predicted by the model are 9.29 MJ/kg, 119.96 MJ/kg, 0.34 MJ/kg and 8.15 MJ/kg, respectively. They are plotted in Figure 5.15 left graph, by means of their calorific value in MW, and varying according to the percentage of syngas that goes to the CC. All streams trends follow a linear behaviour. The slopes are 5 for syngas, -4 for H_2, -0.2 for CO_2 and -1 for PSA purge gas. The slopes values not only express the differences among LHV's, but also the differences among the portions of syngas treated into each concerned unit and the efficiency of the carbon capture process (defined as in Eq. 3.9). Injection of a 100% stream of pure H_2 to the CC, that represents a 75% of the calorific value of the carbon removal train outlet streams, produces less power than a CC powered by syngas. This is due to an $Eff_{CCapture}$ of 69% in the carbon removal step. Even with an increased up to 89%, when the PSA flue gas is used for

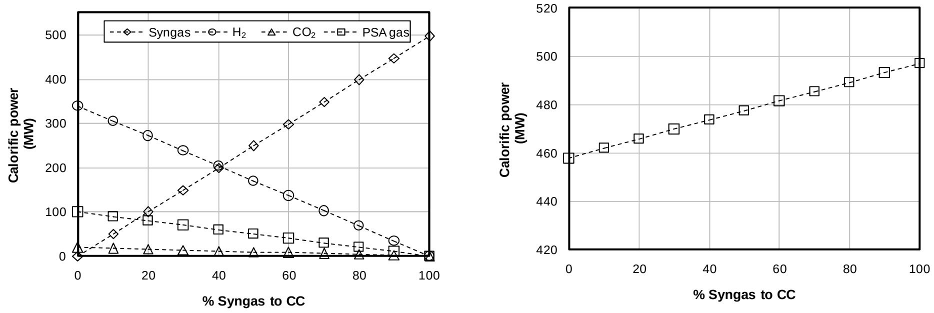

Figure 5.15: Calorific value variation of the final gas unit's outlet streams separately (left side) and all together (right side).

Table 5.9: Comparison between electricity and H_2 production.

	Syngas to CC	Pure H_2 to market	Pure H_2 to market-PSA to CC	H_2 to CC
Eff_{global} (%)	42	-	5.4	33.3
$Eff_{global_{H_2}}$ (%)	-	51	51	-
Gross Power (MW)	315	0	85	273
Net Power (MW)	285	-46	37	226

power purposes, H_2 burning remains a less efficient option than burning syngas. The plot of the calorific value of the four streams together is shown Figure 5.15 right graph. Overall, the addition of other processes after the syngas obtaining, if using them to produce gaseous streams to generate power, diminishes the useable calorific value of the gas. In this case, the decrease has as upper value an 8%.

The base case, in which all the syngas is consumed in the CC, is compared with the extreme cases, in which all the syngas is used to produce pure H_2 to be sold on the market, with PSA purge gas profit or not, or to produce relatively pure H_2 to be burnt in a CC, therefore, in an hypothetical hydrogen turbine, analogous to the one described in this chapter. As suspected before, the advantage of burning H_2 is not on the plant efficiency optimisation, but on the GHG emissions decrease. In all four scenarios, the amount of air that goes to the GT is controlled by a design specification in Aspen Plus to adjust TOT at 540°C. The production of only H_2 induces several inherent changes in the flowsheet: the HRSG cannot be used, no air enters the GT to be burnt in the combustor or to be used for turbine refrigeration and the waste N_2 should be sent somewhere else rather than to the GT cycle. In this case, it is used in the feeding system. Nonetheless, when PSA purge gas is used in the CC, the HRSG as well as the GT refrigeration system are employed.

Table 5.9 lists the global efficiencies (Eqs. 3.8 and 3.10) and the final gross and net powers for each case study. In the scenario with pure H_2 production, the net power is negative mainly because the GT compressor work to provide compressed air to the ASU. The use of the PSA purge gas in the CC demonstrates its benefit in terms of energy profitability, but its low calorific value does not justify the presence of such a CC. The efficiency penalty is 8.7% when comparing a CC working with syngas with

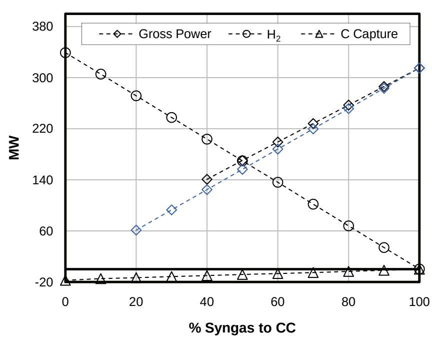

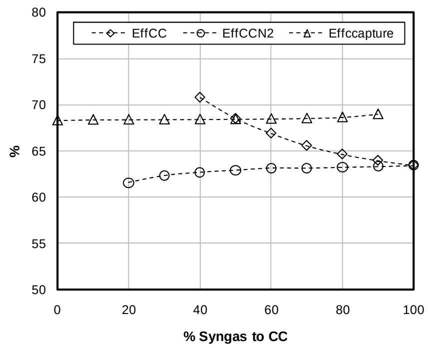

Figure 5.16: Power plant productions, carbon capture units consumption (left side) and CC and carbon capture units efficiencies (right side). Line in blue referes to gross power with waste N_2 separation.

a CC working with H_2. This percentage includes the penalisation of carbon removal train consumption. A feedstock (coal:petcoke) increase of 21% on a mass basis should equal the power produced by H_2 combustion to the power produced when burning syngas.

Figure 5.16 left graph illustrates how the percentage of syngas that goes to the CC affects on the gross power, the calorific value of the H_2 stream and the electricity consumed by the carbon capture train of units. When the split fraction is 50%, the calorific value of the H_2 and the gross power produced are similar. It is therefore deduced that both applications, the CC and the carbon capture train, have comparable efficiencies. Figure 5.16 (right side) presents the efficiencies dependency with the split fraction of syngas to CC. The production of H_2 is almost constant at 68%, while the gross power exhibits two behaviours, depending on the use of the waste N_2 from the ASU. Eff_{CC} refers to the base case configuration: all waste N_2 is fed to the GT combustor. Eff_{CCN_2} considers a fraction of waste N_2 splitted and used in the feeding system, the same as the percentage of syngas that is splitted. This is also plotted in Figure 5.16 (left side) in blue. The waste N_2 stream has a flowrate of 246000 kg/h, at 384°C and 20 bar. It considerably increases the GT flowrate, that relies on a syngas stream at 147°C. The issue with this waste stream is that for low percentage of syngas to CC it refrigerates too much the combustion mixture, which prevent to maintain the TOT design temperature. That is the reason why, when considering N_2 separation, the range of operation is broader, but the power produced diminishes. Both efficiencies show different trends in the right hand graph, with Eff_{CC} showing more disparity .

5.5.1 Aspen Hysys-Aspen Plus superstructure results

The different case studies exposed in Table 5.8 are compared between them in terms of net energy and flue gas emissions. Net energy and emissions have been normalised for comparison purposes considering the mass flow of inlet C (C_{in}). In Figure 5.17 left graph, the relative energy is represented. It decreases as the proportion of coal decreases. Exhaust gas emissions, NO_x and SO_2, in relative terms, are plotted in right graph. NO_x emissions decrease as the proportion of petcoke increases. C1 is the scenario with less relative sulphur emissions. The scenario with 100% coal gasification

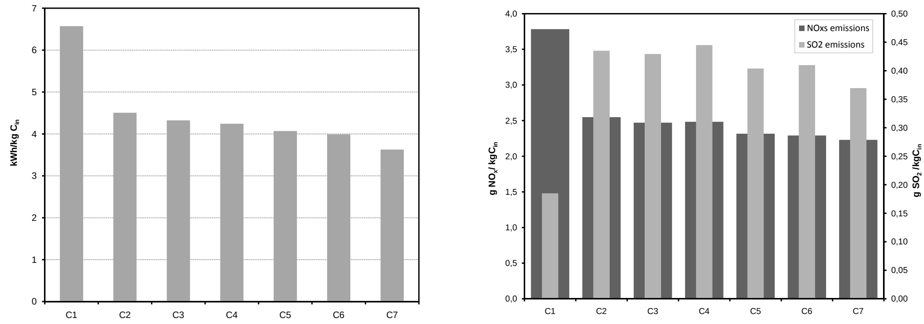

Figure 5.17: Net energy and emissions per kg C_{in} for the simulated feedstock mixtures.

is the preferred one in terms of relative energy produced, but the nitrogen oxides emissions are the highest. These are directly influenced by the composition of the inlet material.

The main limitations in this approach, and deduced from the performance obtained, are attributed to the origin of the gasification model (this is an exhaustive model for coal gasification) and the use of too precise ANN's conceived to work for a specific range of working conditions.

5.6 Final considerations

This chapter has provided an overall view of the superstructure developed for IGCC-CCS plants, showing the degree of flexibility and versatility of the tool. The modelling approach achieves discrepancies lower than 10%, which is accurate enough in a conceptual design stage. It has been proven that more explicit models, as exemplified by the case of the gasifier, that should be derived from more specific applications, are leading to bigger discrepancies when used with other plant datasets than the ones serving to conceive the model. Thus, the modelled superstructure conceived should be general enough to accept the versatility required at this conceptual stage of IGCC-CCS plants design.

The efficiency penalty of the CO_2 capture block is around 8.7% in net power terms if H_2 is used in the CC. In order to maintain the same power level than that obtained with the combustion of syngas, the feedstock should be increased by 21% on a mass basis. The PSA flue gas use in the CC enhances the overall efficiency of the plant. The integrated nature of the plant limits co-production to certain range of syngas to CC split fractions, mainly due to the GT performance and TOT limitation.

This superstructure development stage form the basis for optimisation anaylises presented in the next chapter.

Notation

Latin letters

a	activity

A	pre-exponential factor
b, c, d, e, f	Henry coefficients
B, C, D, E	K_{eq} coefficients
Eff	efficiency
E_a	activation energy
f	fugacity
k	reaction rate constant
K	equilibrium constant
K_{eq}	equilibrium constant
m	mass or molar flow
n	number of stages
H	Henry's law constant
P	pressure
p	partial pressure
R	universal gas constant
r	reaction rate
T	temperature
x	mole fraction in the liquid phase
X	molar concentration
y	mole fraction in the gas phase

Greek symbols

β	steam-to-CO ratio in a WGS reactor
γ	activity coefficient of liquid species
ϕ	fugacity coefficient
ρ	bulk density

Superscripts and subindices

cat	catalyst
cg	clean gas
f	forward
$gasif$	gasification
i	species
L	lower
o	atmospheric conditions
r	reverse
rg	raw gas
st	global number of stages
tg	total concentration of gases
U	upper

Acronyms

ANN	artificial neural network
ar	as received basis
ASU	air separation unit
CC	combined cycle
CCS	carbon capture and storage
CGE	cold gas efficiency
C_{in}	kg of inlet carbon
COS	carbonyl sulphide
CSTR	continuous stirred tank reactor
daf	dry and ash free basis
dry	dry basis

ELECNRTL	NRTL with electrolytes formation
EOS	equation of state
ER	equivalence ratio
GHG	greenhouse gases
GT	gas turbine
HEN	heat exchangers network
HHV	higher heating value
HP	high pressure
HRSG	heat recovery steam generator
IGCC	integrated gasification combined cycle
IP	intermediate pressure
LHV	lower heating value
LLE	liquid-liquid equilibrium
LP	low pressure
MC	moisture content
MDEA	methyldiethanol amine
NRTL	non-random two liquid
PFR	plug flow reactor
P_r	pressure ratio
PR	Peng-Robinson equation of state
PR-BM	Peng-Robinson equation of state with the Boston-Mathias alpha function
PSA	pressure swing adsorption
SA	sensitivity analysis
SG	solid-gas
ST	steam turbine
TIT	turbine inlet temperature
TOT	turbine outlet temperature
VLE	vapour and liquid phases in equilibrium
WGS	water gas shift
WHB	waste heat boiler

Chapter 6

IGCC-CCS Superstructure Results and Process Optimisation

In this chapter, the developed superstructure for the synthesis, pre-design and retrofit of IGCC-CCS plants is used to investigate various co-gasification and co-production cases in terms of technical, economic and environmental performances. The objective in this conceptual design stage is to achieve the most efficient, financially-viable and environmentally-friendly scenarios for a given plant configuration. The results characterising each considered scenario are analysed on the basis of Pareto fronts to deal with the multiple-criteria decision analysis (MCDA). This tool can be used to explore ways to improve the plant operation and to analyse the influence of raw materials and units operational parameters, not only for IGCC power plants, but also for any other type of gasification plant, through the appropriate changes in the plant layout.

6.1 Introduction

The most recent trends in gasification industry are to increase the percentage of biomass use, extend the capture of anthropogenic CO_2, employ more efficient cleaning methods that could comply with higher temperatures and construct and operate economically viable plants (NETL, 2007). As example for the last point, the tendency is to substitute the ASU by more economic new methods or by gasification configurations with air.

Since the aim of conceptual design is to elucidate the best process flowsheet among competing alternatives and determine the optimum design conditions, the role of the superstructure here is focused on the selection of optimum processes layouts, offering at the same time decision-making support to identify the best compromise design in a multiple objective scenario-based optimisation. The scenarios or case studies performed are classified into Set 1 and Set 2, as further described in Section 6.4.

6.2 IGCC-CCS superstructure

The superstructure is performed in Aspen Plus. The modelling strategy has been described in Chapters 4 and 5. Table 6.1 summarises all the modelled units and their implementation in the commercial software.

Table 6.1: Summary of all modelled units.

Block	Aspen Plus model
Feedstock dust preparation	Dust preparation: crusher Combustion chamber: Gibbs reactor Dryer: stoichiometric reactor Bag filters: two phase (VL) flash separator Lock hopper: mixer
Gasification and WHB	Gasifier: yield and Gibbs reactors Solid removal: component splitter WHB: heating units and a compressor for gas recycling
Syngas cleaning	Venturi scrubber: RadFrac column and two phase (VL) flash separator Sour water stripper: RadFrac columns COS hydrolyser: stoichiometric reactor MDEA absorber: RadFrac columns Claus plant: stoichiometric and Gibbs reactors and two phase (VL) flash separators WGS reactor: two equilibrium reactors Rectisol process: RadFrac columns PSA unit: component splitter Liquefactor: flash separator and compressor
CC and HRSG	Turbines, compressors and heating units Combustor: Gibbs reactor Saturator: two phase (VL) flash separator HRSG: heating units
ASU	Compressors and heating units, and component splitter

As already mentioned in Section 5.5, once the H_2 is separated from the CO_2, it could be exploited in different ways: to produce electricity in a CC or to be sold as pure H_2. The PSA purge gas can be fed or not to the CC to use its calorific value. Figure 6.1 provides the detailed arrangement of these units, extracted from Figure 5.2.

Figure 6.2 shows the detail of the IGCC-CCS superstructure: the diagram compiles all the technical possibilities that an IGCC plant offers. Among all the options that a general IGCC plant presents to be optimised, the dashed lines in red indicate the design choices that are taken into account in this thesis approach. Raw materials can be from different origins. Pre-treatment block contemplates energy and matter densifications, as further described and developed in Chapter 7. Feedstock mixture and final syngas usage elections, for electricity of H_2 productions, are carried out in this Chapter with MCDA. See in Figure 6.3 the snapshot of the superstructure of process flowsheet modelled using Aspen Plus. Note the use of stream splitters and mixers to perform the choice of different unit operations executing the same part of the process. Operating conditions subject to changes between case studies are T_{gasif} and turbine outlet temperature (TOT).

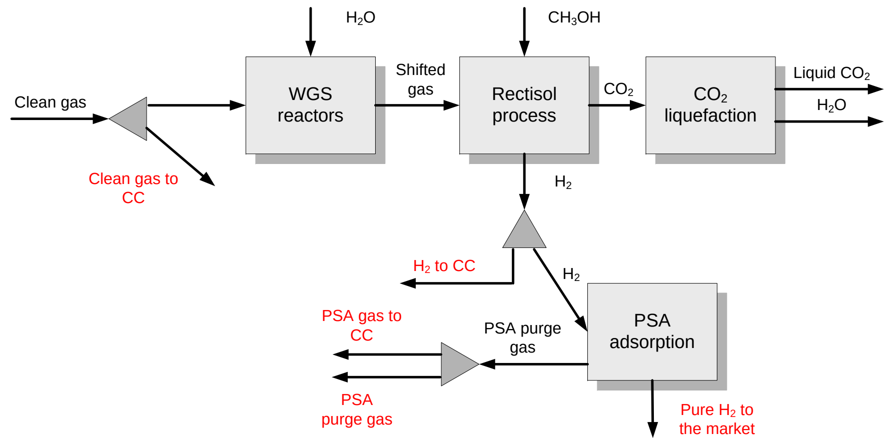

Figure 6.1: CO_2 capture/H_2 production-CC process superstructure.

6.2.1 Superstructure application to IGCC and NGCC configurations

In order to show the capabilities of the superstructure scenario-based optimisation approach, the IGCC and the natural gas-combined cycle (NGCC) modes of operation are compared in terms of their key performance indicators (KPI) evaluation. In essence, the CC can be used for both, syngas or NG combustion. Figures 6.4 and 6.5 show the layout and the mass balances for both plant configurations (Coca, 2003). The main differences consist in inlet feedstocks and utilities flows. For instance, in the case of IGCC mode, the mass flowrate of coal:petcoke mixture is three times higher than the mass flowrate of NG. NG is directly introduced into the GT together with pressurised air. IGCC operation requires from the feedstock preparation, gasification, WHB and gas cleaning units. In the case of IGCC, the selected air/fuel ratio is 10 while in the case of NG is 50, to achieve the same flowrate, as well as the same LHV as GT inlet. In both cases, the ST cycles work at three different pressures: HP, 125 and 80 bar; IP, 30 and 15 bar and LP, 5 and 3 bar, for IGCC and NGCC configurations, respectively.

The considered scenarios are SC1, SC2 and SC3: IGCC configuration base case, IGCC configuration with coal:petcoke:orujillo (45:45:10% on a mass basis), and NGCC configuration. Eff_{global} is calculated following Eq. (3.8). The economic metric is the COE, as described in Eq. (3.16). Figure 6.6 shows the comparison of COE's breakdown for IGCC and NGCC modes of operation.

A comparative environmental impact assessment has been carried out in both cases by means of ISO14040 guidelines. The study of both configurations is organised following the ISO standard 4-steps, as further described in Section 3.5.3:

- Goal definition and scope. The example is focused on the environmental contribution change attained by the different mixtures of raw materials and different raw materials, as well as topological changes. The simulated IGCC and NGCC plants consider extraction and processing of raw materials up to the power production, which constitutes the cradle to gate approach. Emissions from waste water treatment plants, inert solid disposal (ashes) and flue gases are also taken into account. The obtained sulphur is considered to be an environmental credit,

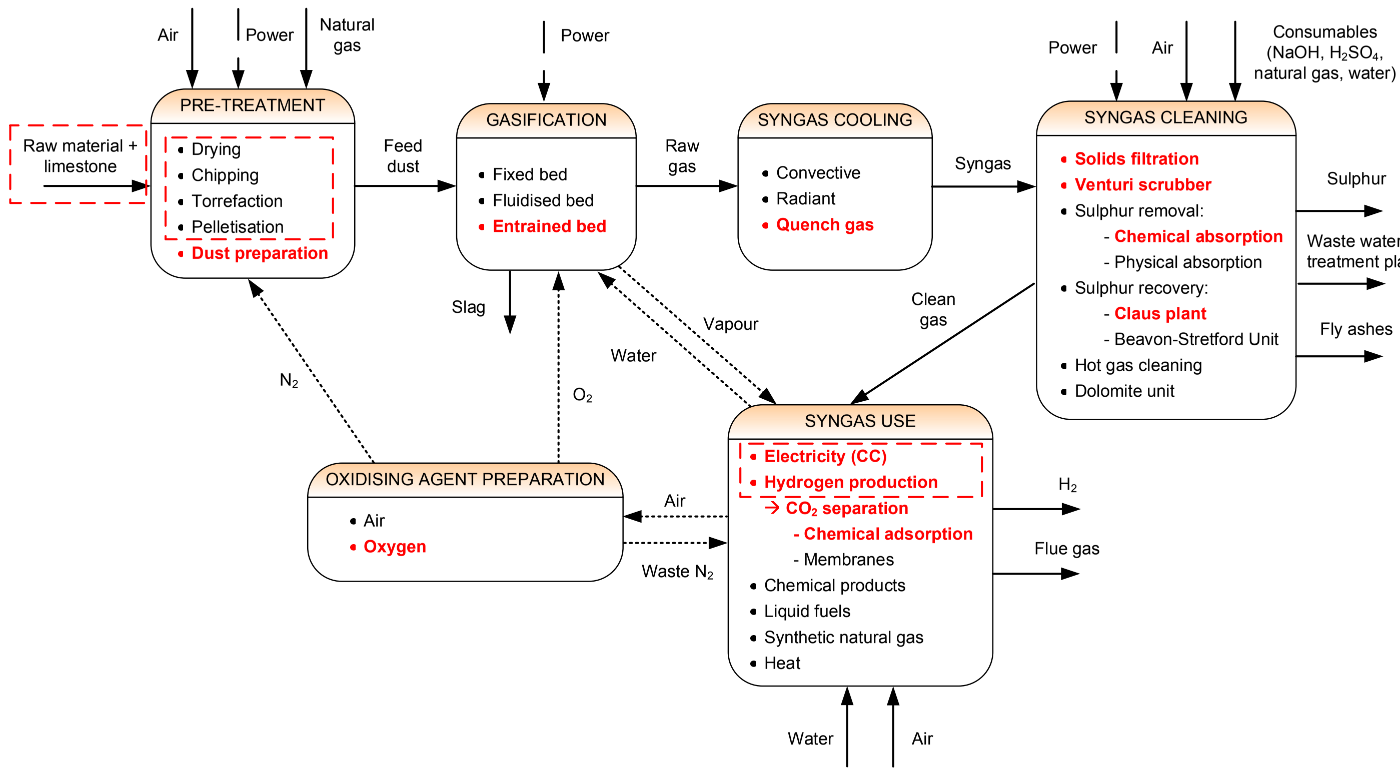

Figure 6.2: IGCC-CCS superstructure. Dashed lines in red indicate the options considered in this thesis. The modelled flowsheet, among the different units alternatives, is in red. Integration flows are in dotted lines.

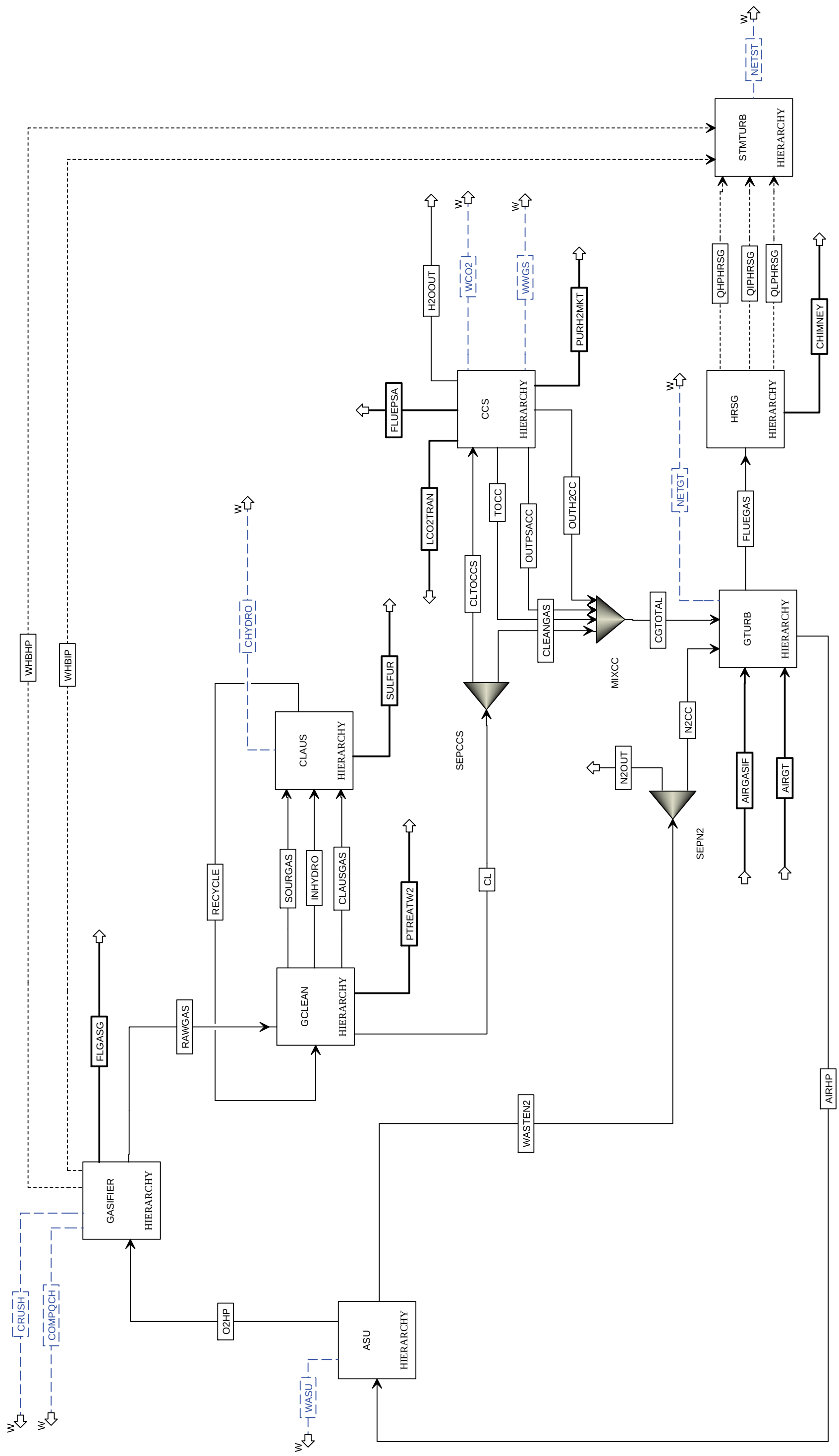

Figure 6.3: IGCC-CCS superstructure as it appears in Aspen Plus.

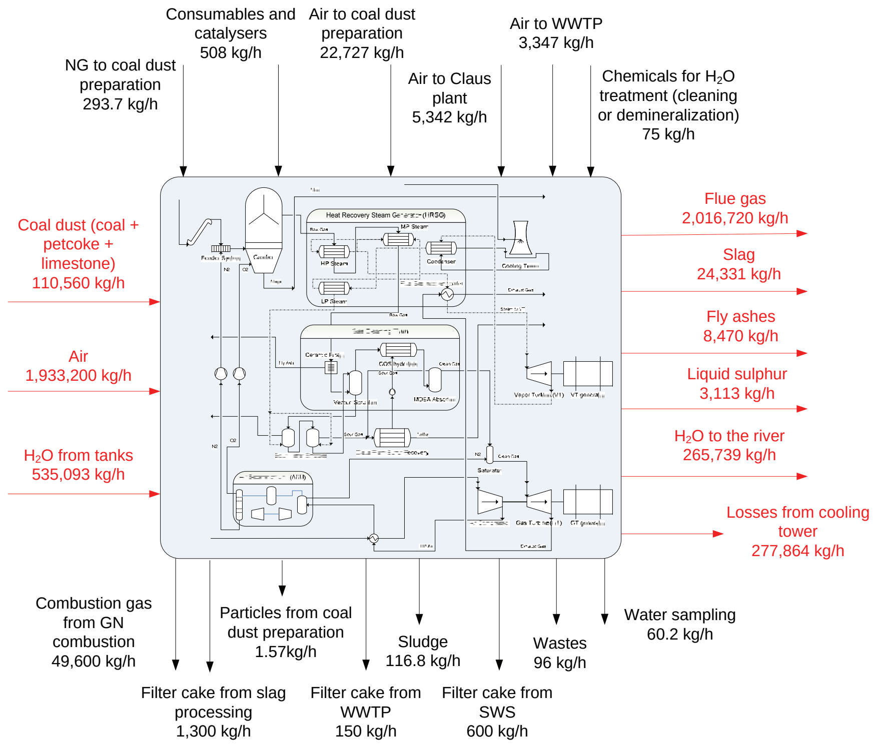

Figure 6.4: Main and secondary mass streams for IGCC mode of operation (base case).

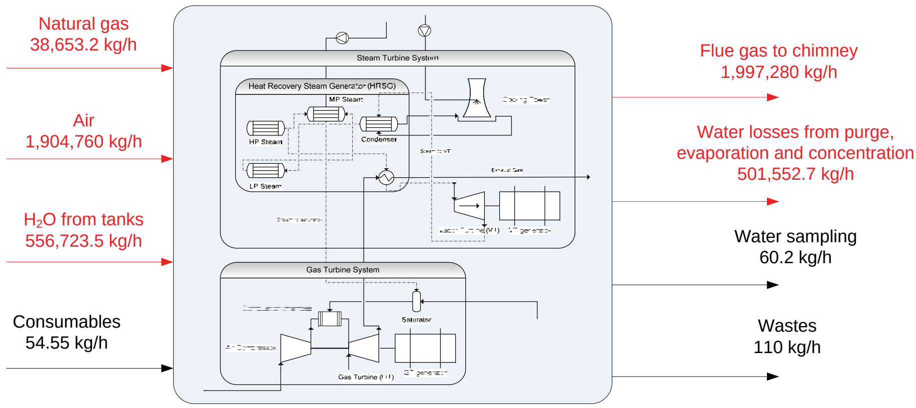

Figure 6.5: Main and secondary mass streams for NGCC mode of operation.

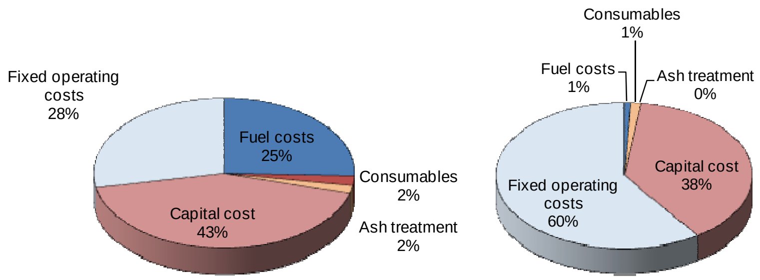

Figure 6.6: Breakdown of COE for IGCC mode (left side) and NGCC mode (right side).

since it reduces the pressure on virgin materials. All scenarios are compared based on 1 MJ as functional unit (FU). The working hours of each mode are pondered according to one year of ELCOGAS service.

- The life cycle inventory (LCI) is gathered for SC1, SC2 and SC3. The use of simulation software enforces mass and energy balances to be closed. For all other studied echelons, production/extraction of raw materials and transport, their corresponding LCIs are retrieved from Ecoinvent-V1.3 (2006). Coal, petcoke, NG and other commodities production impacts are required given their consumption for plant operation, as shown in Table 6.2. Ecoinvent LCI information has been assembled considering that the plant is located in Spain (ES). The European average (RER) has been selected when data for Spain is not available. Table 6.2 shows that SC2 achieves the lowest fuel consumption. Solid wastes are considered inert and sent to a landfill, while waste water effluent is sent to a waste water treatment plant. Consumables are handled as inorganic chemicals and an approximate LCI is used considering the average production for the first 20 most important inorganic compounds. For the sulphur stream, a LCI based on the production from raw material has been used. This decreases the overall impact of IGCC operation.

- The LCIA, based on the previous LCI's, is performed. Several environmental impact indicators are available to assess different environmental issues involved in electricity generation. Those issues are (i) climate change that uses global warming potentials (GWPs) as indicator, (ii) regional acidification using acidification potentials (APs) and (iii) virgin resources consumption using abiotic depletion potentials (ADPs). The metrics can be calculated using different ready-to-use LCIA methodologies. Table 6.3 shows the LCIA for different metrics; cumulative energy demand (CED), cumulative exergy demand (CExD), ecological footprint (EF), equivalent emissions of carbon dioxide (CO_{2eq}) and Impact2002+ overall environmental impact values.

- Life cycle assessment (LCA) results interpretation. It is found that operation using NG instead of solid fuels reduces the CED and CExD. For the first metric, operation using IGCC requires approximately 60% more than the total amount of energy required in the NGCC. In the case of CExD, nearly three times more exergy is required for IGCC than for NGCC. This indicates the low LHV from syngas compared to NG. The differences found in the case of EF are not as

Table 6.2: Summary of SC1, SC2 and SC3 LCI results, expressed in kg/MJ.

Inputs	SC1	SC2	SC3
Hard coal (ES)	$5.50{\cdot}10^{-2}$	$4.99{\cdot}10^{-2}$	0
Petcoke (RER)	$5.50{\cdot}10^{-2}$	$4.99{\cdot}10^{-2}$	0
Limestone milled (RER)	$3.82{\cdot}10^{-3}$	$3.59{\cdot}10^{-3}$	0
Natural gas (RER)	$3.39{\cdot}10^{-6}$	$1.52{\cdot}10^{-6}$	$1.98{\cdot}10^{-5}$
H_2O decarbonised (RER)	$5.51{\cdot}10^{-1}$	$5.56{\cdot}10^{-1}$	$7.39{\cdot}10^{-1}$
Consumables: (Inorganics-RER)	$6.01{\cdot}10^{-4}$	$6.06{\cdot}10^{-4}$	$7.2{\cdot}10^{-5}$
Ouputs			
CO_2	$22.33{\cdot}10^{-2}$	$21.19{\cdot}10^{-2}$	$13.73{\cdot}10^{-2}$
SO_2	$3.12{\cdot}10^{5}$	$2.55{\cdot}10^{-5}$	$7.08{\cdot}10^{-6}$
NO_x	$9.99{\cdot}10^{-5}$	$8.68{\cdot}10^{-5}$	$1.77{\cdot}10^{-4}$
Particles	$4.20{\cdot}10^{-7}$	$4.23{\cdot}10^{-7}$	$6.62{\cdot}10^{-7}$
Solid inert waste	$2.96{\cdot}10^{-2}$	$2.96{\cdot}10^{-2}$	$1.50{\cdot}10^{-4}$
Water to waste treatment	$55.98{\cdot}10^{-2}$	$55.98{\cdot}10^{-2}$	$66.56{\cdot}10^{-2}$
Sulphur produced	$3.23{\cdot}10^{-3}$	$3.21{\cdot}10^{-3}$	0

significant as in the CExD case. The same holds for the CO_{2eq}. The Impact 2002+ results indicate that the lowest impacts refer to the case of operation using NGCC configuration followed by IGCC operation using orujillo.

Figure 6.7 shows the results of Impact 2002+ assessment methodology distributed along the different mid and end-point categories of the LCIA and along the different supply chain (SC) echelons. In the case of mid-point categories the largest impacts are associated to non-renewable energy and GWP, which are mimicked by the end-point categories, resources and climate change. Small differences are found for the end-point categories human health and ecosystem quality, which cannot be traced directly to a single mid point impact as in the case of resources and climate change. In the three electricity production scenarios, regarding end-point impacts, human health impact and ecosystem quality account for less than 13% of the total impact, while the remaining is almost evenly partitioned between resources and climate change impacts. In the case of IGCC operation, the biggest overall impact is related to the plant operation itself. In second and third place, raw material production is found. Coal production is seen more environmentally-friendly than petcoke production. In all the former environmental metrics, the life cycle stages associated to most impact are raw materials production, for the case of resources, while climate change is due to the IGCC/NGCC plant level.

See in Table 6.3 a summary of all the KPIs for SC1, SC2 and SC3. Economic values are in €$_{2007}$. NGCC operation is found to have the lowest COE and the highest efficiency among the considered scenarios. This mode of operation counts with two values for the price of the energy due to the difference on investment costs. The most expensive value refers to NGCC as a mode of operation of an IGCC plant, not as a plant itself. Total capital requirement (TCR) and total operating costs (TOC) for SC3 are the cheapest.

LCA results favours NGCC instead of IGCC and co-gasification. CED and EF are good proxy metrics for electricity generation, in which raw material usage and climate change impacts are more important. Moreover, for those metrics that are related to

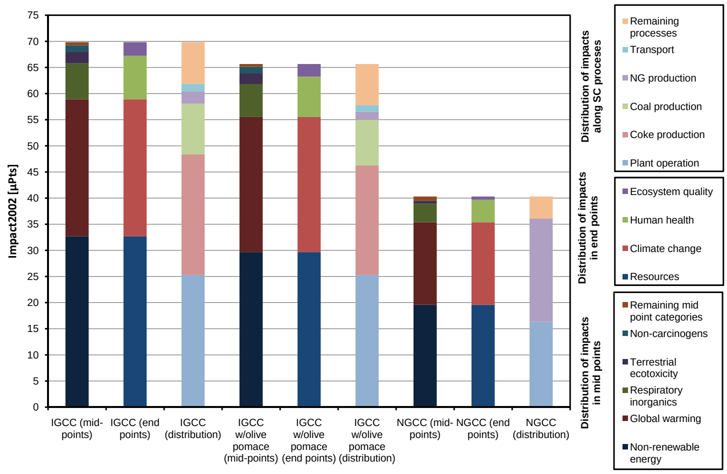

Figure 6.7: Results for EI estimation using Impact2002+ assessment methodology. This is shown distributed along mid and end point indicators and SC levels.

raw material origin, they penalise the use of non-renewable fuels such as coal and petcoke. In this sense, the petcoke has been assigned 3% of emissions associated to the overall refinery crude oil consumption (Ecoinvent-V1.3, 2006). Consequently, its energy and exergy demands are high. This is also found by using Impact 2002+. Here, toxicological effects, i.e. human health or ecosystem quality, are relatively small.

Table 6.3: KPIs for the considered scenarios.

Metric	SC1	SC2	SC3
CED (MJ_{eq})	5.0	4.5	2.8
CExD (MJ_{eq})	9.2	8.3	3.1
EF (m^2)	0.70	0.69	0.41
IPCC GWP ($kgCO_{2eq}$)	0.27	0.27	0.16
Impact 2002+ (μpts)	69.8	65.7	40.3
COE (€/kWh)	0.0619	0.0593	0.0537 0.0249
TCR (€/kW)	3119	2987	1026
TOC (€/kWyr)	273	261	108
Eff_{global} (%)	42.1	41.6	53.12

6.3 Overall model behaviour for co-gasification

In this section, the use of coal, petcoke and orujillo is considered individually and together in mixtures (see in Table 4.4 their ultimate and proximate analyses). The influence of the feedstock on gasification and on the IGCC mode of operation by changing the equivalence ratio (ER) and H_2O ratio is assessed. In Figure 6.8, the H_2 production in the gasifier is assessed when it is fed by pure raw materials. In all cases, they present a similar behaviour to that found in the base case, in which the maximum

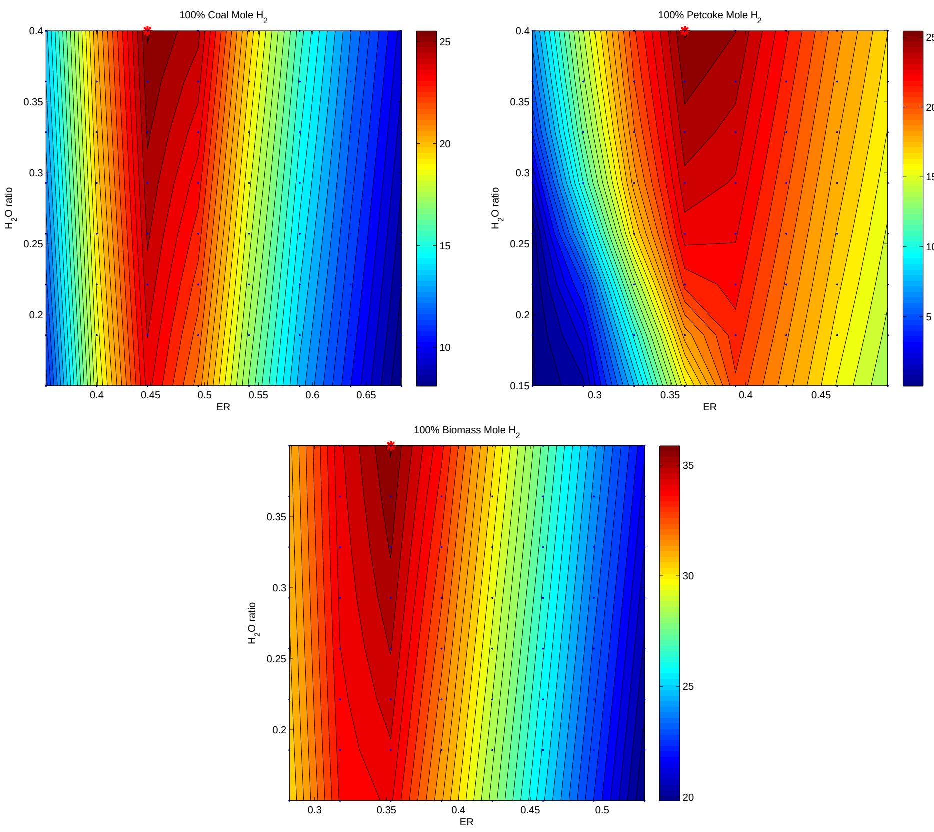

Figure 6.8: Iso-lines for H_2 production (molar fraction % in dry basis) of the three pure components.

amount of H_2 is produced for the highest ratios of H_2O (see also Figure 5.11). The use of orujillo, which contains the highest proportion of oxygen and hydrogen in its composition, achieves the highest proportion of H_2 (to around 35% on a mole basis) with the lowest ER values. It is followed by petcoke, which has a very similar value. Coal leads to a higher ER, for a higher H_2 production.

Figures 6.9 and 6.10 compare ternary blends in terms of cold gas efficiency (CGE) and Eff_{CC}. Firstly, the overall trend in CGE results is the same for all the blends, even though the absolute value is higher for mixtures with lower proportions of biomass. This is due to the effect of petcoke, which is the fuel component with the highest proportion of inlet carbon, leading to a more significant presence of CO in the syngas. In addition, the effect of the H_2O ratio is only noticeable at lower ER values, at which lower steam ratio values imply higher CGEs. Secondly, Eff_{CC} has slightly higher values when higher percentages of biomass are considered. This is due to TOT and syngas flowrate influences on the final power, rather than the syngas composition itself. For this efficiency value, the steam ratio does not have any significant influence, as shown by the parallel isolines. Note that CGE and Eff_{CC} still follow opposite trends when ER is increased. This trade-off must be solved in order to set an ER value that maximises Eff_{global}. Higher values of Eff_{CC} are associated with higher values of ER (marked with red stars in Fig. 6.10).

6.4 Overall model behaviour for topological changes: electricity and H_2 production

Topological changes refer to syngas use to feed the CC or the carbon removal train by setting the appropriate split fractions in the superstructure. In this section, results have been generated using two sets of data. Set 1 includes complete generation of electricity or H_2 by changing the feedstock mixture. The reference used in all scenarios is the *plant feed flowrate*, i.e. the load of the plant is maintained for all case studies at approximately 110 t/h. Section 6.3 and results from Set 1, let anticipate that blends behaviours are expected to exhibit intermediate behaviours of the pure components mixed. Therefore, in order to decrease the number of case studies, in Set 2, four topological changes are considered for the base case mixture and for the pure fuels.

6.4.1 Production of 100% electricity or 100% H_2 with feedstocks mixtures

Table 6.4 compiles the main data for the nine selected case studies, including the base case. *Outputs* values refer to the main parameters selected after gasification and after syngas cleaning units, which remain the same despite of the final syngas application. The LHV of the syngas just after the gasifier (LHV_{rg}) is different for each feed. It is highest for the petcoke, followed by the base case, the orujillo and the coal scenario. For C6-C9, it varies according to the amount of biomass introduced in the system. It depends on the LHV of the raw materials and their composition, as occurs with the CGE. The produced liquid sulphur depends on the feedstock composition, and therefore on the sulphur percentage according to the ultimate analyses. The sulphur release efficiency is approximately 96% in all case studies. The final value of CO_2 emissions to the atmosphere, after the syngas combustion in the CC, is also indicated. This is in agreement with the C composition of the feedstock. Therefore, the petcoke emits more CO_2 in absolute values than the other raw materials. H_2 production is described by its efficiencies and final products and by-products. $Eff_{global_{H_2}}$ follows an analogous trend than Eff_{global}: they diminish while the biomass fraction in the feedstock mixture increases. Again, the petcoke performs best, as it produces H_2 with the highest efficiency. The final amount of hydrogen is not proportional to the final amount of hydrogen produced in the gasifier. This is due to the CO composition: the final amount of hydrogen recovered depends on the H_2/CO ratio before the WGS reaction. Therefore, this ratio should be optimised in carbon capture applications, rather than the value of H_2 alone.

The flowrate of the captured CO_2, which is sent to geological storage, is also reported. This stream differs from the CO_2 stream from the flue gas in the final amount of CO_2 that is emitted to the atmosphere through the PSA purge gas. Case studies with higher CO_2 emissions in flue gas, result in scenarios with lower ratios of carbon to carbon storage. Again, this is due to the WGS reactors: the equilibrium constants of the two reactors at different temperatures depend on the composition of the reactants. Therefore, the syngas composition is a critical parameter.

To sum up, the feedstock compositions that produce the highest amount of

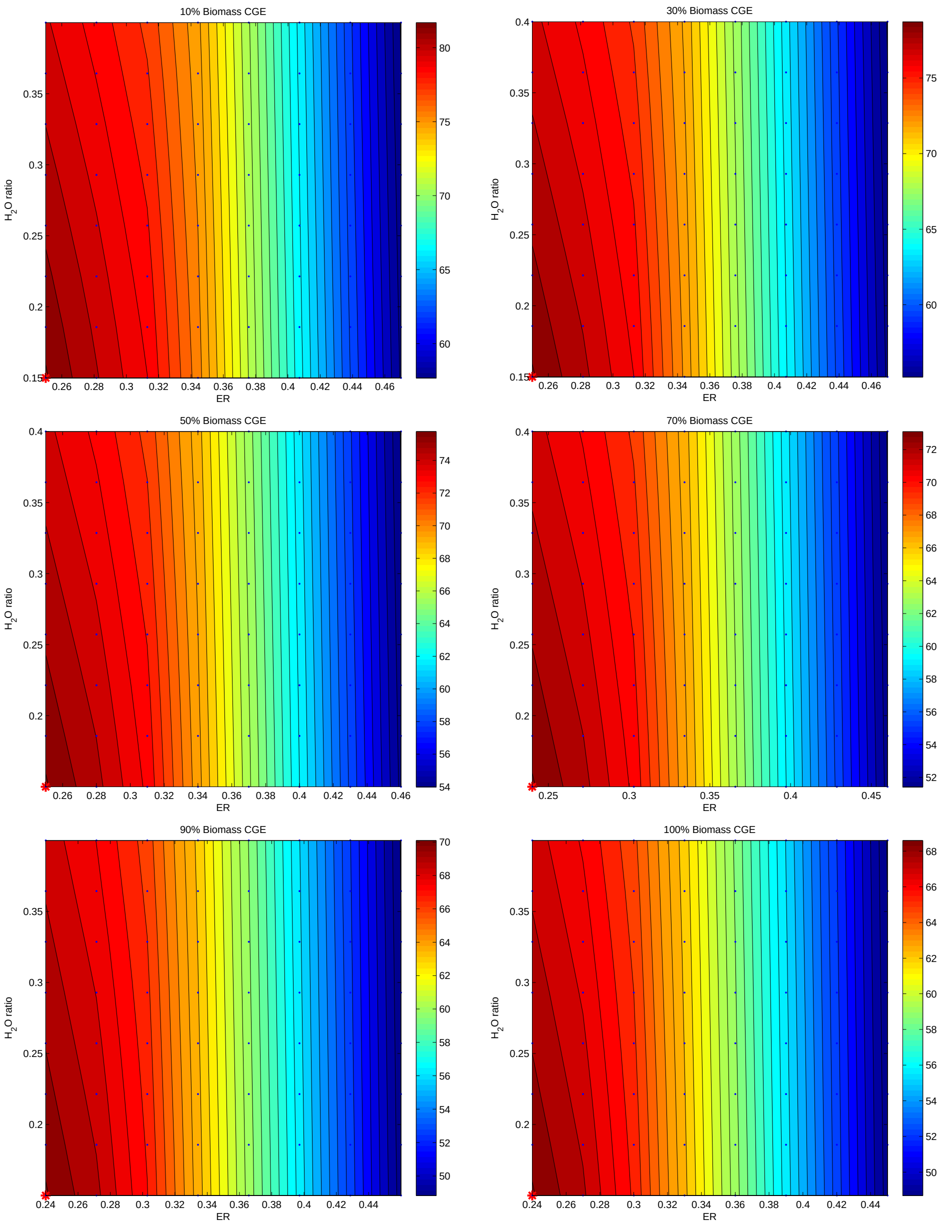

Figure 6.9: Iso-lines for CGE values (%) of the different biomass blends.

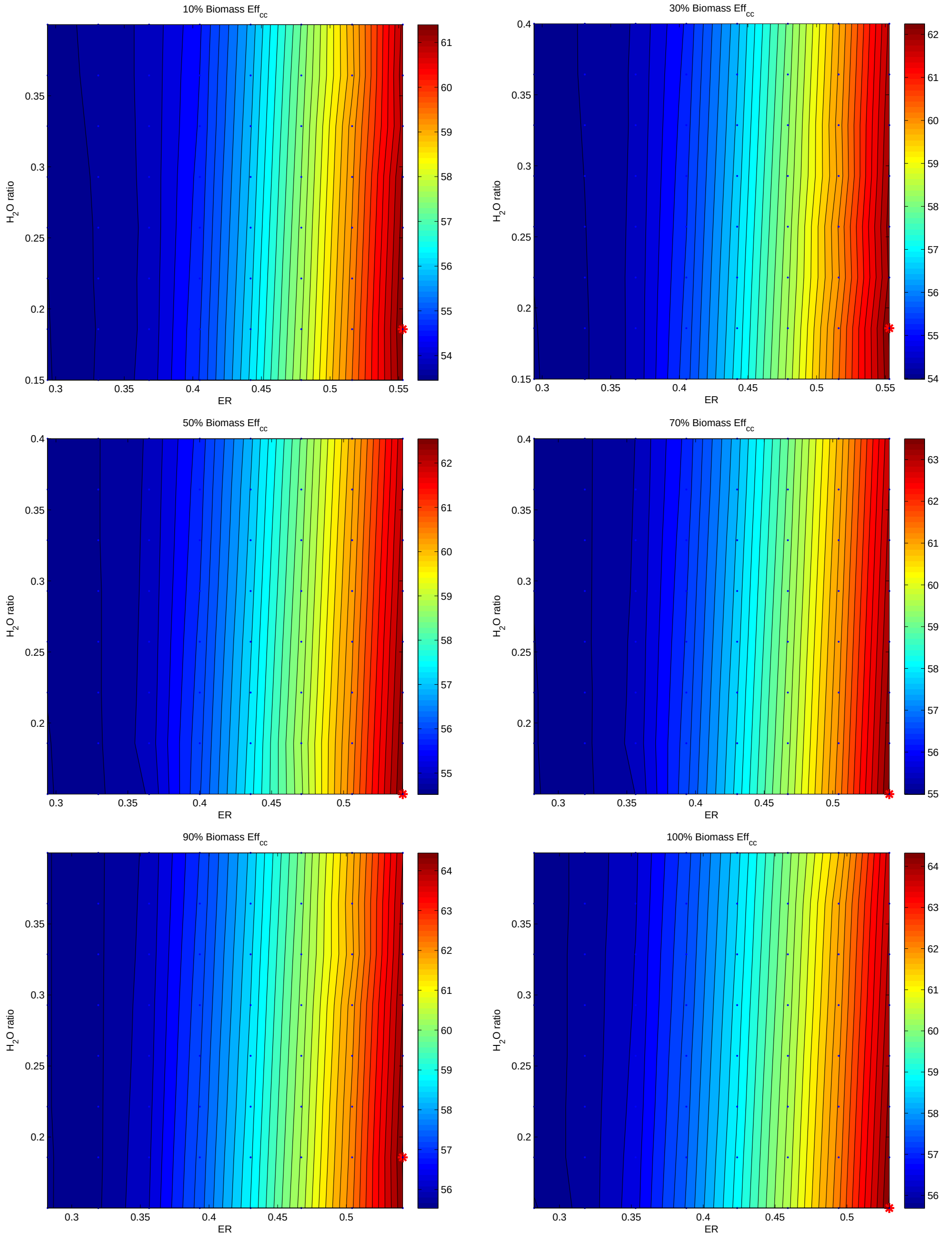

Figure 6.10: Iso-lines for the CC efficiency evaluation (%) of the different biomass blends.

electricity also produce the highest quantity of hydrogen. In addition, the H_2/CO ratio should be optimised for the final carbon capture application.

6.4.2 CC powered by syngas or H_2, H_2 production and PSA purge gas combustion using pure feedstocks

Set 2 of scenarios are used in this section. Table 6.5 summarises the main input variables that stay constant for those case studies that use the same feedstock (cases Cnj). The main output values, those that do not change if the final application changes, are also reported. Table 6.5 review all the needed data to perform a LCA. The simulated scenarios are denominated as: Cij, in which $i-th$ value represents the fuel used while $j-th$ represents the different topological options. i is 1 for coal:petcoke blend, 2 for coal, 3 for petcoke and 4 for orujillo. In turn, the code for topological changes is 1 for syngas to CC (fraction of syngas to $H_2 = 0$), 2 for H_2 to CC (fraction of sygnas to $H_2 = 1$), 3 for H_2 production and 4 for H_2 production and PSA purge gas to CC. For instance, C34 is the scenario where petcoke is used as fuel and all syngas produces H_2 to be sold on the market.

In Table 6.5, the intrinsic characteristics of each feed imply different oxygen requirements to enforce T_{gasif} equal to 1450 °C. NG consumption varies since it depends on feed humidity, as well as on the other consumables. Water fed to venturi scrubber depends on the syngas flowrate and on the gasifier H_2S formation. Concerning the invariable outputs among the different syngas usages, the gas composition that results from the NG combustion in the dryer is reported. Ashes and slag flowrates correspond to ashes and limestone flows. The LHV_{rg} just after the gasifier is different for each feed, being highest for petcoke, followed by the base case, orujillo and coal, respectively. It depends on the LHV of the materials and their inlet composition. The same holds for with the CGE. Water to treatment is the water flowrate that exits the system after the sour water stripper. It depends on the inlet water stream to venturi scrubber.

Sixteen scenarios are simulated to scan all possible combination options between the considered different feeds and topological changes. Each of the scenarios is analysed using the three points of view described in Chapter 3, i.e. engineering, economic and environmental, and farther discriminated in terms of their KPI's values: COE, Eff_{total} and environmental impact (EI) using the Impact 2002+ metric.

Plant engineering point of view

The net power and the H_2 equivalent power content are reported in Table 6.6 for Set 2 case studies, listed in Table 6.5. The net equivalent power has been calculated as the final amount of disposable energy, not distinguishing between power and equivalent energy content.

When PSA purge gas is sent to the CC, more electricity than that required for self-supply is produced. In contrast, when this gas is discharged to the atmosphere, a consumption of electricity from the grid is needed, except for C43. In order to evaluate which scenario uses the fuel energy available more efficiently, global and total efficiencies are calculated (as in Eqs. 3.8, 3.10 and 3.14) and represented in Figure 6.11. The production of electricity based on H_2 combustion is the least efficient use, as shown by the total efficiency values for scenarios Ci2. The effect of purge gas use in the CC is always positive, particularly for scenario C34.

Table 6.4: Set 1: co-gasification of coal, petcoke and orujillo results.

	C1	C2	C3	C4	C5	C6	C7	C8	C9
Inputs									
Coal (mass fraction)	0.5	1	0	0	0.45	0.35	0.25	0.15	0.05
Petcoke (mass fraction)	0.5	0	1	0	0.45	0.35	0.25	0.15	0.05
Orujillo (mass fraction)	0	0	0	1	0.1	0.3	0.5	0.7	0.9
ER	0.422	0.520	0.370	0.406	0.420	0.418	0.414	0.411	0.408
H_2O ratio (from gasifier)	0.16	0.16	0.16	0.16	0.16	0.16	0.16	0.16	0.16
Outputs									
LHV_{rg} (MJ/kg)	9.5	6.6	11.4	7.9	9.4	9.1	8.8	8.4	8.1
CGE (%)	75.2	59.9	82.9	60.7	74.0	71.1	68.3	65.3	62.3
Liquid sulphur (t/h)	3.32	0.98	5.74	0.11	3.00	2.37	1.73	1.08	0.43
Electricity production (fraction of syngas to H_2 = 0)									
O_2 ratio CC	2.45	2.13	2.54	2.45	2.48	2.46	2.46	2.45	2.44
Eff_{CC} (%)	57.7	58.3	57.5	60.8	57.9	58.5	59.1	59.7	60.4
Net power (MW)	285.3	151.9	423.2	243.9	281.6	273.6	265.3	256.9	248.4
Eff_{global} (%)	42.1	34.3	45.7	36.8	41.6	40.6	39.6	38.5	37.4
CO_2 in flue gas (t/h)	223.2	131.8	317.9	170.4	217.9	207.2	196.6	186.1	175.6
Hydrogen production (fraction of syngas to H_2 = 1)									
$Eff_{CCapture}$ (%)	68.9	69.4	61.3	70.7	69.0	69.3	69.6	69.9	70.4
H_2 (t/h)	10.4	5.5	13.6	8.6	10.1	9.7	9.4	9.0	8.7
$Eff_{global_{H_2}}$ (%)	50.2	40.8	50.9	42.8	49.6	48.1	46.6	45.1	43.6
Net power (MW)	-91.9	-43.1	-120.9	-35.2	-75.3	-52.1	-47.3	-42.2	-43.5
CO_2 to final disposal (t/h)	207.3	124.9	277.6	158.5	202.6	191.9	180.8	171.6	155.1

Table 6.5: Set 2: input and output values associated to feedstock dust preparation, gasification and syngas cleaning.

	C1j	C2j	C3j	C4j
Inputs				
Coal (mass fraction)	0.5	1	0	0
Petcoke (mass fraction)	0.5	0	1	0
Orujillo (mass fraction)	0	0	0	1
Feed flowrate (kg/h)	106856.2	106856.2	106856.2	106856.2
Limestone (kg/h)	3703.8	3703.8	3703.8	3703.8
Natural gas (kg/h)	300.0	376.6	223.4	242.6
Air (kg/h) to gasifier	362995.9	274555.2	442957.3	268437.0
Air (kg/h) (Feeding system and Claus plant)	28940.0	23582.0	34743.0	21645.7
O_2 to gasifier (kg/h)	93090.4	70409.8	113596.5	68840.7
H_2O to gasifier (kg/h)	10031.4	6195.0	14062.8	7886.5
ER	0.42	0.52	0.37	0.41
H_2O ratio (from gasifier)	0.16	0.16	0.16	0.16
NaOH (kg/h)	445.5	335.1	559.3	426.1
H_2SO_4 (kg/h)	57.3	43.1	71.9	54.8
H_2O to venturi scrubber (kg/h)	17739.1	13343.0	22267.5	16964.3
Outputs				
Combustion gas from feed preparation (kg/h)	30458.2	30360.6	29177.7	29289.8
CO_2 (kg/h)	2775.0	2775.0	2775.0	2775.0
NO (kg/h)	2.89	2.89	2.89	2.89
NO_2 (kg/h)	0.02	0.02	0.02	0.02
H_2O (kg/h)	8900.9	8803.3	7620.4	7732.5
Ashes/slag (kg/h)	26405.5	47636.2	3982.2	9914.4
LHV_{rg} (MJ/kg)	9.5	6.6	11.4	7.9
CGE (%)	75.2	59.9	82.9	60.7
H_2O to treatment (kg/h)	7310.0	8454.3	6715.7	13591.8
Liquid sulphur (kg/h)	3317.8	975.5	5739.7	102.3

Table 6.6: Power produced for Set 2 scenarios.

Option	Scenario	Net Power Produced (MW)	H_2 produced (MW)	Net equivalent power (MW_{eq})
Electricity production from syngas	C11	285.3	0.0	285.3
	C21	151.9	0.0	151.9
	C31	423.2	0.0	423.2
	C41	243.9	0.0	243.9
Electricity production from H_2	C12	225.6	0.0	225.6
	C22	115.3	0.0	115.3
	C32	331.5	0.0	331.5
	C42	195.1	0.0	195.1
H_2 production	C13	-45.9	346.1	300.2
	C23	-7.1	184.7	177.6
	C33	-55.3	452.0	396.7
	C43	0.7	287.8	288.5
H_2 production with PSA purge gas-CC	C14	26.4	340.7	367.2
	C24	3.4	181.3	184.7
	C34	56.7	468.1	524.8
	C44	26.5	283.8	310.3

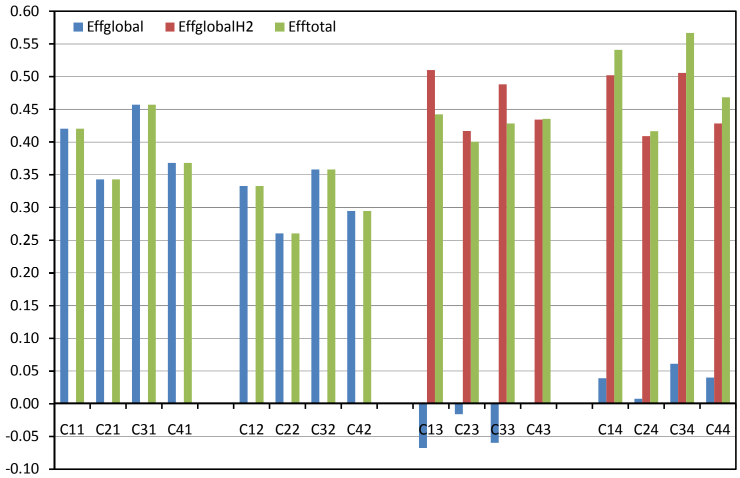

Figure 6.11: Total and global efficiencies for Set 2 scenarios.

Economic point of view

The cost of energy (COE) (Eq. 3.16) is the economic metric used. It takes into account a kWh_{eq} that measures electricity and H_2 production in units of energy. Economies of scale are of concern to calculate the TCR. Life time of the plant is assumed to be 25 years and the interest rate is 5% (which is a typical figure for this type of large investment projects). Annual costs (AC) constitutes 4% of TCR. Prices for coal, petcoke and orujillo are 45 €/t, 75 €/t and 65 €/t, respectively. The annual load is 7200 h. Costs are reported in €$_{2007}$. The COE for the different scenarios have been calculated according to two plant references: (i) the same feeding mass flowrate (around 110 t/h), and (ii) the same output. Therefore, concerning the reference values, for the former, the plant output (kWh_{eq}) is different in all case studies. In the latter, the feed flowrate is variable and the reference value is obtained from scenario C11 (the base case) (285.3 MW_{eq}).

TCR is influenced by the reference plant, as shown by the breakdown in Figures 6.12 and 6.13 for Set 2 case studies. In Figure 6.12, for Ci1 and Ci2 scenarios, in which syngas or H_2 are sent to the CC, the most important investment comes from the electricity generation section. This part encompasses gas turbine (GT), steam turbine (ST), HRSG and WHB. As the LHV of the raw material decreases (compare for instance C21 - with coal, and C31 - with petcoke), the electricity generation investment item decreases as well, while the gasification and ASU costs gain prominence. In H_2 based scenarios, the most important investment comes from the H_2 production section or from the gasification and ASU block, depending on the feed type. For Ci3 cases, the electricity generation item is composed by the WHB and the ST cycles, not operated in CC mode since GT and HRSG cannot be used. In contrast, for Ci4 cases, the electricity generation item gains relevance, but this is still less significant than the H_2 production item. In these last case studies, the TOT is adapted to the LHV of the PSA purge gas, i.e. around 350 °C. Thus, the HRSG is working with less heat recovery than when operating with syngas or hydrogen. Moreover, the production of electricity in Ci3 and Ci4 scenarios is penalised somehow by the WGS consumption of water. Due

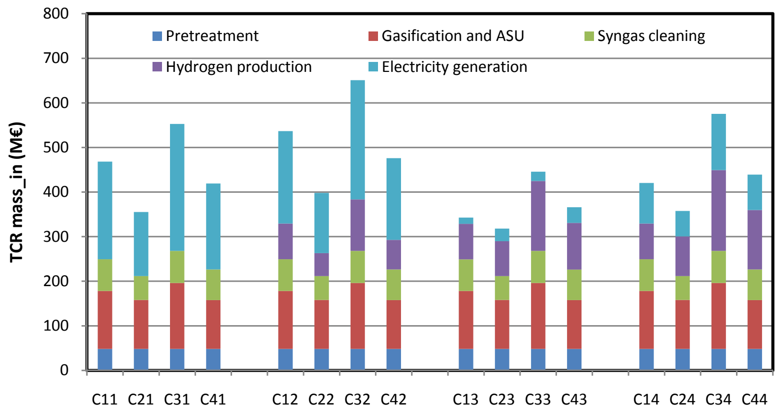

Figure 6.12: Breakdown of TCR for 106.8 t/h of feedstock.

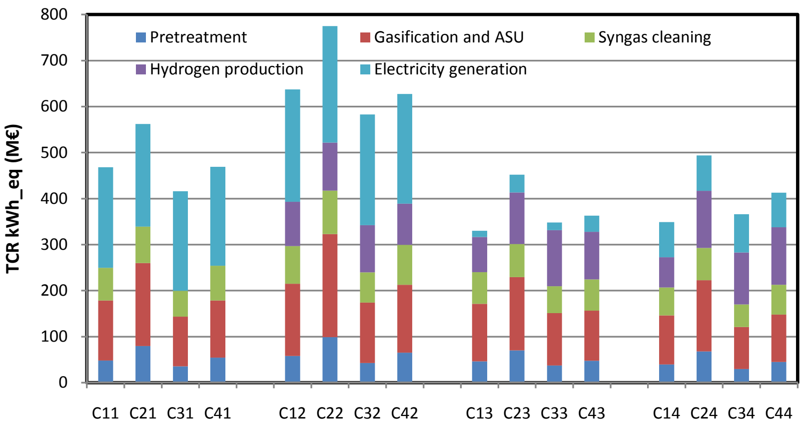

Figure 6.13: Breakdown of investment costs for 2.05 GWh_{eq} of product.

to the reference plant criteria in Figure 6.12, pre-treatment costs are the same for all the cases, independently of the feedstock type. Moreover, gasification, ASU and syngas cleaning costs remain the same for all the C1j, C2j, C3j and C4j cases. The difference between case studies in TCR remains basically in the final syngas application which is highly influenced by the LHV of the feedstock.

Figures 6.12 and 6.13 show different profiles. According to Figure 6.13, Ci2 scenarios are more expensive than Ci1, Ci3 or Ci4, explicitely 35-36% higher than Ci1 case studies. Ci1 cases, as well as Ci2 and Ci4 exhibit approximately the same TCR share for the electricity generation item, since the amount of electricity produced is the same. Final syngas application, followed by syngas generation, have the main TCR contribution.

In Figure 6.14, feedstock costs (FdC) are plotted reflecting the feedstock consumption variation to obtain the reference power. The scenarios follow the same

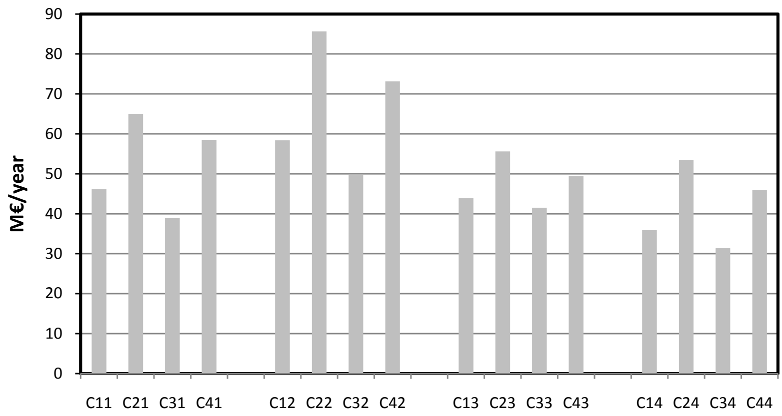

Figure 6.14: FdC per year considering 2.05 GWh_{eq} of product.

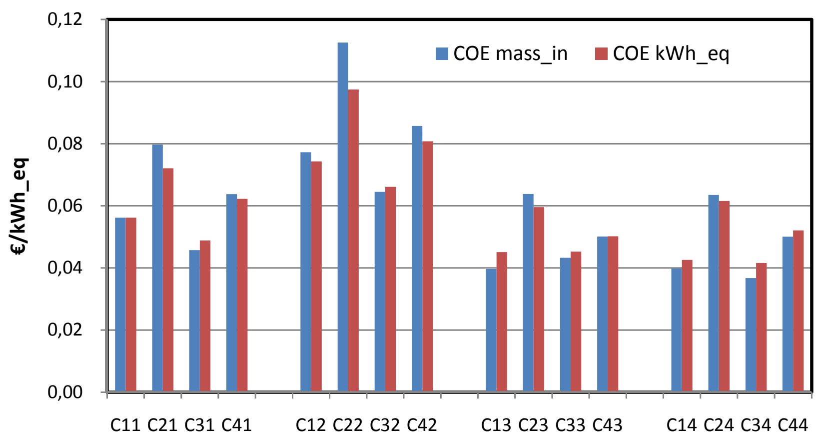

Figure 6.15: COE values for different scenarios considering both reference scenarios fixed inlet flow or product.

profile as in Figure 6.13. Higher feedstock needs are appreciated for Ci2 cases, where H_2 is combusted to produce power. H_2 production scenarios (Ci3 and Ci4) present lower costs, since H_2 has a high calorific value, which is not "penalised" by the combustion process efficiency. Notice that, when compared to C11 scenario (base case), all other cases behave by increasing or decreasing their feedstock costs according to their LHV.

Figure 6.15 compares the different COE values obtained for the 16 case studies for the two reference plants. Lower COE values are found for H_2 production cases (Ci3 and Ci4) when compared with their homologous Ci1 and Ci2. Coal-based cases yield the highest COE values, while petcoke and biomass produce very similar values.

CO_2 metrics. The costs of avoided and captured CO_2 are calculated for Ci1 and Ci2 case studies, with Eqs. 3.18 and 3.19. Ci1 are the reference scenarios for equations calculation. The approach followed here does not consider the energy requirements for CO_2 transportation and storage. Therefore, avoided and captured CO_2 have the same value. The values obtained are 2.5 cts€/tCO_2, 5.85 cts€/tCO_2, 1.75 cts€/tCO_2 and 3.45 cts€/tCO_2 for base case composition, coal, petcoke and orujillo, respectively. These numbers show that the use of coal will require higher CO_2 market prices or higher government subsidies.

Environmental point of view

Each of the Set 2 scenarios are compared in terms of environmental impact following the ISO standards described in Chapter 3. The FU, given that co-production is feasible, is 1 MJ of equivalent energy from electricity or H_2. Therefore, environmental impacts, which are proportional to mass/energy flows, are normalised by the total amount of energy produced in each scenario. The system boundaries have been drawn from cradle-to-gate with the following assumptions:

- Transport of fuel materials has been neglected, mimicking the geographical considerations of ELCOGAS.
- CO_2 disposal does not include transportation and injection to formation, but considers liquefaction.
- For H_2 production, transportation is not considered. It is assumed available at high pressure (HP) in the plant.
- Excess electricity needs comes from the Spanish grid. NG is also represented using data from Spain.
- Allocation of emissions is done for co-products, CO_2 and sulphur.
- Waste water treatment and slag disposal are considered, and emissions associated to their treatment are included within boundaries.

For each case study, the LCIs for raw materials use, electricity and others are gathered from the Ecoinvent database (Ecoinvent-V1.3, 2006). Using the data from Table 6.1 together with the results from each scenario, the LCIs are assembled. From those values, the LCIA can be calculated (Humbert *et al.*, 2005).

Figure 6.16 shows the results of the total environmental impact for each scenario. The highest values are obtained for the case of electricity production using coal (C21), while the lowest is found for the cases C43 and C44, in which orujillo is used to produce H_2. By comparing cases Ci2 and Ci1, it can be seen that the production of electricity directly from syngas is less environmental friendly than its production from H_2. This is mainly due the reduction of climate change impacts due to the CO_2 capture.

The EI can be subdivided in terms of end-point categories. Therefore, impacts to different areas of protection can be grasped: human health, ecosystem quality, climate change and natural resources use. Moreover, the same approach can be distributed along the different activities in the SC: raw materials (fuel consumption), energy consumption (electricity from the grid and natural gas), utilities and IGCC operation. The utilities category includes the consumption of limestone, NaOH, H_2SO_4, water and slag disposal, while IGCC or IGCC-CCS operation encompasses all the impacts associated with its activity, which in this case are mainly related to air emissions (CO_2,

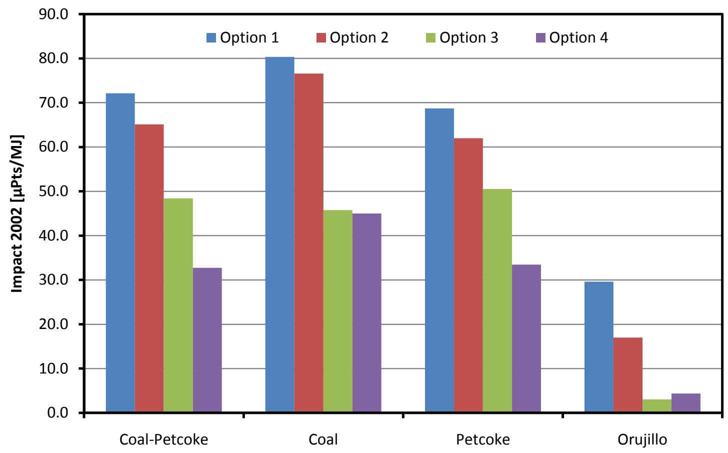

Figure 6.16: Environmental impact for each case study.

CO, and other species). Figures 6.17 to 6.20, they represent the impact of the different topology options for each feedstock, show the clear reduction in the climate change category obtained by shifting from electricity from syngas to electricity from H_2. In the case of coal and petcoke use (see Figures 6.18 and 6.19), global climate change and the resource use are the most influenced areas, while in the case of the orujillo use, the resource use impact is nearly negligible (see Figure 6.20). Concerning the items of the SC that are more responsible for the environmental impact, in the case of coal and petcoke, the production of fuels, under the raw materials category, has the largest share of the impact, while in the case of biomass use, IGCC operation is the most important aspect. In all the cases, the use of utilities impacts are not significant, while energy consumption is noticeable in C13, C23 and C33 scenarios, in which electricity from the grid is required.

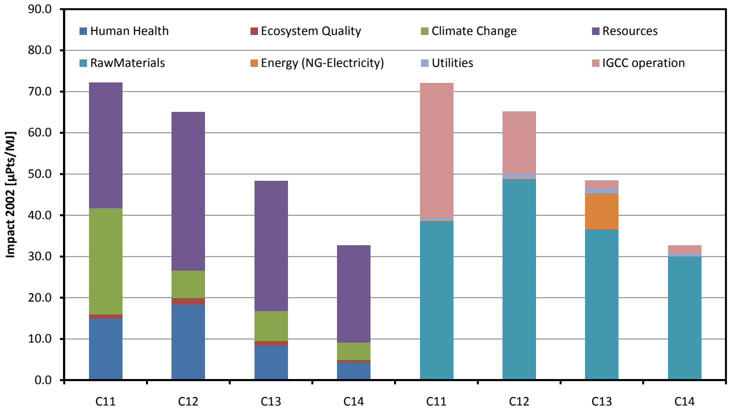

Figure 6.17: EI for C1j scenarios distributed along end-point categories and SC activities.

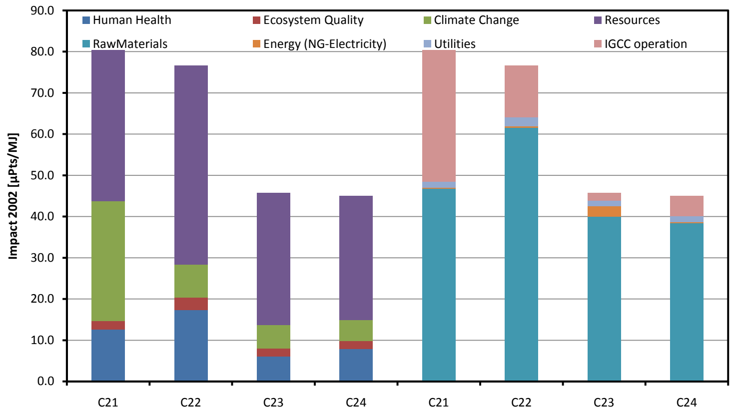

Figure 6.18: EI for C2j scenarios distributed along end-point categories and SC activities.

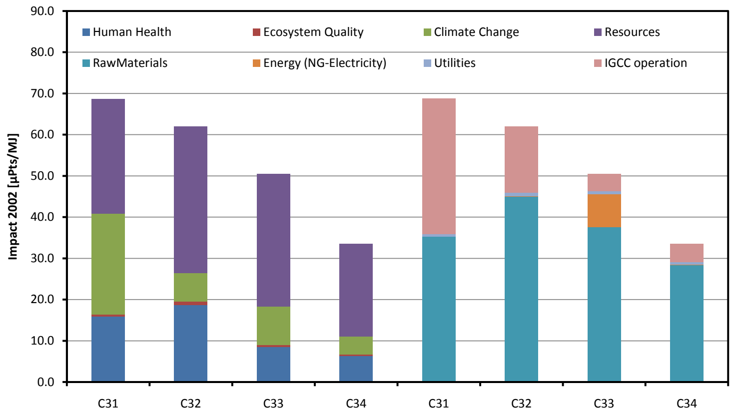

Figure 6.19: EI for C3j scenarios distributed along end-point categories and SC activities.

6.5 Overall model behaviour for co-production

Four sensitivity analyses (SA) with feedstock and product variations are performed. 3D graphs are used to represent the variation in the chosen variables, in terms of the split fraction of syngas that goes to H_2 production and the fraction of orujillo introduced into the 50:50 coal and petcoke mixture. The representative variables that best describe the co-production scenarios, according to Figure 6.21, are the net power produced when the plant is working in IGCC mode, the amount of MW of H_2 produced when it is working with carbon removal units, the revenue, and the Eff_{total} (Eq. 3.14).

Figure 6.21 (top-left) shows that as the fraction of syngas to hydrogen increases, the power obtained decreases to negative values. At these values, all the syngas produces H_2 and, as a result, the power produced by the ST only (which works using steam from the WHB) is not enough for the system internal electricity consumption. The analysis shows that higher fractions of biomass, produce less net power. The top-

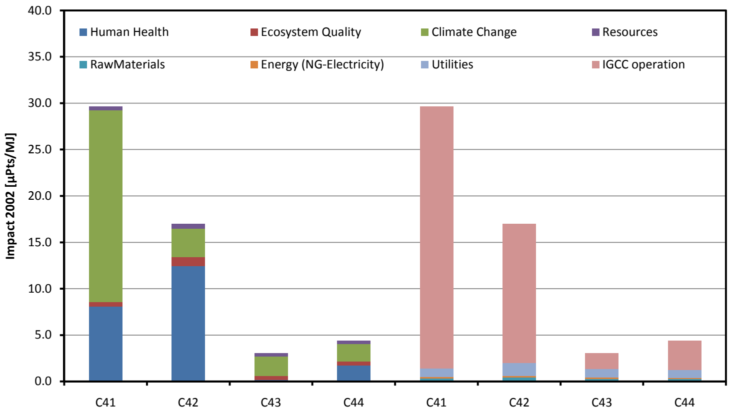

Figure 6.20: EI for C4j scenarios distributed along end-point categories and SC activities. Vertical scale has been reduced if compared with the previous figures for better representation.

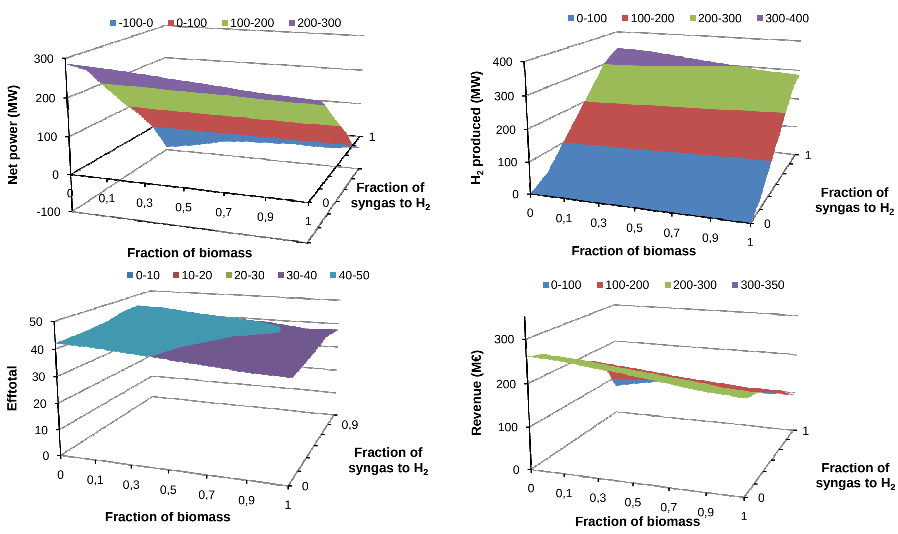

Figure 6.21: Effect of biomass fraction variation with co-production of electricity and H_2.

right graph shows the opposite behaviour, in feedstock terms. In this case, the highest H_2 energy flowrate is obtained when the biomass fraction is null and the H_2 split fraction is 1 (no electricity production). Matching both performances, the bottom-left graph displays a behaviour that is fairly stable compared with the previous graphs: Eff_{total} has a value that ranges between 35%-43%. The highest values are found for the lowest fractions of biomass in the feedstock mixture, and for the highest fractions of H_2 produced. Finally, for the assumed prices, the bottom-right graph suggests an opposite behaviour to that observed in the previous graph: even when the efficiency is not at its maximum, scenarios with higher production of electricity are favoured.

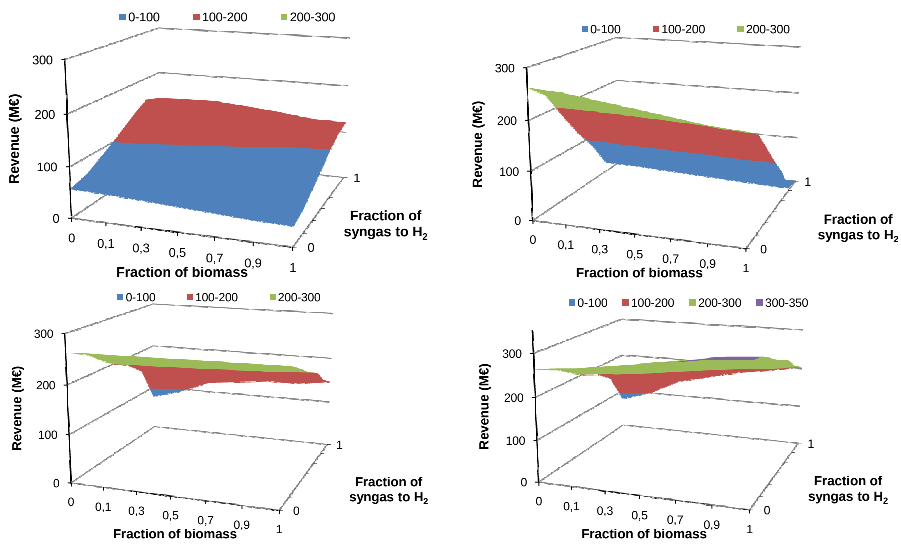

Figure 6.22: Effect of the price on the revenue behaviour. Top-left graph has a decrease on the electricity price. Top-right graph, on H_2 price. Bottom-left and bottom-right graphs vary the biomass price: first, it is set to zero; then, the cost is negative.

From Figure 6.22 it is deduced that a price-based indicator can be very subjective, since changes in prices can drastically alter the identification of the best case study. For instance, these graphs exhibit how the revenue plot changes if the prices are modified. The top-left graph exposes the behaviour of the scenarios when the price of the electricity is reduced to 0.05 €/kWh. The trend is similar than for Eff_{total} plot and favours the hydrogen production case studies. The top-right graph uses an H_2 selling price of 1 €/kg. In this case, the best behaviour is shown by the same scenarios as in the bottom-right graph from Figure 6.21, favouring the use of no biomass and producing only electricity. When the biomass price is zero, as in the bottom-left graph, electricity production is favoured at any biomass fraction. In the bottom-right graph, 75 €/t is the price paid for collecting the biomass. In this case, the optimal scenario is the one with the highest biomass fraction and the production of 100% electricity.

6.6 Global approach: Pareto fronts

6.6.1 Trade-off for Set 1

The evaluation criteria for different case studies include a set of model outputs that include a mixture of co-production parameters, thereby considering a multi-objective approach. For Set 1 scenarios it includes the gasifier efficiency (CGE), the raw material cost, the CO_2 relative emissions in IGCC mode, the net power produced in IGCC mode and the H_2 (in MW) produced when carbon capture units are used. Figure 6.23 shows the different solutions in two-dimensional graphs. Given that five indicators are considered in this case, then ten Pareto curves can be obtained by binary criteria comparison.

In this case, the aim is to identify the feedstock compositions that maximise the production of H_2 to be sold to the market as pure H_2 or that maximises the produced electricity. Therefore, the objective for each indicator is as follows: low raw material cost, low CO_2 relative emissions, high CGE and a high value of H_2 (in MW) or high production of net power.

The simulation results for each case study shows that C3 is the best scenario in the view of maximising H_2 production, net power and CGE all together. There is a trade-off between the raw material costs and the relative CO_2 emissions and all the other parameters. Consequently, only seven out of the ten possible Pareto curves are depicted (since there no exists trade-off among the other values).

For each Pareto curve in Figure 6.23:

- If CGE and raw material costs are considered, then the frontier is determined by C3-C1-C2. These are the base case and the case studies that use only coal and petcoke as raw materials.

- In the case of CO_2 emissions with raw material costs the Pareto frontier contains all the scenarios except C3. Consequently, for the same (or lower) amount of relative carbon emissions there are cheaper options than petcoke.

- When raw material costs are compared with the hydrogen and produced power, the result is the same Pareto frontier made up of the C3-C1-C2 scenarios.

- When CO_2 emissions are compared with the net power and with the CGE, the result is a Pareto frontier formed by C4-C9-C8-C7-C3. The highest producers of power are not necessarily the highest producers of emissions on the basis of produced GWh. Moreover, optimal CGE leads to optimal overall results in terms of energy produced.

- CO_2 emissions against produced hydrogen, results in a Pareto frontier delimited by C4-C9-C8-C7-C3, which is identical to that in the previous case.

Thus, C3 is always on the Pareto frontiers, except in the comparison of carbon emissions with raw material cost. In contrast, C1 and C2 are favoured by the raw material cost. Although they have low values of CGE, net power produced and hydrogen produced, they are the cheapest options. Scenarios with 100% of biomass and the highest proportions of it (C7-C8-C9) are favoured according to the criteria defined in these Pareto frontiers.

Therefore, for the purposes outlined here, the best options involve co-gasification with biomass, which is either used alone or with petcoke. Coal and co-gasification of coal and petcoke are good choices from an economical aspect. Financial criteria follow market laws, which are not necessarily governed by the most efficient choices, being as a consequence a volatile indicator. Moreover, changes in prices modify the Pareto frontiers.

6.6.2 Trade-off for Set 2

In Set 2 scenarios, three KPIs are contrasted. The COE can have two values for each scenario, (a) one for constant feedstock and (b) another one for constant output. Table 6.7 summarises the results for the scenarios considered. Bold values mark the best

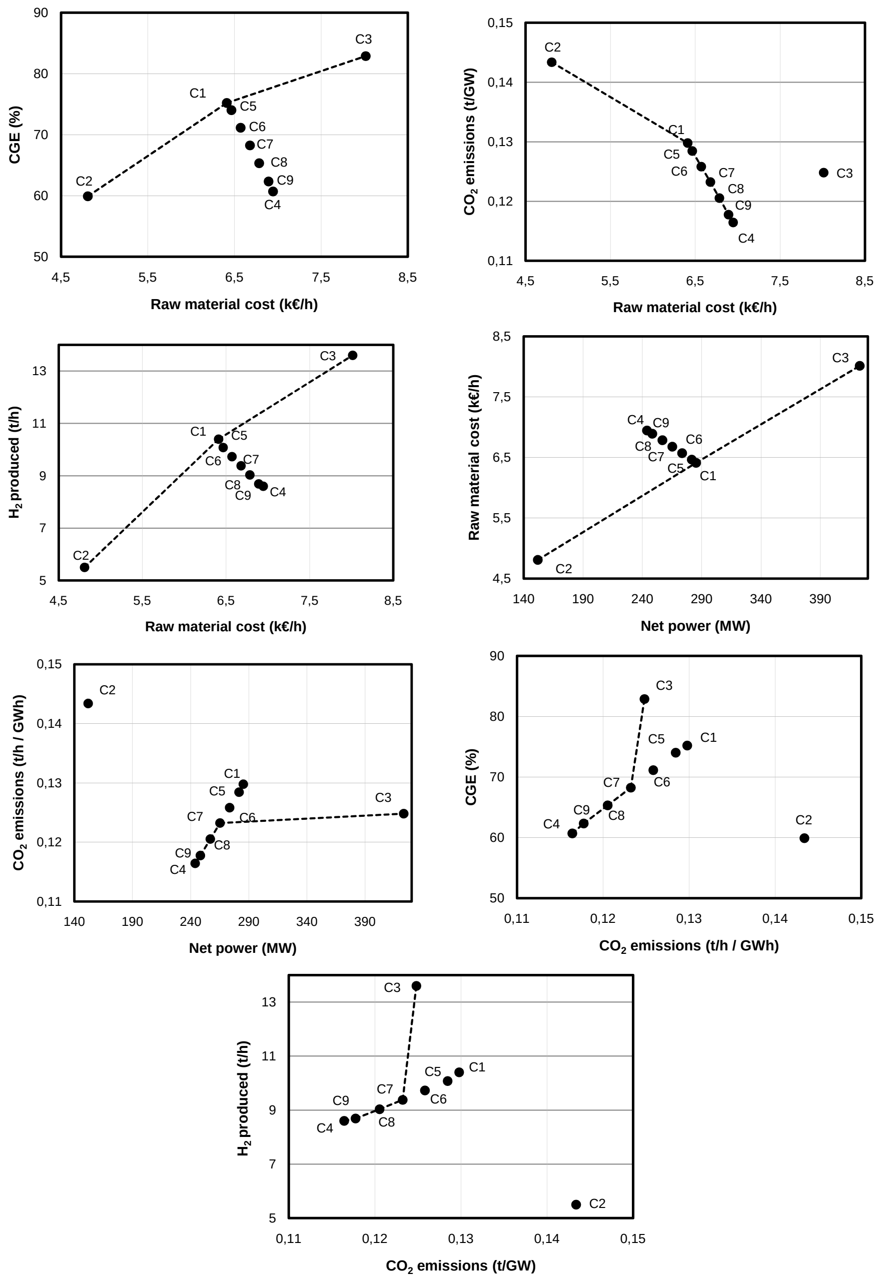

Figure 6.23: Pareto fronts representation for Set 1 scenarios.

Table 6.7: KPIs results for Set 2 scenarios.

	Eff_{total} (%)	COE_a (cts€/kWh$_{eq}$)	COE_b (cts€/kWh$_{eq}$)	EI (μPts/MJ)
C11	42.05	5.62	5.62	72.13
C21	34.28	7.97	7.21	80.35
C31	45.72	4.58	4.89	68.72
C41	36.83	6.38	6.22	29.62
C12	33.25	7.73	7.43	65.12
C22	26.02	11.26	9.75	76.59
C32	35.82	6.45	6.61	62.01
C42	29.46	8.57	8.08	16.99
C13	44.24	3.97	4.51	48.42
C23	40.08	6.38	5.96	45.76
C33	42.85	4.33	4.53	50.53
C43	43.56	5.01	5.02	**3.05**
C14	54.12	3.98	4.26	32.74
C24	41.67	6.35	6.16	45.00
C34	**56.70**	**3.67**	**4.16**	33.46
C44	46.86	5.01	5.21	4.38

scenarios for each metric: scenario C43 is the best when considering the EI and the COE_a, while C34 is the best one when maximising efficiency and minimising COE_b.

Given that there is no coincidence for the best scenario selection, a systematic approach should help in the decision-making task. For this set of scenarios, the TOPSIS decision rule is applied to select the best option (see Section 3.3). In the following figures, blue circles show dominated scenarios, blue dots exhibit dominating solutions (or Pareto front) and stars denote utopian and nadir points. In turn, the red cross indicates the scenario farthest from nadir solution, and the red circle the scenario closest to the utopia solution. Figure 6.24 shows the results for Eff_{total} and EI. The Pareto front includes C43-C44-C14-C34. This clearly demonstrates that scenarios Ci4, for H_2 production and PSA purge gas use, for blends and petcoke and orujillo dominates all other scenarios. The closest case study to utopian point is C44, while the farthest from nadir is C43: it is deduced that regarding EI and efficiency, biomass is the chosen feedstock.

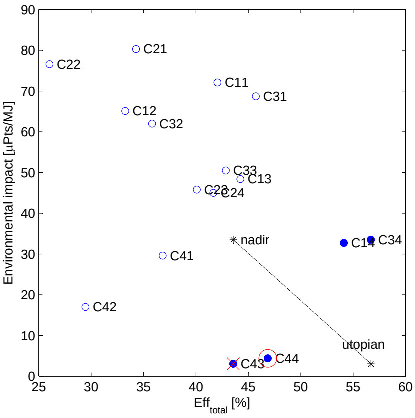

Figure 6.24: Set 2 scenarios trade-off by means of Eff_{total} and EI.

Figure 6.25 represents Eff_{total} vs. the two calculated COEs. In this case, only

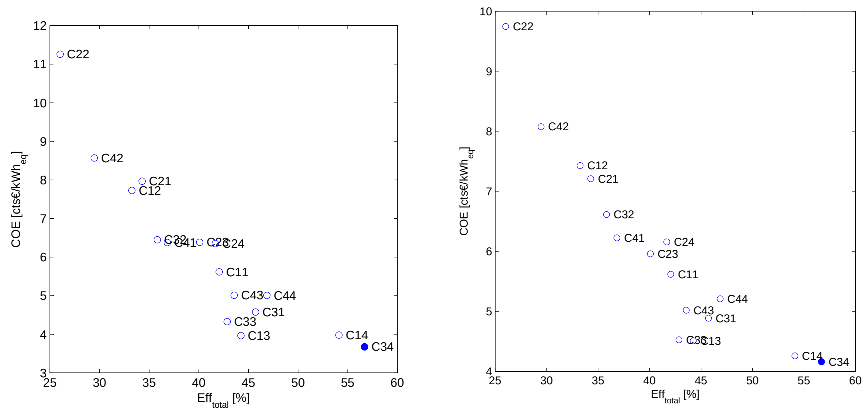

Figure 6.25: Set 2 scenarios trade-off by means of Eff_{total} and COE$_a$ and COE$_b$.

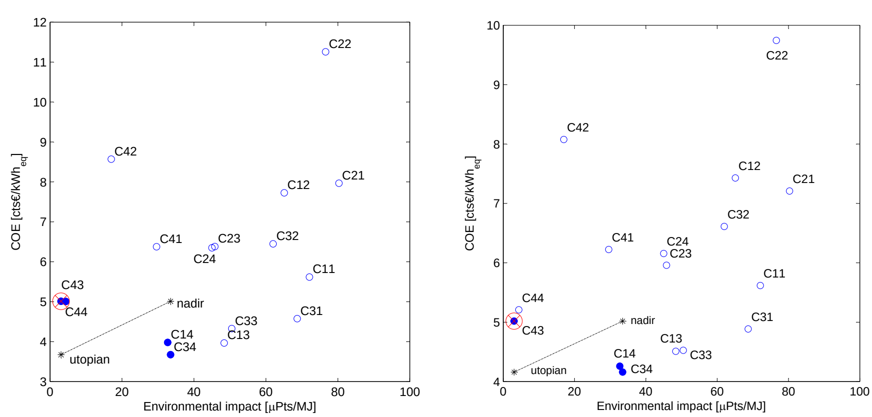

Figure 6.26: Set 2 scenarios trade-off by means of EI and COE$_a$ and COE$_b$.

one scenario dominates all the others: C34 for both criteria. Therefore, petcoke for H_2 production is the most efficient and profitable option.

Figure 6.26 represents the trade-off between COEs and EI. The Pareto front is constituted by C43-C44-C14-C34, which is the same as in Figure 6.24. Nevertheless, for COE$_b$, C44 is not in the Pareto front. Following the TOPSIS methodology, the selected scenario is again C43.

6.7 Final considerations

The choice of an appropriate mixture of feedstocks and amount of products is dependent on many criteria and is subject to the decision-maker interests. These co-gasification and co-production analyses carried out in this chapter demonstrate that the production of H_2 and electricity is a more efficient process, in terms of Eff_{total}. The end-user has to consider that the Eff_{global} is reduced when carbon capture units are added to an already existing IGCC power plant. Accordingly, the feedstock should be increased to maintain amount the electricity production. This shows the importance of each case study and each specific context, such as the demands to satisfy, or the raw material and product prices.

Oxygen has been shown to have a greater influence on gasification than steam. Biomass gasification and biomass co-gasification with coal and petcoke are attractive choices for climate change mitigation and traditional fuels independence. The simulation results analysed by means of Pareto curves show that biomass is a suitable choice for net power and H_2 production, as it offers higher efficiencies and lower carbon-related emissions. High CGE values lead to optimal overall results in terms of the produced electricity. The prices of raw materials follow market laws, which are not necessarily governed by the most efficient choices. Concerning feedstocks and co-production, the feedstock compositions that lead to the most electricity production also offer the best H_2 production results.

The results provided by this IGCC model validated show its prediction capability. The procedure involves the use of evaluation scenarios, which facilitates and assists the decision-making task taking into account multiple objectives. Therefore, the modelling superstructure conceived is able to accept changes in raw materials and in operation units, thus constituting an enabling tool in conceptual design of IGCC systems. Moreover, comparisons tests indicate that the simulation results show good agreement with real data from power plant.

Emphasis in the development of the present tool has been placed on optimising plant conceptual design. Depending on the final interests, this tool suggests through discrimination design options for planned changes or can be used to identify the effect of specific parameters.

Notation

Latin letters

Eff	efficiency
P	pressure
T	temperature

Superscripts and subindices

cg	clean gas
CC	combined cycle
$CCapture$	carbon capture units
e	electric
eq	equivalent; when adding power and H_2 calorific value in co-production case studies
$global$	considering the plant as a whole, when only electricity is produced
H_2	produced hydrogen
rg	raw gas
th	thermal
$total$	considering the plant as a whole in co-production scenarios

Acronyms

ADP	abiotic depletion potential
AC	annual costs

ANN	artificial neural network
ar	as received basis
AP	acidification potential
ASU	air separation unit
CC	combined cycle
CCS	carbon capture and storage
CED	cumulative energy demand
CExD	cumulative exergy demand
CGE	cold gas efficiency
COE	cost of energy
COS	carbonyl sulphide
EF	ecological footprint
EI	environmental impact
ES	Spain
ER	equivalence ratio
FdC	feedstock costs
FU	functional unit
GHG	greenhouse gases
GT	gas turbine
GWP	global warming potential
HP	high pressure
HRSG	heat recovery steam generator
IGCC	integrated gasification combined cycle
KPI	key performance indicator
LCA	life cycle assessment
LCI	life cycle inventories
LCIA	life cycle impact assessment
LHV	lower heating value
MCDA	multiple-criteria decision making
MDEA	methyldiethanol amine
NG	natural gas
NGCC	natural gas combined cycle
PSA	pressure swing adsorption
RER	European average
SA	sensitivity analysis
SC	supply chain
ST	steam turbine
TCR	total capital requirement
TOC	total operating costs
TOPSIS	technique for order by similarity to ideal solution
TOT	turbine outlet temperature
VL	vapour-liquid
WGS	water gas shift
WHB	waste heat boiler

Chapter 7

Bio-based Supply Chain Optimisation in Centralised Energy Systems

This chapter describes the use of mathematical modelling for bio-based suplly chains (BSC) based on biomass as a feedstock, to support decision-making. This approach is used in three different case studies exemplifying different contexts: (i) centralised energy systems taking into account biomass as raw material for electricity and hydrogen production, (ii) biomass co-combusted with coal in thermal power plants and (iii) a decentralised energy system for rural electrification, this last described in Chapter 8. The problem is formulate as a multi-objective optimisation mixed integer linear program (MOO-MILP) taking into account two main criteria: the net present value (NPV) and the environmental impact through Impact 2002+ indicator.

Both case studies using centralised energy systems (CES) are located in Spain. The first one comprises different supply chain (SC) components distributed over the country, aiming at finding the best gasification plants allocation to produce electricity and hydrogen. For comparison purposes, this first SC is contrasted to one using coal as raw material. The second case study is focused on co-combustion of coal and biomass in existing conventional thermal power plants aiming to obtain the best biomass distribution chain. The findings of this second case study include solid and liquid biomass for raw material transportation comparison and search to elucidate the role of subsidies in this sector while setting a possible coal substitution by means of locally-available biomass.

7.1 Introduction

A SC model, for the specific case of energy from biomass sytems, is developed and exemplified in the present chapter and in the next one by representative case studies. It concerns an analytical methodology for the design and planning (in the conceptual design framework, implying long term decisions) of a multiple source - multiple product BSC taking into account economic and environmental issues. The model includes different biomass wastes as sources. It identifies the most appropriate pre-treatment technologies, feedstock suppliers and processing plants, in the view of providing the electricity and hydrogen demand in one case (case study 1), to substitute a percentage of coal to produce electricity on another (case study 2), and to provide the basic electricity demand in a rural case, for the last one (case study 3).

Chapter 2 Section 2.2.3 has highlighted the main drawbacks of biomass as fuel: high moisture content (MC), low bulk density (BD) and low LHV, and poor grindability. Therefore, an appropriate design of the whole SC should alleviate these problems, with minimum costs and environmental impact, as considered in this chapter. The SC goals concern biomass transportation along long distances (even more important when considering international trade of biomass) and biomass usage in large scale reactors, specially when feedstock size reduction is crucial. As a consequence, transportation, process and handling must be facilitated. As was depicted in Figure 2.5, there exist five main blocks in a BSC: biomass collection, pre-treatment to enhance biomass properties, storage, transport and treatment to obtain the final product. The main characteristic of a BSC compared with a conventional SC is the pre-treatment echelon, which is needed to enhance biomass properties and has led to the development of new technologies to improve biomass quality as a fuel. In this chapter, torrefaction and fast pyrolysis are the state-of-the-art technologies contemplated, while the well-known pelletisation is also used alone, or in combination with torrefaction. Biomass can be characterised by its grindability, proximate and ultimate analyses. For gasification or combustion as final treatments, the chosen properties to be introduced in the model and evaluated throughout the whole SC are MC (%) and dry matter (DM) (%), LHV (in ar basis, MJ/kg) and BD (kg/m^3).

7.1.1 Biomass pre-treatments

The pre-treatment echelon of the SC is the bottleneck of biomass as a fuel if compared with other organic fuels. This chapter is focused on choosing the best SC network enhancing biomass properties according to several units inlet conditions. The pre-treatment characteristics are briefly described as follows.

Torrefaction

This is a thermal step at relatively low temperature (225°C-300°C, depending on the type of biomass) performed at atmospheric pressure in an inert atmosphere. The heating rate is low, approximately 50°C/min (Prins *et al.*, 2006a). The final solid product is a uniform solid with lower MC and higher calorific value than the raw material. By-products are a condensable liquid and a non-condensable gas. It is a relatively new technique applied to biomass, but the benefits have been already perceived on the BD and grindability, as the energy required for milling is significantly reduced (Prins *et al.*, 2006b; Uslu *et al.*, 2008). Prins *et al.* (2006a) have demonstrated that higher gasification efficiencies can be obtained by means of an O/C ratio decrease and MC reduction. Their simulated case studies comprise a circulating fluidised bed and a entrained flow gasifier, gasified with air or oxygen, at atmospheric pressure. During torrefaction the biomass reaches a 0% of humidity, but it captures some environmental moisture after the process. This capture of humidity is limited since torrefied biomass has a hydrophobic nature. Moreover, torrefaction limits biological degradation (Bergman *et al.*, 2005). Couhert *et al.* (2009) have conducted several pilot analyses with torrefied woods in an entrained flow gasifier. They have concluded that the syngas produced has a better quality, i.e. higher calorific value, than the syngas produced by gasifying not torrefied wood. Moreover, char from torrefied biomass is less reactive with steam. As additional example, the work by Deng *et al.* (2009) have evaluated the performance of torrefied agricultural residues in co-gasification with coal. They have demonstrated that torrefied biomass can be grinded to lower diameters, resulting in properties more similar to coal than untreated biomass. Torrefaction homogenises the appearance of the torrefied product, coming from different biomass sources.

Pelletisation

Mass densification and homogenisation, implying a higher BD, ease the handling, transport and storage of the biomass as fuel due to the uniform size, the high density and the low MC of the pellet (Maciejewska *et al.*, 2006). They also limits biological degradation. Drawbacks are moisture uptake, decreased mechanical resistance towards crushing and dust formation. A pellet is a cylinder of 6-8 mm diameter, and pelletisation requires drying, milling, conditioning, shaping and cooling. Usually, lignin acts as binding agent, which avoids external additives. Nowadays, the market share of pellets is growing, and this is the usual standard biomass shape used to commercialise biomass as fuel. Wood is the most usual raw material transformed (Sultana *et al.*, 2010). Pelletisation of torrefied biomass is described in Maciejewska *et al.* (2006) and Uslu *et al.* (2008), calling the product TOP pellets. The combination of both processes can overcome the main pellet and torrefied biomass disadvantages: biomass is completely dry after torrefaction, its humidity uptake is limited and biological degradation is practically completely inhibited, but torrefied biomass has a relatively low energy density. The storage of TOP pellets can be further simplified. As a result, the TOP pellets production process consumes less energy than conventional pelletisation. Torrefaction gas can be used for raw material drying at the beginning of the process. In contrast to conventional pellets, the TOP pellets can be produced from a wider variety of feedstocks, such as sawdust, willow, larch, grass, demolition wood, straw, yielding similar physical properties.

Fast pyrolysis

Pyrolysis can be defined as the thermal decomposition of biomass in the absence of oxygen, in a range of 400°C-800°C. It produces gas, liquid and char, at variable proportions depending on the pyrolysis method, the biomass type and the reaction parameters (Uslu *et al.*, 2008). Pyrolysis methods comprise slow and fast pyrolysis. The latter is the one considered here. This pyrolysis takes into account a high heating rate, taking place at 450°C-550°C. This option allows to obtain a liquid product called pyrolysis oil or bio-oil, consisting in 70% oxygenated organics and 30% water (on a mass basis) (Maciejewska *et al.*, 2006). The proportion of water can cause corrosion problems. Pyrolysis can provide a cheaper transport and handling, due to the liquid state of the bio-oil. This oil can be used as a transport fuel, even directly in a diesel engine. The works by Wu *et al.* (2010) and Abdullah *et al.* (2010) have used bioslurry from mallee biomass as fuel to be transported. The bioslurry is formed by combining bio-oil and biochar, which is the solid product that results from the fast pyrolisis, milled into fine particles (due to its favourable grindability) and suspended into the bio-oil. In that way, the LHV of the bioslurry profits from the energy concentration of char, enhancing the efficiency of the process.

Uslu *et al.* (2008) and Magalhaes *et al.* (2009) have evaluated the use of pre-treatment technologies in a BSC. In the first study, those are seen as alternatives to promote international trade. Among the considered options, TOP pellets are selected, while pyrolysis has a main drawback from the economic point of view. In the second study, three different pre-treatment technologies are evaluated to select the most profitable and the most environmentally-friendly option, in terms of CO_2 emissions, in a biomass-to-liquid SC. The final numbers favour the case study with rotating cone reactor to perform a fast pyrolysis, vs. fast pyrolysis in a fluidised bed, torrefaction, and torrefaction combined with pelletisation. Large scale vs. small scale plants issue is also presented by means of different scenarios evaluation. Efficiencies increase and cheaper biomasses would enhance the financial pattern.

Storage

Storage is not a pre-treatment but it can change the biomass properties, such as MC, LHV and DM content because of microbiological degradation processes. A critical parameter here is the temperature of the pile of biomass. In order to alleviate biomass degradation, biomass stored should be homogeneous and with low MC (usually under 20% on a mass basis). The work by Rentizelas *et al.* (2009d) points out that biomass waste can be a seasonal fuel. Therefore, storage is crucial to meet the demand of each period. A BSC should be a multi-source SC that coherently considers transportation costs and embedding storage as a part of them. The type of storage depends on the type of biomass to be stored. Usually, during summer or in tropical climates, open-air storage is used to dry the biomass. For pre-treated biomass, usually a closed storage such as in silos or bunkers is used. Liquids while stored unusually change their properties.

The different pre-treatments can imply changes on MC, DM, LHV and the BD of the biomass. All pre-treatments enhance transportation costs. Examples of enterprises that commercialise those state-of-the-art processes are Dynamotive Inc. or BTG group for the fast pyrolysis technology, and Topell BV, for the torrefaction. Note that those technologies are still in a development phase. All the SC steps, except storage, need energy, i.e. electricity or liquid/solid fuel such as diesel or biomass itself, to be run. Table 7.1 briefly summarises the biomass properties that change during the SC echelons.

7.2 The bio-based supply chain

The *mathematical model* of the BSC allows taking different decisions: (i) active SC nodes and links among them (a node can be represented by processing or distribution activities), (ii) facilities capacity expansion into each period, (iii) the product portfolio per plant and (iv) its utilisation level, (v) transportation links and (vi) the amount of final products to be sold, subjected to the optimisation of the objective function(s). Therefore, the overall economical profit as well as the environmental impact associated to each SC node or echelon can be identified. All of them in the planning horizon, or as described in this thesis, in the conceptual design stage.

Table 7.1: Biomass properties manipulation depending on the BSC activity.

	MC (%)	Matter loss (%)	BD (kg/m^3)	Energy loss (%)	Inlet restrictions
Chipping		√	√		
Drying	√				
Torrefaction	√	√	√	√	MC
Torrefaction + pelletisation	√	√	√	√	MC
Pelletisation	√		√		MC
Fast pyrolysis	√		√	√	MC
Fast pyrolysis + char grinding	√		√	√	MC
Storage	√	√			
Transportation					

The BSC is defined as a number of potential locations where processing sites or distribution centers, or both of them can be installed. Suppliers are at fixed locations, where biomass is available. The final product can be produced at several plant sites. The characteristics of the raw biomass are enhanced by means of the pre-treatment units, so as to allow treated biomass to meet the characteristics required to be used in subsequent steps in the SC, and diminishing transportation costs. The production capacity of each processing site is modelled by relating the nominal production rate per activity to the availability of the equipment per year, i.e. the number of working hours per year and equipment. Distribution centres and the distribution or transportation activity are modelled by considering upper and lower bounds based on their biomass handling capacity. Distribution centres can be supplied from more than one pre-treatment plant. Given the way the problem is modelled, materials flow between facilities may appear if selecting such flow improves the performance of the SC. The market demand of electricity or hydrogen, can be satisfied by more than one site.

A general outline of the modelled BSC for case studies 1 and 2, is shown in Figure 7.1. It comprises four main blocks: sourcing, pre-treatment, product generation and product distribution. The *sourcing block* consists of the available biomass collection from different regions and suppliers. Each type of biomass, which in all case studies is biomass waste (pine waste, forest wood residues, olive pomace, agricultural woody residues, forestry residues and cassava waste), has its own characteristic attributes: MC, DM, LHV and BD. The *pre-treatment block* considers the activities described in Section 7.1, to modify the quality of biomass, in terms of energy and matter densifications. Those processes are chipping, drying, torrefaction, pelletisation or fast pyrolysis. Some of these activities can be mandatory provided that some other following technologies in the BSC, concerning *product generation* may be restricted to a maximum value of MC and/or require a specific shape or maximum size to be able to process the biomass. *Product distribution* mainly concerns electricity supply through the grid.

7.3 The multi-objective optimisation

All the abovementioned decisions will be taken by considering the optimisation of an economic (NPV) and an environmental impact metric (Impact 2002+) in a defined planning horizon. Each metric is further described in Chapter 3.

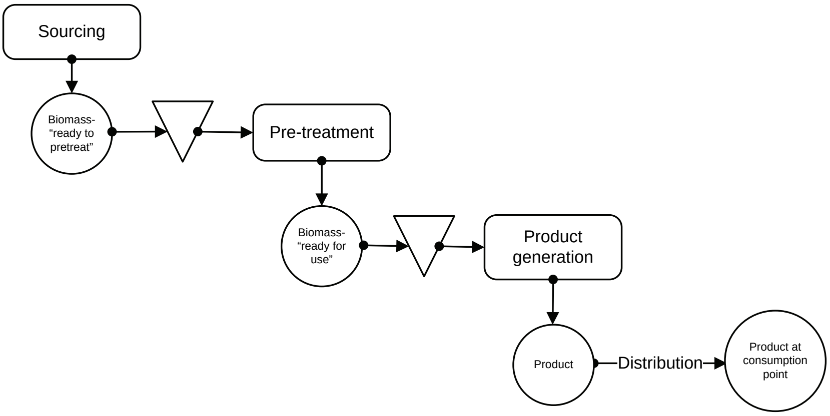

Figure 7.1: General scheme considered here for a BSC.

7.3.1 The mathematical formulation

The resulting model is solved by using a MOO-MILP algorithm, which allows observing the trade-off between environmental damage categories and economic indicator. The mathematical formulation is described here. The *variables* and *constraints* from the model are classified into three groups: (i) process operations constraints given by the SC topology (the so-called design-planning model), (ii) economic metric requirements and (iii) environmental metric requirements. They are described as follows.

Design-planning model

The design-planning model presented here is a translation of the state task network (STN) formulation (Kondili *et al.*, 1993) to the SC modelling, adapted from Laínez-Aguirre *et al.* (2009). This formulation can collect all the SC node information through a single variable. This eases the economic and environmental metrics formulation. The SC node characteristics are modelled by means of a single equation set, since manufacturing nodes, distribution centres, production and distribution activities are treated in the same way. Therefore, the most important variable of the model is $P_{ijff't}$, which represents the particular activity of task i, performed using technology j during period t, whose origin is location f and destination is location f'. Concretely, the task is described by the couple biomass type (as raw material, and pre-processed biomass)-technology used. In the case of production activities, they must receive and deliver material within the same site ($P_{ijff't}$). In contrast, in a distribution activity, facilities f and f' must be different. The separation among tasks and technologies allows for a flexible formulation of different case studies. The equations are described in the following paragraphs.

Mass balance must be satisfied at each node. The expression for the mass balance for each type of biomass s (that can be raw material and pre-processed biomass), consumed at each potential site f in every time period t is presented in Eq. (7.1). Parameter α_{sij} is defined as the mass fraction of biomass s that is produced by task i using technology j. T_s set refers to tasks that produce s, while $\bar{\alpha}_{sij}$ and $\bar{T}_s$ set, refer to tasks that consume s.

$$S_{sft} - S_{sft-1} = \sum_{f'} \sum_{i \in T_s} \sum_{j \in (J_i \cap \tilde{J}_{f'})} \alpha_{sij} P_{ijf'ft} - \sum_{f'} \sum_{i \in \bar{T}_s} \sum_{j \in (J_i \cap \tilde{J}_f)} \bar{\alpha}_{sij} P_{ijff't} \qquad \forall s, f, t \tag{7.1}$$

The model assumes that process parameters such as conversions, separation factors or temperatures, are fixed for all the activities, to enforce the linearity of the problem. In this sense, the parameters α_{sij} and $\bar{\alpha}_{sij}$ gives the recipe for a given activity. Nevertheless, there are activities where it is desirable to let the model specify the mixture of inputs in order to achieve a given value of a specific biomass property, for instance, a specific MC. For such activities, the combination of feedstocks, therefore, the proportion of each feedstock is variable. In order to take into account those activities, the mass balance is modified as shown in Eq. (7.2). Note that Eq. (7.1) is a simplification of Eq. (7.2)

$$\begin{aligned} S_{sft} - S_{sft-1} = &\sum_{f'} \sum_{i \in T_s} \sum_{j \in (J_i \cap \tilde{J}_{f'})} \alpha_{sij} P_{ijf'ft} - \sum_{f'} \sum_{i \in \bar{T}_s} \sum_{j \in (J_i \cap \tilde{J}_f)} \bar{\alpha}_{sij} P_{ijff't} \\ &+ \sum_{i \in T_s} \sum_{j \in (J_i \cap \tilde{J}_{f'})} Pv_{sijfft} - \sum_{i \in \bar{T}_s} \sum_{j \in (J_i \cap \tilde{J}_{f'})} Pv_{sijf't} \qquad \forall s, f, t \end{aligned} \tag{7.2}$$

For these flexible activities, it is necessary to verify that the *energy balance* is satisfied. For the activities that have fixed biomass properties at the inlet and the outlet of the technology, the energy balance is achieved during the definition of the streams. The energy balance is represented by Eq.(7.3). Here, HV_{si} is the heating value of material s in activity i. Notice that each different type of biomass has a different heating value. A specific activity changes the heating value of the output stream if it is a pre-treatment task that modifies explicitly the calorific value of the biomass, or if it is a task whose main objective is the change of shape, but it is receiving a mixture of biomasses as input.

$$\sum_{s \in S_i} HV_{si} Pv_{sijfft} = \sum_{s \in \bar{S}_i} HV_{si} Pv_{sijf't} \qquad \forall i \in \bar{I}, j, f, t \tag{7.3}$$

The flexible activities must accomplish a final MC, fixed by the user. In that case, the constraint Eq. (7.4) must be satisfied. The parameters $Water_s$ and $Water_{ij}^{max}$ represent the MC for material s, and the maximum MC allowed for task i performed in equipment j, respectively.

$$\sum_{s \in S_i} Water_s Pv_{sijfft} \leq Water_{ij}^{max} \sum_{s \in \bar{S}_i} Pv_{sijf't} \qquad \forall i \in \bar{I}, j, f, t \tag{7.4}$$

Eq. (7.5) represents the temporal change in facility capacities, such as in distribution activities, demonstrating the model capability for design and SC retrofit.

Eq. (7.6) is used for total capacity F_{jft} bookkeeping taking into account the capacity augment during the planning period t (FE_{jft}).

$$V_{jft}FE^{L}_{jft} \leq FE_{jft} \leq V_{jft}FE^{U}_{jft} \qquad \forall f, j \in \tilde{J}_f, t \tag{7.5}$$

$$F_{jft} = F_{jft-1} + FE_{jft} \qquad \forall f, j \in \tilde{J}_f, t \tag{7.6}$$

Eq. (7.7) is used to ensure a total plant production rate greater than a minimum production rate fixed by the user, lower than the available capacity. Parameter β_{jf} defines a minimum utilisation rate of technology j in site f. Parameter $\theta_{ijff'}$ represents the resource utilisation factor. This is the capacity utilisation rate of technology j by task i whose origin is location f and destination location f'.

$$\beta_{jf}F_{jft-1} \leq \sum_{f'}\sum_{i\in I_j}\theta_{ijff'}P_{ijff't} \leq F_{jft-1} \qquad \forall f, j \in \tilde{J}_f, t \tag{7.7}$$

$\theta_{ijff'}$ is one of the key factors to be determined when addressing aggregated planning problems, considering strategic and tactical decisions in continuous and in semi-continuous processes. For continuous problems, the capacity utilisation factor is a conversion factor that allows taking into account the equipment j capacity in site f in terms of task i per unit of produced material and unit of time. The factor is consequently the maximum throughput per planning period. For batch problems, this parameter is closely related to the operation time of the different tasks. Here, the time period scale utilised in aggregated planning is usually larger than the time that a task (production/distribution activity) requires to be performed. Therefore, the sequencing-timing problem of short term scheduling is transformed into a rough capacity problem where aggregated figures are used. The capacity is expressed as equipment j available time during one planning period, then $\theta_{ijff'}$ represents the time required to perform task i in equipment j per unit of produced material. Thus, once operation times are determined, this parameter can be estimated without problems. Eq. (7.8) guarantees that the amount of raw biomass s purchased in site f at each time period t is lower than an upper bound given by physical limitations A_{sft}. Eq. (7.9) is used to express that the demand can be partially satisfied, due to biomass production or supplier capacity limitations: the sales of product s carried out in market f during the time period t should be less or equal to the demand.

$$\sum_{f'}\sum_{i\in \bar{T}_s}\sum_{j\in J_i} P_{ijff't} \leq A_{sft} \qquad \forall s \in RM, f \in Sup, t \tag{7.8}$$

$$\sum_{f'}\sum_{i\in T_s}\sum_{j\in J_i} P_{ijf'ft} \leq Dem_{sft} \qquad \forall s \in FP, f \in Mkt, t \tag{7.9}$$

Economic model

The expressions to calculate the operating revenue, the operation costs and the total capital investment, needed for NPV calculation according to Eq. (3.15)), are described as follows.

The *operating revenue* is calculated taking into account the net sales reached during normal SC activities. The total revenue is expressed in Eq. (7.10) as the product sales during period t.

$$ESales_t = \sum_{s \in FP} \sum_{f \in Mkt} \sum_{f' \notin (Mkt \cup Sup)} Sales_{sf'ft} Price_{sft} \qquad \forall t \tag{7.10}$$

The *operating costs* include fixed and variable costs: Eq.(7.11) describes the total fixed costs of operating a SC, with $FCFJ_{jft}$ as fixed unitary capacity cost of using technology j at site f.

$$FCost_t = \sum_{f \notin (Mkt \cup Sup)} \sum_{j \in \tilde{J}_f} FCFJ_{jft} F_{jft} \qquad \forall t \tag{7.11}$$

In turn, as variable costs, the cost of purchases from supplier e, includes raw material obtaining, transport and production resources, as shown in Eq. (7.12). The purchases of raw materials ($Purch_{et}^{rm}$) made to supplier e is evaluated in Eq. (7.13). It should be noted that in this formulation and for the case of raw material suppliers and transport providers each one of them uses a different technology. The variable χ_{est} represents the cost associated to raw material s purchased to supplier e. Transportation and production variable costs are determined by Eqs. (7.14) and (7.15), respectively. $\rho_{eff't}^{tr}$ denotes the e provider unitary transportation cost associated to material movement from location f to location f' during period t. τ_{ijfet}^{ut1} represents the unitary production cost associated to perform task i using technology j, whereas τ_{sfet}^{ut2} represents the unitary inventory costs of material s storage at site f. Both of them count with provider e during period t. The parameter τ_{ijfet}^{ut1} entails restrictions associated with α_{sij} and $\bar{\alpha}_{sij}$, given that the amount of utilities and labour spent are proportional to the amount of raw material processed. This assumption neglects the benefits of economies of scale, since higher production rates, linearly deals to higher production costs.

$$EPurch_{et} = Purch_{et}^{rm} + Purch_{et}^{tr} + Purch_{et}^{prod} \qquad \forall e, t \tag{7.12}$$

$$Purch_{et}^{rm} = \sum_{s \in RM} \sum_{f \in F_e} \sum_{i \in \bar{T}_s} \sum_{j \in J_i} P_{ijfft} \chi_{est} \qquad \forall e \in E_{rm}, t \tag{7.13}$$

$$Purch_{et}^{tr} = \sum_{i \in Tr} \sum_{j \in J_i \cap \bar{J}_e} \sum_{f} \sum_{f'} P_{ijff't} \rho_{eff't}^{tr} \qquad \forall e \in \bar{E}_{tr}, t \tag{7.14}$$

$$Purch_{et}^{prod} = \sum_{f} \sum_{i \notin Tr} \sum_{j \in (J_i \cap \hat{J}_f)} P_{ijfft} \tau_{ijfet}^{ut1} + \sum_{s} \sum_{f \notin (Sup \cup Mkt)} S_{sft} \tau_{sfet}^{ut2} \qquad \forall e \in \tilde{E}_{prod}, t \tag{7.15}$$

The *total capital investment* on fixed assets is calculated by means of Eq. (7.16). This equation includes the investment made to expand the technology's capacity j in facility site f in period t ($Price_{jft}^{FJ} FE_{jft}$) and the investment required to open a manufacturing plant in location f, in case it is opened at period t ($I_{ft}^{J} JB_{ft}$).

$$FAsset_t = \sum_{f} \sum_{j} Price_{jft}^{J} FE_{jft} + I_{ft}^{J} JB_{ft} \qquad \forall t \tag{7.16}$$

Finally, Eq. (7.17) calculates the profit in period t, as operating revenues minus fixed and variable operating costs. The NPV is calculated as in Eq. (7.18) using the mathematical programming terminology.

$$Profit_t = ESales_t + Net_t^{co_2} - (FCost_t + \sum_e EPurch_{et}) \qquad \forall\ t \tag{7.17}$$

$$NPV = \sum_t \left(\frac{Profit_t - FAsset_t}{(1+i_r)^t} \right) \tag{7.18}$$

Environmental model

The application of the life cycle assessment (LCA) methodology to the SC model requires four steps, as described in Chapter 3: goal definition and scope, life cycle inventory (LCI), life cycle impact assessment (LCIA) and results interpretation. Environmental interventions are translated into metrics related to environmental impact as end-points or mid-points metrics by the usage of characterisation factors. Eq. (7.19) calculates IC_{aft}: it represents the mid-point environmental impact a associated to site f, as a consequence from activities in period t. In turn, $\psi_{ijff'a}$ is the a characterisation factor of the environmental category impact for task i performed using technology j, receiving materials from node f and delivering them at node f'.

$$IC_{aft} = \sum_{j \in \tilde{J}_f} \sum_{i \in I_j} \sum_{f'} \psi_{ijff'a} P_{ijff't} \qquad \forall\ a, f, t \tag{7.19}$$

Analogously to α_{sij} and $\bar{\alpha}_{sij}$, the value of $\psi_{ijff'a}$ is fixed and constant, since all environmental impacts are considered linearly proportional to the activity performed in the node (variable P_{ijfft}) (Heijungs & Suh, 2002). Environmental impacts associated to transportation, has as a common functional unit (FU), the amount of kg of transported material over a given distance (kg·km). Consequently, the value of the mid-point environmental impact $\psi_{ijff'a}$ associated to transport, is calculated as in Eq. (7.20), where $\psi^T_{ijff'a}$ represents the a characterisation factor of the environmental category impact for the transportation of a mass unit of material over a unit of lenght. The impact is assigned to the origin node. The environmental impacts associated to production (Eq. 7.19) or transport (Eq. 7.20), can be performed by setting the indices summation over the corresponding tasks ($i \in Tr$ or $i \in NTr$).

$$\psi_{ijff'a} = \psi^T_{ija} distance_{ff'} \qquad \forall\ i \in Tr, j \in J_i, a, f, f' \tag{7.20}$$

Eq. (7.21) introduces $DamC_{gft}$, which is a weighted sum of all mid-point environmental interventions. They are combined using g end-point damage factors ζ_{ag}, normalised with $NormF_g$ factors. Moreover, Eq. (7.22) calculates g normalised end-point damage along the SC ($DamC_g^{SC}$).

$$DamC_{gft} = \sum_{a \in A_g} NormF_g \zeta_{ag} IC_{aft} \qquad \forall\ g, f, t \tag{7.21}$$

$$DamC_g^{SC} = \sum_f \sum_t DamC_{gft} \qquad \forall\ g \tag{7.22}$$

Eqs. (7.23) and (7.24) sum the end-point environmental damages for each site f and for the whole SC, respectively.

$$Impact_f^{2002} = \sum_g \sum_t DamC_{gft} \qquad \forall\ f \tag{7.23}$$

$$Impact_{overall}^{2002} = \sum_f \sum_g \sum_t DamC_{gft} \tag{7.24}$$

$DamC_g^{SC}$ or $Impact_{overall}^{2002}$ can be used as objective functions in the MOO-MILP formulation.

Objective functions

The SC network can be optimised as:

$$\begin{gathered}\underset{\mathscr{X},\mathscr{Y}}{\text{Min}} \left\{-NPV, DamC_g^{SC} or Impact_{overall}^{2002}\right\} \\ \text{subject to} \\ \text{Eqs. (7.1)-(7.24);} \\ \mathscr{X} \in \{0,1\}; \mathscr{Y} \in \mathbb{R}^+\end{gathered}$$

Where, $\mathscr{X}$ denotes the binary variables set, while $\mathscr{Y}$ corresponds to the continuous variable set.

7.4 Case study 1: a BSC located in Spain using gasification

This first case study evaluates the generation of electricity and H_2 from biomass wastes compared to coal, using IGCC plants. The SC under study comprises biomass collection sites, processing sites where biomass is pre-treated and used and product distribution (see Figure 7.1). The boundaries considered are from cradle-to-gate.

A simplified network is proposed for Spain, as depicted in Figure 7.2. The feedstock is supposed to be available at Córdoba (LA), Lugo (LB), Cuenca (LC), Santander (LD) and Oviedo (LE). This last site supplies coal. The possible facilities (pre-treatment and treatment plants) are Lugo ($F1$), Ciudad Real ($F2$) and Burgos ($F3$). Electricity and H_2 are fed to the Spanish electricity grid and sold, respectively, at their respective generation places and in marketplaces located at Madrid ($M1$), Valencia ($M2$) and Barcelona ($M3$).

Raw materials used

Different biomass wastes, which can be found in Spain according to Gómez *et al.* (2010b), are taken into account, characterised by their own LHV and MC: forest wood residues, pine waste, almond tree prunings, olive pomace (orujillo) and olive pit. In this case study, no changes in BD are considered. Table 7.2 summarises their main characteristics: approximate availability, costs and MCs are based on data published in Gómez *et al.* (2010b), Van Dyken *et al.* (2010), Rentizelas *et al.* (2009d) and Panichelli and Gnansounou (2008). LHVs are from ECN-Biomass (2010). Coal is assumed a dry material that does not require any pre-treatment. It is interesting to observe that

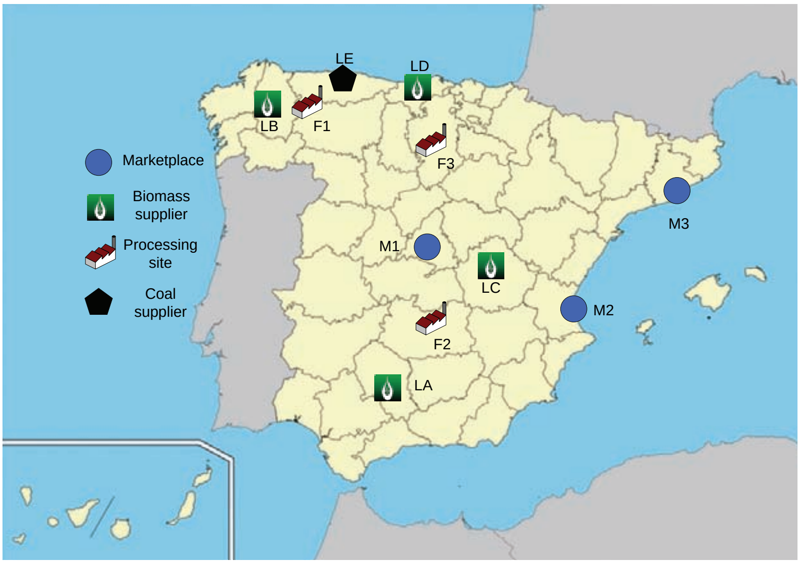

Figure 7.2: Location map of the potential BSC network.

higher MC's are present in forest and wood residues. Olive residues have lower MC and higher LHV, which is comparable to the one of the sub-bituminous coal considered here. A specific seasonality has been estimated for each raw material.

Table 7.2: Feedstock properties for case study 1.

Biomass	Cost (€/t)	LHV_{ar} (MJ/kg)	MC (%wt)	Seasonality	Monthly available (t)	Source location
Forest wood residue	25	8.597	48.9	None	40500	LB
Pine waste	35	10.450	40	None	3350	LD
Almond tree prunings	40	11.313	40	December to February	12400	LC
Olive pomace	65	19.098	7.6	January to March	73400	LA
Olive pit	35	18.778	6.1	February to May	27900	LA
Coal	45	15.000	-	None	65000	LE

Used technologies

The biomass must be pre-treated before being final processing. Figure 7.3 depicts the different pre-treatment processes that may be applied to the biomass (BM) to achieve the adequate conditions set up by the user, which are needed to follow up later processes. Those properties are MC, shape and LHV as specific inlet biomass characteristics to be able to enter the different plants. Pre-treatment plants modify MC and DM of biomass, modifying as a consequence its LHV. Each pre-treatment characteristics appear in Table 7.3, and are further described here:

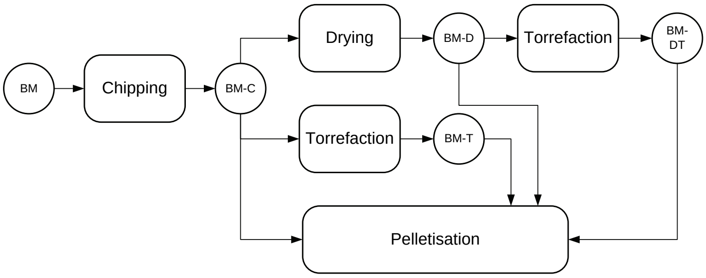

Figure 7.3: Pre-treatment activities layout for a generic biomass, in case study 1.

- Chipping. This activity transforms biomass as received into chips. This is the first biomass size reduction step, and mandatory for all the biomass sources considered: shape homogenisation is crucial for an integrated BSC. MC is not modified, but there exists a loss of DM.

- Drying. An active dryer is needed when the different sources have variable MC's. The threshold condition to activate this step is a humidity higher than 7%. Passive drying is assumed not to be significant according to the unit of time that the model considers. The DM loss is insignificant compared with the moisture loss.

- Torrefaction. Its main objective is the LHV increase through volatiles release in an inert atmosphere. The biggest DM loss is achieved here, while a drying process also takes place. The condition to pass through this unit is to have a LHV lesser than 15 MJ/kg.

- Pelletisation. Biomass must be transformed into pellets before its final transformation. No moisture or dry matter losses occur. This unit requires as input biomass with MC equal or lower than 7%. This requirement may be fulfilled by mixing different types of pre-treated materials, as described for flexible units in Eqs. (7.2), (7.3) and (7.4).

Table 7.3: Pre-treatment processes considered in case study 1 and their main modelling assumptions (Hamelinck *et al.*, 2005; Panichelli & Gnansounou, 2008).

Activity/ Equipment	Moisture losses (%)	Dry matter losses (%)	Operating costs (€/t)	Capacity (t/h)	Investment (M€)	Electricity consumption (MWh/t)
Chipping	0	0.17	2.5	30	0.370	5
Drying	88	0.08	55	100	5.000	20
Torrefaction	55	19	40	20	0.100	37
Pelletisation	0	0	3.5	6	0.485	30

Gasification is the final technology used to provide electricity and H_2: IGCC and IGCC-CCS plants are considered. Efficiencies of 40% and 30% are assumed for each plant respectively, as has been calculated in Chapter 6. It is assumed that the lowest capacity that can be installed for the electricity generator is 85 MWh. Other relevant information concerning these technologies is presented in Table 7.4. Note that the described activities do not take into account economies of scale to calculate investment or operational costs.

Biomass transportation price is estimated at 0.03 €/t·km, and H_2 transportation price at 0.05 €/t·km, from current economical trends. It is assumed that the demand must be completely satisfied. The demand of H_2 is evenly distributed along the three markets ($M1$, $M2$ and $M3$), while the demand of electricity has to be supplied to the grid, from any of the facilities location.

The time period t is a month. According to the number of biomass wastes considered and the number of possible products, s has 26 different states. In turn, j has 6 different states in accordance with the different pre-treatment and treatment technologies. i has 21 states depending on the couple biomass-activity. Finally, this case study works with biomass mass; no volumetric performance is considered.

Table 7.4: Parameters for electricity and H_2 generation plants, in case study 1 (Coca, 2003; IEA-GHG, 2008).

Activity/ Technology	Operating costs (€)	Capacity	Investment (M€)	Product price (€)	Total monthly demand
Electricity	34.2/MWh	300MW	860	0.151/kWh	75000 MWh
H_2	1880/t	33.6 t/h	1500	3/kg	650 t

Environmental impact

To assess the environmental impact associated to BSC, the available LCI values are retrieved from the LCI database Ecoinvent-V1.3 (2006) using B.V. (2004), and they are directly converted into the Impact 2002+ mid-point indicators (LCIA step). For the activities that are not available in the former database, the impacts are taken assuming similar products or activities. For biomass impacts estimation, wood, softwood and chips from different origins are retrieved from the database. The environmental impact for the different feedstock's production can be found in Table 7.5, which does not consider impacts associated to transportation. The environmental impacts associated to electricity generation, H_2 production and pre-treatment processes without feedstock or transport considerations, as well as to transportation, are found in Table 7.6. Those impacts depend on the energy consumption during the operation, for each unit, translated into equivalent tonnes of biomass. Note that the impact for electricity generation from coal and biomass has been estimated taking into account the IGCC power plant outputs taken from the superstructure (Chapter 6).

Cherubini and Stromman (2011) have made a state-of-the-art of the performed LCA's for bioenergy systems. They concluded that most studies report a significant net reduction of GHG emissions when bioenergy substitutes fossil energy. Nevertheless, the main issue of all these studies is that they chooses different input data, functional units, allocation methods and reference systems. There exists a lack of methodological guidelines, and the environmental impacts taken into account depend on the user criteria. A standardisation in GHG balance evaluation is needed, as well as the reduction of uncertainties in key issues related to bioenergy such as land use change or impacts on biodiversity. The work by Forsberg (2000) assesses a life cycle inventory of the possible logistic systems available for biomass as raw material, including biomass recollection, on-site processing, pre-treatment methods

Table 7.5: Environmental impacts in terms of Impact 2002+ metric, associated to feedstock's production (Ecoinvent-V1.3, 2006), in pts/t.

Mid-point categories	Forest wood residue	Pine waste	Almond tree prunings	Olive pomace	Olive pit	Coal
Carcinogens	$2.12{\cdot}10^{-5}$	$2.18{\cdot}10^{-5}$	$1.96{\cdot}10^{-5}$	$2.84{\cdot}10^{-5}$	$9.40{\cdot}10^{-6}$	$1.51{\cdot}10^{-4}$
Non-Carcinogens	$1.37{\cdot}10^{-5}$	$1.31{\cdot}10^{-5}$	$1.53{\cdot}10^{-5}$	$3.28{\cdot}10^{-5}$	$1.76{\cdot}10^{-6}$	$2.52{\cdot}10^{-4}$
Respiratory inorganics	$1.16{\cdot}10^{-3}$	$1.19{\cdot}10^{-3}$	$1.08{\cdot}10^{-3}$	$1.11{\cdot}10^{-3}$	$4.36{\cdot}10^{-4}$	$2.89{\cdot}10^{-2}$
Ionising radiation	$2.62{\cdot}10^{-5}$	$2.42{\cdot}10^{-5}$	$3.12{\cdot}10^{-5}$	$4.77{\cdot}10^{-6}$	$2.64{\cdot}10^{-7}$	$9.37{\cdot}10^{-5}$
Ozone layer depletion	$1.05{\cdot}10^{-7}$	$1.07{\cdot}10^{-7}$	$1.00{\cdot}10^{-7}$	$8.00{\cdot}10^{-8}$	$3.70{\cdot}10^{-8}$	$1.42{\cdot}10^{-6}$
Respiratory organics	$5.52{\cdot}10^{-6}$	$6.22{\cdot}10^{-6}$	$3.71{\cdot}10^{-6}$	$2.25{\cdot}10^{-6}$	$4.95{\cdot}10^{-6}$	$2.28{\cdot}10^{-5}$
Aquatic ecotoxicity	$1.24{\cdot}10^{-6}$	$1.15{\cdot}10^{-6}$	$1.44{\cdot}10^{-6}$	$1.89{\cdot}10^{-6}$	$6.60{\cdot}10^{-8}$	$2.13{\cdot}10^{-4}$
Terrestrial ecotoxicity	$5.05{\cdot}10^{-5}$	$4.91{\cdot}10^{-5}$	$5.42{\cdot}10^{-5}$	$1.10{\cdot}10^{-4}$	$6.64{\cdot}10^{-6}$	$8.41{\cdot}10^{-3}$
Terrestrial acid/nutri	$1.89{\cdot}10^{-5}$	$1.97{\cdot}10^{-5}$	$1.67{\cdot}10^{-5}$	$1.68{\cdot}10^{-5}$	$8.28{\cdot}10^{-6}$	$6.78{\cdot}10^{-4}$
Land occupation	$1.90{\cdot}10^{-3}$	$1.62{\cdot}10^{-3}$	$2.62{\cdot}10^{-3}$	$4.80{\cdot}10^{-3}$	$1.38{\cdot}10^{-3}$	$1.63{\cdot}10^{-4}$
Aquatic acidification	0	0	0	0	0	0
Aquatic eutrophication	0	0	0	0	0	0
Global warming	$1.08{\cdot}10^{-3}$	$1.05{\cdot}10^{-3}$	$1.16{\cdot}10^{-3}$	$4.50{\cdot}10^{-4}$	$1.88{\cdot}10^{-4}$	$1.57{\cdot}10^{-2}$
Non-renewable energy	$1.49{\cdot}10^{-3}$	$1.43{\cdot}10^{-3}$	$1.65{\cdot}10^{-3}$	$5.72{\cdot}10^{-4}$	$1.97{\cdot}10^{-4}$	$1.84{\cdot}10^{-1}$
Mineral extraction	$6.52{\cdot}10^{-8}$	$6.69{\cdot}10^{-8}$	$6.05{\cdot}10^{-8}$	$6.75{\cdot}10^{-7}$	$3.59{\cdot}10^{-8}$	$7.72{\cdot}10^{-7}$

and electricity production through combustion. No significant differences are observed between domestic bioenergy use and electricity or biomass exportation: bioenergy can be considered as a commodity to be transported long distances.

The project is evaluated along a planning horizon of 25 years, considering monthly planning decisions, and considering 7200 average working hours per year. The model has been implemented in GAMS. The formulation of the SC-LCA model leads to a MILP with 4159 equations, 41221 continuous variables, and 96 discrete variables. It takes 61 CPU seconds to reach a solution with a 0.1% integrality gap on a 2.0 GHz Intel Core 2 Duo computer using the MIP solver of CPLEX 9.0.

7.4.1 Results

The results performed correspond to the two extremes of the Pareto frontier. Figure 7.4 shows the obtained BSC network that *maximises the NPV*. It is found that the three potential locations are used having more than one facility opened. All pre-treatment technologies are installed in location $F1$ besides the required plant to produce H_2. From this site, the overall H_2 demanded is produced and delivered to all the markets. $F1$ collects all forest wood residues (located in LB). By establishing $F1$, which is near to LB collection site, significant savings in transportation are obtained. All the needed electricity is generated in site $F2$: it is able to supply the requirements of the three markets, by injecting the electricity to the grid. In the same site, equipments to perform chipping, drying and pelletisation are installed. $F2$ receives olive residues (pomace and

Table 7.6: Environmental impacts in terms of Impact 2002+ metric, associated to SC tasks (Ecoinvent-V1.3, 2006), for case study 1.

Mid-point categories	Chipping (pts/t)	Drying (pts/t)	Torrefaction (pts/t)	Pelletisation (pts/t)	Electricity generation (pts/GJ)	H_2 generation (pts/t)	Transportation (pts/tkm)	Electricity generation from coal (pts/GJ)
Carcinogens	$2.16{\cdot}10^{-6}$	$8.64{\cdot}10^{-6}$	$1.60{\cdot}10^{-5}$	$1.30{\cdot}10^{-5}$	0	0	$6.93{\cdot}10^{-8}$	0
Non-Carcinogens	$9.28{\cdot}10^{-6}$	$3.71{\cdot}10^{-5}$	$6.86{\cdot}10^{-5}$	$5.57{\cdot}10^{-5}$	0	0	$4.93{\cdot}10^{-7}$	0
Respiratory inorganics	$4.18{\cdot}10^{-4}$	$1.67{\cdot}10^{-3}$	$3.10{\cdot}10^{-3}$	$2.51{\cdot}10^{-3}$	$2.09{\cdot}10^{-3}$	$2.49{\cdot}10^{-1}$	$2.38{\cdot}10^{-5}$	$2.21{\cdot}10^{-2}$
Ionising radiation	$6.03{\cdot}10^{-6}$	$2.41{\cdot}10^{-5}$	$4.46{\cdot}10^{-5}$	$3.62{\cdot}10^{-5}$	0	0	$5.17{\cdot}10^{-9}$	0
Ozone layer depletion	$1.23{\cdot}10^{-8}$	$4.93{\cdot}10^{-8}$	$9.11{\cdot}10^{-8}$	$7.39{\cdot}10^{-8}$	0	0	$2.58{\cdot}10^{-9}$	0
Respiratory organics	$6.01{\cdot}10^{-8}$	$2.40{\cdot}10^{-7}$	$4.45{\cdot}10^{-7}$	$3.61{\cdot}10^{-7}$	0	0	$3.43{\cdot}10^{-8}$	0
Aquatic ecotoxicity	$3.40{\cdot}10^{-7}$	$1.36{\cdot}10^{-6}$	$2.51{\cdot}10^{-6}$	$2.04{\cdot}10^{-6}$	0	0	$2.23{\cdot}10^{-8}$	0
Terrestrial ecotoxicity	$6.50{\cdot}10^{-6}$	$2.60{\cdot}10^{-5}$	$4.81{\cdot}10^{-5}$	$3.90{\cdot}10^{-5}$	0	0	$5.34{\cdot}10^{-6}$	0
Terrestrial acid/nutri	$5.75{\cdot}10^{-6}$	$2.30{\cdot}10^{-5}$	$4.26{\cdot}10^{-5}$	$3.45{\cdot}10^{-5}$	$6.91{\cdot}10^{-5}$	$8.23{\cdot}10^{-3}$	$5.13{\cdot}10^{-7}$	$7.33{\cdot}10^{-4}$
Land occupation	$1.30{\cdot}10^{-7}$	$5.20{\cdot}10^{-7}$	$9.63{\cdot}10^{-7}$	$7.80{\cdot}10^{-7}$	0	0	$1.61{\cdot}10^{-10}$	0
Aquatic acidification	0	0	0	0	0	0	0	0
Aquatic eutrophication	0	0	0	0	0	0	0	0
Global warming	$2.57{\cdot}10^{-4}$	$1.03{\cdot}10^{-3}$	$1.90{\cdot}10^{-3}$	$1.54{\cdot}10^{-3}$	$2.06{\cdot}10^{-2}$	2.45	$1.37{\cdot}10^{-5}$	$2.19{\cdot}10^{-2}$
Non-renewable energy	$3.22{\cdot}10^{-4}$	$1.29{\cdot}10^{-3}$	$2.39{\cdot}10^{-3}$	$1.93{\cdot}10^{-3}$	0	0	$1.34{\cdot}10^{-5}$	0
Mineral extraction	$2.96{\cdot}10^{-9}$	$1.19{\cdot}10^{-8}$	$2.19{\cdot}10^{-8}$	$1.78{\cdot}10^{-8}$	0	0	$4.54{\cdot}10^{-12}$	0

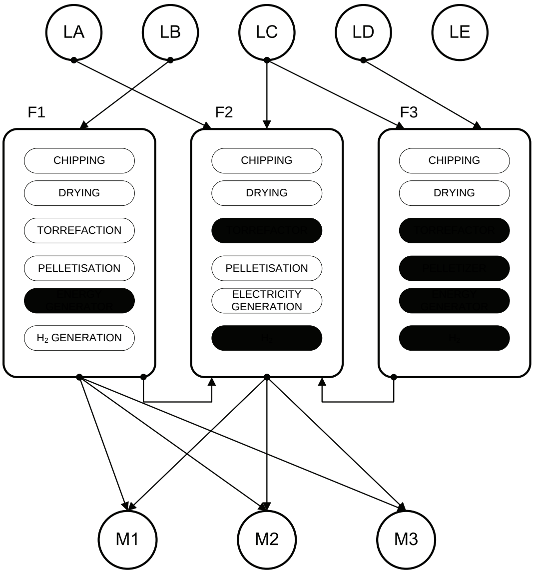

Figure 7.4: Optimum NPV network configuration for the BSC described in case study 1.

Table 7.7: Equipment capacity for the optimum NPV BSC described in case study 1.

	Facility		
Equipment	F1	F2	F3
Chipping (t/h)	67.5	60.4	40.0
Drying (t/h)	47.4	20.7	20.0
Torrefaction (t/h)	55.8	-	-
Pelletisation (t/h)	23.2	60.3	-
Electricity (GJ/h)	-	450.0	-
H_2 (t/h)	1.1	-	-

pit) and almond tree prunings. Site $F3$ is just used as a distribution centre for chipped and dried biomass. All pine waste (that has the minimum production of the considered wastes) and part of the almond tree prunings production are pre-processed here. Note that all collection sites supply biomass waste to the closest processing sites, according to Figure 7.2. Coal is not used here: all biomass wastes produced are enough to supply the market demand. Some inter-site flows are observed: dried and torrefied forest wood residue are sent from site $F1$ to $F2$, while $F3$ transfers dried pine waste and dried almond tree pruning to location $F2$ for conversion into electricity. By having materials flows of pre-treated biomass, the transportation costs are reduced, since energetically denser material is transported. Thus, this is the chosen option when biomass wastes should be transported long distances. Table 7.7 shows the calculated capacity to be installed per equipments at every site.

The optimal configuration that *minimises Impact 2002+* is shown in Figure 7.5. For this BSC network, $F3$ is not considered: all the biomass wastes are sent to locations $F1$ and $F2$. The electricity demand is satisfied from $F1$ and $F2$, while the whole amount of H_2 required comes from $F2$. There is one inter-site flow: it corresponds to a flow of dried olive pomace, which is the biomass with highest LHV. Thus, it diminishes the environmental pressure of the transportation activity. Table 7.8 presents the capacity proposed to be installed, per equipment.

As mentioned during the case study description, the pelletisation activity has been modelled as a flexible task: the model decides how to mix the biomass wastes to achieve a given specified biomass property. In this case, a 7% of MC should be assured before entering the pelletisation site. To give an example, there are periods (months) in which the model proposes the following mix: 1.4% forest wood residues, 30.3% dried and torrefied forest wood residues, 10.5% dried pine waste, 14.4% dried almond tree prunings, and 43.5% chipped olive pomace, on a mass basis. Their MC are: 10%, 6%, 7%, 7% and 7%, respectively. The humidity of this mix is 7%.

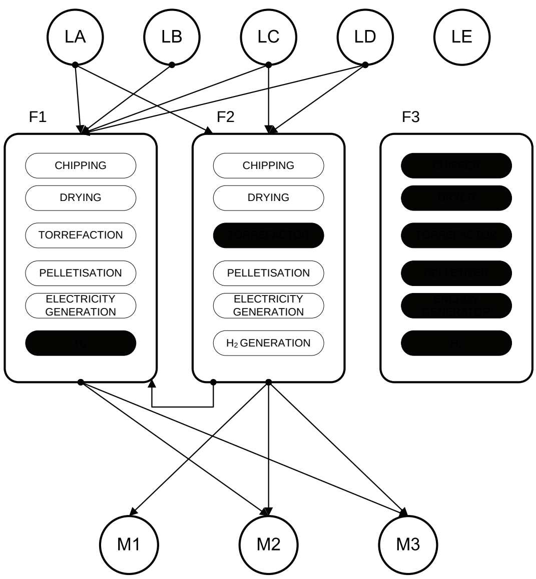

Figure 7.5: Optimum Impact 2002+ network configuration for the BSC described in case study 1.

Table 7.8: Equipment capacity for the optimum Impact 2002+ BSC described in case study 1.

Equipment	F1	Facility F2	F3
Chipping (t/h)	73.1	70.3	-
Drying (t/h)	54.4	20.7	-
Torrefaction (t/h)	51.7	-	-
Pelletisation (t/h)	40.0	62.7	-
Electricity (GJ/h)	300.0	300.0	-
H_2 (t/h)	-	1.1	-

The following results compare both optimal solutions. Tables 7.9 and 7.10 summarise the most representative values for the two networks proposed, regarding economic and environmental aspects. By regarding Table 7.9, the NPV correspondent to the BSC configuration that maximises the NPV is 228.51 M€. This value decreases of 3% if the environmental-friendly network is considered. This is mainly due to the difference among scenarios on investment and transportations costs. The transportation activity is lower when the environmental criterion is optimised. For the case of NPV maximisation, the installation of an electricity generation plant only at location $F2$ implies larger amounts of biomass to be processed here. The purpose of the distribution centre located at $F3$ is to reduce additional costs by transporting pre-processed biomass among longer distances instead of raw biomass. The reduction in capacity investment if compared with the environmental-friendly network compensates the increase in the transportation cost and the extra costs associated to the pre-treatment of biomass. Table 7.9 also shows the payback periods and the internal rate of return for both solutions.

Table 7.9: Economic aspects arising from single objective function optimisation results, in M€(taking into account the period of 25 years).

	NPV optimisation	Impact 2002+ optimisation
Investment	148.13	170.21
Biomass cost	819.87	820.16
Transportation cost	122.65	92.73
Production cost	2224.02	2222.77
Sales	3987.00	3987.00
Profit	820.46	851.34
NPV[1]	228.51	220.59
IRR (%)[2]	27.38	24.02
Payback period (years)	4.51	5.00

[1] Based on a return rate of 8%.
[2] Based on a planning horizon of 25 years.

Table 7.10 regards environmental interventions: the NPV optimum solution has an environmental impact of 117682 pts, while the Impact 2002+ optimum scenario is 2% lower. The impacts for each damage category (human health, ecosystem quality, climate change and resources) are very similar. The highest impact of the proposed case study 1 is on climate change: it represents 78% of the overall impact. Figure 7.6 depicts the environmental impact per SC echelons: transportation contribution is the most different among the optimised networks. The production activity (gasification to produce electricity or H_2) is the most contributing activity to the overall impact of both scenarios, while biomass sourcing is the least impacting issue. It is directly seen that biomass as a source has a minimal environmental impact. Thus, the attention should be focused on improving the efficiencies of treatment technologies.

Table 7.10: Environmental impacts arising from single objective function optimisation results, in Impact 2002+ pts (results per year).

End-point impact category	NPV optimisation	Impact 2002+ optimisation
Human health	17267.21	16255.29
Ecosystem quality	3610.96	3375.79
Climate change	90950.66	90383.37
Resources	5852.73	5292.64
Impact 2002+	117681.56	115307.09

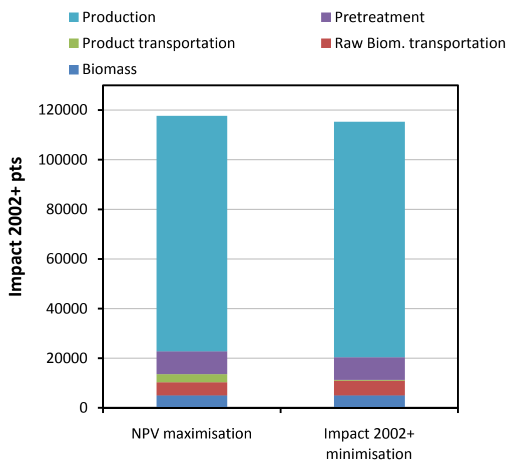

Figure 7.6: Distribution of environmental impacts for single objective optimisation solutions, according to the different SC activities (results per year).

Figure 7.7 analyses the effect of the electricity price on the optimised network considering the maximisation of the NPV, by means of the internal rates of return. The price of the electricity during the optimisation step is 0.151 €/kWh (see Table 7.4). Assuming an electricity price reduction of 50% (0.075 €/kWh), the NPV at the end of the planning horizon (25 years) is negative and equal to -553 M€. The price that equals the internal rate of return to the interest rate (8%) for the temporary horizon of 25 years is 0.129 €/kWh. Any price below this value would require a subsidy.

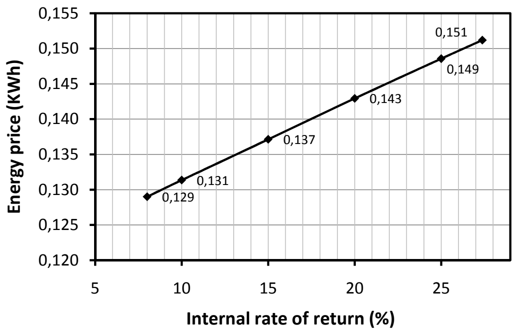

Figure 7.7: Energy price vs. internal rate of return for the BSC network optimised to obtain the maximum NPV.

For comparison purposes, the *optimal coal-based SC* is also investigated. The optimal NPV configuration proposes to deliver electricity from location $F1$, which is the closest site to the coal supplier. The capacity installed is 450 GJ/h, while the H_2 is produced at location $F3$, with a capacity of 1.1 t/h. The minimum Impact 2002+ network for this raw material is the same as the one obtained by the NPV optimisation. This is due to the fact that the only way to decrease environmental impacts is via transportation impact reduction. Since no pre-treatment is needed for coal, the transportation distance is the same in both configurations. The optimum network performances are summarised in Tables 7.11 and 7.12. The NPV is 219% higher than the optimum NPV for the BSC. This is due to the different investment and production costs, which are higher when pre-treatment activities are mandatory.

Table 7.11: Economic aspects arising from single objective optimisation for the coal-based SC, in M€.

	Optimisation
Investment	111.74
Coal cost	839.55
Transportation cost	181.70
Production cost	1136.10
Sales	3987.00
Profit	1829.65
NPV[1]	729.40
IRR (%)[2]	112.75
Payback period (years)	1.53

[1] Based on a return rate of 8%.
[2] Based on a planning horizon of 25 years.

Looking at environmental impacts, Impact 2002+ is increased in 203% compared with the BSC. The impact associated with the climate change category is similar for both cases: CO_2 is also emitted when using biomass, even if this source can be considered negative or zero emissions, as further discussed in Chapter 1 (which is not contemplated). This emphasizes the crucial importance of an overall impact indicator instead of a partial indicator such as CO_2 kg: comparing both SC's by means of CO_2 kg, there no exists any environmental improvement to motivate the use of biomass instead of coal. Nevertheless, the other impact categories are significantly increased when using coal, specially resources and human health. Figure 7.8 depicts the environmental impacts associated to the different SC activities for the coal-based SC. In this scenario, the production activity represents 46% of the overall impact, while the other remarkable activity is coal production, with 50% of the overall impact. Disregarding the raw material sourcing impact, the BSC and the coal-based SC would have an impact of 112701 pts and 178225 pts, respectively. This highlights the significance of integrating to the whole SC, instead of focusing on single activities.

Table 7.12: Environmental impacts arising from single objective optimisation for the coal-based SC, in Impact 2002+ pts (results per year).

End-point impact category	Optimisation
Human health	109640.53
Ecosystem quality	11077.16
Climate change	95334.48
Resources	140605.89
Impact 2002+	356658.06

7.4.2 Case study 1 conclusions

Case study 1 contemplates a BSC located in Spain, taking into account five different biomass wastes as sources and gasification plants as potential plants to produce demanded amounts of electricity and H_2. The most profitable and the most environmentally-friendly networks have been presented and compared. The optimal NPV is around 230 M€ for the considered 25 years. The sensitiveness of the optimal solutions to changes in prices is demonstrated, showing that the same network configuration can easily have positive or negative NPV's depending on the product price. This type of approaches can be useful to calculate the subsidy policies to drive industry practices towards more environmentally-friendly practices, which are not always the most profitable solutions. A coal-based SC is also solved, showing the importance of using an overall environmental impact rather than partial metrics, such as CO_2 emissions, when comparing different fossil fuels. The need for overall SC's comparison, rather than activity by activity is demonstrated.

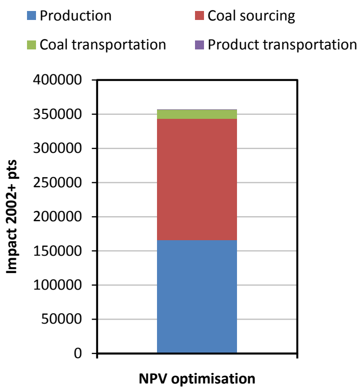

Figure 7.8: Distribution of environmental impacts for the coal-based SC.

7.5 Case study 2: a BSC located in Spain using co-combustion

This case study contemplates the co-combustion of biomass and coal in already existing power plants in Spain. The SC comprises biomass harvesting/collection sites, processing sites where biomass is pre-treated and treated to produce electricity; storage centres and transport. Concretely, given a net constituted by biomass collection sites, and biomass treatment plants (the thermal power plants), the SC model will help on the decision-making task related with: type and capacity of pre-treatment plants to be used, allocation of pre-treatment plants and allocation of the distribution centres. The kind of pre-treatment influences the way of transportation, since different trucks for solids or liquids are used. The boundaries considered are from cradle-to-gate. The currency used is $€_{2008}$. See again in Figure 7.3 the main SC echelons considered. It is assumed that electricity is supplied to the grid at the generation point without a final distribution step.

Raw materials and coal combustion plants

As described in Chapter 2, co-firing or co-combustion is defined as the simultaneous combustion of two or more fuels in the same combustion plant, using biomass along with coal in this case. This is the cheapest biomass application. The main reason to perform BSC optimisation to identify the most appropriate match between the percentage of substituted coal and the type and quality of used biomass.

The reported co-firing experiences in Chapter 2, Section 2.2.1, are principally with wood, which presents its highest compatibility with coal. This is why from the available data by Gómez *et al.* (2010a), where a deep analysis of the agricultural and forestry residues in Spain and their possible use is performed, forestry wood residues and agricultural woody residues are the selected biomass wastes to be used in this chapter. Table 7.13 provides their main characteristics. 2% of ashes is assumed for biomass properties calculation, in compliance with ECN-Biomass (2010). The possible feedstock supply site's coordenates and biomass amounts have been obtained from Gómez *et al.* (2010a). The quantity of available biomass for energy purposes, is estimated through a hierarchy of potential. It integrates physical, geographical and technical limitations: the authors consider the situation of the productive sites in Spain, the possibility of collection and the limitation due to access and environmental considerations. Therefore, the values considered in Gómez *et al.* (2010a) and hence, in this chapter, represent an upper bound of the potential energy content from forest and agricultural residues in Spain. There are 106 places that produce forest wood residues and 157 places that produce agricultural woody residues. In this work it is assumed that only the sites with an energy potential larger than around 550000 GJ/yr are considered for the BSC for co-combustion plants. Through this restriction, 73 and 34 positions result, respectively for each biomass type. Note that the most dispersed source is the agricultural woody residue, while the "best" biomass source (higher LHV and lower MC) is the forestry residue. See in Figure 7.9 the location and the relative size, in energy terms, of the considered biomass suppliers.

Table 7.13: Feedstock properties for case study 2 (Gómez *et al.*, 2010a).

Biomass	Cost (€/t)	LHV_{ar} (MJ/kg)	MC (%wt)	Seasonality	Yearly available (kt)
Forest wood residues	66	12.5	30	None	7748.023
Agricultural woody residues	61	10.8	40	Summer and winter	3882.567

Biomass can be co-fired by means of different technological options: blending biomass with coal (co-milling) before the reactor, separate injection and parallel co-firing in separate combustors and gasification with the subsequent co-combustion of the blend formed by syngas and coal. In this case study, co-milling has been chosen. Among the reported data from Section 2.2.1, the maximum amount of coal to be substituted in a plant without any efficiency penalty is 15% on a thermal basis. Therefore, the overall plant energy efficiency for only coal and blends of coal with biomass is merely one value, around 36% on a LHV_{ar} basis (Berndes *et al.*, 2010). The needed investment for plant modification to allow co-firing with liquid and solid biomass is 201€/kW_{th} (Basu *et al.*, 2011). The assumed operation and maintenance costs are 4% the investment

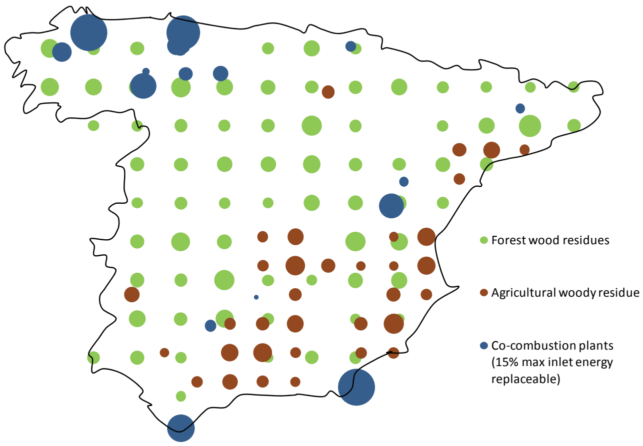

Figure 7.9: Location map of the feedstocks sites and the power plants, distinguishing between forest wood residues and agricultural woody residues. They are represented according to their relative GJ/yr production for sources, and according to their relative GJ/yr thermal input demand for power plants.

(Gómez *et al.*, 2010b). This chapter considers the complete group of coal combustion power plants existing in Spain[1]. See in Figure 7.9 the situation of those plants in the country, among the biomass sites identified. Note that the plants are represented according to their maximum 15% of inlet thermal power, which is susceptible to be replaced by biomass. See in Tables 7.14 and 7.15 the main characteristics of those power plants, ordered by Spanish regions, and the key features of the types of coal used (López-Vilariño *et al.*, 2003), respectively. Power and energy data come from 2008. The reported energy values do not correspond to the installed capacity but to the used capacity. Escatrón power plant, did not supply electricity to the grid during 2008. In order to establish the coal prices (Table 7.15), the four different types of coal have been divided into two big groups according to their origin: local and imported coal[2].

Concerning the biomass potential per year (Table 7.13) and coal power plants inlet power per year, the substitutive potential of biomass against coal is around 41%. This replacement is limited here to 15%, due to technological restrictions. Considering an electricity price in the power plants market of 0.05711 €/kWh[3], the total revenue of the power plants is 1934 M€/yr. The depreciation period is 10 years, since the plants are built-up before 2008, and according to Table 7.16, the minimum average life of a BSC unit is 10 years. The average working hours is 4000 h/yr, according to *Red Eléctrica de España*[4].

In the works by Rentizelas *et al.* (2009d) and Rentizelas *et al.* (2009c), a major issue concerning logistics expenses is biomass storage, specially when the resource availability is seasonal. Therefore, in order to guarantee a continuous provision of biomass, it is crucial to match the availability of each raw material, referred to as a

[1] This information is from www.ree.es.
[2] The prices are taken from www.enerclub.es.
[3] Price from www.cne.es for year 2008.
[4] www.ree.es.

Table 7.14: Thermal power plants in Spain. Data for 2008, from www.ree.es and López-Vilariño *et al.* (2003).

Model name	Name	Power (MW)	Energy (GWh)	Type of coal
m1	Puentes García Rodríguez	1468	5816	Coal 1
m2	Meirama	563	1618	Coal 1
m3	Aboño	916	4876	Coal 3
m4	Lada	513	710	Coal 3
m5	Soto de la Ribera	604	1417	Coal 3
m6	Narcea	595	826	Coal 3
m7	Anllares	365	263	Coal 3
m8	Compostilla	1171	2819	Coal 3
m9	La Robla	655	783	Coal 3
m10	Guardo	516	980	Coal 3
m11	Pasajes de San Juan	217	523	Coal 4
m12	Cercs	162	393	Coal 2
m13	Escatrón	80	0	Coal 2
m14	Teruel	1102	2717	Coal 2
m15	Escucha	159	416	Coal 2
m16	Litoral de Almería	1159	5804	Coal 4
m17	Los Barrios	568	3219	Coal 4
m18	Puertollano	221	98	Coal 3
m19	Puentenuevo	324	583	Coal 3
Total		11358	33861	

Table 7.15: Types of coal used. Data for 2008, from www.ree.es, www.enerclub.es and López-Vilariño *et al.* (2003).

	Type	Origin	LHV_{ar} (MJ/kg)	Cost (€/t)
Coal 1	Sub-bituminous 1	Local	12.57	80
Coal 2	Sub-bituminous 2	Local	17.81	80
Coal 3	Bituminous 1	Local	22.63	80
Coal 4	Bituminous 2	Imported	27.03	125

multi-source biomass problem, with the demand. Figure 7.10 provides the yearly profile of the forest wood residues and agricultural woody residues production[5], as well as power plants thermal demand[6]. In this figure it is appreciated that the demand of biomass to provide the 15% of the power plants thermal input is below the resources limit. The model will favour the use of the closest sites to power plants, diminishing transportation costs, with minimal restriction coming from the biomass availability. This reduces the impact of seasonality.

In the mathematical formulation, e corresponds to biomass generation sites, having 107 different states and m represents the power plants, therefore having 19 states. t, the model time period, is a year. Even if t is a year, the maximum storage period of biomass is considered to be two months. Figure 7.11 shows the different biomass combinations introduced into the mathematical model, implicitly representing biomass properties, which depend on the month of storage. The main change is the decrease on MC due to natural drying. B_0 is the biomass collected during the current month. B_1 corresponds to biomass stored during one month. Similarly, B_2 corresponds to biomass stored during two months. Biomass or biomass mixtures (B_{Dn}) that have

[5]Seasonal biomass availability according to Mr. Ignacio López, from Centre Tecnológic Forestal de Catalunya (CTFC), Spain

[6]Information from www.ree.es.

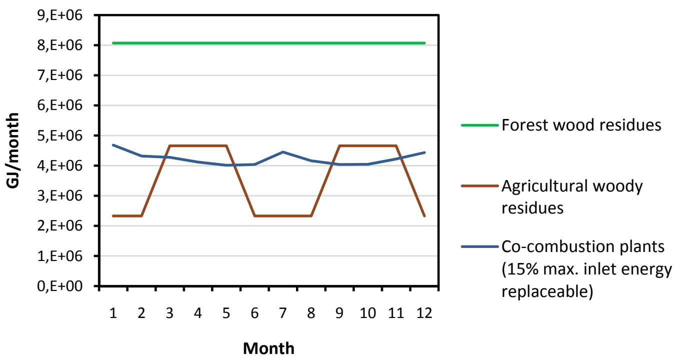

Figure 7.10: Seasonal biomass availability and power plants maximum demand.

already spent two months in storage are in red. Those biomass mixtures correspond to biomass of different combined collection months. Forest wood residues and agricultural woody residues are not merged.

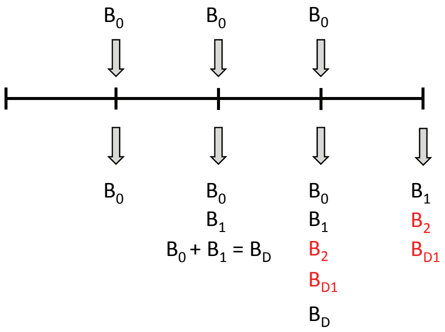

Figure 7.11: Biomass possible combinations during two months of storage.

Technologies used for pre-treatment

Biomass should be homogeneous and enhance its properties in the view of transportation, to be used as a sustainable commodity. For co-firing, biomass should mimic the properties of coal as far as possible. Figure 7.12 depicts the different pre-treatment processes considered in this case study, which are needed to obtain the desired biomass characteristics. Torrefied biomass (TOR), torrefied pellets (TOP), pellets (PEL) and bio-oil (OIL) or bioslurry (SLU) are the state-of-the-art techniques considered. Biomass storage can be done after harvesting/collection and/or after pre-treatment sites. Storage of raw biomass allows for the mixture of the same type of biomass, gathering it from diverse sites. The biomass properties, i.e. MC, DM, BD and LHV, are assumed to change in all the BSC echelons, except in processed biomass storage. Power plants only process pre-treated biomass, i.e. TOR, TOP, PEL, OIL and SLU. The selection of the biomass type principally influences the logistics costs and the investment, since the power produced by the plant must be preserved. The distances between biomass collection sites and power plants, as well as the demands, i.e. the percentages of coal thermal input replaced, are the main variables. Only restrictions of maximum MC are stated in the pre-treatment inlet streams, as indicated in Figure 7.12. Trucks, adapted to carry solids or liquids are in charge of biomass transportation.

The main issues at each pre-treatment site, storage and transportation, concerns MC, DM, LHV and BD variations, and are summarised here after. The reported percentages and proportions are used to linearly model the activities inside the mathematical program. The assumed capacities have been set according to literature data. Chipping and drying are mandatory for all the flows before entering the pre-treatment sites, since biomass has lower transportation costs after homogenisation. The assumed average working hours is 2400 h/yr.

- Chipping. A roll crusher is considered. This unit increases the BD of raw biomass through conversion into chips, to 240 kg/m^3. A loss of 2% of raw matter is assumed, homogeneously distributed among MC and DM (Hamelinck *et al.*, 2003). Therefore, the final percentages of humidity and dry matter are the same than the percentages from raw biomass. The capacity to be installed ranges between 10t/h and 80t/h.

- Drying. A rotatory drum dryer is considered. This element is used to decrease the MC of the inlet mixture to 15%, 10% or 5%, according to the pre-treatment unit requirement. Chipped biomass changes LHV, MC and DM content, according to the amount of evaporated water (Hamelinck *et al.*, 2005). The capacity to be installed is between 40 and 100 t/h.

- Torrefaction. This unit needs biomass at 15% MC. This operation considers a fixed bed reactor. Torrefied biomass contains 70% of its initial weight and 90% of the early energy content, both of them expressed on a daf basis. The remaining humidity is 6% at the inlet amount. The final BD is 230 kg/m^3, with mass and volume decreasing here (Uslu *et al.*, 2008). The capacity is between 10 MW and 160 MW of inlet energy content.

- Torrefaction and pelletisation. After torrefaction, pre-treated biomass is pelletised. The modelling of torrefaction as reported before is enlarged with the characterisation of pelletisation. TOP process increases the BD to 800 kg/m^3. MC decreases to 5% of the inlet biomass humidity (Uslu *et al.*, 2008). The capacity to be installed ranges 10 MW and 160 MW of inlet energy content.

- Pelletisation. This activity processes biomass with 10% MC. Bulk density is the main parameter that varies here: its final value is 575 kg/m^3. The remaining humidity is a 17% of the inlet value. This percentage is calculated using the data from Uslu *et al.* (2008). The energy loss is assumed to be 94%. The capacity to be installed ranges 10 MW and 160 MW of inlet energy content.

- Fast pyrolysis. This activity processes biomass with the lowest MC value, 5%. Bio-oil represents 73% of the initial weight and 66% of the inlet energy content on a daf basis. The remaining humidity is 64% the inlet value, since the yield of water produced is between 5%-15% on dry feed. The BD is increased to 1200 kg/m^3 (Uslu *et al.*, 2008; Magalhaes *et al.*, 2009). The capacity to be installed ranges 20 MW and 160 MW of inlet energy content.

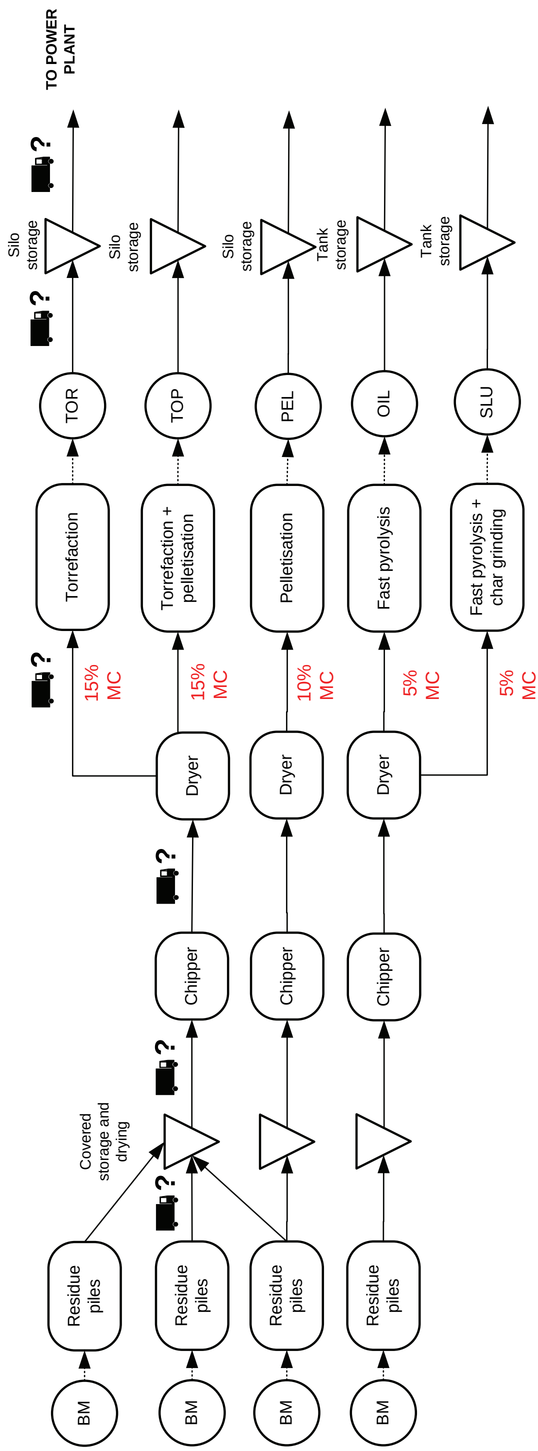

Figure 7.12: Pre-treatment activities network and MC inlet restrictions.

- Fast pyrolysis and char grinding. This pre-treatment is a modification of the previous one. The inlet MC is the same. The bioslurry is 74% of the initial weight and 92% of the inlet energy content on a daf basis, since it profits from the energy content in the produced char. The final MC is 53% the inlet humidity. The BD is 1200 kg/m^3 (Uslu *et al.*, 2008; Magalhaes *et al.*, 2009). This unit capacity ranges between 1t/h - 20 t/h.

- Storage. According to Rentizelas *et al.* (2009c), on-field storage reduces the cost but yields significant biomass matter losses. As indicated by Maciejewska *et al.* (2006), MC needs to be low (usually under 20%) to limit material losses under storage. The present case study considers open air covered storage for raw material. Covering relies on a paperboard to keep MC down. After a month of open-air covered storage, the resulting raw biomass has 2% less MC and 0.25% less DM. Storage in silos is considered for TOR, TOP and PEL. This choice causes a MC loss of 1.5% and a DM loss of 1.8% per month. Liquid biomass (OIL and SLU) are stored in tanks. In this case, MC and DM diminishes by 2% altogether. Storage in silos and tanks are modelled with no properties changes over the year, due to programming simplification purposes (Hamelinck *et al.*, 2003).

- Transportation. Inside and outside the collection site transportation can be distinguished (Yu *et al.*, 2009). In this case study, only the second type is considered. Raw and pre-treated biomass is transported to power plants by trucks. Trucks for any type of solid biomass can handle a maximum of 130 m^3. Trucks for liquid biomass allows a maximum of 33 m^3 (Hamelinck *et al.*, 2003). The distances are estimated as direct distances from the site to the power plant or to another site, expressed in km. The winding or tortuosity factor is assumed of 1.4 (Gómez *et al.*, 2010b; Yu *et al.*, 2009), representing the road network.

Figure 7.13 illustrates the abovementioned properties changes along the SC, for a stream of forest wood residues, starting from the inlet conditions described in Table 7.13. The process with the highest efficiency is torrefaction combined with pelletisation, followed by torrefaction, pelletisation, fast pyrolysis with char grinding and finally, fast pyrolysis. Fast pyrolysis yields products with the highest bulk density, and torrefied products and bioslurry have the highest energy densities.

The economic evaluation is based on estimations of investment and annual operation and maintenance (O&M) costs. The total capital requirement is spent only at the beginning of the project. This is calculated including economies of scale, where the specific investment cost decreases as the size of the plant increases. The scale factor is 0.7 (Uslu *et al.*, 2008; Yu *et al.*, 2009). Table 7.16 summarises the values used for costs estimation, including storage, transportation and utilities consumption. Investments are introduced into the MILP model by linear functions adjusted to the plant size. t_{input} corresponds to the tonnes of pre-processed biomass. Utilities, i.e. diesel and electricity prices are 1001.08 €/t[7] and 0.07181 €/kWh[8], respectively. The cheapest pre-treatment technology is fast pyrolysis, followed by pelletisation and torrefaction combined with pelletisation.

The possible sites chosen to allocate chipping, drying, torrefaction, torrefaction + pelletisation, pelletisation or fast-pyrolysis, and storage, correspond to the provision

[7] www.mityc.es
[8] www.cne.es

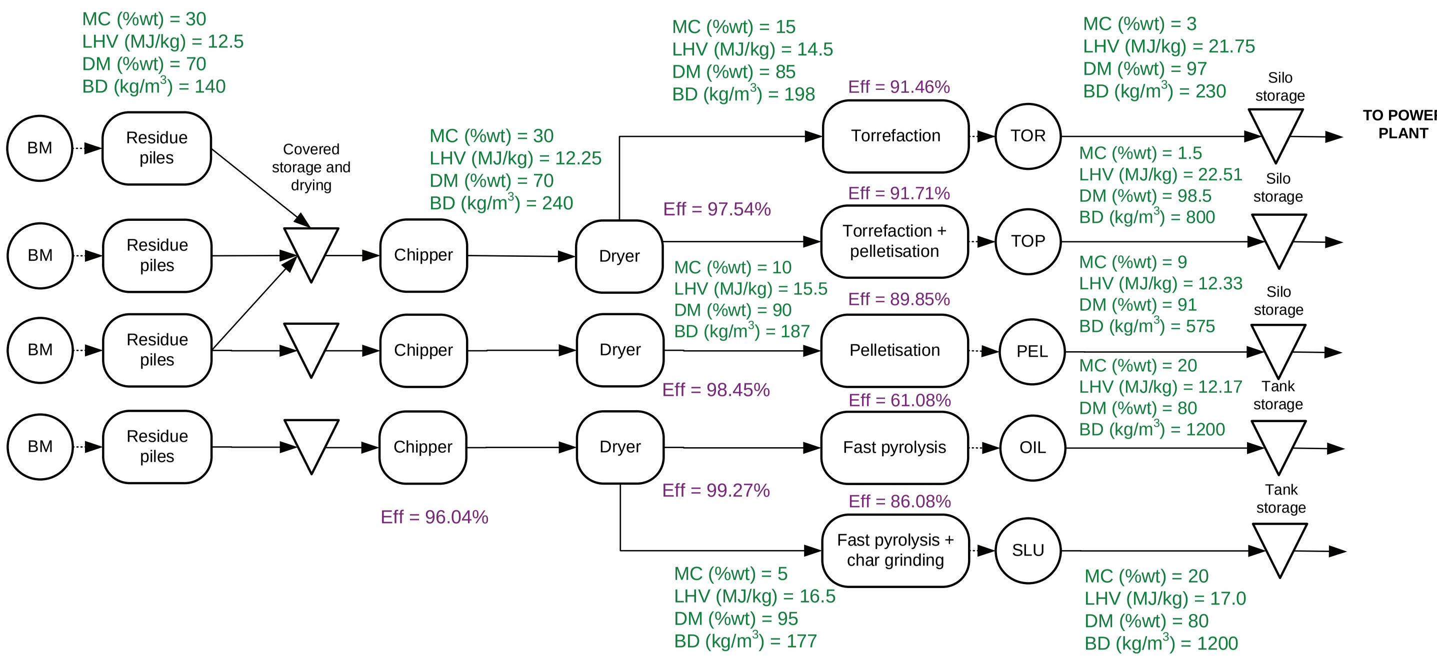

Figure 7.13: Technical comparison of the properties of a forest wood residue stream along the pre-treatment BSC for case study 2. LHV is in ar basis. Eff is defined in terms of LHV in ar basis.

Table 7.16: Economic parameters of pre-treatment and storage units and transportation. Data from Hamelinck *et al.* (2003), Uslu *et al.* (2008) and Magalhaes *et al.* (2009).

	Base scale	Base investment	O&M (% of investment)	Utility consumption	Lifetime (yr)
Chipping	80 t/h	0.8 M€	20	Bond law $0.15 \cdot t_{input}$ (kW)	15
Drying	100 t/h	7.2 M€	3	$0.06 \cdot t_{H_2Oev}$ (t diesel)	15
Torrefaction	40 $MW_{th_{in}}$	6.5 M€	5	92 kWh/t_{input}	10
Torrefaction + pelletisation	40 $MW_{th_{in}}$	7.8 M€	5	102 kWh/t_{input}	10
Pelletisation	40 $MW_{th_{in}}$	6.2 M€	5	129 kWh/t_{input}	10
Fast pyrolysis	40 $MW_{th_{in}}$	11 M€	4	75 kWh/t_{input}	25
Fast pyrolysis + char grinding	5 t/h	5.1 M€	5	95 kWh/t_{input}	25
Open air covered storage			0.6 €/m^3month		
Silo storage	5000 m^3	0.5M€	3		25
Tank storage	2272 m^3	1.2M€	3		25
Transportation solid			0.5 €/m^3 0.85 €/km		
Transportation liquid			0.5 €/m^3 1.24 €/km		

sites that produce higher amounts of biomass, to avoid expenses on transportation. Those sites are restricted to a minimum production around 1100000 GJ/yr and are shown in Figure 7.14.

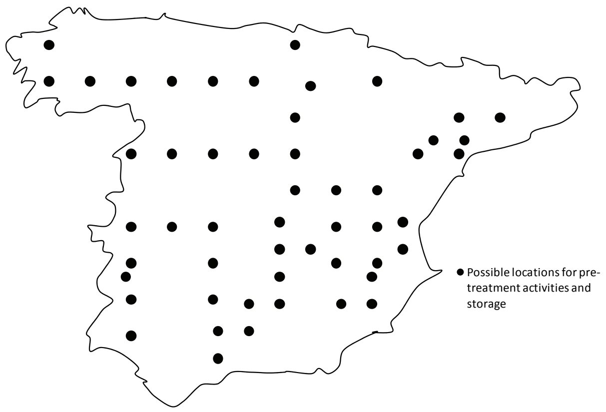

Figure 7.14: Location map of the potential pre-treatment and storage sites.

The described approach for co-combustion in Spain, counts with various parameters to determine its performance: biomass collection window, raw material costs, equipment capacity, capital and O&M costs, utilities consumption (power, diesel), transportation distance and capacity, final conversion efficiency and biomass characteristics at every SC echelon. The network components will be selected, but there is a limited degree of freedom in the alternatives selection, since in this case, drying only processes chipped biomass, and torrefaction, pelletisation and fast pyrolysis have a maximum value for inlet stream MC.

The mathematical model does not include flexible units (Section 7.3). Forest wood residues and agricultural woody residues have independent routes. In relation to model parameters, s, as biomass states, according to the number of biomass wastes considered and the number of possible products, has a value of 100. This arises from the assumption of two possible months in open air storage, and its subsequent biomass mixtures. As t is a year for the following results, the s used, only correspond to raw material processed along the different echelons. The number of tasks i is 98 by combining materials and activities, and the number of equipments j is 11, according to the different technologies considered for pre-treatment and transportation.

Objective functions

The objective functions for optimisation integrate economic and environmental aspects. Those are related to the reference scenario with only coal as raw material. The objectives functions are therefore the increase of investment, at a constant level of incomes, since the produced electricity is the same, and the reduction on environmental impact, attributed to the proportion of coal replaced by biomass. Both objective functions should be maximised.

Similarly to the process developed for the previous case study, the environmental impact associated to the BSC, LCI values are retrieved from Ecoinvent-V1.3 (2006) database using B.V. (2004). They are directly converted into Impact 2002+ mid-point indicators (LCIA step). The amount of pts associated to the biomass production without transportation are in Table 7.5: forest wood residues and almond tree prunnings, the latter chosen as representatives of agricultural woody residues, are used. Table 7.17 lists the impact associated to the production of coal for the reference scenario. Here, the impact of electricity generation from coal, is considered as a whole, including transportation impacts. Table 7.17 summarises the considered impacts associated to the SC tasks, including transportation for solid and liquid biomass. The impact associated to each unit is proportional to utilities consumption. The pts are given by tonnes of diesel consumed or GJ of spent electricity. The impact of electricity production by means of gasification (case study 1) is less than the amount of points generated by combustion. The last column correspond to the generation of electricity from biomass combustion. Global warming estimation depends on the inlet flowrate of carbon that finally produce CO_2 emissions.

The project is evaluated along a planning horizon of 10 years, considering yearly planning decisions. The model is implemented in GAMS. The formulation of the SC-LCA model leads to a MILP with 18019 equations, 694337 variables. It takes a maximum of 6000 CPU seconds to reach a solution integrality gap of 2.5% on a 2.0 GHz Intel Core 2 Duo computer using the MIP solver of CPLEX 9.0.

7.5.1 Results

The results performed correspond to the two ends of the Pareto frontier. This section is divided into three parts, according to the overall share of inlet thermal power of coal replaced by biomass: 5%, 10% and 15%, corresponding this last one to the maximum biomass share without incurring in technological problems and exempt of power plant efficiency penalty. These values are introduced into the model as constraints. The

Table 7.17: Environmental impacts in terms of Impact 2002+ metric, associated to SC tasks (Ecoinvent-V1.3, 2006), for case study 2.

Mid-point categories	Coal supply (pts/t)	Electricity at power plant from coal (pts/GJ)	Diesel (pts/t)	Transport solid (pts/tkm)	Transport liquid (pts/tkm)	Electricity generation (pts/GJ)
Carcinogens	$3.21 \cdot 10^{-4}$	$2.26 \cdot 10^{-4}$	$2.48 \cdot 10^{-3}$	$4.56 \cdot 10^{-7}$	$3.45 \cdot 10^{-7}$	0
Non-Carcinogens	$4.87 \cdot 10^{-4}$	$1.81 \cdot 10^{-3}$	$2.86 \cdot 10^{-3}$	$6.87 \cdot 10^{-7}$	$4.54 \cdot 10^{-7}$	0
Respiratory inorganics	$3.31 \cdot 10^{-2}$	$4.56 \cdot 10^{-2}$	$7.37 \cdot 10^{-2}$	$2.01 \cdot 10^{-5}$	$7.54 \cdot 10^{-6}$	$2.44 \cdot 10^{-3}$
Ionizing radiation	$1.18 \cdot 10^{-4}$	$1.45 \cdot 10^{-5}$	$2.19 \cdot 10^{-4}$	$4.80 \cdot 10^{-8}$	$2.95 \cdot 10^{-8}$	0
Ozone layer depletion	$1.67 \cdot 10^{-6}$	$2.25 \cdot 10^{-7}$	$6.87 \cdot 10^{-5}$	$3.94 \cdot 10^{-9}$	$2.53 \cdot 10^{-9}$	0
Respiratory organics	$2.99 \cdot 10^{-5}$	$4.76 \cdot 10^{-6}$	$2.51 \cdot 10^{-4}$	$3.18 \cdot 10^{-8}$	$2.30 \cdot 10^{-8}$	0
Aquatic ecotoxicity	$3.39 \cdot 10^{-4}$	$5.00 \cdot 10^{-5}$	$5.14 \cdot 10^{-4}$	$3.80 \cdot 10^{-8}$	$2.37 \cdot 10^{-8}$	0
Terrestrial ecotoxicity	$1.35 \cdot 10^{-2}$	$1.74 \cdot 10^{-3}$	$1.77 \cdot 10^{-2}$	$4.13 \cdot 10^{-6}$	$2.47 \cdot 10^{-6}$	0
Terrestrial acid/nutri	$7.90 \cdot 10^{-4}$	$6.68 \cdot 10^{-4}$	$1.09 \cdot 10^{-3}$	$5.11 \cdot 10^{-7}$	$1.66 \cdot 10^{-7}$	$8.07 \cdot 10^{-5}$
Land occupation	$7.80 \cdot 10^{-4}$	$9.63 \cdot 10^{-5}$	$3.44 \cdot 10^{-4}$	$1.24 \cdot 10^{-7}$	$6.58 \cdot 10^{-8}$	0
Aquatic acidification	0	0	0	0	0	0
Aquatic eutrophication	0	0	0	0	0	0
Global warming	$1.81 \cdot 10^{-2}$	$2.92 \cdot 10^{-2}$	$4.94 \cdot 10^{-2}$	$1.65 \cdot 10^{-5}$	$1.02 \cdot 10^{-5}$	0.101 pts/tCO_2
Non-renewable energy	$1.87 \cdot 10^{-1}$	$2.21 \cdot 10^{-2}$	$3.60 \cdot 10^{-1}$	$1.83 \cdot 10^{-5}$	$1.17 \cdot 10^{-5}$	0
Mineral extraction	$7.74 \cdot 10^{-6}$	$1.35 \cdot 10^{-6}$	$1.80 \cdot 10^{-5}$	$9.31 \cdot 10^{-9}$	$7.42 \cdot 10^{-9}$	0

resolution of the present case study relies on the mathematical formulation described in section 7.3.

Replacement by biomass up to 5% of coal

Figure 7.15 and Tables 7.18 and 7.19 provide the BSC network that *maximises the economic criteria*. Figure 7.15 depicts the relative GJ/yr of biomass used from each production site and the replaced thermal potential. Tables 7.18 and 7.19 describe the connections among biomass sources, pre-treatment sites and power plants, by specifying the amount of kt of biomass used and the amount of GJ replaced, per site. Moreover, Table 7.18 indicates the percentage of biomass used from the overall biomass production per location. Figure 7.16 and Tables 7.20 and 7.21, describe in an analogous way the BSC network that *maximises the environmental criteria*.

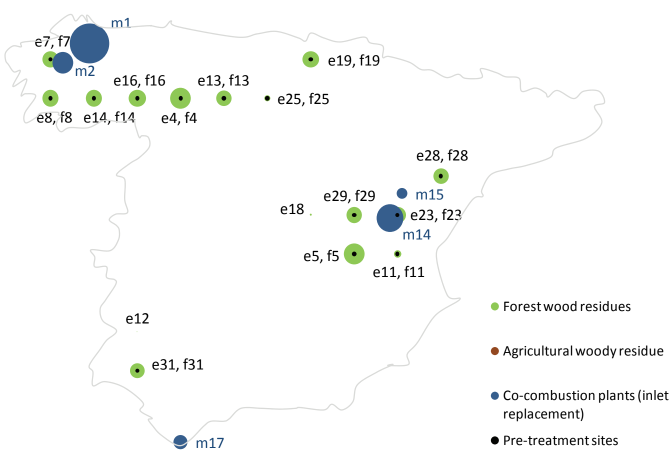

Figure 7.15: Optimum economic network configuration for replacement by biomass up to 5% thermal input of coal.

The optimum configuration for the economic criteria substitutes coal in 5 of the 19 Spanish power plants. It uses 16 biomass generation points, and 15 pre-treatment locations. Only 2 pre-treatment sites are not at the same biomass generation place. More than 70% of the biomass sites use more than 50% of the resource capacity. Among this 70%, 75% use more than 80% of the resource capacity. The proposed BSC network is placed in three regions: north-west, middle-east and south of Spain, the latter being the smallest. Power plants in north-west area, $m1$ and $m2$, are the two closest plants of the district, $m1$ has the highest power capacity of the country, as shown in Table 7.14. The selected biomass sourcing locations are placed close to the final consumption points.

The optimum configuration in the view of the environmental criterion differs from the economic optimum network. In the former chain, the most favoured area is placed in the middle and south-east of the country. The selected biomass sourcing locations are also placed close to the power plants. This case contemplates the use of 18 biomass sourcing places and 17 pre-processing spots. Here, 6 pre-treatment sites are placed in

Table 7.18: Sites connection (between biomass sourcing–pre-treatment sites) for the optimum economic network configuration for 5% thermal input of coal replacement.

Biomass site	kt/yr consumed	% total production	Pre-treatment site
e4	192.00	94.44	f4
e5	192.00		f5
e5	7.77	100.00	f29
e7	118.06	68.37	f7
e8	118.06	68.67	f8
e11	25.67	17.01	f11
e12	0.18	0.12	f31
e13	108.00	76.14	f13
e14	118.06	83.54	f14
e16	131.79	93.69	f16
e18	1.84	1.35	f29
e19	118.06	88.05	f19
e23	119.10	100.00	f23
e25	14.45	12.74	f25
e28	107.75	100.00	f28
e29	107.41	100.00	f29
e31	99.43	99.99	f31

Table 7.19: Sites connection (between pre-treatment sites–power plants) for the optimum economic network configuration for 5% thermal input of coal replacement.

Pre-treatment site	GJ/yr replaced	Power plant
f4	1939.43	m1
f5	1267.75	m1
f7	101.68	m1
f13	1581.99	m1
f14	1264.34	m1
f16	1264.34	m1
f19	1267.75	m1
f29	36.70	m1
f7	1162.66	m2
f8	1264.34	m2
f5	1038.80	m14
f23	1264.34	m14
f28	529.94	m14
f29	1227.64	m14
f28	624.00	m15
f5	27.99	m17
f31	1066.79	m17

different spots than biomass sourcing places. Biomass substitution percentage is the highest in $m16$, which is one of the largest power plants in the country.

The following paragraphs compare the two solutions provided by optimisation in the view of economic and environmental criteria. Table 7.22 shows the percentage of thermal power replaced by biomass. Plants $m2$, $m14$ and $m17$ are used in both optimum configurations. Figure 7.17 presents the breakdown of investment and annual costs. The investment for the optimum BSC economic configuration is 549.16 M€, while this is 550.24 M€ for the optimum BSC environmental configuration, i.e. only 0.2% higher. In the first scenario, the largest contribution to the investment share comes from power plants adaptation. The pre-processing biomass units that perform torrefaction (TOR) and torrefaction combined with pelletisation (TOP) are the most efficient units, according to Figure 7.13. These are the selected units by the model. The

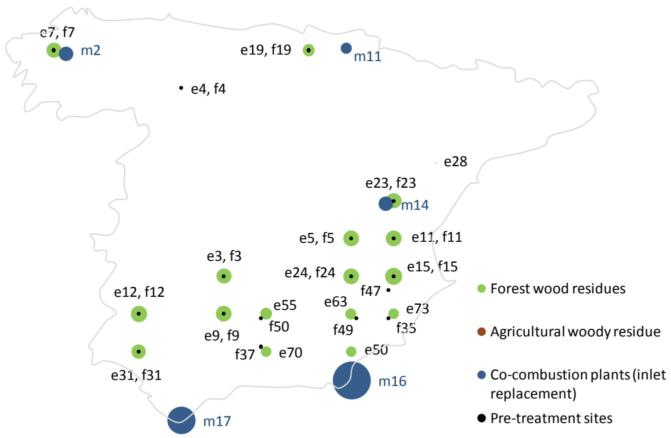

Figure 7.16: Optimum environmental network configuration for replacement by biomass up to 5% thermal input of coal.

Table 7.20: Sites connection (between biomass sourcing–pre-treatment sites) for the optimum environmental network configuration for 5% thermal input of coal replacement.

Biomass site	kt/yr consumed	% total production	Pre-treatment site
e3	113.09	53.97	f3
e4	7.37	3.62	f4
e5	117.92	59.03	f5
e7	117.92	68.29	f7
e9	117.92	72.28	f9
e11	117.92	78.15	f11
e12	136.40	95.03	f12
e15	141.32	100.00	f15
e19	73.24	54.62	f19
e23	117.92	99.00	f23
e24	118.72	100.00	f24
e28	0.59	0.55	f28
e31	99.43	100.00	f31
e50	1.63		f35
e50	54.57	69.55	f49
e55	70.88	100.00	f50
e63	63.34	100.00	f49
e70	56.34	100.00	f37
e73	54.04	100.00	f35

Table 7.21: Sites connection (between pre-treatment sites–power plants) for the optimum environmental network configuration for 5% thermal input of coal replacement.

Pre-treatment site	GJ/yr produced	Power plant
f7	1263.10	m2
f4	78.94	m9
f19	784.50	m11
f23	1263.10	m14
f28	6.36	m15
f3	172.18	m16
f5	1263.10	m16
f11	1263.10	m16
f15	1263.10	m16
f24	1263.10	m16
f35	605.38	m16
f37	603.47	m16
f47	250.23	m16
f49	1263.10	m16
f50	759.25	m16
f3	1039.21	m17
f9	1263.10	m17
f12	1263.10	m17
f31	1263.10	m17

Table 7.22: Thermal input replacement per plant for the optimised networks, for an overal 5% thermal input replacement.

Power plant	% thermal input replaced
Economic optimisation	
m1	15.00
m2	15.00
m14	14.95
m15	15.00
m17	3.40
Environmental optimisation	
m2	7.81
m11	15.00
m14	4.65
m16	15.00
m17	15.00

investment share of the two items together results in a higher investment contribution than the power plants. A stricking difference among the two optimum scenarios, is the exclusive use of TOR in the environmentally-friendly one. Here, the largest investment contribution comes from this unit alone (TOR), followed by the power plants adaptation. In both cases, chipping has the cheapest contribution, followed by drying. The BSC economic optimisation network requires 15.2 M€ for transport, 24.7 M€ for utilities and 25.1 M€ for O&M costs, which are the largest. In the BSC environmental optimum configuration, those costs are 19.4 M€, 33.2 M€ and 24.9 M€, respectively. It must be emphasized that the storage activity, with the subsequent O&M costs, only appears in the second scenario, diminishing drying costs. The highest fraction is from utilities consumption. The abovementioned shares for annual costs show that torrefaction without pelletisation is the preferred pre-treatment option, despite its slightly lower efficiency.

Looking at the environmental impacts, Table 7.23 compares them on the basis of Impact 2002+ pts for each BSC optimum network, and its homologous chain

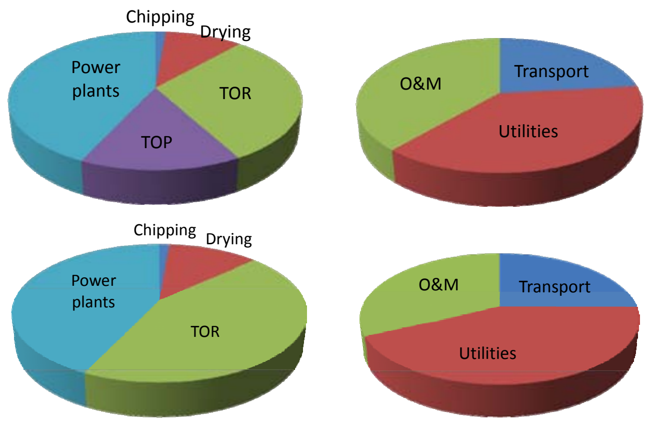

Figure 7.17: Breakdown of costs for economic and environmental optimised networks (up and down, respectively), for 5% thermal input replacement. Left side: investment share. Right side: annual costs share.

Table 7.23: Environmental impacts arising from economic and environmental optimisations, in Impact 2002+pts, for an overall 5% thermal input replacement. Impacts for biomass used and coal replaced are characterised (results per year).

End-point impact category	Economic optimisation	Environmental optimisation
Biomass		
Human health	40146.80	38376.27
Ecosystem quality	5436.43	5302.17
Climate change	291723.15	290809.57
Resources	19513.68	17710.74
Impact 2002+	356820.07	352198.75
Coal replaced		
Human health	291009.33	297744.66
Ecosystem quality	15783.18	18368.60
Climate change	178912.43	187970.26
Resources	135858.97	146565.57
Impact 2002+	621563.90	650649.08

using coal, i.e. the replaced amount of coal. The used power plants are different into each optimum scenario, so do the coal SC impact, being highest the impact of coal for the configuration depicted in the environmental optimisation scenario. The BSC environmental optimum network has an impact of 352199 pts, which is 1.3% less than the economic optimum one. In the case of the environmental optimum coal-equivalent network, the impact is of 650649 pts, which is 4.5% larger than the impact of the coal SC associated to the economic optimum BSC configuration. The most contributing impact categories are climate change for biomass, and human health followed by climate change for coal. Figure 7.18 depicts the environmental impacts resulting from the different BSC activities. Due to the biomass dispersion along the country, transportation impact is insignificant when compared to the other echelons. Electricity generation activity by biomass combustion predominantly contributes to the overall impact in both scenarios, followed by pre-treatment activities.

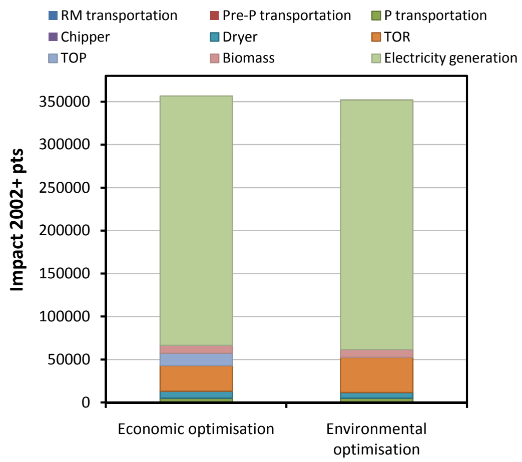

Figure 7.18: Distribution of environmental impacts for each optimisation solution (5% thermal input replacement), according to the different SC activities (results per year).

Replacement by biomass up to 10% of coal

In an analogous way as in the previous case, Figures 7.19 and 7.20 show the two optimal BSC's networks configurations according to the two selected criteria. Tables 7.24 to 7.27 describe the link between the different sites placed in the two figures, by means of mass and energy flows.

The optimum configuration for the economic criteria fulfills the demand of 12 over the 19 Spanish power plants. It uses 28 biomass generation points, and 25 pre-treatment locations. The used biomass sourcing locations exploited in the BSC is around 80%. The proposed BSC network is well dispersed along the country. The highest share of thermal input replaced is in the north of Spain.

The optimum configuration for the environmental criteria differs from the previous optimum network in terms of number of sites used throughout the country. Nevertheless, the selected power plants are the same, even though the share of thermal input substituted is different in 2 of the 12 plants selected. It uses 30 biomass generation points, and 25 pre-treatment locations.

Table 7.28 lists the used power plants and the thermal power replaced in both solutions. Plants $m10$ and $m19$ have different percentages in both scenarios. Figure 7.21 presents the different items contribution to investment and annual costs. The investment for the BSC optimum economic network is 1111.5 M€, while this is 0.28% lower for the environemental one. The largest contribution arises from the power plant investment. TOR and TOP are present in both situations. The economic network invests more in TOP, while the environmentally-friendly version invests equally among TOP and TOR. As in the previous scenario, the pre-treatment units investment is higher than the power plant's investment. In this case, intermediate storage is only considered for the economic optimisation network. The share of annual costs is fairly similar for both optimum networks. The main difference concerns transportation costs. The overall annual costs for the BSC economic network is 130.5 M€, with utilities consumption constituting the highest share. The costs for the other optimum

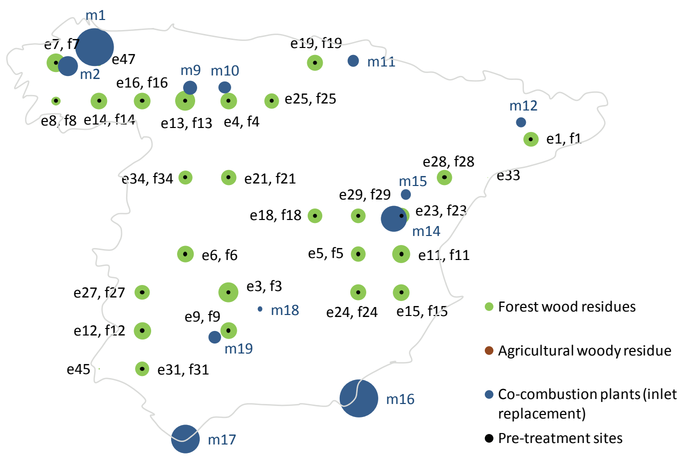

Figure 7.19: Optimum economic network configuration for replacement by biomass up to 10% thermal input of coal.

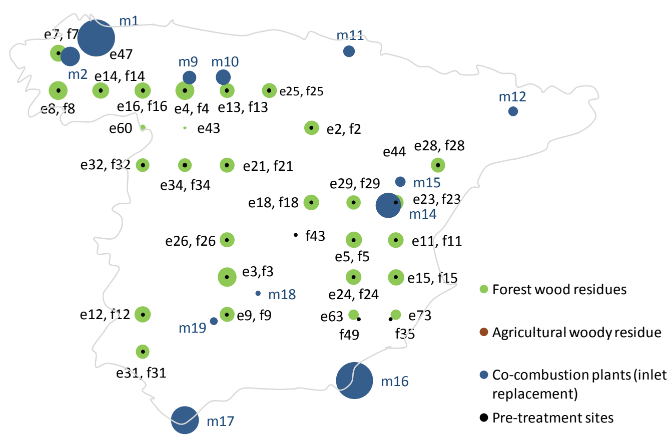

Figure 7.20: Optimum environmental network configuration for replacement by biomass up to 10% thermal input of coal.

configuration are 1% higher.

Table 7.29 provides the environmental analysis by comparing Impact 2002+ pts for each BSC optimum solution and the correspondent coal-based SC. The economic optimisation network results in 717070 pts. The environmental optimised system is only 0.18% lower. The associated coal-based SC impacts are very similar for both configurations, since they differ by 0.17%, the impact of the environmental configuration being slightly higher. As in the previous case, the most important category for biomass and coal are climate change and human health, respectively. Figure 7.22 represents the environmental impacts associated to the different SC activities. Electricity generation activity from biomass combustion contributes the most to the overall impact of both scenarios. Pre-treatment activities follow. The main

Table 7.24: Sites connection (between biomass sourcing–pre-treatment sites) for the optimum economic network configuration for 10% thermal input of coal replacement.

Biomass site	kt/yr consumed	% total production	Pre-treatment site
e1	108.00	42.68	f1
e3	192.00	91.62	f3
e4	192.00	94.44	f4
e5	108.00		f5
e5	0.59	54.36	f29
e6	136.00	74.21	f6
e7	172.67	100.00	f7
e8	39.73	23.11	f8
e9	136.00	83.36	f9
e11	150.88	100.00	f11
e12	136.00		f12
e12	7.54	100.00	f31
e13	136.00	95.88	f13
e14	138.06	97.70	f14
e15	132.87	94.02	f15
e16	136.00	96.68	f16
e18	108.00	79.16	f18
e19	128.12	95.55	f19
e21	108.00		f21
e21	6.36	89.45	f34
e23	119.10	100.00	f23
e24	118.72	100.00	f24
e25	108.00	95.25	f25
e27	108.00	98.47	f27
e28	107.75	100.00	f28
e29	107.41	100.00	f29
e31	99.43	100.00	f31
e33	0.25	0.26	f28
e34	95.28	100.00	f34
e45	1.03	1.19	f31
e47	19.33	22.87	f7

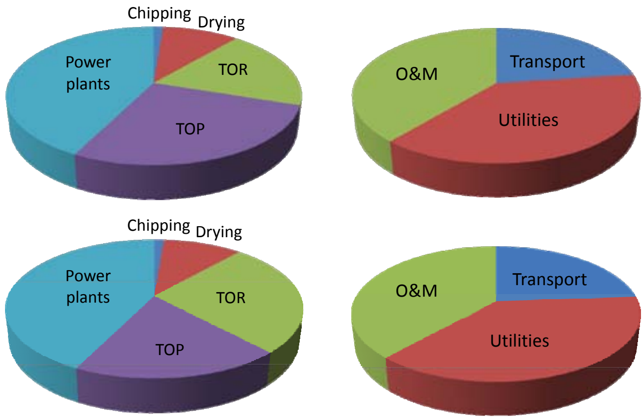

Figure 7.21: Breakdown of costs for economic and environmental optimised networks (up and down, respectively), for 10% thermal input replacement. Left side: investment share. Right side: annual costs share.

Table 7.25: Sites connection (between pre-treatment sites–power plants) for the optimum economic network configuration for 10% thermal input of coal replacement.

Pre-treatment site	GJ/yr replaced	Power plant
f4	1159.51	m1
f6	203.96	m1
f7	105.09	m1
f13	1267.75	m1
f14	1264.34	m1
f16	1544.33	m1
f21	1267.75	m1
f25	841.59	m1
f34	1069.67	m1
f7	2427.00	m2
f4	1174.50	m9
f19	479.84	m10
f25	426.16	m10
f19	784.50	m11
f1	589.50	m12
f1	40.60	m14
f11	1264.34	m14
f18	1264.34	m14
f23	241.87	m14
f29	1264.34	m14
f1	624.00	m15
f3	1313.04	m16
f5	1267.75	m16
f6	31.73	m16
f9	1267.75	m16
f15	1267.75	m16
f23	1025.88	m16
f24	1264.34	m16
f28	1267.75	m16
f6	1032.06	m17
f12	1264.34	m17
f27	1267.75	m17
f31	1264.34	m17
f3	147.00	m18
f3	874.50	m19

share difference is on TOR and TOP impacts between the two optimum systems.

The two networks for 10% of coal replacement by biomass are more similar in all the analysed aspects than the two networks for 5% of coal replacement.

Replacement by biomass up to 15% of coal

In this case, the scenarios for both criteria of optimisation result in a unique network. Analogously to the preceding cases, the map and the links among the sites are presented in Figure 7.23 and Tables 7.30 and 7.31. In this scenario, the maximum replacement of the thermal inlet potential (15%) is enforced in all power plants. The optimum configuration counts with 42 biomass collection sites and 39 pre-treatment locations. Only 7 pre-treatment units are placed away from biomass collection points. In average, 90% of the biomass production sites are used in this network. Comparing with the total number of biomass disponibility (see Figure 7.9), 58% corresponds to forest wood residues sites. Agricultural woody residues are not needed for this maximum thermal share substitution. Therefore, residual biomass remains unused and can serve for other purposes.

Figure 7.24 shows the investment share with power plants being the main item, followed by TOP and TOR. The overall investment for this thermal share is 1640

Table 7.26: Sites connection (between biomass sourcing–pre-treatment sites) for the optimum environmental network configuration for 10% thermal input of coal replacement.

Biomass site	kt/yr consumed	% total production	Pre-treatment site
e2	108.00	50.27	f2
e3	186.56	89.03	f3
e4	180.78	88.92	f4
e5	136.00	68.08	f5
e7	136.00		f7
e7	6.80	82.71	f8
e8	171.93	100.00	f8
e9	118.06	72.37	f9
e11	122.69	81.32	f11
e12	136.00		f12
e12	0.68	95.23	f31
e13	118.06	83.24	f13
e14	141.32	100.00	f14
e15	132.51	93.77	f15
e16	136.00	96.68	f16
e18	120.48	88.30	f18
e21	108.00	84.48	f21
e23	119.10	100.00	f23
e24	118.72	100.00	f24
e25	108.00	95.25	f25
e26	112.28	100.00	f26
e28	107.75	100.00	f28
e29	107.41	100.00	f29
e31	99.43	100.00	f31
e32	99.04	100.00	f32
e34	95.28	100.00	f34
e43	4.33	4.99	f34
e44	0.25	0.29	f28
e47	5.62	6.65	f14
e60	19.02	29.10	f32
e63	53.96	85.19	f35
e73	54.04	100.00	f35

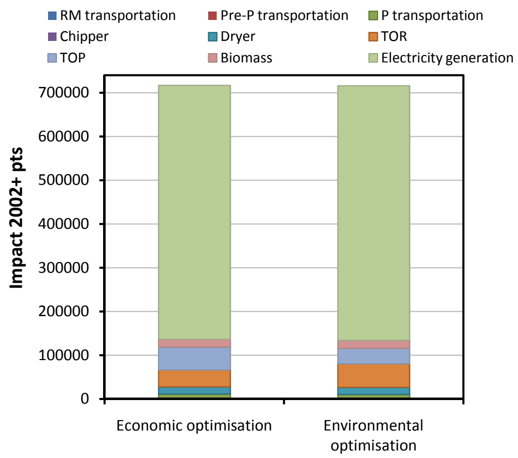

Figure 7.22: Distribution of environmental impacts for each optimisation solution (10% thermal input replacement), according to the different SC activities (results per year).

Table 7.27: Sites connection (between pre-treatment sites–power plants) for the optimum environmental network configuration for 10% thermal input of coal replacement.

Pre-treatment site	GJ/yr produced	Power plant
f4	763.34	m1
f7	101.68	m1
f8	673.49	m1
f14	1939.43	m1
f16	1264.34	m1
f21	577.50	m1
f25	1069.67	m1
f32	1267.75	m1
f34	1066.79	m1
f7	1162.66	m2
f8	1264.34	m2
f4	1174.50	m9
f2	183.38	m10
f13	1264.34	m10
f2	784.50	m11
f28	589.50	m12
f2	278.56	m14
f18	1264.34	m14
f23	1264.34	m14
f28	3.91	m14
f29	1264.34	m14
f28	624.00	m15
f3	369.02	m16
f5	1267.75	m16
f11	1267.75	m16
f15	1264.34	m16
f21	582.23	m16
f24	1264.34	m16
f26	1267.75	m16
f35	1264.34	m16
f43	79.23	m16
f49	79.23	m16
f3	1032.06	m17
f9	1264.34	m17
f12	1267.75	m17
f31	1264.34	m17
f3	147.00	m18
f3	391.36	m19

Table 7.28: Thermal input replacement per plant for the optimised networks, for an overall 10% thermal input replacement.

Power plant	% thermal input replaced
Economic optimisation	
m1	15.00
m2	15.00
m9	15.00
m10	9.24
m11	15.00
m12	15.00
m14	15.00
m15	15.00
m16	15.00
m17	15.00
m18	15.00
m19	15.00
Environmental optimisation	
m1	15.00
m2	15.00
m9	15.00
m10	14.77
m11	15.00
m12	15.00
m14	15.00
m15	15.00
m16	15.00
m17	15.00
m18	15.00
m19	6.71

Table 7.29: Environmental impacts arising from economic and environmental optimisations, in Impact 2002+pts, for an overall 10% thermal input replacement. Impacts for biomass used and coal replaced are characterised (results per year).

End-point impact category	Economic optimisation	Environmental optimisation
Biomass		
Human health	81749.35	80839.30
Ecosystem quality	11053.81	10939.42
Climate change	584204.93	584657.87
Resources	40062.22	39374.57
Impact 2002+	717070.31	715811.16
Coal replaced		
Human health	589535.19	590539.56
Ecosystem quality	34008.32	34062.14
Climate change	366954.29	367570.37
Resources	282145.41	282611.85
Impact 2002+	1272643.21	1274783.91

Table 7.30: Sites connection (between biomass sourcing–pre-treatment sites) for the optimum network configuration for 15% thermal input of coal replacement.

Biomass site	kt/yr consumed	% total production	Pre-treatment site
e1	55.05	21.75	f1
e2	195.92	91.20	f2
e3	171.43	81.81	f3
e4	192.00	94.44	f4
e5	180.78	90.49	f5
e6	146.94	80.18	f6
e7	172.67	100.00	f7
e8	171.93	100.00	f8
e9	136.00	83.36	f9
e10	122.45	76.04	f10
e11	122.45	81.16	f11
e12	143.54	100.00	f12
e13	141.84	100.00	f13
e14	141.32	100.00	f14
e15	122.45		f15
e15	18.87	100.00	f47
e16	140.66	100.00	f16
e17	136.00	98.19	f17
e18	118.06	86.53	f18
e19	134.08	100.00	f19
e21	127.85	100.00	f21
e22	119.44	100.00	f22
e23	118.06	99.12	f23
e24	118.72	100.00	f24
e25	108.00	95.25	f25
e26	108.96	97.05	f26
e27	108.00	98.47	f27
e28	95.30	88.44	f28
e29	107.41	100.00	f29
e30	104.16	100.00	f30
e31	99.43	100.00	f31
e32	99.04	100.00	f32
e34	95.28	100.00	f34
e38	11.95	13.12	f51
e46	86.01	100.00	f51
e47	19.33		f7
e47	42.54		f8
e47	22.68	77.13	f14
e50	13.80	17.07	f49
e55	70.88	100.00	f50
e62	63.79	100.00	f8
e63	63.34	100.00	f49
e70	56.34	100.00	f37
e71	56.26	100.00	f52
e73	54.04	100.00	f35

Table 7.31: Sites connection (between pre-treatment sites–power plants) for the optimum network configuration for 15% thermal input of coal replacement.

Pre-treatment site	GJ/yr produced	Power plant
f6	1267.75	m1
f7	2056.20	m1
f8	553.03	m1
f14	1953.26	m1
f16	47.14	m1
f27	664.59	m1
f30	1118.53	m1
f32	1063.49	m1
f8	2427.00	m2
f2	2103.82	m3
f10	1029.66	m3
f17	673.79	m3
f19	1439.36	m3
f25	1015.45	m3
f51	1051.91	m3
f10	238.09	m4
f13	47.14	m4
f18	779.77	m4
f4	1002.19	m5
f21	606.58	m5
f22	516.73	m5
f18	487.98	m6
f22	751.02	m6
f4	89.84	m7
f21	304.66	m7
f6	309.28	m8
f16	1264.34	m8
f21	461.60	m8
f26	1170.09	m8
f34	1023.18	m8
f4	1174.50	m9
f10	47.01	m10
f13	1264.34	m10
f22	14.75	m10
f25	143.90	m10
f17	784.50	m11
f1	589.50	m12
f5	1264.34	m14
f23	1264.34	m14
f28	396.56	m14
f29	1150.25	m14
f28	624.00	m15
f3	550.38	m16
f5	673.49	m16
f11	1314.89	m16
f15	1314.76	m16
f24	1274.87	m16
f35	578.71	m16
f37	604.96	m16
f47	202.60	m16
f49	826.12	m16
f50	761.12	m16
f52	604.08	m16
f3	717.37	m17
f9	1009.24	m17
f12	1540.59	m17
f27	495.14	m17
f31	1066.16	m17
f3	147.00	m18
f3	424.55	m19
f9	449.95	m19

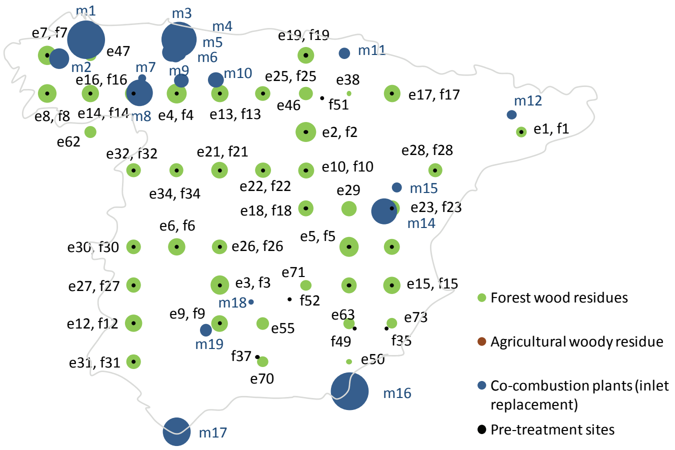

Figure 7.23: Optimum network configuration for replacement by biomass up to 15% thermal input of coal.

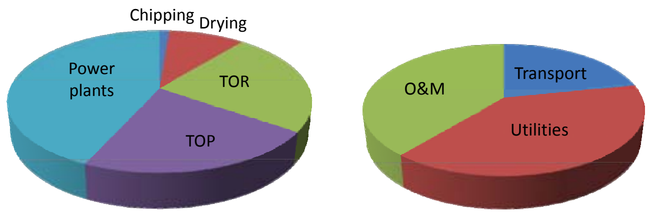

Figure 7.24: Breakdown of costs for the optimised network, for 15% thermal input replacement. Left side: investment share. Right side: annual costs share.

M€. Annual costs are very similar to the previous situations: utilities contribute predominantly. Overall annual costs are 191.6 M€. No intermediate storage is contemplated.

Table 7.32 and in Figure 7.25 provide the results based on the environmental criterion. The BSC network counts 1075470 Impact 2002+ pts. The coal-based SC is 75% higher. Again, electricity generation is the most influencing SC echelon, followed by TOP and TOR.

Scenarios results comparison

Table 7.33 lists the values of the objective functions for all the scenarios. The discrepancy between the three optimum configurations diminishes as the share of thermal input increases. Table 7.34 compiles the percentage extracted from the ratio among the difference of NPV's and the calculated amount of revenues associated to the complete park of power plants, within a period of 10 years (19338 M€). This expresses the theoretical increase of the electricity price or the potential subsidy required to face a BSC for co-combustion. The value ranges from 5.84% to 20.25%, depending on the thermal share replacement.

Table 7.32: Environmental impacts arising from the optimisation, in Impact 2002+pts, for an overall 15% thermal input replacement. Impacts for biomass used and coal replaced are characterised (results per year).

End-point impact category	Economic and environmental optimisations
Biomass	
Human health	122773.85
Ecosystem quality	16537.04
Climate change	876171.22
Resources	59987.93
Impact 2002+	1075470.03
Coal replaced	
Human health	879849.40
Ecosystem quality	49563.55
Climate change	545033.85
Resources	416971.54
Impact 2002+	1891418.34

Table 7.33: Economic and environmental aspects for the three scenarios.

	5%	10%	15%
Economic optimisation (M€)	-1129.892	-2455.948	-3915.110
Impact 2002+ difference (pts/yr)	264743.84	555572.89	813013.61
Environmental optimisation (pts/yr)	301568.12	558972.74	813013.61
NPV decrement (M€)	-1370.097	-2465.371	-3915.110

Table 7.34: Revenue's increase to cover BSC costs.

	5%	10%	15%
Economic optimisation (%)	5.84	12.70	20.25
Environmental optimisation (%)	7.08	12.75	20.25

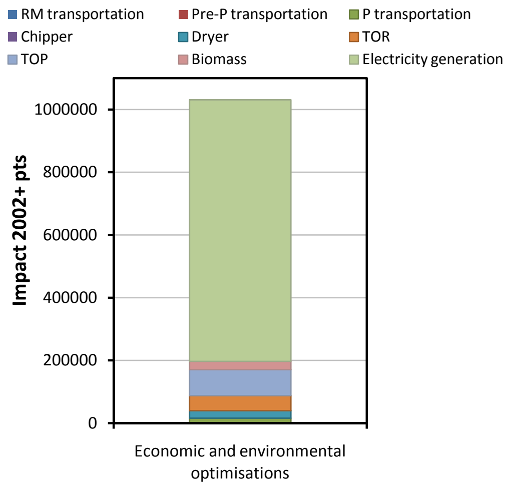

Figure 7.25: Distribution of environmental impacts for the optimisation solution (15% thermal input replacement), according to the different SC activities (results per year).

Table 7.35: Transportation annual costs for all the scenarios.

	5%	10%	15%
Economic optimisation (M€)	15.17	29.86	41.83
Environmental optimisation (%)	19.44	31.48	41.83

A drawback of biomass as raw material is transportation but, in the present case study, this is not the main cost item or the main BSC echelon in terms of environmental impact, because of the raw material dispersion. Transportation costs per year are summarised in Table 7.35. The difference between 5% and 10% scenarios is higher than the difference among 10% and 15% scenarios. Contemplating all the scenarios solutions, TOP and TOR are the only pre-treatment technologies selected, because of efficiency and investment costs reasons.

7.5.2 Case study 2 conclusions

Case study 2 considers a BSC located in Spain, including the estimation of the overall potential of woody biomass residues, and the real coal power plants park existing in the country. The objective has been to provide the optimum BSC networks in the light of different policies of coal inlet thermal power replacement: 5%, 10% or 15%. Economic and environmental criteria have enabled the discrimination of the optimum networks, allowing for the calculation of subsidy policies or prices increase to promote or to justify such a project. The value ranges from 5.84% to 20.25%, depending on the thermal share replacement. It has been shown that the main benefit of co-combustion is principally environmental. The proposed criteria to be optimised are related to the coal-based SC.

Biomass waste remains after coal substitution in all the configurations found. This suggests a potential for the production of standard pre-processed biomass for exportation, in the form of pellets, for instance.

The transportation problem is not a major hurdle in the present case study. The investment for such a project ranges from 549.16 M€ to 1640 M€, depending on the percentage of replacement.

7.6 Final remarks

This chapter presents an approach for the efficient design and planning BSC. The model relies on multi-period MILP for multi-objective optimisation of economic and environmental interventions. The model considered the long-term strategic decisions, i.e. establishing of pre-treatment trains of units and their respective location, selection of biomass sources, location of processing sites, and distribution centres.

The case studies have been solved with exhaustive data found in the literature. This chapter has demonstrated the capability of the developed tool to perform biomass-to-energy projects. The data should be refined to support more specific analyses.

Future work should focus on biomass properties calculation, including biomass types combinaisons, long-term storage and seasonality. A more accurate match between the raw material and its demand is needed to achieve this aim. Transport policies and taxes, specific for each contry, are of concern when studying international transport of biomass.

Notation

Superscripts and subindices

ar	as received basis
daf	dry and ash free basis
D	biomass mixture
e	electric
ev	evaporated
i_r	interest rate
n	project life
th	thermal

Acronyms

BD	bulk density
BM	biomass
BSC	bio-based supply chain
CCS	carbon capture and storage
CES	centralised energy systems
CTFC	Centre Tecnològic Forestal de Catalunya
DM	dry matter
FU	functional unit
IGCC	integrated gasification combined cycle
LCA	life cycle assessment
LCI	life cycle inventory
LCIA	life cycle impact assessment
LHV	lower heating value

MC	moisture content
MILP	mixed integer linear programming
MOO	multiple objective optimisation
NPV	net present value
OIL	bio-oil
O&M	Operation and maintenance
PEL	pellet
SC	supply chain
SLU	slurry
STN	state task network
TOP	torrefied and pelletised biomass
TOR	torrefied biomass

Mathematical formulation

Indices

a	mid point environmental impact categories
e	suppliers
f, f'	facility locations
g	end point environmental impact categories
i	tasks
j	equipment technology
s	materials (states)
t, t'	planning periods

Sets

A_g	set of midpoint environmental interventions that are combined into endpoint damage factors g
E_{rm}	set of suppliers e that provide raw materials
$\hat{E}_{prod}$	set of suppliers e that provide production services
$\bar{E}_{tr}$	set of suppliers e that provide transportation services
F_e	set of locations f where supplier e is placed
FP	set of materials s that are final products
I_j	set of tasks i that can be performed in technology j
$\bar{J}_e$	technology j that is available at supplier e
$\tilde{J}_f$	technology j that can be installed at location f
J_i	technologies that can perform task i
Mkt	set of market locations
RM	set of materials s that are raw materials
Sup	set of supplier locations
T_s	set of tasks producing material s
$\bar{T}_s$	set of tasks consuming material s
Tr	set of distribution tasks

Parameters

A_{sft}	maximum availability of raw material s in period t in location f
Dem_{sft}	demand of product s at market f in period t
$distance_{ff'}$	distance from location f to locationf'
$FCFJ_{jft}$	fixed cost per unit of technology j capacity at location f in period t
I^J_{ft}	investment required to establish a processing facility in location f in period t

$NormF_g$	normalising factor of damage category g
$Price_{sft}$	price of product s at market f in period t
$Price^J_{jft}$	investment required per unit of technology j capacity increased at facility f in period t
$rate$	discount rate
$Water_s$	Moisture for material s
$Water^{max}_{ij}$	Maximum moisture for task i performed in equipment j

Greek symbols

α_{sij}	mass fraction of task i for production of material s in equipment j
$\bar{\alpha}_{sij}$	mass fraction of task i for consumption of material s in equipment j
β_{jf}	minimum utilisation rate of technology j capacity that is allowed at location f
ζ_{ag}	g end-point damage characterisation factor for environmental intervention a
$\theta_{ijff'}$	capacity utilization rate of technology j by task i whose origin is location f and destination location f'
$\rho^{tr}_{eff't}$	unitary transportation costs from location f to location f' during period t
τ^{ut1}_{ijfet}	unitary cost associated with task i performed in equipment j from location f and payable to external supplier e during period t
τ^{ut2}_{sfet}	unitary cost associated with handling the inventory of material s in location f and payable to external supplier e during period t
χ_{est}	unitary cost of raw material s offered by external supplier e in period t
$\psi_{ijff'a}$	a environmental category impact CF for task i performed using technology j receiving materials from node f and delivering it at node f'
ψ^T_{ija}	a environmental category impact CF for the transportation of a mass unit of material over a length unit

Binary Variables

V_{jft}	1 if technology j is installed at location f in period t, 0 otherwise
$\mathscr{X}$	set of binary variables
$\mathscr{Y}$	set of continous variables

Continuous Variables

$DamC_{gft}$	normalised endpoint damage g for location f in period t
$DamC^{SC}_g$	normalised endpoint damage g along the whole SC
$EPurch_{et}$	economic value of purchases executed in period t to supplier e
$ESales_t$	economic value of sales executed in period t
$FAsset_t$	investment on fixed assets in period t
$FCost_t$	fixed cost in period t
$Fjft$	total capacity of technology j during period t at location f
FE_{jft}	capacity increment of technology j at location f during period t
IC_{aft}	midpoint a environmental impact associated to site f which rises from activities in period t
$Impact^{2002}_f$	total environmental impact for site f
$Impact^{2002}_{overall}$	total environmental impact for the whole SC
$P_{ijff't}$	specific activity of task i, by using technology j during period t, whose origin is location f and destination is location f'
$Profit_t$	profit achieved in period t

$Purch^{pr}_{et}$	amount of money payable to supplier e in period t associated with production activities
$Purch^{rm}_{et}$	amount of money payable to supplier e in period t associated with consumption of raw materials
$Purch^{tr}_{et}$	amount of money payable to supplier e in period t associated with consumption of transport services
$Sales_{sff't}$	amount of product s sold from location f in market f' in period t
S_{sft}	amount of stock of material s at location f in period t
Superscripts	
L	lower bound
U	upper bound

Chapter 8

Bio-based Supply Chain Optimisation in Distributed Energy Systems

The approach developed and used in Chapter 7 is applied to a third BSC case study, based on a distributed energy system (DES) located in Atebubu district (Ghana), which uses cassava waste as raw material. The problem is defined as a multi-objective mixed integer linear program (MILP) taking into account two main criteria, the net present value (NPV) and the environmental impact through the Impact 2002+ indicator. The mathematical formulation is provided in Chapter 7. In the present case study, the purpose is to extend and adapt the decision tool for the analysis of rural development in a developing country. As was discussed in Chapter 2, there is a lack of energy models for such situations: this chapter seeks to a systematic approach contemplating the social point of view. The technology used for the supply of electricity demands is a BG-GE plant.

Small scale gasification technology should provide appropriate answers to those issues reported in Figure 2.10, concerned with raw material homogenisation, tars production, gas cleaning and gas engine performance. Waste heat recovery is presented in this chapter as an alternative to increase the overall BG-GE plant efficiency.

8.1 Introduction

Small scale gasification systems are employed to meet the specific requirements of DES using biomass available at or near the point of use, or pre-treated biomass, such as pellets, bought from an established market. Small scale gasification systems can be employed in rural or urban contexts in both, industrialised or developing areas (for further discussion, see Sections 1.1.1 and 2.3.1). In the first context presented, the main system requirements are sustainability, i.e. resource sustainability and no need of grid support, high efficiency, demand accomplishment, consumer implication and fossil fuels independency, to an efficient electrification alternative. In the second context, the main intention is to save energy consumption from the grid and/or to be self-sufficient. This option belongs to residential building programs. Both options contribute to mitigate climate change by using clean and efficient systems.

The technology is similar for rural electrification or residential building programs despite the different circumstances. *Waste heat recovery* or *co-generation* covers the production of heat, cooling or chilling and electricity. Among these options, two strategies can be distinguished: passive strategies, in which the energy is recycled back to the same process, and active systems, in which the heat is used by other systems. In co-generation, heat that would normally be lost in the production of one form of energy, is recovered. The overall efficiency of a co-generation plant is 70%-80%, vs. a 35%-45% of an utility power plant, such as an IGCC power plant. An important issue affecting heat recovery equipment limitation is the presence of contaminants in flue gases. Depending on the size and the heated stream, mainly air or water, the heat exchangers can be recuperators, economisers, regenerators, heat recovery steam generators (HRSG's) or waste heat boilers (WHB's). Waste heat can be transferred to liquid or gaseous process units, as well as to solids, directly through pipes, or indirectly by means of a secondary fluid (i.e. steam, oil), through heat exchangers. It can be used to produce either, heat, or air conditioning or refrigeration. To synthesize the final waste heat recovery system, the composition, temperature and flowrate of the waste heat fluid as well as the composition, maximum allowable temperature (or minimum, depending on the case) and flowrate of the heated fluid, are required (Thumann & Mehta, 2008; Doty & Turner, 2009). In order to evaluate the most appropriated method for the recovery of heat, rather than the amount, the quality, i.e. the temperature of the heat must be evaluated. Three temperature ranges can be distinguished. The high temperature range refers to temperature above 650℃. The medium temperature range between 232℃- 650℃ and the low temperature range is below 232℃. Depending on this scale, different options are presented.

- High temperature waste heat. This is typical for flue gases. It can be used to produce process steam, pre-heat combustion air or mechanical energy in gas and steam turbines.
- Medium temperature waste heat. Such stream is useful to produce steam, pre-heat combustion air, boiler feedwater, or to be converted into mechanical energy in gas and steam turbines cycles.
- Low temperature waste heat. This heat of limited use, can be promoted to higher quality heat stream using a heat pump, which consumes mechanical work. It can be used also to pre-heat boiler feedwater.

Strictly speaking, co-generation is not only a matter of heat recovery, but also a tool to satisfy an existing heat, cooling or mechanical/electrical demand. These systems aim at extracting the maximum available energy from the feedstock. A co-generation system comprises an electricity system generator, a system of heat exchangers and usually, an operating control system. The three must common types of electricity generators are (Thumann & Mehta, 2008; Doty & Turner, 2009):

- Steam turbines. Steam turbine co-generation plants consist of a boiler, a turbine and a heat exchangers system for one of the aforementioned applications.
- Combustion gas turbines. The combustion gases drive a turbine to generate electricity. Usually, high-temperature flue gases can be exploited by a HRSG (as

in the IGCC power plant). Those units are common for industrial and commercial applications.

- Combustion engines. In internal combustion engines (ICE) and external combustion engines, the energy can be recovered from the cooling system of the exhaust gases. The co-generation plants that use ICEs generate the highest amount of electricity per amount of heat produced: hot water can be produced from the engine cooling jacket, and low pressure steam can be generated from the flue gas, as well as heating the process itself. Compared with turbines, ICEs have lower efficiency, as well as higher operation and maintenance (O&M) costs. Small and large reciprocating gas engines are comprised into this category. Any reciprocating engine uses pistons to convert pressure into a rotation movement. According to their mode of ignition, compression or spark ignitions, they are classified into diesel and Otto engines. ICE's are for instance the two-stroke or four-stroke piston engines, or even gas turbines mentioned before. Stirling engine, organic rankine cycle and steam engine are external combustion engines, that use heat from an external source, transferred to the working fluid through the engine wall or a heat exchanger.

The evaluation of the co-generation systems is performed by a feasibility study of the needed utilities: the determination of the thermal and electric loads is required, by taking into account the timing of maximum use of each energy source. The *load factor* is characterised by the average consumption rate for each service between its peak consumption rate over a given period of time. In the best case, all the electricity and all the heat produced are consumed. A common parameter which is calculated for co-generation systems is the *heat-to-power ratio*. It takes into account the net power and heat productions. The *overall efficiency* is calculated in Eq. (8.1), being therefore possible to calculate electrical and thermal efficiencies separately, by only taking into account the utility of concern (Thumann & Mehta, 2008; Doty & Turner, 2009).

$$\eta_{overall} = \frac{\text{Electricity}_{net} + \text{Heat}_{net}}{\text{Feedstock}_{in}} \tag{8.1}$$

The operating strategies of a co-generation system can give priority to the electric or to the thermal demand, or to the both of them. The *electric dispatch* mode sizes the co-generation plant to meet the annual peak or base-load demand, with some additional capacity to accomodate demand growing. It operates independently from the grid. In turn, the *thermal dispatch* mode sizes the plant according to the facility annual peak or base-load demand. In this case, the grid supplies part of the needed electricity demand. A *hybrid strategy* minimises O&M costs while maximising the return of investment. The heat or electricity peaks may not be satisfied. Therefore, additional boilers and electricity from the grid are needed.

8.1.1 Micro-generation

This chapter uses electricity *micro-generation* systems, since the BG-GE system produces power below 10-20 kW_e for domestic applications, according to Thiers *et al.* (2010). As indicated by Incorporated (2008), micro-generation appliances deliver a maximum of 15 kW_e, implying approximately up to 39 kW_{th}. In Doty and Turner (2009), the term *distributed generation* is used to describe the generation of heat and

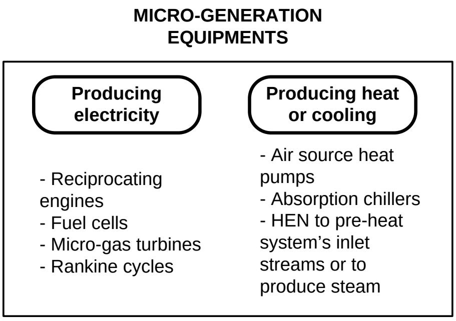

Figure 8.1: Summary of the equipments used in micro-generation.

power by means of small units, comprising from several kW's to 25 MW_e. A micro or distributed generator is located close to the consumer, and can be connected to the grid or not, depending on the facility services. Typical fuels used here are natural gas, liquefied petroleum gas, kerosene and diesel. The available technologies at this range are reciprocating engines, air source heat pumps, fuel cells, Stirling engines, steam engines and micro-gas turbines, this last for more than 30 kW_e (Cockroft & Kelly, 2006; Thiers *et al.*, 2010). Rentizelas *et al.* (2009a) and Cockroft and Kelly (2006) state that micro-generation is financially viable if the system run a minimum of 4500 h/yr, while an efficiency of more than 80% is required to obtain GHG emissions savings. Figure 8.1 summarises the technical solutions for micro-generation.

An extension of co-generation is *tri-generation*, in which the generation of electricity, heat and cooling are contemplated, specially in warm climates where the generation of heat is of lower interest. Absorption chillers or refrigerators, that consume heat as source to produce cooling, are principally applied in space refrigeration. Rentizelas *et al.* (2009a) use combustion and gasification processes to provide district heating and cooling networks, depending on the yearly demand. They present an organic Rankine cycle as an alternative to produce electricity by using low quality heat streams, which heat streams used in conventional Rankine cycles. Organic cycles are a well proven technology for power generation up to 1000 kW_e.

8.1.2 The BSC

Biomass for feeding micro-generation plants, can be transformed into a gas (by means of digestion or gasification), into a liquid (through fast pyrolysis) or directly combusted as a solid. To produce electricity, gas and liquid products can be directly used in ICE's. The producer gas can be moreover utilised in a fuel cell. The heat from combustion should be used in both Rankine cycles, organic or conventional. Biomass should be pre-treated to enhance its properties and to be more efficiently used as a feedstock (for further discussion see Chapters 2 and 7). The trade-off when using biomass in CES and DES characterises the price of minimally centralising and pre-processing it against the cost of the usage of the dispersed sources by means of pre-processing plants close to the raw material.

Co-generation installations can be designed to supply the *base-load* or the *peak-load* heat or electricity demands, depending on each context. For instance, in a grid-independent installation, peak-load is the demand to be satisfied. For domestic application in urban contexts, where the key features are energy savings, the base-load should be covered, while the peak-load can be supplied by the grid, or in the case of heat peak-loads, by gas boilers, or, in contrary, the design can be performed to alleviate utility peak demand problems. In co-generation, does not exist a unique solution. The solution depends on the needs and the context of the user. It is strongly influenced by rural and urban environments in developing or industrialised countries. Urban areas provided by CES, are focused on energy consumption reduction, enhancing the overall efficiency of the whole energy provision system. Better insulated buildings influence the heat-to-power ratio. Micro-generation systems should imply annual energy and thermal savings. Rural areas, with no other alternative for electricity generation, seek for a complete autonomy. Rural and domestic applications have different driving motives, and their physical situation leads to different supply chains (SC's): for domestic application, the BSC can be defined as in Chapter 7. For rural electrification, the bio-based SC (BSC) can be stated as in the present chapter.

On the topic of *rural electrification*, Andrade *et al.* (2011) identify several lessons learnt from Brazil. Electricity should arrive with advice, population education and social inclusion. The people involved should be informed in advance, and the installation should be specifically dimensioned taking into account their specific needs and growing potential. People should be trained concerning the news trends derived from electrification. Above all, initiatives should be sustainable in time, and the final objective must be the autonomy of the local population. Chapter 2 identified several trends concerning DES: a lack of systematic energy models that promote the use of biomass, specially in rural areas from developing countries, for exportation and for local use. Moreover, there is also a lack of energy models for rural development that take into account economic, environmental and social issues of the communities.

This chapter is focused on rural areas in developing countries. The approach can be however extended to handle DES in developing and industrialised countries. The objectives are savings in money and GHG emissions, by enhancing the efficiency of the modular units. A large number of social and environmental studies promotes the suitability of DES promotion to mitigate climate change and fossil fuels depletion effect, and to overcome poverty zones inequalities. This chapter promotes rural electrification by means of efficient technology and through economic, environmental and social considerations.

8.1.3 Linking social and environmentally-friendly systems

Small scale gasification for rural electrification in this specific case, and for economic development in general, should take into account social and ecological aspects, for sustainability related to resources management and population involvement. This social-environmental concern takes into account an adaptive management that deals with the unpredictable interactions between people and ecosystems, and among themselves. It means that no pre-conceived management and rural electrification issues usually works as stipulated solutions for all the scenarios. Figure 8.2 shows the main points to be considered for the local social system to develop management practices based on knowledge of the environment. One main characteristic to all the factors is their principally qualitative rather than quantitative nature. Social issues such as population increase, urbanisation problems, changing gender roles or the varying knowledge. may be identified as priorities. Those issues cannot be tackled

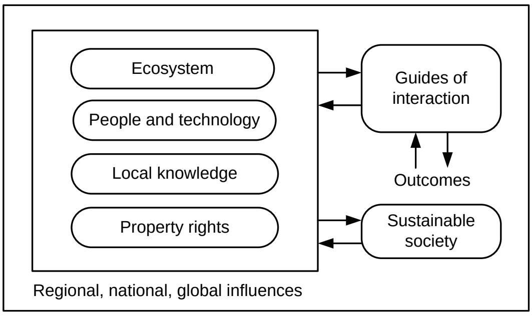

Figure 8.2: Factors influencing social guidelines. Based on Berkes and Folke (2000).

neglecting their dynamic nature, and without respectful appraisal for local knowledge and experience (Berkes & Folke, 2000).

At the design-planning level, the implementation of social-environmental issues is a challenge of a multiple-objective optimisation problem, since qualitative and dynamic concerns are involved. Some studies make reference to the possibility of considering past successful experiences as a starting point, and as a knowledge of the social-environmental interaction. Many design-planning rural projects, take into account the social factor in the light of generation of jobs exclusively (see for instance Ravindranath *et al.* (2004) or Silva and Nakata (2009)). The work by Fleskens and de Graaff (2010) defines a social function based on employment and liveability, as maximum hired labour input that people can pay assuring a minimum level of life. Nidumolu *et al.* (2007) further include the land use in the analysis. Thus, their social objective seeks to maximise food production. This is an example of a *surrogate criterion*, where issues that cannot be quantified directly (in this case, m^2 to be used for energy purposes), are modelled through a related effect (the need of food).

Note that social concerns in industrialised and developing countries can involve completely different desired consequences. As described in Bojarski (2010), social criteria concerning process design and operation in industrialised countries are security patterns and working conditions enhancements. In contrast, in developing countries, those social factors aim at reflecting parameters that promote economic development and satisfaction of basic needs.

8.2 Small scale gasification

The chosen technology for micro-generation is gasification linked to an ICE. The considered BG-GE plant belongs to small scale gasification systems, whose main purpose is to proportionate electricity. Therefore, the approach followed in case study 3 is *electric dispatch*, that aims at operating co-generation plants supplying electric requirements as first priority, in order to be completely independent from other CES.

According to Kirkels and Verbong (2011), gasification application is still having problems regarding tar, operation, maintenance and economic feasibility. Research on coal and/or biomass gasification proliferated during oil crisis (world wars) and climate change regulations, mainly in Japan, China, USA and India. It is a recurrent technology that has not been definitely incorporated into the energy share of the different countries and is highly dependent on government regulation and assistance. Kirkels and Verbong (2011) conclude that small scale biomass gasification has been successful in a few niche markets, even if it is still in an early commercial step. The biomass gasification market is characterised by a lack of focus and proper impetus.

In the same line, the work by Verbong *et al.* (2010) points out a strategic niche management of biomass gasification, based on the Indian experience. The management of gasification projects should deal with the social network composition of actors, for instance private and/or public actors, consumers as clients or as active actors, and with the proper expression of expectations. Lessons learnt from real case studies reflect the need of improving the technology and enhancing economic efficiencies (need of subsidies, since positive cash flows are difficult to obtain), as well as the finding of appropriate application domains. There is a lack of well trained technicians in the field, as well as of monitoring and evaluation programs of biomass gasification small scale plants. In Mechanical wood products branch, Forest industries division (1986) the most important concerns with a biomass gasifier include ashes, soot, slag and tarry condensates, safety rules, equipment failures caused by design mistakes, the choice of inadequate materials and incomplete instructions on O&M.

The *niche approach* is focused on the specific needs of the target market. The identified drawbacks reveal the difficulty of scaling-up the biomass gasification technology for high dissemination: variations in the energy need among the different users groups, availability and type of biomass, financial, human and institutional resources, economies of scale difficulty. Thereby, the approach should be application-specific or tailor-made (Ghosh *et al.*, 2006).

Biomass gasification plants can compete in the market with other modular gasification plants, biomass combustion plants and any micro-cogeneration plant. The producer gas can be used in fuel cells, microturbines, gas engines, dual fuel engines, gas turbines and combined cycles, this last for larger scales (see Section 2.3.2). The benchmark of commercial gasification plants indicates an atmospheric-pressure flowsheet with a simplified fuel processing step prior gasification (generally drying), the gasifier itself, gas cleaning, gas cooling, an ICE and the electric generator. Gas cleaning includes wet and dry gas scrubbing, tar cracking, filters and cyclones.

Table 8.1 summarises of the major companies commercialising gasifiers for small power generation (from Kirkels and Verbong (2011) and the Bioenergy list[1]). An extensive list of manufacturers can be found from China and India. Most of them are small companies with limited sources and oriented to the regional market. For most of the suppliers, gasification is not their core business. Thus, the devices are not mass produced. The enterprises cited in Table 8.1 use fixed bed gasifiers. Most of them specifies biomass type and properties to be used in standardised units. However, each project requires from a particular study. It is appreciated that the majority of the enterprises offers co-production of electricity and heat.

In Section 2.3.2, several experiences have been identified and reported concerning rural electrification by means of gasification. The layout of a typical BG-GE plant has been presented. Section 2.3.3 describes in-depth the current challenges on gasification pilot plants. These are raw material characterisation and homogenisation, better operation of the gasifier (in the view of generation of tars and the producer gas composition), more efficient cleaning units, mainly in terms of tars, and an overall optimal performance of the BG-GE plant, to guarantee an efficient and sustainable

[1] www.gasifiers.bioenergylists.org

Table 8.1: Principal micro-generation gasifier manufacturers.

Company	Type of gasifier; Application
Europe	
AHT Pyrogas Vertriebs (Germany)	Fixed bed; heat and electricity
Babcock Volund (Denmark)	Updraft; heat and electricity
Bioneer (now Foster Wheeler) (Finland)	Updraft; heat
Biomass Engineering Ltd (UK)	Downdraft; heat and electricity
Biosynergi (Denmark)	Fixed bed; heat and electricity
ITI Energy (UK)	Propietary design; heat and electricity
Thomson Spaven (UK)	Downdraft; heat and electricity
America	
Community Power Corporation (USA)	Downdraft; heat and electricity
Frontline Bioenergy (USA)	Fixed bed; heat and electricity
Gasifier Experimenters Kit (GEK) (USA)	Downdraft and updraft; electricity
Planet Green Solutions (USA)	Fixed bed; electricity
PRM Energy Systems Inc (USA)	Updraft; heat and electricity
Asia	
Ankur Scientific Energy Technologies (India)	Downdraft; heat and electricity
Africa	
Carbo Consult Ltd (South Africa)	Downdraft; heat and electricity
Oceania	
Fluidyne Gasification (New Zealand)	Fixed bed; electricity

process, at a minimum cost. A standard BG-GE layout is used in Section 8.2.2 to consider co-generation and to characterise the main parameters to be included in the MILP model.

8.2.1 Waste heat recovery

From the micro-generation equipments listed in Figure 8.1, the chosen equipment to be coupled in the BG-GE system is the Stirling engine (STE). This option uses waste heat to produce power by means of producer gas heat recovery, since the objective of the BG-GE system is to produce electricity. The STE works in the range of high temperature waste heat. In this chapter, the possibility of generating more electricity than the one supplied by the ICE is evaluated: this option allows to face growing demand. Corria *et al.* (2006) have presented an evaluation of the STE's used for distributed energy systems in Brazil, as alternative generation energy systems, with lower environmental impacts. The Stirling engine is defined as an external combustion engine with a working gas that expands when heated from an external heating source and moves a piston that produces work. The expanded volume is then cooled and compressed before the next cycle. As a difference from the GE, STE works in a continuous mode. The efficiency is evaluated in 30%. The main disadvantages of this technology are the relatively high costs, due to low volumes of production, few test realised with producer gas, and the available data on the durability is sparse. This chapter considers the most common α-type STE, based on two pistons and cylinders. This is a technology in pre-commercial phase due to the market availability, even though the technology is well developed. Examples of companies in the field are SOLO Stirling GmbH, now Stirling Systems GmbH (Germany and Switzerland) and Stirling Thermal Motors Inc (USA).

Podesser (1999) exemplify electricity production in rural areas using a Stirling engine, heated by the flue gas produced from biomass combustion. Their study highlights the applications of Stirling engines at small companies and communities. The engine is an α-type that uses air as working gas. The advantages of using air are availability and price, not only of the gas itself, but also for the auxiliary equipment, such as the compressor, or the sealing. Moreover, the efficiency of the engine is not influenced by the working gas. The study by McGovern *et al.* (2010) simulates a combined cycle formed by a stationary ICE and a STE, for small and medium scale power generation. The thermal source of the STE is the exhaust gas from the ICE. Knight and Ugursal (2005) published an exhaustive review of ICE's, STE's and fuel cells as co-generation systems.

ICE and STE are generally modelled for heat and electrical power generation. The considered flowsheet in this chapter uses a ICE to exploit the calorific power of the producer gas generated by gasification, and a STE to use one of the waste heat sources of the system (see Section 8.2.2), using air as a working fluid. ICE and STE are based on the Otto and the Stirling cycles, respectively. The main difference between both cycles is the replacement in ideal conditions of the adiabatic processes in the Otto cycle by isothermal processes in the Stirling cycle. The maximum STE efficiency theoretically matches the Carnot efficiency. The Stirling electrical efficiency is in practice in the range of 20%-35% (Knight & Ugursal, 2005). The used ICE in the BG-GE flowsheet is a spark-ignited gas engine. The electrical efficiency ranges 25%-30% (Knight & Ugursal, 2005). According to Thumann and Mehta (2008), domestic hot water supply is around 80°C.

8.2.2 Conceptual design - superstructure

The objective of this section is to find the main flowsheet values to characterise the BG-GE system considered here, with waste heat recovery to produce more power and hot water, for micro-generation purposes. As referred in Chapter 1, large and small scale gasification plants have different operating conditions, but the gasification and gas cleaning principles remain the same. Therefore, the developed superstructure in Chapter 6 is applied here to BG-GE plant. The following describes the main model parameters and adaptations implemented into the Aspen Plus superstructure.

The layout of the plant follows standard process description in Section 2.3.3 and the specific flowsheet of the pilot plant built at UPC, and financed by VALTEC08-2-0020 project. This project follows the design recommendations of the company *Waste Technology S.L.* The main characteristic introduced in this new design is a dry method to clean the gas, avoiding water pollution by means of a venturi scrubber. This unit uses a reactor with CaO as catalyst, for tars and, to a low degree, for any sulphur removal.

The outline of the plant is shown in Figure 8.3 by the considered blocks. This gasifier operates with 100% biomass. Specifically, at the current conceptual level and for characterisation purposes, wood pellets are used (see Table 8.2 for its characterisation). This is an Imbert downdraft gasifier working at atmospheric pressure. The moisture content (MC) is assumed here of 8.5%, which lies within the range found in the literature (from 7% to 25%). The ER is between 0.25 and 0.9 using the oxygen-based definition, being 0.25 the typical value. The complete oxidation of biomass defined as mass of oxygen/mass of biomass is of 1.476, while the complete oxidation with air corresponds to 6.36. The pilot plant at UPC is designed to work with 15 kg/h of wood pellets . Therefore, the amount of air ranges between 20.4 kg/h and 73.5 kg/h (calculated with the property set COMB-O2 from Aspen Plus, using a calculator block). The chosen amount of air is 20.4 kg/h, and is heated

Table 8.2: Ultimate and proximate analysis of wood pellets (ECN-Biomass, 2010). The LHV is calculated by QVALNET property set from Aspen Plus.

% mass basis (dry)	Wood pellets
Ultimate analysis	
C	50.12
H	6.07
O	43.20
N	0.09
S	0.01
Cl	0.01
Proximate analysis	
Moisture	8.50
Ashes	0.50
Fixed carbon	18.00
Volatiles	81.5
LHV_{dry} (MJ/kg)	21.80

when cooling down the producer gas after the gasifier. The producer gas temperature before the CaO unit should be around 550℃, as design condition. There exists another stream of cooling air before the gas engine, to cool down the producer gas till around 80℃, which is the referred temperature in Mechanical wood products branch, Forest industries division (1986) (see Figure 8.4). This hot air flowrate is the one used in the STE. The most important parameter in the biomass gasifier, which influences the producer gas composition, is the amount of inlet air (therefore, the ER). The second is the MC.

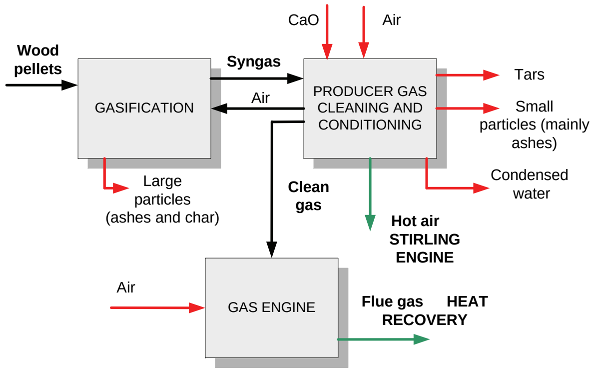

Figure 8.3: BG-GE plant layout, with waste heat recovery options in bold and capital letters.

See in Figure 8.3 the outline of the considered BG-GE plant. A blower embedded in the producer gas trajectory to the flare or to the engine is in charge of its movement. The most common layout includes as main elements a cyclone, wet scrubber and several filters to clean the gas from tars and particulates. This flowsheet uses a cyclone, a CaO reactor and a filter to clean the gas before combustion in the gas engine. Those systems are operated in batch mode, but a continuous stationary operation mode is assumed at the present early stage of development.

The considered main engine is the gas engine. Its performance modelling in the

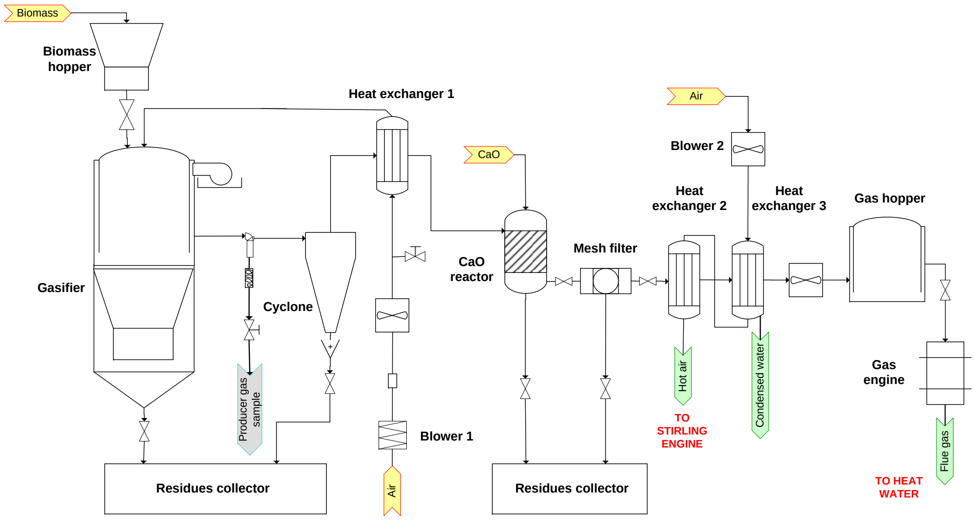

Figure 8.4: BG-GE plant layout showing the principal flowsheet units.

Aspen Plus superstructure follows the approach from Mechanical wood products branch, Forest industries division (1986). It takes into account an air/gas ratio of 1.1. In the state-of-the-art, the char bed porosity in the gasifier, which depends on the type of feedstock (chips, pellets or other shapes), is the most important factor for the pressure drop calculation along the flowsheet. The pressure drop is estimated in the Aspen Plus model by taking into account distances, diameter, elbows, valves and tees according to the UPC pilot plant design. The pressure drop in the considered reactors and units (gasifier, cyclone, heat exchangers and filter) are estimated using the criteria found in Ulrich and Vasudevan (2004). The overall value before the blower installed to move the producer gas is around 0.0553 bar. The streams inlet conditions to the flowsheet i.e. biomass, air and water, are 1 atm and 15℃. The superstructure designed for IGCC-CCS systems (see Figure 6.2) is used, and units selection and operation conditions are adapted to the BG-GE system. The GE and the STE, have been represented as gas and steam turbines, respectively, for simplification purposes. Water to be heated uses heat from the GE from 121℃ to 30℃ (from the flue gas cooling). The resulting overall efficiency is 27%. This is far from the 70%-85% efficiencies reported in bibliography for co-generation systems. This is due to the maximum amount of heat used in the STE, which is around 5 kW$_{th}$, which is already 5.5% of the total inlet amount of energy in the raw biomass. For heating purposes, recent bibliography for the engines co-generation functions include moreover, the heat recovered from jacket water and lube oil heat in the case of the GE (all the engine coolant) (Knight & Ugursal, 2005). Furthermore, those high efficiencies obtained in co-generation are reported for highly integrated systems, using natural gas or gases from a combustion (at around 1400℃), which is the double of the temperature from the producer gas that goes out from the gasifier. For comparison, the IGCC power plant reported in Chapters 5 and 6, had a 42% of efficiency using a well integrated flowsheet, performed by a combined cycle (CC), a HRSG and a WHB.

The most important results are summarised in Table 8.3: T_{gasif}, as the temperature

Table 8.3: Principal output values.

Parameter	Values
T_{gasif} (°C)	702
Producer gas composition (on a mole basis)	
CO	23.93
CO_2	10.49
N_2	37.07
H_2	20.88
CH_4	3.58
H_2O	4.03
Flowrate (kg/h)	35.33
LHV (MJ/kg)	6,32
CGE (%)	68
Power GE (kW_e)	15.80
η_{GE} (%)	25
η_{BG-GE} (%)	**17**
Power STE (kW_e)	1.50
η_{STE} (%) (%)	30
η_{BG-GE} with STE (%)	19
Heat (kW_{th})	6.89
η_{heat} (%)	8
η_{GE} with heat recovery (%)	37
η_{BG-GE} with STE and heat recovery	27
Heat-to-power ratio	0.40

of the producer gas at the gasifier outlet, producer gas composition and LHV, power and heat outputs, as well as partial and overall efficiencies of the system. The efficiency can increase by 10% if the abovementioned waste heat recovery options are implemented.

8.3 The bio-based supply chain

The aim in this chapter mirrors Chapter 7. The BSC seeks to take decisions such as active nodes and links among them, units capacity and final sold products, subjected to the optimisation of the objective function(s), within the conceptual design stage context. The BSC comprises potential locations for processing or distribution centres. The potential suppliers and clients are inputs of the model. Biomass as raw material is conditioned before being processed into the gasification plant. Materials fluxes among facilities may appear. The demand of electricity is supplied by more than one site. As depicted in Figure 7.1, the BSC comprises four main blocks: sourcing, pre-treatment, product generation and product distribution. The biomass attributes modelled and characterised along the SC are MC, dry matter (DM), LHV and bulk density (BD).

For this case study 3, the BSC has been adapted as represented in Figure 8.5. The main differences with the previous case studies in Chapter 7 lies in the CES-DES distinction:

- Taking advantage of the local biomass wastes needs short or negligible distances between clients and sites where raw material is generated.
- Because of the rural configuration, no long distances should be overcome; chipping and drying are the only pre-treatment considered.

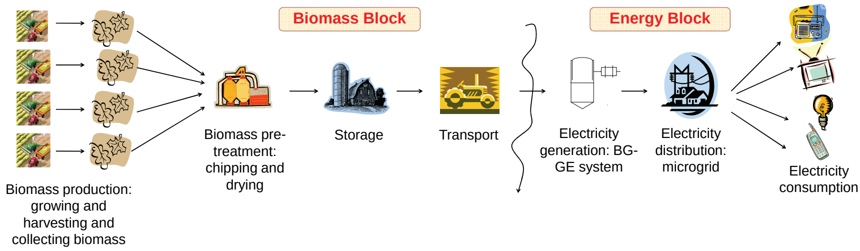

Figure 8.5: BSC echelons considered for DES.

- It is assumed that no grid exists. Thus, a DES is closer to the customers than a CES, and this is usually interconnected to a microgrid or directly to the customer's facilities. In this chapter, the investment needed for the microgrid construction is contemplated.
- The electricity demand in a rural area from a developing country can increase significantly if the economic activity of the area experiences an important development.
- One of the objectives functions includes a social criterion.

Two blocks can be distinguished in the layout depicted in Figure 8.5, i.e. the biomass block and the energy block. Multi-biomass sources and electricity demands at multiple sites are considered.

The biomass block includes all the stages from biomass production to its delivery in the generation power plant(s). This step includes three major elements:

- Biomass sourcing. Biomass waste from agricultural or forest origin are of concern. Availability, in terms of amount and seasonality, locations and costs are considered.
- Pre-treatment. Biomass waste is pre-processed before gasification to obtain the adequate shape, LHV and MC. The homogeneisation of biomass shape is important to reduce volume for transportation and a required characteristic for the raw material entering the gasification plant. Storage serves as a biomass reservoir, matching productions from several sites, or when the storage is needed as a buffer for the periods when biomass waste is not produced. Fast pyrolysis, torrefaction and pelletisation are disregarded since the small biomass quantities required for rural electricity demand satisfaction does not allow to take profit from economies of scale. Moreover, those are too complicated technologies for rural areas in developing countries[2]. Another business case should be the possibility of centralised processing sites to transform biomass into pellets, torrefied biomass or bio-oil, for local consumption and exportation. This is however a CES problem.
- Transportation. The transportation is achieved by people, by animal traction or by tractors. The distance to be covered is a parameter to be considered.

[2]Information from conversations with Ms. Dagmar Zwebe, from Biomass Technology Group (BTG) company.

The energy block contains the electricity generation and distribution systems.

- BG-GE microplant. It contemplates the generation of producer gas, its cleaning and use in a gas engine to produce electricity.
- Microgrid. The microgrid delivers electricity to the consumption points. Two microgrids are considered: the low voltage (LV) distribution line, whose objective is the intra-community distribution and the medium voltage (MV) line, of 36 kV, which connects different communities.
- Consumption. The demand is distributed among different sites.

The energy block is the most versatile part of the model in DES configuration: this part can be easily adapted to other microgeneration sources, such as wind, hydraulics or solar, or even to investigate the use of more than one renewable source in hybrid systems. In contrast to biomass, the other renewable sources have the advantage of being captured at the same point of use. Therefore, the model adaptation passes through the modification of the equations that represent the electricity generation technology and through the introduction of the main parameters that characterise the sources or raw materials.

8.4 The multi-objective optimisation

The abovementioned options are investigated in the light of optimisation of economic (NPV), environmental (life cycle assessment, LCA, through Impact 2002+ pts evaluation) and social criteria. Similar to the previous chapter, the extremes of the Pareto frontier are obtained, by optimising each criterion individually. The social indicator is the sole new feature that requires an adaptation of the mathematical formulation described in the previous chapter (see Section 7.3).

Social model

As described in Chapter 2, Section 2.3.1, the lack of an integrated approach for rural electrification planning, principally in developing countries, has hindered so far the spreading of renewable energy technologies in modular configuration. Rural electrification projects can be financially sustainable, if they integrate appropiate and reliable data on the location of sources and clients, type of sources, income levels and energy demand. Moreover, there exists very few systematic energy models that can promote international trade. Biomass should be promoted in developing areas for exportation and local use. As previously indicated in Section 8.1.3, environmental and social points of view must be considered in DES problems. A social criterion is in essence qualitative, but must be expressed in quantitatively for implementation in a MILP problem. This is achieved here by using a surrogate criterion.

The proposed approach consists in a criterion that counts the number of demand sites that have a treatment or pre-treatment system installed. The aim is to install as many as possible of them, to promote working places in the widest range of communities or demand sites. Therefore, the social criterion SoC should be maximised (see Eq.8.2). This criterion assigns a value of 1 to each unit installed per site f. V is the binary variable that characterises the number of units installed per site. This is not applied for storage.

$$SoC = \sum_j \sum_f V_{jft} \qquad \forall\, j, f, t \tag{8.2}$$

Objective functions

The SC network can be optimised as:

$$\begin{gathered}\underset{\mathscr{X},\mathscr{Y}}{\text{Min}} \left\{-NPV, DamC_g^{SC} or Impact_{overall}^{2002}, -SoC\right\} \\ \text{subject to} \\ \text{Eqs. (7.1)-(7.24) and Eq. (8.2)} \\ \mathscr{X} \in \{0,1\}; \mathscr{Y} \in \mathbb{R}^+\end{gathered}$$

Where, $\mathscr{X}$ denotes the binary variables set, while $\mathscr{Y}$ corresponds to the continuous variable set.

8.5 Case study 3: a BSC located in Ghana using gasification

Case study 3 exemplifies the benefits of the approach via the design of a BSC in a specific rural area of a developing country, Ghana (Africa). Nine communities in Atebubu-Amantin or Atebubu district, in Brong Ahafo Region (see Figure 8.6) are of concern. The communities, from the highest to the lowest populated are Kumfia, Fakwasi, Abamba, Old Kronkompe, Boniafo, Bompa, Trohye, Seneso and Nwunwom. The biomass considered as raw material is cassava waste. Cassava is a tropical crop highly extended in the country, used to provide food. The boundaries considered are from cradle-to-gate. The currency is $\$_{2010}$. The objective is to supply the electricity demand of the selected communities that currently share a common characteristic: all are equipped with a multi-functional platform (MFP) that supplies the current electricity needs, mainly for cell phone's battery charge, water refrigeration, lighting, radio, TV, computer and machines for maize and cassava processing. The proposal is to install BG-GE systems able to work in synergy with the MFP's. The producer gas can run a diesel engine, saving diesel. This case study exemplifies the niche approach described in Section 8.2, i.e. gasification projects at small scale are application specific projects. In contrast, the methodology applied for different BSC resolutions can be the same.

Data for the BSC characterisation is provided by Dr. Ahmad Addo, from the Energy Center, in Kwame NKrumah University of Science and Technology (KNUST), in Ghana, and Mr. Ishmael Edjekumhene and Mr. Clement Nartey from the NGO Kumasi Institute of Technology, Energy and Environment (KITE) (Ghana). The MFP's matter in Atebubu district has been executed in collaboration with KITE, and the local NGO called Women and Children Support Organisation (WACSO). The contact person here is Mr. Jacob Salifu. Prices for transportation and utilities valorisation, as well as specific information about the cassava crop, have been obtained during an on-field travel. The applied currency conversion is 1 Ghana cedi = US\$0.65946[3].

[3] www.oanda.com

Figure 8.6: Location of Atebubu district.

Atebubu district context

Atebubu district is located in Ghana, Sub-Saharan Africa. This belongs to a developing country with tropical climate. The climate conditions limit biomass characteristics and uses.

The general context of Sub-Saharan Africa is nowadays characterised by globalisation, as social and economic force. The United Nations's Millenium Development Goals put their attention on social and economic issues such as hunger and poverty. The role of global institutions such as the World Bank, the International Monetary Fund, and the World Trade Organisation is crucial in the determination of trade and developing policies in Sub-Saharan countries. This is also in the framework of climate change, deforestation and desertification mitigation. Local human agents in Africa play a key role in the globalisation process: their input is decisive in ensuring the success of the initiatives.

African culture significantly differs from Western culture. The group, family and community, as a main force, rather than the individual is considered. As a consequence, the African culture is more cooperative. Wealth is demonstrated by sharing. African countries are not used to assign a monetary value to everything. In those countries, aged people are a symbol of maturity and experience. One important concern is the result of colonialism on land tenures. Traditionally, it has had the tendency of alienating Africans from their possession. This is often not well registered, which maintains informal and illegal tenure arrangements, impacting on land development. This is therefore a complicated task to evaluate land as understood in Western countries, as an investment with its years of amortisation, or as a more or less stable rental fee.

In Sub-Saharan Africa urban and rural dualism is touched by the presence of formal and informal economies, these last operating outside the control of the government. In turn, urban dualism is characterised by commercial and subsistence farmers, the first group being favoured by the government (Attoh, 2010).

The Western point of view should be reformulated and adapted to developing countries realities. This case study is a starting point, that performs a first adaptation of a SC model used in an urban area of an industrialised country with CES, to a rural area of a developing country with DES. Obtaining real and reliable data in this context, such as electricity demand, needs or biomass sources, needs from the collaboration with local partners.

Figure 8.7: Kumfia community. Source: own source.

Electrification not only consists in providing electricity to a community, but also rises the questions of commercial activity sustainability, ways of action and management of the appliances. This is why the 9 communities chosen from Atebubu district have already an established commercial activity through the management of the MFP's. None of them have access to electricity from the grid. These villages mainly use diesel, kerosene, batteries, charcoal and wood as sources to produce electricity and heat. The electricity consumption is seasonal and discontinuous along the day. The willingness to pay is the amount of money that a person is ready to pay to receive some good or service. Those communities suffer from false promises concerning electricity access. In Kumfia (Figure 8.7), the grid extension compromise is still a promise.

The most important economic activity in the area is agriculture, producing mainly cassava, yam and maize. Dressmaking, groundnut harvesting and traditional production of charcoal from dried trees are also found in the district. Farmers seldom own the lands. They usually pay a rent. Charcoal, dresses and food can be sold in the same district, in Kumasi and/or in Accra, which are the two biggest cities of the country. The cassava crop is commercialised to produce principally fufu or gari, both of them for food purposes. Women are usually in charge of trading activities, playing therefore a key role in the development of the zone.

Figure 8.8 represents the 9 communities according to their relative population. The biggest community is Kumfia with 2834 people, and the smallest one is Nwunwom with 122 people.

Multi-functional platforms

The Ghana MFP project is a 3 year project that aimed at installing and assuring the sustainability of 40 platforms, in selected communities with a clear potential to guarantee the core objectives. This is an initiative from the United Nations Development Program's-Regional Energy Poverty Programme. KITE is the Ghanadian local leading implementing partner, and WACSO is the specific area organisation which is in charge of the field tasks, such as installation, maintenance and monitoring. Also external mechanic technicians are engaged for the purpose (Morris *et al.*, 2008).

A MFP consist in "a source of mechanical and electrical energy, provided by a diesel

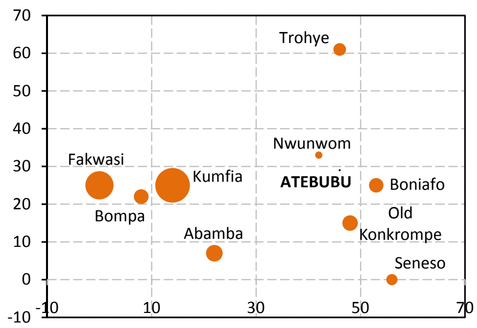

Figure 8.8: Location map of the 9 modelled communities from Atebubu district, represented according to their relative size (estimated population for year 2010). Axes in km. Data provided by KITE.

engine from 6 to 9 kW$_e$, that is mounted on a chassis and to which a variety of end-use equipment can be added following the needs: grinding mills, battery chargers, electric water pumps, vegetable or nut oil presses, welding machines, carpentry tools and mini grids for lighting" (Bre-Hammond & Crole-Rees, 2004). This type of installations includes an annexed warehouse to store the processed crops, built by the community itsself. See in Figure 8.9 a picture of one of the MFP visited, in Seneso. The project is more ambitious, and aims at creating an energy business, by selectioning a women's group, assessing the self-sustaining of the MFP, i.e. social and economic viability, training women on managerial and entrepreneurial skills, adapting a market-based business approach and through monitoring and evaluation.

According to KITE[4], the main social benefits derived from the MFP's implementation are (i) training on income generation activities, i.e. product improvement and business management, (ii) expansion of gari production and trade (collaborating with feeding programs) and (iii) starting rice trade, as a result of the product improvement and management trainings, as demonstrated in Atebubu district. In general, the MFP's have benefited the population in terms of commercial activities engagement, mainly for food trades. Therefore, MFP's revenues are highly seasonal. According to the collected data, the capacity of the installed engines are under-used.

Raw materials used

Cassava is also called manioc, manihoc, yuca, mandioca, aipin, catelinha, macaxeira and tapioca (Pattiya, 2010). This is a basic food source in tropical countries. According to Serpagli *et al.* (2010), this is important for food security and for poverty alleviation in rural areas. It has a future strategic dimension, to feed the growing population. Five markets are identified for cassava: traditional food market, feed market, food-grade food market, starch and derivatives market and ethanol market.

The cassava waste is pilled in the farms and used for fertilisation or to feed pigs or poultry. Leaves from cassava crops are used for food (soups). The stalk is used to replant the crop. According to Ubalua (2007), peels from hand peeling can constitute 20%-35% of the total tuber weight. Cassava peels degradation produce unpleasant

[4] Conversations with Mr. Clement Nartey (KITE).

Figure 8.9: Worker in a MFP, in Seneso. In the picture, the diesel engine and the cassava grater. Source: Pol Arranz-Piera.

Table 8.4: Feedstock properties for case study 3.

Biomass	Cost ($/t)	LHV_{ar} (MJ/kg)	MC (% wt)	BD (kg/m^3)	Seasonality	Yearly available (t)
Cassava waste	0	5.574	66	340	June-October	1252.73

odours and polluted air that may cause infection for human and animals. Inappropriate storage is a problem during rainfall periods. Peels are not used by its low digestibility and high levels of hydrocyanic acid. Therefore, cassava peels constitute the selected raw material for gasification, which does not compete with food needs.

The cassava is planted once a year, in April, during the rainy season[5] and does not need any special care. It takes 3 to 6 months to grow, depending on the type (there exist five different types of cassava). The harvesting period is assumed to be between June and October. A mixture of cassava peels is considered as raw material, with 66% MC and 5.574 MJ/kg LHV (Serpagli *et al.*, 2010). As the produced wastes have no current alternative use, the cost of acquisition is assumed to be zero. See in Table 8.4 a summary of the main properties used for case study 3. The last column sums up the total amount of cassava waste produced by the 9 communities. It means an overall value of 6982.7 GJ/yr, by considering fresh cassava.

Figure 8.10 shows the assumed production of cassava waste per community, in GJ/month of fresh cassava. It has been estimated proportional to the population of each community based on the 264649 t of fresh cassava produced during 2009 in the whole Atebubu district (Serpagli *et al.*, 2010). 20% of this amount is assumed to be converted into peels, among which 50% can serve for gasification in the worst case. Agricultural activity is assumed evenly divided among the communities, and that the final cassava peel disposal is at the same community. See in the same Figure the aggregated demand assumed for the nine communities. This is expressed in terms of thermal demand.

[5] Conversation with people from Seneso.

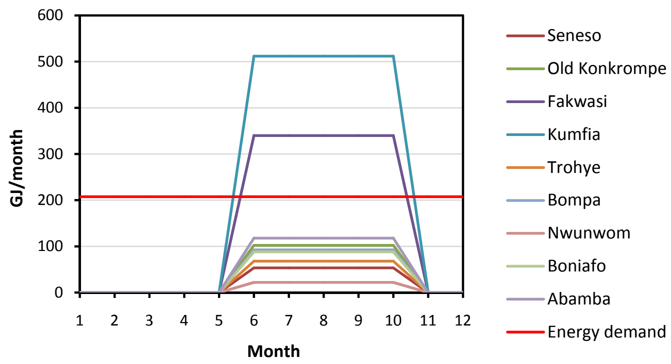

Figure 8.10: Seasonal cassava waste production and thermal power demand.

Technologies used and electricity demand

Biomass that goes to the gasifier must meet shape (chips) and MC requirements (20%), involving pre-treatment prior to use. Comparing with case studies 1 and 2, case study 3 counts with basic pre-treatment actions: drying and chipping. It is assumed that the only possible biomass storage is carried out before chipping and gasification, as on-field storage, being the cheapest and simplest option. Figure 8.11 shows the layout of the different pre-treatment processes applied to the biomass (BM). The biomass properties that change along the network are MC, shape and LHV, as in case study 1.

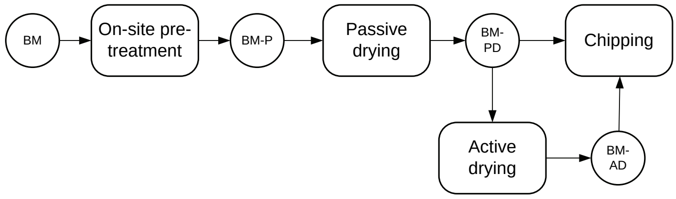

Figure 8.11: Pre-treatment activities layout for a generic biomass, in case study 3.

The main issues of each pre-treatment site as well as the main characteristics concerning transportation, by means of MC, DM and LHV, are summarised. The reported percentages and proportions are used to linearly model the activities in the mathematical formulation. It is assumed that the gasifier (therefore, all the network) works in average 8h/day and the project has a lifespan of 7 years (Stassen, 1995). The range of unit's capacity have been fixed by taking into account the processed maize in a MFP during one day and the total production of cassava estimated per year. The investment and O&M costs are taken from case study 2. No economies of scale are considered since the low electricity demand penalises the investment. In this first approach, a lineal estimation is regarded.

- On-site pre-treatment. In this task the biomass waste is generated. Here, the cassava is peeled and cut. The place of generation also serves as a place for on-site storage. Therefore, open air storage, in open air piles, is considered here.

The case of no coverage is assumed in contrast to case study 2.

- Drying. This stage contemplates passive or active drying. Passive drying is a consequence of the abovementioned open air storage. According to Hamelinck *et al.* (2003), storage at the roadside, for instance, is free, and has negligible O&M cost. If the raw biomass has a MC higher than 20%, dry matter loss per month is 3%, and MC loss per month is 2%. Figure 8.10 reveals the need of cassava storage. Dry matter and moisture content losses per month are calculated and introduced into the mathematical model. It is assumed a maximum period of storage of 12 months. Those calculations reveals that dry matter losses highly penalises the raw biomass waste: at the worst case, after 12 months of storage, cassava peels loss 95% of its thermal potential (resulting in a LHV of 680 MJ/kg). Active drying takes place into a rotatory drum. This unit is used to decrease the inlet MC till 20%, which is the humidity required before the gasification process. Biomass changes its MC and its LHV according to the tonnes of water evaporated. This unit has an energy efficiency of 99%. It consumes diesel as utility. The available capacities are between 0.1-5 t/h.

- Chipping. In this case study chipping is placed after drying, assuming location of chipping units close to the gasifiers, due to its electricity consumption. The electricity is provided by the gasifier. This unit has an energy efficiency of 96%. The available capacities are in the range of 0.1-5 t/h.

- BG-GE system. The microplant has an efficiency of 17% as calculated in Section 8.2.2. Concerning waste heat recovery issues, the Stirling engine will be used after the network resolution to evaluate growing demand possibilities, while heating water has no sense in Atebubu district context. The gasification units work in the range of 5 to 100 kW_e according to the enterprise *Ankur*.

- Transportation. Solid biomass can be displaced from its point of generation to a common storage place or to a pre-treatment node by tractors, within a capacity of 10 t for biomass[6]. Lineal distances are assumed between sites and they are expressed in km. A tortuosity factor of 1.5 is taken into account, which differs from the previous case study in Chapter 7, since road connexion in Atebubu district is more deficient.

- LV and MV networks. LV line is used if the electricity is produced and used at the same community. A MV line is used if the electricity is provided by a BG-GE microplant installed in another community. The LV distribution implies 5% losses on energy terms. It is assumed that there exists 1% additional energy loss in the gasifier itself. The MV distribution line takes into account losses estimated by Merino (2003), which are proportional to the power demand.

The economic evaluation is based on estimations of investment and annual O&M costs. It is assumed that the total capital requirement is spent only at the beginning of the project. Table 8.5 lists the parameters for costs estimation, including pre-treatment units, BG-GE plant and transportation. The diesel price is \$1133.31/t[7]. According to Serpagli *et al.* (2010), the electricity price in Brong Ahafo Region is

[6] On-field data and conversations with Mr. Jacob Salifu (WACSO).
[7] On-field data.

Table 8.5: Economic parameters for pre-treatment units, BG-GE plant, transportation and utilities consumption. Data from Hamelinck *et al.* (2003), Hamelinck and Faaij (2002), Ankur, KITE and WACSO.

	Base scale	Base investment	O&M (% of investment)	Utility consumption	Lifetime (yr)
Drying	100 t/h	M$10.5	3	$0.06 \cdot t_{H_2Oev}$ (t diesel)	15
Chipping	80 t/h	M$1.2	20	Bond law 0.15·t input (kW)	15
BG-GE microplant[2]	20 kW$_e$	M$0.05[1]	4		7
Transportation biomass		Tractor full $0.32/km·t	Loading and offloading $1.32/t		
MV network[3]		$5000/km			

[1] LV network costs are included here.
[2] CaO consumption is disregarded.
[3] Transformer cost is 1000€.

around $0.335/kWh. This case study assumes an electricity price of $0.233/kWh, as the value that the communities are willing to pay. It has been calculated by taken into account the consumption of diesel and batteries, with the subsequent prices, based on the community of Seneso.

The electricity demand, as the cassava production, has been estimated proportional to the population of each community. The values are based on a similar previous project, on rural electrification in a West Africa community, from the enterprise *Trama Technoambiental*. The demand estimate takes into account residential, community and commercial electricity requirements. The highest demand is 448.65 kWh/day from Kumfia, while the lowest is 21.17 kWh/day from Nwunwom. The demand has been assumed constant for all the year. The mathematical model is used at this point to predict the power that the raw material is able to satisfy: the results show that cassava peels can supply only a 25% of the estimated power need. Therefore, the optimisation procedure takes into account those adjusted power needs. These are 269.21 kWh/day for Kumfia, and 12.71 kWh/day for Nwunwom. The work by Al-Faris (2002) points out that communities in developing countries should be able to install sufficient power to meet the expected electricity demand: the supply in those countries are characterised by capacity constraints, and fast population growing. Figure 8.12 depicts the nine communities represented by their relative GJ/yr of demand, and in black, the locations selected for pre-treatment and treatment locations. Note that all the communities are considered as potential locations. Four more intermediate sites have been also defined as potential locations.

The time period t is a month. According to the number of biomass status s has 40 different states. In turn, j has 6 different states (in accordance with the different pre-treatment and treatment technologies, and transportation). i has 79 states depending on the couple biomass-activity (including transportation). f considers sites location, being overall 31 of them, by considering suppliers, pre-treatment and treatment possible locations and markets. This case study works with biomass mass.

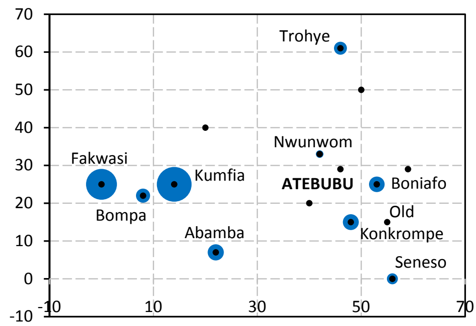

Figure 8.12: Communities representation by means of their relative energy demand. Black points mark the possible pre-treatment and treatment sites locations. Axes in km.

Environmental impact

Similar to case studies 1 and 2, the environmental impact is calculated from Impact 2002+ metric, evaluated in pts. Life cycle inventory (LCI) values are retrieved from LCI database Ecoinvent-V1.3 (2006) using B.V. (2004), and they are directly converted into Impact 2002+ mid-point indicators, which is the life cycle impact assessment (LCIA) step. The BSC associated and evaluated tasks are biomass production without transportation, transportation by tractors, pre-treatments and generation of electricity by means of biomass gasification, as listed in Table 8.6. This last column has been adapted from case study 1, according to the difference in efficiencies between an IGCC plant and the BG-GE microplant.

The project is evaluated for a planned horizon of 7 years, with yearly planning decisions. The interest rate is assumed at 5%, as in the previous case study. The model has been implemented in GAMS. The formulation of the SC-LCA model leads to a MILP with 26643 equations, 817547 variables. It takes a maximum of 1456 CPU seconds to reach a solution on a 2.0 GHz Intel Core 2 Duo computer using the MIP solver of CPLEX 9.0.

8.5.1 Results

The results presented here correspond to the three extremes of the Pareto frontier, according to the three selected criteria. Figure 8.13 depicts the network that *maximises the NPV*. Three types of matters, i.e. raw, dried and chipped matter, and no electricity, are transported between locations. The material fluxes among communities are shown: they may correspond to different periods, since the depicted networks represent the flux of matter for a year, while the modelled period contemplates months. Table 8.7 lists the calculated capacity of the equipments installed at the sites. The model recommends to install a BG-GE plant in each community but dispatches the needed pre-processing facilities in four sites: Fakwasi, Kumfia, Boniafo and Abamba. This shows that even though a BG-GE installation can provide more than one community, the demand is not high enough to motivate the implementation of a MV microgrid. The four sites with pre-processing units are strategically located to best handle the biomass of all the communities. The minimum chipping capacity is installed (10 t/h) in the three

Table 8.6: Environmental impacts in terms of Impact 2002+ metric, associated to SC tasks (Ecoinvent-V1.3, 2006), for case study 3.

Mid-point categories	Cassava peels (pts/t)	Chipper (pts/t)	Dryer (pts/t)	Transportation by tractor (pts/t·km)	Electricity generator (pts/GJ)
Carcinogens	$1.96\cdot10^{-5}$	$2.16\cdot10^{-6}$	$8.64\cdot10^{-6}$	$1.66\cdot10^{-6}$	0
Non-Carcinogens	$1.53\cdot10^{-5}$	$9.28\cdot10^{-6}$	$3.71\cdot10^{-5}$	$2.78\cdot10^{-5}$	0
Respiratory inorganics	$1.08\cdot10^{-3}$	$4.18\cdot10^{-4}$	$1.67\cdot10^{-3}$	$5.81\cdot10^{-5}$	$5.16\cdot10^{-3}$
Ionizing radiation	$3.12\cdot10^{-5}$	$6.03\cdot10^{-6}$	$2.41\cdot10^{-5}$	$1.78\cdot10^{-7}$	0
Ozone layer depletion	$1.00\cdot10^{-7}$	$1.23\cdot10^{-8}$	$4.93\cdot10^{-8}$	$5.38\cdot10^{-9}$	0
Respiratory organics	$3.71\cdot10^{-6}$	$6.01\cdot10^{-8}$	$2.40\cdot10^{-7}$	$7.98\cdot10^{-8}$	0
Aquatic ecotoxicity	$1.44\cdot10^{-6}$	$3.40\cdot10^{-7}$	$1.36\cdot10^{-6}$	$1.73\cdot10^{-7}$	0
Terrestrial ecotoxicity	$5.42\cdot10^{-5}$	$6.50\cdot10^{-6}$	$2.60\cdot10^{-5}$	$7.47\cdot10^{-5}$	0
Terrestrial acid/nutri	$1.67\cdot10^{-5}$	$5.75\cdot10^{-6}$	$2.30\cdot10^{-5}$	$9.12\cdot10^{-7}$	$1.71\cdot10^{-4}$
Land occupation	$2.6\cdot10^{-3}$	$1.30\cdot10^{-7}$	$5.20\cdot10^{-7}$	$1.18\cdot10^{-6}$	0
Aquatic acidification	0	0	0	0	0
Aquatic eutrophication	0	0	0	0	0
Global warming	$1.16\cdot10^{-3}$	$2.57\cdot10^{-4}$	$1.03\cdot10^{-3}$	$3.08\cdot10^{-5}$	$5.09\cdot10^{-2}$
Non-renewable energy	$1.65\cdot10^{-3}$	$3.22\cdot10^{-4}$	$1.29\cdot10^{-3}$	$3.21\cdot10^{-5}$	0
Mineral extraction	$6.05\cdot10^{-8}$	$2.96\cdot10^{-9}$	$1.19\cdot10^{-8}$	$1.55\cdot10^{-7}$	0

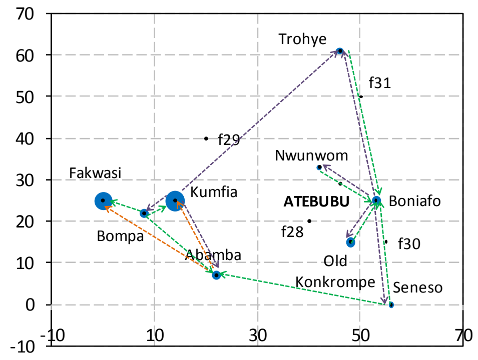

Figure 8.13: Optimum NPV network configuration for the BSC described in case study 3. See in green, the raw matter flow, in orange the dry matter flow and in purple the chipped matter flow.

Table 8.7: Equipment capacity for the optimum NPV BSC described in case study 3.

	Dryer (t/h)	Chipper (t/h)	BG-GE (MJ/h)
Seneso			18.00
Old Konkrompe			18.00
Fakwasi	0.13	0.10	40.44
Kumfia	0.21	0.10	51.34
Trohye			18.00
Bompa			18.00
Nwunwom			18.00
Boniafo	0.12	0.10	18.00
Abamba	0.10		18.00

communities, which is enough to process all the cassava peels. Therefore, Fakwasi, Kumfia, Boniafo and Abamba are centralised processing sites of cassava peels, being four of the five most populated communities. The purpose of the pre-treatment units located in Abamba is to dry enough biomass for its own consumption, as well as that for Fakwasi and Kumfia. The high investment costs associated to an intermediate site ($f28$ to $f31$), since the MV microgrid is needed, prevent their use. The results show that this case study requires from biomass storage in the view of supplying the constant electricity demand. The maximum storage is of 8 months.

Figure 8.14 shows the optimal configuration that *minimises Impact 2002+*. Table 8.9 provides the overview of the installed capacities. For this BSC network, material fluxes are characterised by chipped biomass. The units are installed by means of its minimum capacity at all the sites, except at the two largest, Fakwasi and Kumfia, which relies on adapted dryers and BG-GE units. Nwunwom, which is the smallest community, is not equiped with any pre-treatment unit. Therefore, satisfying the low demand of this community constitutes most of the biomass transportation efforts within the network. The transportation costs are minimised by means of the environmental impact optimisation. Analogously to the previous case, no MV microgrid is installed and the maximum storage period is 8 months.

The third network depicted *maximises the SoC*. In contrast to the two previous criteria, the model installs each type of unit at each location, thus maximising the

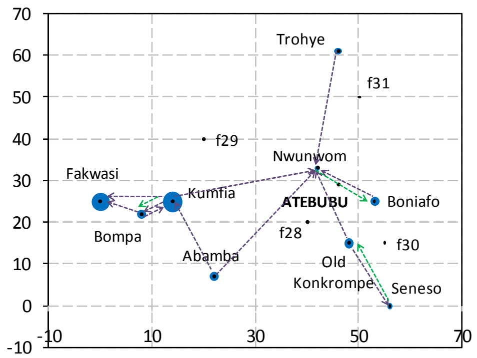

Figure 8.14: Optimum Impact 2002+ network configuration for the BSC described in case study 3. See in green, the raw matter flow, in orange the dry matter flow and in purple the chipped matter flow.

Table 8.8: Equipment capacity for the optimum Impact 2002+ BSC described in case study 3.

	Dryer (t/h)	Chipper (t/h)	Gasifier (MJ/h)
Seneso			18.00
Old Konkrompe	0.10	0.10	18.00
Fakwasi	0.12	0.10	40.44
Kumfia	0.17	0.10	51.34
Trohye	0.10	0.10	18.00
Bompa	0.10	0.10	18.00
Nwunwom			18.00
Boniafo	0.10	0.10	18.00
Abamba	0.10	0.10	18.00

number of working people involved in the project. Pre-treatment units are also installed at their minimum capacity, even for the largest communities. Therefore, the chipped material net is much more complicated than in the two previous networks. Fluxes of raw material exist to supply the largest communities, since they are not able to process all the biomass they need. Similarly to the optimised network for the environmental criterion, the BG-GE units are scaled to meet the demand in Fakwasi and Kumfia, the minimum available capacity being otherwise enough to supply locally the rest of the communities. The maximum storage period is again 8 months.

The following results compare the three optimal solutions. Table 8.10 summarises the three criteria evaluated for each optimal network. The economic value corresponding to the BSC configuration that maximises the NPV is -\$261212.6, which reveals the infeasibility of the project. This value is decreased by 10% in the environmental friendly network, and by 30% in the social network. The differences are mainly due to higher investment costs arising from the decrease on transportation and from the installation of all the units into each location, respectively. For the environmental parameter, it can be deduced that the difference among configurations mainly falls on transportation of pre-processed biomass. The Impact 2002+ value is reduced by 1.5 pts, i.e. 4%, if the LCA instead of the NPV is optimised. The environmental impact for the social BSC network is approximately the same than the optimal environmen-

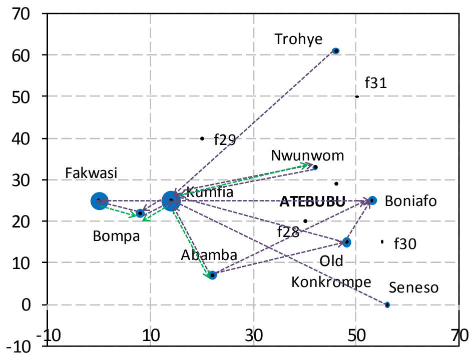

Figure 8.15: Optimum social network configuration for the BSC described in case study 3. See in green, the raw matter flow, in orange the dry matter flow and in purple the chipped matter flow.

Table 8.9: Equipment capacity for the optimum social BSC described in case study 3.

	Dryer (t/h)	Chipper (t/h)	Gasifier (MJ/h)
Seneso	0.10	0.10	18.00
Old Konkrompe	0.10	0.10	18.00
Fakwasi	0.10	0.10	40.44
Kumfia	0.10	0.10	51.34
Trohye	0.10	0.10	18.00
Bompa	0.10	0.10	18.00
Nwunwom	0.10	0.10	18.00
Boniafo	0.10	0.10	18.00
Abamba	0.10	0.10	18.00

tal impact. The maximum value for the social criterion is 27, installing 3 units per site. Intermediate sites ($f28$ to $f31$) are not used, since MV microgrids are not viable for such a range of electricity demand. The comparison between economic and social configurations focuses two extreme scenarios: (i) the capacity of the installed units is adapted to match the demand or, (ii) units are installed and then operated to meet the demand. Thus, minimal centralisation is needed in DES to ensure the sustainability of the network.

Figure 8.16 depicts the investment and the annual costs breakdown for each BSC optimised. Investment costs are \$104778, \$135296 and \$163899 for NPV, Impact 2002+

Table 8.10: Economic, environmental and social aspects for optimised networks.

NPV optimisation (\$)	-261212.6
Impact 2002+ (pts/yr)	38.4
Social criterion	16.0
NPV (\$)	-288090.6
Impact 2002+ optimisation (pts/yr)	36.8
Social criterion	23.0
NPV (\$)	-339819.5
Impact 2002+ (pts/yr)	36.9
Social optimisation	27.0

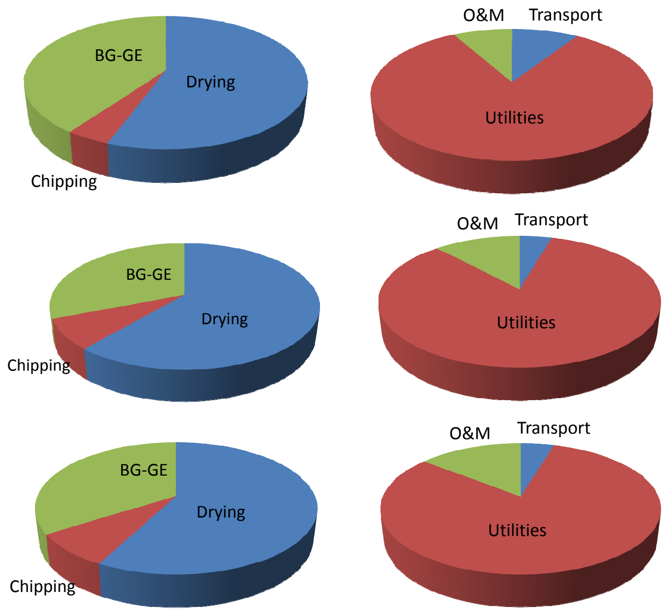

Figure 8.16: Breakdown of costs for NPV, Impact 2002+ and social optimised networks, respectively. Left side: investment share. Right side: annual costs share.

and social optimised scenarios, respectively. The utilities costs for each BSC are around \$44100/yr, which is too large in comparison with the investment. The reason is the diesel consumption of the dryer. The most relevant features that can be deduced from the breakdown of costs concern the penalisation in costs terms, derived from the installation of more units/capacity than the strictly needed, thus diminishing the transportation costs. Analogous observations can be retrieved from Figure 8.17, where the environmental impact is depicted per SC echelon. The contribution that changes the most among the optimised networks is that of transportation. Biomass pre-processing and electricity generation constitute the major share among contributions; the increase of the efficiency of these processes is crucial.

Table 8.11 lists environmental interventions: the NPV optimum solution has an environmental impact of 38.40 pts, whereas the Impact 2002+ optimum scenario has 36.80 pts and the social optimum network has 36.91 pts. The impacts for each damage category, i.e. human health, ecosystem quality, climate change and resources, are comparable. The highest impact is on climate change and constitutes 67% of the whole impact.

For comparison purposes and looking for a sustainable net able to supply the whole electricity demand of the communities in a viable way, an alternative case study has been defined. It is derived from the input conditions of case study 3. Here, the LHV_{ar} of cassava waste is hypothetically increased to 11.5 MJ/kg and seasonality is neglected. Moreover, the price of the electricity sold is \$0.335/kWh, the one for Atebubu district (Serpagli *et al.*, 2010). In Section 8.5 was pointed out that cassava peels were only able to supply a 25% of the predicted demand: under these assumptions, the model indicates that the overall demand estimated per community can be satisfied without storage.

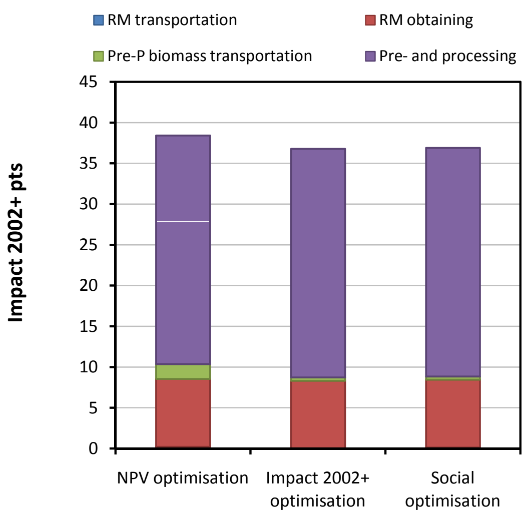

Figure 8.17: Distribution of environmental impacts for single objective optimisation solutions, according to the different SC activities (results per year).

Table 8.11: Environmental impacts arising from single objective function optimisation results, in Impact 2002+ pts (results per year).

End-point impact category	NPV optimisation	Impact 2002+ optimisation	Social optimisation
Human health	6.21	5.58	5.62
Ecosystem quality	4.19	3.64	3.67
Climate change	24.40	24.13	24.14
Resources	3.70	3.45	3.47
Impact 2002+	38.40	36.80	36.91

To study the distribution or the centralisation sensitivity of the potential network, instead of using the social criterion, this case study considers capacity restrictions on the BG-GE systems. Therefore, the case study is divided into two scenarios, one with a maximum capacity of 20 kW_e and other with 40 kW_e, which are in the range of the electricity demand.

In contrast to the original optimised networks, the solution passes through MV microgrids installation. The network configurations found that maximise the NPV and minimise the environmental impact are identical. Figures 8.18 and 8.19 detail the biomass fluxes and the electricity networks for each capacity installed. In the 20 kW_e scenario, the NPV is -M\$1.7, and the Impact 2002+ metric is 46 pts. The maximum capacity allowed per site is installed in almost all the communities. The network obtained is complex and expensive, and not economically viable. Production activities predominantly affect the environmental impact and transportation costs are very similar to the investment. Because the BG-GE system capacity is limited, the maximim equipment size is installed even in communities that do not need the produced electricity. This requires sending raw biomass to these locations for processing, which increases the transportation costs and further requires a microgrid. In the 40 kW_e scenario, the environmental impact is similar but the NPV differs, being M\$0.94. Due

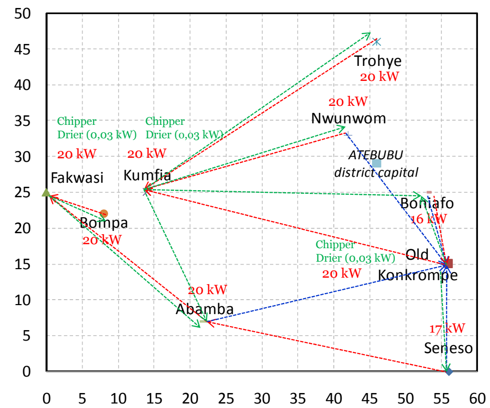

Figure 8.18: Optimum NPV and Impact 2002+ network configuration for 20 kW_e of maximum power allowed per site. Lines in blue are raw material fluxes, lines in green are processed biomass fluxes, and lines in red are needed MV grids.

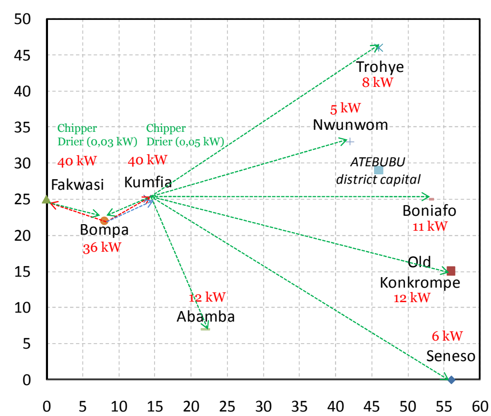

Figure 8.19: Optimum NPV and Impact 2002+ network configuration for 40 kW_e of maximum power allowed per site. Lines in blue are raw material fluxes, lines in green are processed biomass fluxes, and lines in red are needed MV grids.

to the allowed capacity, the resultant network configuration favours the self-supply of raw materials and electricity. The network is consequently highly distributed. Pre-processed biomass forms the basis of the connection between communities. Again, the highest environmental impact comes from the microplant activity, while the highest costs contribution is from investment.

Figure 8.20 analyses the effect of the electricity price on the optimised network considering the maximisation of the NPV, on the NPV itself. See that due to a decrease in the electricity price of 10%, the viability of the network breaks down. Therefore, prices lower than approximately \$0.3/kWh, would require a subsidy policy.

The optimal networks for this case study 3 variation, are completely different from the networks obtained using the original case study 3. The precise knowledge of the

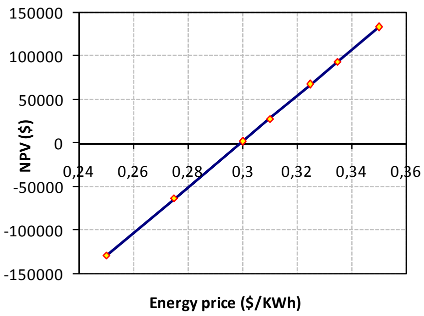

Figure 8.20: Electricity price vs. NPV for the BSC network optimised to obtain the maximum NPV.

raw material characteristics is mandatory to perform the final layout of the network. The thresholds for sustainability passes through a range of final product prices that should be known.

Implementation of waste heat recovery options would yield a more efficient BG-GE system, allowing a reduction of the environmental impact in the production echelon. A Stirling engine costs around $1143/kWh (Corria *et al.*, 2006) and would allow savings when combined with a gasification installation, since its minimum installed capacity can be as low as 1.5 kW_e and its relative cost is 20% lower than the cost of a new oversized gasifier.

8.6 Final remarks

This chapter has demonstrated the capabilities for a DES network design of the mathematical model described in Chapter 7. There does not exist any unique and global approach to tackle such a problem: the strategy must be adapted depending on the used raw material, the pre-treatment units and the final energy purpose. Case study 3 shows the cheap on-the-field storage of biomass is not favourable since it does not avoid high losses of matter. It suggests that advanced pre-treatment method, i.e. pelletisation, torrefaction or pyrolysis, should be used. Yet, it has been demonstrated that the implementation of such units, as commercialised in Western countries, can lead to oversized and unsustainable networks in developing countries. Distributed approaches should rely on a certain level of centralisation to be feasible on time, even if they may seek to favour the economy of the areas.

The trade-off between quality, understood as a high LHV and a low MC, and seasonality of the used raw material, the involvement of more or less advanced pre-treatment methods and the mitigation of matter degradation governs the capability to satisfy the demand and thus, to determine an optimal solution. Co-generation and tri-generation should be evaluated in future works, as an alternative to enhance the efficiency.

Notation

Latin letters

T	temperature

Greek symbols

η	efficiency

Superscripts and subindices

ar	as received basis
daf	dry and ash free basis
e	electric
$gasif$	gasification
i_r	interest rate
n	project life
th	thermal

Acronyms

BD	bulk density
BG	biomass gasification
BM	biomass
BTG	Biomass Technology Group
BSC	bio-based supply chain
CES	centralised energy systems
CC	combined cycle
CCS	carbon capture and storage
CGE	cold gas efficiency
CCHP	combined cooling, heat and power
CHP	combined heat and power
COE	cost of energy
DES	distributed energy systems
DM	dry matter
EO	equation-oriented
EOS	equation of state
FU	functional unit
GE	gas engine
GHG	greenhouse gas
HEN	heat exchangers network
HRSG	heat recovery steam generator
ICE	internal combustion engine
IGCC	integrated gasification combined cycle
KITE	Kumasi Institute of Technology, Energy and Environment
KNUST	Kwame NKrumah University of Science and Technology
LCA	life cycle assessment
LCI	life cycle inventory
LCIA	life cycle impact assessment
LHV	lower heating value
LV	low voltage
MC	moisture content
MFP	multi-functional platform
MILP	mixed integer linear programming
MV	medium voltage
NGO	non-governmental organisation
NPV	net present value
O&M	operation and maintenance

SC	supply chain
SCM	supply chain management
STE	Stirling engine
WACSO	Women and Children Support Organisation
WHB	waste heat boiler

Mathematical formulation

Indices

e	suppliers
f, f'	facility locations
i	tasks
j	equipment technology
s	materials (states)
t, t'	planning periods

Binary Variables

V_{jft}	1 if technology j is installed at location f in period t, 0 otherwise
$\mathscr{X}$	set of binary variables
$\mathscr{Y}$	set of continous variables

Continuous Variables

$DamC_{gft}$	normalized endpoint damage g for location f in period t
$DamC_g^{SC}$	normalized endpoint damage g along the whole SC
$Impact_f^{2002}$	total environmental impact for site f
SoC	social criterion value per site

Part III

Conclusions and Outlook

Chapter 9

Conclusions and Future Work

9.1 Conclusions

In the emerging bioenergy sector, new standards and legislation are needed to guarantee the sustainability of the biomass and to promote market implementation. The biomass potential of each country must be revealed and understood to develop efficient processing methods that satisfy energy needs while limiting environmental damage. Biomass wastes for energetic purposes are of special concern, because of land controversy reasons and residues disposal problems. This thesis investigates bioenergy along two main lines: centralised and distributed energy systems are evaluated in the light of engineering, economic, environmental and social aspects. Centralised and distributed energy systems place different constraints on the use of biomass. For large scale use, biomass can be adequately co-used with fossil fuels, for co-gasification or co-combustion in already existing power plants. Multiple products can be derived taking advantage from the syngas versatility. Polygeneration mimics the energy efficiency of oil refineries through the production of fuels, power and chemicals from biomass. For small scale use, such as residential applications in urban areas or electricity generation in rural areas, waste heat recovery is crucial to enhance the performance of the technology. At present, the use of biomass for micro-generation may only consider local resources and so neglect the possibility of an integrated resource networks, taking into account even international prospects. Tailor-made approaches are needed to account for the characteristics of each possible system and to provide appropriate optimal solutions from the available biomass and the energy demand.

This thesis has developed a systematic and versatile decision-making tool for biomass use at large and small scale, in different contexts. The methodology is based on conceptual design using modelling, simulation and optimisation techniques. On this basis, simulation and multiple criteria decision analysis are used to support the decision-making task. Decision-maker criteria selected in this thesis focus on (i) plant engineering, (ii) economic, (iii) environmental and (iv) social considerations. Those are, respectively, (i) different partial and global efficiency parameters, (ii) NPV, COE and

CO_2 metrics, (iii) a LCA approach with Impact 2002+ environmental metric and (iv) promotion of working places in the widest range of communities. With this framework and within the bounds of conceptual design, the preliminary design of biomass gasification projects can be systematically and consistently tackled, by discriminating the different process alternatives and retrofitting solutions of existing ones. The outcomes are the best type, scale and description of the bio-based network. The same approach and tools are used for centralised and distributed energy systems, showing that both schemes follow the same principles, despite their different characteristics. The modelling framework is implemented in Aspen Plus and Aspen Hysys , for the evaluation of mass and energy balances of the biomass-to-energy systems, and GAMS is used for the mathematical optimisation of the bio-based supply chain. Two base cases have been selected for the simulation of each energy system category: ELCOGAS IGCC power plant and the UPC BG-GE pilot plant layouts.

The Part I of this thesis provides a brief introduction to the subject, covering the key issues of the utilised approach. Then, a detailed overview of the state-of-the-art identifies the main trends and challenges of the bioenergy sector, followed by a description of the methods and tools used for its analysis.

Part II, composed by five chapters, starts with the superstructure conception and build-up with modelling gasification systems purposes. Chapters 4 and 5 focus on the detailed modelling and validation of the gasifier, the gas cleaning units, the combined cycle and the carbon capture and storage components. The simulated gasifier is a PRENFLO gasifier working at 1450°C and 25 bar, with a residence time of 7.7 s. The equilibrium model exhibits good agreement with ELCOGAS plant data. This validation highlights that model fitting is highly dependant on the specific gasification conditions (the agreement is better at higher temperatures and/or longer residence times) as well as on the raw materials introduced in the reactor. In this view, if co-gasification with biomass is of concern, tars and synergetic effects should be known to adequately represent the gasification behaviour. Feedstock composition must be considered to select the appropriate gasification agents and their proper amount. In contrast, gasifier temperature and pressure are somehow pre-fixed by the ashes melting point and the final syngas applications, respectively. The gas cleaning train embraces a venturi scrubber, a sour water stripper, a COS hydrolyser, an MDEA absorber and the Claus plant. CCS units in pre-combustion configuration, are performed by a WGS reactor, followed by a Rectisol process and a PSA system. The final CO_2 stream is compressed for geological storage. The combined cycle includes the gas and steam cycles to produce power, the HRSG and the waste heat recovery system to exploit the residual heat of the plant. The IGCC-CCS plant is integrated by means of steam and nitrogen nets. The complete modelling approach achieves discrepancies with experimental data lower than 10%, which is of sufficient accuracy for conceptual design.

After model validation, sensitivity analyses and multi-objective optimisations are performed to provide guidelines in co-gasification and co-production strategies, at a process system level. In Chapter 6, the multi-objective optimisation problem identifies the trade-off between techno-economic and environmental criteria in 25 scenarios, based on different feedstock mixtures and on topological changes. Those considerations comprise different coal, petcoke and biomass combinations, and electricity generation from syngas, electricity generation from H_2 and purified H_2 production without and with PSA purge gas use in the combined cycle. On the one hand, co-gasification analyses reveal that the oxygen inlet flow to the gasifier influences notably the IGCC plant performance, in contrast to the steam inlet flow, which mainly acts as a temperature moderator. Higher oxygen fractions lead to better combined cycle efficiency, but affect the gasification efficiency. Therefore, the overall efficiency of the system should be optimised depending on the final syngas use, that drives the characteristics of the syngas composition, or H_2/CO ratio. On the other hand, for topological changes, the feedstock compositions that produce the most electricity are also able to produce the highest hydrogen quantity. From an engineering point of view, the production of electricity based on H_2 combustion is the least efficient route. From an economic point of view, the most important investment is on the electricity generation section. For H_2 production, the highest investment concerns the CCS units or the gasification and ASU sections, depending on the feed type. The highest COE values are found for coal based cases, while petcoke and biomass shows nearly similar values.

The analysis of CO_2 metrics demonstrates that the use of coal will require of higher CO_2 market prices or higher government subsidies. Investigation from an environmental prospects reveals that the highest impact values are obtained for electricity production by means of coal, while the lowest is found for orujillo used to produce H_2. The production of electricity directly from syngas causes higher environmental impact than its production from H_2. This is mainly due the reduction of climate change impacts because of CO_2 capture. In the case of coal and petcoke, the production of fuels constitutes the largest share of the impact, while in the case of biomass use, IGCC operation is the most important aspect. Utilities use impacts are not significant, except for those cases of H_2 production, in which electricity from the grid is required. The Pareto frontier analyses reveal that the scenario with petcoke as feedstock for H_2 production with PSA purge gas use is the best in terms of techno-economic considerations. The scenario with residual biomass, in this case orujillo, without PSA purge gas use is the best in terms of lowest environmental damage. CCS technology implementation leads to an efficiency penalty of 8.7% of net power if H_2 is used in the combined cycle. To maintain the same power level than that obtained with the combustion of syngas, the feedstock should be increased by 21% on a mass basis. The integrated nature of the plant limits co-production.

The conceptual design framework and the superstructure notion are applied to propose and optimise two bio-based supply chains in Spain, which exemplifies co-gasification and co-combustion of biomass with coal in large gasification plants, in centralised energy systems. Co-combustion of biomass with coal is presented as the cheapest and most immediate bioenergy alternative. Chapter 7 describes the mathematical formulation of a bio-based supply chain, which is formulated as a multi-objective optimisation mixed integer linear program that embeds the NPV and the environmental impact by means of Impact 2002+ indicator. Supply chain case studies highlight, for Spain, the huge potential of biomass that can be optimally used to produce electricity and hydrogen by investing on new IGCC-CCS power plants, or to be co-combusted in the existing power plants. Case study 1 comprises different SC elements distributed over the country, finding the best 100% biomass large scale gasification plants allocation to produce electricity and hydrogen. The optimal NPV is around 230 M€ for a considered time period of 25 years. The sensitivity of the optimal solutions on changes in prices is demonstrated. The same network configuration can easily yield positive or negative NPV's depending on the product price. The price that equals the internal rate of return to the interest rate (8%) for the temporary horizon of 25 years is 0.129 €/kWh. Any price below this value would require a subsidy. For comparison purposes, this first supply chain is contrasted to another using coal as raw material. The NPV is 219% higher than the optimum NPV for the bio-based supply chain. This is due to the different investment and production costs, which are higher when pre-treatment activities are mandatory. Looking at environmental impacts, Impact 2002+ is 203% higher for the coal supply chain if compared with the bio-based supply chain. Case study 2 is focused on co-combustion of coal and biomass in already existing conventional thermal power plants aiming at obtaining the best biomass distribution chain. The emphasis here is placed on understanding the implication of solid and liquid biomass for pre-processed matter transportation comparison and on the clarification of the role of the subsidies in this sector while setting a possible coal substitution by means of locally available biomass. The pre-treatment techniques considered are torrefaction, pelletisation and fast pyrolysis. The results reveal that Spanish power plants can substitute their coal consumption by 15% on an inlet thermal basis that is the mechanical limit allowed, while important amount of biomass waste still remain unused. This action would require a subsidy or an electricity price increases of 20.25%. The involved investment is about 1640 M€. The chosen pre-treatment is torrefaction combined with pelletisation.

The superstructure developed for large-scale gasification is adapted to small-scale in Chapter 8. The process modelling reveals that the BG-GE system has an efficiency of 17%, which is susceptible to be increased to 27% by incorporating a Stirling engine and heating water application. In the field of micro-generation, the proposed plants can be used in residential applications and for rural electrification. A supply chain in a specific community from Ghana is proposed and optimised in the framework of rural electrification. The case study contemplates 9 communities and an overall electricity demand of 118 MWh/yr, to be satisfied by cassava peels. This biomass waste has a huge amount of moisture content, 66%, and is characterised here by its seasonality. The pre-treatments taken into account are open air storage, drying and chipping, since the BG-GE plant requires raw material in the shape of chips with a moisture content of 20%. Multi-objective optimisation contemplates NPV, Impact 2002+ and social criteria optimisations. The social criterion promotes the implementation of the maximum number of units, in order to promote working places. The results reveal an unviable network, with a NPV of $-261212.6, an Impact 2002+ of 36.8 and a social parameter of 27, for each optimised point of view. The main causes of unviability of the project approach can be attributed to the need of storage to supply the demand, of a low quality biomass resource, without the usage of an advanced pre-treatment to enhance the biomass properties to be stored. It is demonstrated that the units commercialised in Western countries, can lead to oversized and not sustainable networks in developing countries. From the resulting networks, distributed approaches need a certain level of centralisation to be feasible on time. The same case study, with modified assumptions on the LHV and the seasonality of the biomass waste, can result in a viable bio-based network to be implemented. This shows that an unique and global approach to tackle a DES network design may not be possible to develop, and that each problem should be tackled by its own characteristics and context. The precise knowledge of the raw material characteristics is mandatory to perform the final layout of the network. The thresholds for sustainability passes through a range of final product prices that should be known.

Bioenergy complies with the requirement of the emerging energy paradigm: it offers decisive advantages in terms of environmental and social impacts. Its deployment is already straightforward to support with current energy conversion technologies. Challenges concern the improvement of biomass pre-treatment processes and storage, to meet the standards for energy generation. Despite all the striking advantages, biomass conversion, combined with carbon capture and storage needs political incentives to enter definitely and extensively the market, as would be the case for any energy conversion alternative.

9.2 Future work

The greatest opportunities identified in this thesis are from the emerging nature of IGCC-CCS systems and BG-GE projects, and from the potential of biomass as a resource. Despite these results, the bioenergy topic still offers a wide range of challenges for future research work. The propositions here can be seen as steps following the work completed in this thesis.

- The IGCC-CCS model can be enlarged for other syngas promising applications such as Fischer-Tropsch process, or synthetic natural gas. Processes intensification and hot gas cleaning can be included to enhance the plant efficiency. CCS is an emerging sector not only in the energy sector, but also in the industrial sector. The developed model can be adapted to provide guidance in industrial CCS development.

- Alternatives to exploit waste heat recovery in BG-GE systems must be investigated further. These comprise for instance adding engine models, with a special attention on the heat streams. The BG-GE model can be enlarged to evaluate the performance with fuel cells. Tars behaviour should be studied and modelled.

- MILP formulation must be enlarged with additional or refined performance indicators, and potentially switched to MINLP. Emergent issues in the bioenergy field may contemplate emissions trade and hybrid systems with biomass and other renewable sources. Extensive efforts are needed on the determination of social objectives.

- There is a crucial need for more accurate and experimentally-validated biomass properties calculation procedures, to capture and predict correctly the effects of biomass type combinations, degradation during storage and seasonality. This will enable to propose better strategies to increase the effective availability of biomass, thus better track the demand.

- Transport policies and taxes, along with their specificities among countries must be better modelled. This requires forcing the link between engineering and political/social aspects.

- Optimal configurations may not use all the available biomass waste for energy generation. The remaining amount can serve for other purposes, which highlights business and trade opportunities at local or international scale. This could be tackeld using a model of an extended huge supply chain.

Appendixes

Appendix A

Publications

This is a list of the works carried out within the scope of this thesis.

A.1 Journal publications

M. Pérez-Fortes, J.M. Laínez-Aguirre, A.D. Bojarski, L. Puigjaner, Bio-based supply chain modelling for biomass co-combustion in thermal power plants. Biomass and Bioenergy (submitted for publication).

Publications submitted after invitation:

M. Pérez-Fortes, A.D. Bojarski, L. Puigjaner, Advanced simulation environment for clean power production in IGCC plants. Computers & Chemical Engineering, 33 (12) (2011).

M. Pérez-Fortes, A.D. Bojarski, E. Velo, J.M. Nougués, L. Puigjaner, Conceptual model and evaluation of generated power and emissions in an IGCC plant. Energy, 34 (2009), 1721-1732.

A.2 Book chapters

Contributions to books were provided after invitation:

L. Puigjaner, Syngas from waste: Emerging Technologies (2011). Springer-Verlag, London, UK (in press). Contributions in 7 of 13 chapters:

- Chapter 3: Raw materials supply. Authors: J.M. Laínez, M. Pérez-Fortes, A.D. Bojarski, L. Puigjaner.
- Chapter 4: Modelling syngas generation. Authors: M. Pérez-Fortes, A.D. Bojarski.

- Chapter 5: Main purification operations. Authors: M. Pérez-Fortes, A.D. Bojarski.
- Chapter 8: Modelling superstructure for conceptual design of syngas generation and treatment. Authors: A.D. Bojarski, M. Pérez-Fortes, J.M. Nougués, L. Puigjaner.
- Chapter 10: Global clean gas process synthesis and optimisation. Authors: M. Pérez-Fortes, A.D. Bojarski.
- Chapter 11: Selection of best designs for specific applications. Authors: A.D. Bojarski, M. Pérez-Fortes.
- Chapter 13: Industrial data collection. Authors: A.D. Bojarski, C.R. Álvarez, M. Pérez-Fortes, P. Coca.

M. Pérez-Fortes, A. Bojarski, E. Velo, L. Puigjaner, IGCC Power Plants: Conceptual Design and Techno-Economic Optimization chapter in: Clean Energy: Resources, Production and Developments, Editor: Harries, A.D. Series: Energy Science, Engineering and Technology (2010). Nova Science Publishers Hauppauge NY, USA.

A.3 Congresses

A.3.1 Contributed talks

M. Pérez-Fortes, P. Arranz-Piera, J.M. Laínez, E. Velo, L. Puigjaner, Optimal location of gasification plants for electricity production in rural areas. *21st European Symposium on Computer Aided Process Engineering - ESCAPE 21*, Chalkidiki, Greece, 29 May - 1st June, 2011.

M. Pérez-Fortes, A. Bojarski, L. Puigjaner, Co-Production of Electricity and Hydrogen from Coal and Biomass Gasification. *14th International Conference on Process Integration, Modelling and Optimisation for Energy Saving and Pollution Reduction - PRES*, Florence, Italy, 8-11 May, 2011.

M. Pérez-Fortes, A. Bojarski, J.M. Nougués, L. Puigjaner, Integrated tool for IGCC power plants design. *AIChE 2009 Annual Meeting*, Nashville, Tennessee, USA, November 8-13, 2009.

M. Pérez-Fortes, A. Bojarski, S. Ferrer-Nadal, C.R Álvarez, G. Kopanos, J.M. Nougués, E. Velo, L. Puigjaner, Conceptual model and evaluation of generated power and emissions from an integrated gasification combined cycle power plant. *CHISA 2008*, Prague, Czech Republic, August 24-28, 2008.

M. Pérez-Moya, M. Pérez-Fortes, E. Capón, A. Calvet, E. Boada, M. Graells, Active learning evaluation in the framework of Lab Project Management *ICEE 2008, International Conference on Engineering Education*, Pécs-Budapest, Hungary, July 28-31, 2008.

M. Pérez-Fortes, A. Bojarski, S. Ferrer-Nadal, G. Kopanos, J.M. Nougués, E. Velo, L. Puigjaner, Valorization of waste in a gasification plant for clean power production. *Clean Technology, 2008*, Boston, Massachusetts, USA, June 1-5, 2008.

M. Pérez-Fortes, A. Bojarski, S. Ferrer-Nadal, G. Kopanos, J.M. Nougués, E. Velo, L. Puigjaner, Enhanced Modeling and Integrated Simulation of Gasification and Purification Gas Units targeted to Clean Power Production. *18th European Symposium on Computer Aided Process Engineering (ESCAPE 18)*, Lyon, France, USA, June 1-4, 2008.

M. Pérez-Fortes, A. Bojarski, S. Ferrer-Nadal, G. Kopanos, N. Mitta, C.A. Pinilla, J.M. Nougués, E. Velo, L. Puigjaner, Conceptual Modeling and Simulation of an Entrained Bed Gasifier Reactor. *AIChE 2007 Annual Meeting*, Salt Lake City, Utah, USA, November 4-9, 2007.

M. Pérez-Fortes, A. Bojarski, E. Velo, L. Puigjaner, Modeling and Analysis of Improved Sour Water Stripping System. *2nd International Congress of Energy and Environment Engineering and Management (IICIIEM 2007)*, Badajoz, June 6-8, 2007.

A.3.2 Poster presentations

M. Pérez-Fortes, P. Arranz-Piera, J.M. Laínez, E. Velo, L. Puigjaner, Bio-based sustainable supply chain modelling for rural electrification. *19^{th} European Biomass Conference and Exhibition - EU BC& E*, Berlin, Germany, 6-9 June, 2011.

B. Escorcia, C. Cuba, M. Pérez-Fortes, P. Arranz-Piera, A. Espuña, E. Velo, Small scale BIO-CHP systems; pilot plant approach. *19^{th} European Biomass Conference and Exhibition - EU BC& E*, Berlin, Germany, 6-9 June, 2011.

M. Pérez-Fortes, P. Arranz-Piera, J.M. Laínez, E. Velo, L. Puigjaner, Biomass supply chain model for rural electrification. *AIChE 2010 Annual Meeting*, Salt Lake City, Utah, USA, November 7-12, 2010.

A. Bojarski, M. Pérez-Fortes, E. Velo, L. Puigjaner, Life Cycle Assessment of Integrated Gasification Power Plants: Conceptual Design and Techno-Economic Evaluation. *23rd International Conference on Efficiency, Cost, Optimization, Simulation and Environmental Impact of Energy Systems (ECOS2010)*, Lausanne, Switzerland, June 14-17, 2010.

M. Pérez-Fortes, A. Bojarski, E. Velo, L. Puigjaner, Biomass and waste gasification: feasible contributions in industrialized and rural areas. *17th European Biomass Congress*, Hamburg, Germany, June 29-July 3, 2009.

M. Pérez-Fortes, E. Capón-García, L. Puigjaner, Statistical models for pollutants forecasting in urban areas. *11th Mediterranean Congress of Chemical Engineering*, Barcelona, Spain, October 21-24, 2008.

M. Pérez-Moya, M. Pérez-Fortes, E. Capón-García, A. Calvet, E. Boada, M. Graells, Competences evaluation criterion in the field of chemical engineering lab. *11th Mediterranean Congress of Chemical Engineering*, Barcelona, Spain, October 21-24, 2008.

G. Kopanos, J.M. Laínez, M. Pérez-Fortes, L. Puigjaner, Biomass for Energy Production Supply Chain Network Design. *11th Mediterranean Congress of Chemical Engineering*, Barcelona, Spain, October 21-24, 2008.

M. Pérez-Fortes, A. Bojarski, S. Ferrer-Nadal, G. Kopanos, N. Mitta, C.A. Pinilla, J.M. Nougués, E. Velo, L. Puigjaner, CAPE-OPEN - Aspen based mathematical modeling for integrated simulation of an entrained bed gasifier. *6th European Congress of Chemical Engineering (ECCE-6)*, Copenhagen, Denmark, September 16-21, 2007.

M. Pérez-Fortes, A. Bojarski, S. Ferrer-Nadal, G. Kopanos, N. Mitta, C.A. Pinilla, J.M. Nougués, E. Velo, L. Puigjaner, Enhanced Model for Integrated Simulation of an Entrained Bed Gasifier Implemented as Aspen Hysys Extension. *2007 International Conference on Coal Science and Technology (2007ICCS&T)*, Nottingham, August 28-31, 2007.

A.3.3 Participation in research projects

AGAPUTE, *Advanced GAs PUrification TEchnologies for co-gasification of coal, refinery by-products, biomass & waste, targeted to clean power produced from gas & steam turbine generator set fuel cells*, supported by the European Community (RFC-CR-04006), 2004-2008.

EHMAN, *Extendiendo los horizontes productivos frente a la paradoja de la integración*, supported by the MICINN with the ERD Funds, (DPI2009-09386), 2010-2012.

MICROTEACHING, *Modular Teaching and Learning Solutions for a needs based education*, supported by Leonardo da Vinci program, European Community (2004-146 157), 2004-2007.

Bibliography

Abdullah, H., D. Mourant, C.Z. Li, & H. Wu. "Bioslurry as a Fuel 3. Fuel and Rheological Properties of Bioslurry Prepared from the Bio-oil and Biochar of Mallee Biomass Fast Pyrolysis." *Energy Fuels* 24: (2010) 5669–5676.

Abe, H., A. Katayama, P.S. Bhuwneshwar, T. Toriu, S. Samy, P. Pheach, M.A. Adams, & P.F. Grierson. "Potential for rural electrification based on biomass gasification in Cambodia." *Biomass and Bioenergy* 31: (2007) 656–664.

Al-Faris, A.R.F. "The demand for electricity in the GCC countries." *Energy Policy* 30: (2002) 117–124.

Altafini, C.R., P.R. Wander, & R.M. Barreto. "Prediction of the working parameters of a wood waste gasifier through an equilibrium model." *Energy Conversion and Management* 44: (2003) 2763–2777.

Andrade, C.S., L.P. Rosa, & N.F. da Silva. "Generation of electric energy in isolated rural communities in the Amazon Region. A proposal for the autonomy and sustainability of the local populations." *Renewable and Sustainable Energy Reviews* 15: (2011) 493–503.

Ansolabehere, S., J. Beer, J. Deutch, A.D. Ellerman, S.J. Friedmann, H. Herzog, H.D. Jacoby, P.L. Joskow, G.J. McRae, R. Lester, E.J. Moniz, E. Steinfeld, & J. Katzer. "The Future of Coal. A interdisciplinary study." *Massachusetts Institute of Technology.* Http://web.mit.edu/coal/.

Anthony, D.B., & J.B. Howard. "Coal Devolatilization and Hidrogasification." *AIChE Journal* 22: (1976) 625.

Arena, U., L. Zaccariello, & M.L. Matellone. "Fluidised bed gasification of waste-derived fuels." *Waste Management* 30: (2010) 1212–1219.

AspenTech. "Aspen Plus user's guide." Technical report, AspenTech INC, 2010.

Attoh, S.A. *Geography of Sub-Saharan Africa.* Prentice Hall, 2010, 3rd Edition.

Ayoub, N., H. Seki, & Y. Naka. "Superstructure-based design and operation for bimoass utilization networks." *Computers and Chemical Engineering* 33: (2009) 1770–1780.

Badzioch, S., & P.G.W. Hawsley. "Kinetics of Thermal Decomposition of Pulverized Coal Particles." *Industrial & Engineering Chemistry Process Design and Development* 9, no. 4: (1970) 521–530.

Baliban, R.C., J.A. Elia, & C.A. Floudas. "Toward Novel Hybrid Biomass, Coal, and Natural Gas Processes for Satisfying Current Transportation Fuel Demands, 1: Process Alternatives, Gasification Modeling, Process Simulation, and Economic Analysis." *Industrial and Engineering Chemistry Research* 49: (2010) 7343–7370.

Bassily, A. M. "Modeling, numerical optimization, and irreversibility reduction of a dual-pressure reheat combined-cycle." *Applied Energy* 81, no. 2: (2005) 127–151.

Basu, P., J. Butler, & M.A. Leon. "Biomass co-firing options on the emission reduction and electricity generation costs in coal-fired power plants." *Renewable Energy* 36: (2011) 282–288.

Baxter, L. "Biomass-coal co-combustion: opportunity for affordable renewable energy." *Fuel* 84: (2005) 1295–1302.

Bayod, A.A., J. Mur, J.L. Bernal, & J.A. Domínguez. "Definitions for distributed generation: a revision." In *International Conference on renewable Energies and Power Quality*. Zaragoza, Spain, 2005.

Bergman, P.C.A., A.R. Boersma, R.W.R. Zwart, & J.H.A. Kiel. "Torrefaction for biomass co-firing in existing coal-fired power stations." Technical report, Energy research Centre of the Netherlands, ECN, 2005.

Berkes, F., & C. Folke. *Linking social and ecological systems: management and practices and social mechanisms*. Cambridge, UK: Cambridge University Press, 2000, 1st Edition.

Berndes, G., J. Hansson, A. Egeskog, & F. Johnsson. "Strategies for 2nd generation biofuels in EU - Co-firing to stimulate feedstock supply development and process integration to improve energy efficiency and economic competitiveness." *Biomass and Bioenergy* 34: (2010) 227–236.

Biagini, E., L. Masoni, & L. Tognotti. "Comparative study of thermochemical processes for hydrogen production from biomass fuels." *Bioresource Technology* 101: (2010) 6381–6388.

Biegler, L.T., I.E. Grossmann, & A.W. Westerberg. *Systematic methods of chemical process design*. Prentice Hall, Upper Saddle River (New Jersey), 1997.

Blunck, M., & E. Dimpl. "Small-scale Electricity Generation from Biomass: Experience with Small-scale Technologies for Basic Energy Supply. Part I: Biomass Gasification." Technical report, GTZ-HERA Poverty-oriented basic energy services, 2010.

Bojarski, A.D. *Life Cycle Thinking and General Modelling contribution to Chemical Process Sustainable Design and Operation*. Ph.D. thesis, UPC, Barcelona, Spain, 2010.

Borel, L., & D. Favrat. *Thermodynamics And Energy Systems Analysis: From Energy To Exergy*. EPFL Press, 2010, 1st english Edition.

Bouffard, F., & D.S. Kirschen. "Centralised and distributed electricity systems." *Energy Policy* 36: (2008) 4504–4508.

Brammer, J.G., & A.V. Bridgwater. "The influence of feedstock drying on the performance and economics of a biomass gasifier-engine CHP system." *Biomass and Bioenergy* 22: (2002) 271–281.

Mechanical wood products branch, FAO forestry department, Forest industries division. "Wood gas as engine fuel." Technical Report FAO forestry paper 72, Food and Agriculture organization of the United Nations (FAO), Italy, 1986.

Bre-Hammond, A., & A. Crole-Rees. "Reducing rural poverty through increased access to energy services." Technical report, United Nations Development Programme, Bamako, Mali, 2004.

Brent, A.C., & W.J.L. Kruger. "Systems analyses and the sustainable transfer of renewable energy technologies: A focus on remote areas of Africa." *Renewable Energy* 34: (2009) 1774–1781.

Bridgwater, A. V. "Renewable fuels and chemicals by thermal processing of biomass." *Chemical Engineering Journal* 91: (2003) 87–102.

Bridgwater, A.V., A.J. Toft, & J.G. Brammer. "A techno-economic comparison of power production by biomass fast pyrolysis with gasification and combustion." *Renewable and Sustainable Energy Reviews* 6: (2002) 181–248.

Brown, D., M. Gassner, T. Fuchino, & F. Maréchal. "Thermo-economic analysis for the optimal conceptual design of biomass gasification energy conversion systems." *Applied Thermal Engineering* 29: (2009) 2137–2152.

Buragohain, B., P. Mahanta, & V.S. Moholkar. "Biomass gasification for decentralized power generation: The Indian perspective." *Renewable and Sustainable Energy Reviews* 14: (2010) 73–92.

B.V., PRé Consultants. "SimaPro 6 LCA software." *The Netherlands* www.pre.nl/simapro/default.htm.

Capros, P., L. Mantzos, N. Tasios, A. De Vita, & N. Kouvaritakis. "EU trends to 2030: update 2009." Technical report, Directorate-General for Energy and the Directorate-General for Climate Action - European Comission, 2010.

Caputo, A.C., M. Palumbo, P.M. Pelagagge, & F. Scacchia. "Economics of biomass energy utilization in combustion and gasification plants: effects of logistics variables." *Biomass and Bioenergy* 28: (2005) 35–51.

Chauhan, S. "Biomass resources assessment for power generation: A case study from Haryana state, India." *Biomass and Bioenergy* 34: (2010) 1300–1308.

Chen, C., & E. S. Rubin. "CO2 control technology effects on IGCC plant performance and cost." *Energy Policy* 37, no. 3: (2009) 915–924.

Cherni, J.A., I. Dyner, F. Henao, P. Jaramillo, R. Smith, & R.O. Font. "Energy supply for sustainable rural livelihoods. A multi-criteria decision-support system." *Energy Policy* 35: (2007) 1493–1504.

Cherubini, F., & A.H. Stromman. "Life cycle assessment of bioenergy systems: State of the art and future challenges." *Bioresource Technology* 102: (2011) 437–451.

Chiaramonti, D., A. Oasmaa, & Y. Solantausta. "Power generation using fast pyrolysis liquids from biomass." *Renewable and Sustainable Energy Reviews* .

Chiesa, P., G. Lozza, & L. Mazzocchi. "Using hydrogen as gas turbine fuel." *Journal of Engineering For Gas Turbines and Power-transactions of the Asme* 127, no. 1: (2005) 73–80.

Coca, M.T. "Tecnología de gasificación integrada en ciclo combinado: GICC. Aplicación real en España: ELCOGAS." Technical report, ENERCLUB, Puertollano, Ciudad Real, Spain, 2003.

Cockroft, J., & N. Kelly. "A comparative assessment of future heat and power sources for the UK domestic sector." *Energy Conversion and Management* 47: (2006) 2349–2360.

Corria, M.E., V.M. Cobas, & E.S. Lora. "Perspectives of Stirling engines use for distributed generation in Brazil." *Energy Policy* 34: (2006) 3402–3408.

Couhert, C., S. Salvador, & J.M. Commandré. "Impact of torrefaction on syngas production from wood." *Fuel* 88: (2009) 2286–2290.

Council, Gasification Technologies. "Gasification: redefining clean energy ." Technical report, (GTC), 2008. Http://www.gasification.org/Docs/Final_whitepaper.pdf.

Damen, K., & A. Faaij. "A greenhouse gas balance of two existing international biomass import chains. The case of residue co-firing in a pulverised coal-fired power plant in The Netherlands." *Mitigation and Adaptation Strategies for Global Change* 11: (2006) 1023–1050.

Demirbas, M.F. "Biorefineries for biofuel upgrading: A critical review." *Applied Energy* 86: (2009) 151–161.

Deng, J., G.J. Wang, J.H. Kuang, Y.L. Zhang, & Y.H. Luo. "Pretreatment of agricultural residues for co-gasification via torrefaction." *Journal of Analytical and Applied Pyrolysis* 86: (2009) 331–337.

Descamps, C., C. Bouallou, & M. Kanniche. "Efficiency of an Integrated Gasification Combined Cycle (IGCC) power plant including CO2 removal." *Energy* 33, no. 6: (2008) 874–881.

Desideri, U., & A. Paolucci. "Performance modelling of a carbon dioxide removal system for power plants." *Energy Conversion and Management* 40, no. 18: (1999) 1899–1915.

Di Blasi, C. "Dynamic behaviour of stratified downdraft gasifiers." *Chemical Engineering Science* 55: (2000) 2931–2944.

Dogru, M., C.R. Howarth, G. Akay, B. Keskinler, & A.A. Malik. "Gasification of hazelnut shells in a downdraft gasifier." *Energy* 27: (2002) 415–427.

Dong, L., H. Liu, & S. Riffat. "Development of small-scale and micro-scale biomass-fuelled CHP systems - A literature review." *Applied Thermal Engineering* 29: (2009) 2119–2126.

Dornburg, V., & A.P.C. Faaij. "Efficiency and economy of wood-fired biomass energy systems in relation to scale regarding heat and power generation using combustion and gasification technologies." *Biomass and Bioenergy* 21: (2001) 91–108.

Doty, S., & W.C. Turner. *Energy Management Handbook*. The Fairmont Press, Inc. and CRC Press (Taylor & Francis Group, 2009, 7th Edition.

Douglas, J.M. *Conceptual design of chemical processes*. McGraw-Hill Chemical Engineering Series, 1988.

ECN-Biomass. "Phyllis, database for biomass and waste." http://www.ecn.nl/phyllis, 2010.

Ecoinvent-V1.3. "The Ecoinvent database V1.3." Technical report, Swiss Centre for Life Cycle Inventories, 2006.

Elia, J., R.C. Baliban, & C.A. Floudas. "Toward Novel Hybrid Biomass, Coal, and Natural Gas Processes for Satisfying Current Transportation Fuel Demands, 2: Simultaneous Heat and Power Integration." *Industrial and Engineering Chemistry Research* 49: (2010) 7371–7388.

Elrich, C., & T.H. Fransson. "Downdraft gasification of pellets made of wood, palm-oil residues respective bagasse: Experimental study." *Applied Energy* 88: (2011) 899–908.

Emun, F., M. Gadalla, T. Majozi, & D. Boer. "Integrated gasification combined cycle (IGCC) process simulation and optimization." *Computers & Chemical Engineering* 34, no. 3: (2009) 331–338.

Faaij, A.P.C. "Bio-energy in Europe: changing technology choices." *Energy Policy* 34: (2006) 322–342.

Fang, K., R. Li, & A. Sudjianto. *Design and modeling for computer experiments*. FL, USA: Chapman & Hall/CRC Taylor & Francis Group, 2006, 1st Edition.

Fermoso, J., B. Arias, M.V. Gil, M.G. Plaza, C. Pevida, J.J. Pis, & F. Rubiera. "Co-gasification of different rank coals with biomass and petroleum coke in a high-pressure reactor for H_2-rich gas production." *Bioresource Technology* 101: (2010) 3230–3235.

Fermoso, J., B. Arias, M.G. Plaza, C. Pevida, F. Rubiera, J.J. Pis, F. García-Peña, & P. Casero. "High-pressure co-gasification of coal with biomass and petroleum coke." *Fuel Processing Technology* 90: (2009) 926–932.

Ferrer-Martí, L., R. Pastor, & G.M. Capó. "Un modelo de ubicación de microaerogeneradores para el diseño de proyectos de electrificación rural con energía eólica." 3rd Internationala Conference on Industrial Engineering and Industrial Management, 2009.

Fiedorow, R., R. Leaute, & I.G.D. Lana. "A study of the kinetics and mechanism of COS hydrolysis over alumina." *Journal of Catalysis* 85, no. 2: (1984) 339–348.

Fleskens, L., & J. de Graaff. "Conserving natural resources in olive orchards on sloping land: Alternative goal programming approaches towards effective design of cross-compliance and agri-environmental measures." *Agricultural Systems* 103: (2010) 521–534.

Forsberg, G. "Biomass energy transport: Analysis of bioenergy transport chains using life cycle inventory method." *Biomass and Bioenergy* 19: (2000) 17–30.

Frey, H. C., & Y. H. Zhu. "Improved system integration for integrated gasification combined cycle (IGCC) systems." *Environmental Science & Technology* 40, no. 5: (2006) 1693–1699.

Frey, H.C. *Probabilistic modeling of innovative clean coal technologies: implications for* *research planning and technology evaluation.* Ph.D. thesis, Carnegie Mellon University, Pennsylvania, USA, 1991.

Frey, H.C., & N. Akunuri. "Probabilistic Modeling and Evaluation of the Performance, Emissions, and Cost of Texaco Gasifier-Based Integrated Gasification Combined Cycle Systems Using ASPEN." Technical report, Computational Laboratory for Energy, Air, and Risk. Department of Civil Engineering. North Carolina State University, 2001.

García-Labiano, F., & J. Adánez. "Sulphur release during the devolatilization of large coal particles." *Fuel* 75, no. 5: (1996) 585–590.

Gassner, M., & F. Maréchal. "Methodology for the optimal thermo-economic, multi-objective design of thermochemical fuel production from biomass." *Computers & Chemical Engineering* 33, no. 3: (2009a) 769–781.

———. "Thermo-economic process model for thermochemical production of Synthetic Natural Gas (SNG) from lignocellulosic biomass." *Biomass & Bioenergy* 33, no. 11: (2009b) 1587–1604.

Gautam, G., S. Adhikari, & S. Bhavnani. "Estimation of Biomass Synthesis Gas Composition using Equilibrium Models." *Energy Fuels* 24: (2010) 2692–2698.

Ghosh, D., A.D. Sagar, & V.V.N. Kishore. "Scaling up biomass gasifier use: an application-specific approach." *Energy Policy* 34: (2006) 1566–1582.

Giampaolo, T. *Gas Turbine Handbook, Principles and Practice.* Fairmont Press, 2006, 3rd Edition.

Giltrap, D.L., R. McKibbin, & G.R.G. Barnes. "A steady state model of gas-char reactions in a downdraft biomass gasifier." *Solar Energy* 74: (2003) 85–91.

Gómez, A., M. Rodrigues, C. Montañés, C. Dopazo, & N. Fueyo. "The potential for electricity generation from crop and forestry residues in Spain." *Biomass and Bioenergy* 34: (2010a) 703–719.

Gómez, A., J. Zubizarreta, M. Rodrigues, C. Dopazo, & N. Fueyo. "An estimation of the energy potential of agro-industrial residues in Spain." *Resources, Conservation and Recycling* 54: (2010b) 972–984.

Gold, S., & S. Seuring. "Supply chain and logistics issues of bio-energy production." *Journal of Cleaner Production* 19: (2011) 32–42.

Govind, R., & J. Shah. "Modeling and Simulation of An Entrained Flow Coal Gasifier." *AIChE Journal* 30, no. 1: (1984) 79–92.

Graves, S.C., & B.T. Tomlin. "Process Flexibility in Supply Chains." *Management Science* 49: (2003) 907–919.

Hamelinck, C.N., & A.P.C. Faaij. "Future propects for production of methanol and hydrogen from biomass." *Journal of Power Sources* 111: (2002) 1–22.

Hamelinck, C.N., R.A.A. Suurs, & A.P.C. Faaij. "International bioenergy transport costs and energy balance." Technical report, Universiteit Utrecht, Copernicus Institute, Science Technology Society, Utrecht, The Netherlands, 2003.

———. "International bioenergy transport costs and energy balance." *Biomass and Bioenergy* 29: (2005) 114–134.

Hamimu, H. "The prospects and challenges of biofuel production in developing countries (Tanzania experience)." In *17th European Biomass Conference and Exhibition.* Hamburg, Germany, 2009, 1755–1759.

Han, J. Y., A. P. J. Mol, Y. L. Lu, & L. Zhang. "Small-scale bioenergy projects in rural China: Lessons to be learnt." *Energy Policy* 36, no. 6: (2008) 2154–2162.

Hasler, P., & T. Nussbaumer. "Gas cleaning for IC engine applications from fixed bed biomass gasification." *Biomass and Bioenergy* 16: (1999) 385–395.

Hawboldt, K.A. *Kinetic modelling of key reactions in the modified Claus plant front end furnace.* Ph.D. thesis, Department of Chemical and Petroleum Engineering, University of

Calgary, Alberta, Canada, 1998.

Heijungs, R., & S. Suh. *The Computational Structure of Life Cycle Assessment.* Kluwer Academic Publishers, Dordrecht The Netherlands, 2002.

Hernández, J.J., G. Aranda-Almansa, & C. Serrano. "Co-Gasification of Biomass Wastes and Coal-Coke Blends in an Entrained Flow Gasifier: An Experimental Study." *Energy Fuels* 24: (2010) 2479–2488.

Hernández-Pacheco, E., M.D. Mann, P.N. Hutton, D. Singh, & K.E. Martin. "A cell-level model for a solid oxide fuel cell operated with syngas from a gasification process." *International Journal of Hydrogen Energy* 30: (2005) 1221–1233.

Highman, C., & M. van der Burght. *Gasification.* Elsevier Science, 2003.

Hiremath, R.B., B. Kumar, P. Deepak, P. Balachandra, R.H. Ravindranath, & B.N. Raghunandan. "Decentralized energy planning through a case study of a typical village in India." *Journal of renewable and sustainable energy* 1: (2009) 043,103–1–043,103–24.

Hsi, C.L., T.Y. Wang, C.H. Tsai, C.Y. Chang, C.H. Liu, Y.C. Chang, & J.T. Kuo. "Characteristics of an Air-Blown Fixed-Bed Downdraft Biomass Gasifier." *Energy and Fuels* 22: (2008) 4196–4205.

Huang, H.M., N. Young, B.P. Williams, S.H. Taylor, & G.J. Hutchings. "High temperature COS hydrolysis catalysed by $\gamma - Al_2O_3$." *Catalysis Letters* 110: (2006) 243–246.

Huang, H.M., N. Young, P. Williams, S.H. Taylor, & G.J. Hutchings. "COS hydrolysis using zinc-promoted alumina catalysts." *Catalysis Letters* 104: (2005) 17–21.

Huang, Y., S. Rezvain, D. McIlveen-Wright, A. Minchener, & N. Hewitt. "Techno-econornic study of CO2 capture and storage in coal fired oxygen fed entrained flow IGCC power plants." *Fuel Processing Technology* 89, no. 9: (2008) 916–925.

Humbert, S., M. Margni, & O. Jolliet. "IMPACT 2002+: User Guide Draft for version 2.1." Technical report, Industrial Ecology & Life Cycle Systems Group, GECOS, Swiss Federal Institute of Technology Lausanne (EPFL), Lausanne, Switzerland, 2005.

Husain, Z., Z.A. Zainal, & M.Z. Abdullah. "Analysis of biomass-residue-based cogeneration system in palm oil mills." *Biomass and Bioenergy* 24: (2003) 117–124.

Iakovou, E., A. Karagiannidis, A.D. Vlachos, A. Toka, & A. Malamakis. "Waste biomass-to-energy supply chain management: A critical synthesis." *Waste Management* 30: (2010) 1860–1870.

Iaquaniello, G., & A. Mangiapane. "Integration of biomass gasification with MCFC." *International Journal of Hydrogen Energy* 31: (2006) 399–404.

IEA-GHG. "Co-production of hydrogen and electricity by coal gasification with CO_2 capture - updated economic analysis." Technical report, International Energy Agency, IEA, UK, 2008.

Incorporated, BCS. "Waste Heat Recovery: Technology and Opportunities in U.S. Industry." Technical report, U.S. Department of Energy, Industrial Technologies Program, 2008.

Jand, N., & P.U. Foscolo. "Decomposition of wood particles in fluidized beds." *Industrial and Engineering Chemistry Research* 44: (2005) 5079–5089.

Janssen, R., D. Rutz, P. Helm, J. Woods, & R. Diaz-Chavez. "Bio-energy for sustainable development in Africa. Environmental and social aspects." In *17th European Biomass Conference and Exhibition.* Hamburg, Germany, 2009, 2422–2430.

Jayah, T.H., L. Aye, R.J. Fuller, & D.F. Stewart. "Computer simulation of a downdraft wood gasifier for tea drying." *Biomass and Bioenergy* 25: (2003) 459–469.

Jurado, F. "Robust control for fuel cell-microturbine hybrid power plant using biomass." *Energy* 30: (2005) 1711–1727.

Kajitani, S., Y. Zhang, S. Umemoto, M. Ashizawa, & S. Hara. "Co-gasification Reactivity of Coal and Woody Biomass in High-Temperature Gasification." *Energy Fuels* 24: (2010) 145–151.

Kambara, S., & T. Takarada. "Relation between Functional Forms of Coal Nitrogen and Formation of NOx Precursors during Rapid Pyrolysis." *Energy & Fuels* 7, no. 6: (1993) 1013–1020.

van de Kamp, W., P. Wild, U. Zielke, & M. Suomalainen. "Tar measurement standard for sampling and analysis of tars and particles in biomass gasification product gas." Technical report, Energy research Centre of the Netherlands, ECN, Petten, Netherlands, 2005.

Kanagawa, M., & T. Nakata. "Assessment of access to electricity and socio-economic impacts in rural areas of developing countries." *Energy Policy* 36: (2008) 2016–2029.

Kanase-Patil, A.B., R.P. Saini, & M.P. Sharma. "Integrated renewable energy systems for off grid rural electrification of remote area." *Renewable Energy* 35: (2010) 1342–1349.

Kanniche, M., & C. Bouallou. "CO_2 capture study in advanced integrated gasification combined cycle." *Applied Thermal Engineering* 27: (2007) 2693–2702.

Kanniche, M., R. Gros-Bonnivard, P. Jaud, J. Valle-Marcos, J. M. Amann, & C. Bouallou. "Pre-combustion, post-combustion and oxy-combustion in thermal power plant for CO2 capture." *Applied Thermal Engineering* 30, no. 1: (2010) 53–62.

Karellas, S., J. Karl, & E. Kakaras. "An innovative biomass gasification process and its coupling with microturbine and fuel cells systems." *Energy* 33: (2008) 284–291.

Kirkels, A.F., & G.P.J. Verbong. "Biomass gasification: Still promising? A 30-year global overview." *Renewable and Sustainable Energy Reviews* 15: (2011) 471–481.

Knight, I., & I. Ugursal. "Residential cogeneration systems: A review of the current technologies." Subtask A of the project entitled 'the simulation of building-integrated fuel cell and other cogeneration systems' (FC-COGEN-SIM) Annex 42, International Energy Agency (IEA), Canada, 2005.

Knoef, H.A.M. "The UNDP/World Bank monitoring program on small scale biomass gasifiers (BTG's experience on tar measurements)." *Biomass and Bioenergy* 18: (2000) 39–54.

———. "BTG Biomass Gasification." Technical report, Biomass Technology Group, BTG, BTG, The Netherlands, 2008.

Kondili, E., C.C. Pantelides, & R.W. Sargent. "A general algorithm for short term scheduling of batch operations." *Computers & Chemical Engineering* 17: (1993) 211–227.

Koukouzas, N., A. Katsiadakis, E. Kariopouios, & E. Kakaras. "Co-gasification of solid waste and lignite - A case study for Western Macedonia." *Waste Management* 28, no. 7: (2008) 1263–1275.

Kreutz, T., R. Williams, S. Consonni, & P. Chiesa. "Co-production of hydrogen, electricity and CO_2 from coal with commercially ready technology. Part B: Economic analysis." *International Journal of Hydrogen Energy* 30: (2005) 769–784.

Kunzing, G.E. *Gas-Solid Transport.* Mc- Graw-Hill Book Company, 1981.

Laínez-Aguirre, J.M. *Integrated Management of the Supply Chain for enterprise Sustainability.* Ph.D. thesis, UPC, Barcelona, Spain, 2010.

Laínez-Aguirre, J.M., G. Kopanos, A. Espuña, & L. Puigjaner. "Flexible design–planning of supply chain networks." *AIChE Journal* 55: (2009) 1736–1753.

Lapuerta, M., J.J. Hernández, A. Pazo, & J. López. "Gasification and co-gasification of biomass wastes: Effect of the biomass origin and the gasifier operating conditions." *Fuel Processing Technology* 89: (2008) 828–837.

Leduc, S., D. Schwab, E. Dotzauer, E. Schmid, & M. Obersteiner. "Optimal location of wood gasification plants for methanol production with heat recovery." *International Journal of Energy Research* 32: (2008) 1080–1091.

Loeser, M., & M.A. Redfern. "Modelling and simulation of a novel micro-scale combined feedstock biomass generation plant for grid-independent power supply." *International Journal of Energy Research* .

Loison, R., & R. Chauvin. "Pyrolyse rapide du charbon." *Chimie et Industrie* 91, no. 3:

(1964) 269–275.

van Loo, S., & J. Koppejan. *The Handbook of Biomass Combustion & Co-Firing.* Biomass energy - Handbooks, manuals, etc. VA, USA: Earthscan, 2008.

López-Vilariño, J.M., G. Fernández-Martínez, I. Turnes-Carou, S. Muniategui-Lorenzo, P. López-Mahía, & D. Prada-Rodríguez. "Behavior of fluorine and chlorine in Spain coal fired power plants with pulverized coal boilers and fluidized bed boiler." *Environmental Technology* 24, no. 6: (2003) 687–692.

Maciejewska, A., H. Veringa, J. Sanders, & S.D. Peteves. "Co-firing of biomass with coal: constraints and role of biomass pre-treatment." Technical report, Institute for Energy and the European Comission, 2006.

Madjera, M. "The necessity of policies in Sub-Saharan Africa (SSA) for the production of energy crops." In *17th European Biomass Conference and Exhibition.* Hamburg, Germany, 2009, 2452–2458.

Magalhaes, A.I.P., D. Petrovic, A.L. Rodriguez, Z.A. Putra, & G. Thielemans. "Techno-economic assessment of biomass pre-conversion processes as a part of biomass-to-liquids line-up." *Biofuels, bioproducts and biorefining* 3: (2009) 584–600.

Mamphweli, N.S., & E.L. Meyer. "Implementation of the biomass gasification project for community empowerment at Melani village, Eastern Cape, South Africa." *Renewable Energy* 34: (2009) 2923–2927.

Mastellone, M.L., L. Zaccariello, & U. Arena. "Co-gasification of coal, plastic waste and wood in a bubbling fluidized bed reactor." *Fuel* 89: (2010) 2991–3000.

Mathews, J.A. "Carbon-negative biofuels." *Energy Policy* 36: (2008) 940–945.

Maurstad, O. "An Overview of Coal based Integrated Gasification Combined Cycle (IGCC) Technology." *Laboratory for Energy and the Environment. Massachusetts Institute of Technology (MIT)* Publication No. LFEE 2005-002 WP.

McGovern, J., B. Cullen, M. Feidt, & S. Petrescu. "Validation of a simulation model for a combined Otto and Stirling cycle power plant." In *Proceedings of ASME 2010, 4th International Conference on Energy Sustainability.* Arizona, USA: American Society of Mechanical Engineers (ASME), 2010.

McIlveen-Wright, D., & D.J. Guiney. "Wood-fired fuel cells in an isolated community." *Journal of Power Sources* 106: (2002) 93–101.

McIlveen-Wright, D.R., B.C. Williams, & J.T. McMullan. "Wood gasification integrated with fuel cells." *Renewable Energy* 223–228.

McKendry, P. "Energy production from biomass (part 1): overview of biomass." *Bioresource Technology* 83, no. 1: (2002a) 37–46.

———. "Energy production from biomass (part 2): conversion technologies." *Bioresource Technology* 83, no. 1: (2002b) 47–54.

Melgar, A., J.F. Pérez, H. Laget, & A. Horillo. "Thermochemical equilibrium modelling of a gasifying process." *Energy Conversion and Management* 48: (2007) 59–67.

Mentzer, J.T., W. DeWitt, J.S. Keebler, S. Min, N.W. Nix, C.D. Smith, & Z.G. Zacharia. "Defining supply chain management." *Journal of business logistics* 22, no. 2: (2001) 1–25.

Merino, J.M. "Electric Energy Efficiency. Volume 3: Electricity transport and distribution." Technical report, CADEM-IBERDROLA, Madrid, Spain, 2003.

Metz, B., O. Davidson, H. Coninck, M. Loos, & L. Meyer. "Special Report on Carbon Dioxide Capture and Storage." Technical report, International Panel on Climate Change (IPCC), Switzerland, 2005.

Milne, T.A., R.J. Evans, & N. Abatzoglou. "Biomass Gasifier -Tars-: Their Nature, Formation and Conversion." Technical report, National Renewable Energy Laboratory, NREL, Springfield, VA, US, 1998.

Mirza, U.K., N. Ahmad, & T. Majeed. "An overview of biomass energy utilization in

Pakistan." *Renewable and Sustainable Energy Reviews* 12: (2008) 1988–1996.

Mitra, I., T. Degner, & M. Braun. "Distributed Generation and Microgrids for Small Island Electrification in Developing Countries: A Review." *Solar Energy Society of India* 18, no. 1: (2008) 6–20.

Monnery, W. D., K. A. Hawboldt, A. Pollock, & W. Y. Svrcek. "New experimental data and kinetic rate expression for the Claus reaction." *Chemical Engineering Science* 55, no. 21: (2000) 5141–5148.

Morris, E., R. King, & J. Winiecki. "Evaluation of the Ghana multi-functional platform pilot project." Technical report, United Nations Development Programme, 2008.

Munir, S., W. Nimmo, & B.M. Gibbs. "The effect of air staged, co-combustion of pulverised coal and biomass blends on NO_x emissions and combustion efficiency." *Fuel* 90: (2011) 126–135.

Muñoz, M., F. Moreno, J. Morea-Roy, J. Ruiz, & J. Arauzo. "Low heating value gas on spark ignition engines." *Biomass and Bioenergy* 18: (2000) 431–439.

Nathen, S.V., R.D. Kirkpatrick, & B.R. Young. "Gasification of New Zealand Coals: A Comparative Simulation Study." *Energy & Fuels* 22: (2008) 2687–2692.

NETL. "Gasification World Database 2007." Technical report, DOE, National Energy Technology Laboratory, 2007.

Nidumolu, U.B., H. van Keulen, M. Lubbers, & A. Mapfumo. "Combining interactive multiple goal linear programming with an inter-stakeholder communication matrix to generate land use options." *Environmental Modelling & Software* 22: (2007) 73–83.

Nikoo, M.B., & N. Mahinpey. "Simulation of biomass gasification in fluidized bed reactor using ASPEN PLUS." *Biomass and Bioenergy* 32: (2008) 1245–1254.

Ongiro, A. O., V. I. Ugursal, A. M. Altaweel, & D. K. Blamire. "Simulation of Combined-cycle Power-plants Using the Aspen Plus Shell." *Heat Recovery Systems & Chp* 15, no. 2: (1995) 105–113.

Ordorica-Garcia, G., P. Douglas, E. Croiset, & L. G. Zheng. "Technoeconomic evaluation of IGCC power plants for CO2 avoidance." *Energy Conversion and Management* 47, no. 15-16: (2006) 2250–2259.

Otto, M. "Trade-offs, risks and opportunities linked to bioenergy for sustainable development." In *17th European Biomass Conference and Exhibition*. Hamburg, Germany, 2009, 71–77.

Panichelli, L., & E. Gnansounou. "GIS-based approach for defining bioenergy facilities location: A case study in Northen Spain based on marginal delivery costs and resources competition between facilities." *Biomass and Bioenergy* 32: (2008) 289–300.

Panwar, N.L., N.S. Rathore, & A.K. Kurchania. "Experimental investigation of open core downdraft biomass gasifier for food processing industry." *Mitigation and Adaptation Strategies for Global Change* 14: (2009) 547–556.

Pathak, B.S., S.R. Patel, A.G. Bhave, P.R. Bhoi, A.M. Sharma, & N.P. Shah. "Performance evaluation of an agricultural residue-based modular throat-type down-draft gasifier for thermal application." *Biomass and Bioenergy* 32: (2008) 72–77.

Pattiya, A. "Bio-oil production via fast pyrolysis of biomass residues from cassava plants in a fluidised-bed reactor." *Bioresource Technology* 102: (2010) 1959–1967.

Perry, M., & F. Rosillo-Calle. "Recent trends and future opportunities in UK bioenergy: Maximising biomass penetration in a centralised energy system." *Biomass and Bioenergy* 32: (2008) 688–701.

Perry, R., & D. Green. *Perry's Chemical Engineers' Handbook*, Vol. Size Reduction and Size Enlargement. McGraw-Hill, 1997.

Pisa, J., L. Serra de Renobales, A. Moreno, & A. Valero. "Evaluación de alternativas en un diseño de planta GICC con gasificador PRENFLO." XII Congreso Nacional de Ingeniería

Mecánica, 1997, 269–278.

du Plessis, V., R. Beshiri, & R.D. Bollman. "Definitions of Rural." Technical report, Statistics Canada, Agriculture Division,, Ottawa, Ontario, 2002.

Podesser, E. "Electricity production in rural villages with a biomass Stirling engine." *Renewable Energy* 16: (1999) 1049–1052.

Pootakham, T., & A. Kumar. "Bio-oil transport by pipeline: A techno-economic assessment." *Bioresource Technology* 101: (2010a) 7137–7143.

———. "A comparison of pipeline versus truck transport of bio-oil." *Bioresource Technology* 101: (2010b) 414–421.

Prausnitz, J.M., R.N. Lichtenthaler, & E. Gómez de Acevedo. *Molecular thermodynamics of fluid-phase equilibria.* Englewood Cliffs, New Jersey: PTR Prentice Hall, 1986, 2nd Edition.

Prins, M.J., K.J. Ptasinski, & F.J.J.G. Janssen. "More efficient biomass gasification via torrefacton." *Energy* 31: (2006a) 3458–3470.

———. "Torrefaction of wood. Part 1. Weight loss kinetics." *Journal of Analytical and Applied Pyrolysis* 77: (2006b) 28–34.

Puigjaner, L., & G. Guillén. "Towards an integrated framework for supply chain management in the batch chemical process industry." *Computers and Chemical Engineering* , no. 32: (2008) 650–670.

Puigjaner, L., P. Ollero, C. de Prada, & L. Jiménez. *Estrategias de modelado, simulación y optimización de procesos quimicos.* Biblioteca de químicas. Madrid, Spain: Editorial Síntesis, 2006.

Ragauskas, A.J., C.K. Williams, B.H. Davison, G. Britovsek, J. Cairney, C.A. Eckert, W.J. Frederick, J.P. Hallet, D.J. Leak, C.L. Liotta, J.R. Mielenz, R. Murphy, R. Templer, & T. Timothy. "The Path Forward for Biofuels and Biomaterials." *Science* 311: (2006) 484–489.

Ramadhas, A.S., S. Jayaraj, & C. Muraleedharan. "Dual fuel mode operation in diesel engines using renewable fuels: Rubber seed oil and coir-pith producer gas." *Renewable Energy* 33: (2008) 2077–2083.

Ravindran, A.R. *Operations research and management science.* Operations Research. NW, USA: CRC Press, Taylor & Francis Group, 2008, 1st Edition.

Ravindranath, N. H., H. I. Somashekar, S. Dasappa, & C. N. J. Reddy. "Sustainable biomass power for rural India: Case study of biomass gasifier for village electrification." *Current Science* 87, no. 7: (2004) 932–941.

Reed, T.B. *Biomass Gasification. Principles and Technology.* Energy technology review. New Jersey USA: Noyes Data Corporation, 1981.

Reed, T.B., & A. Das. "Handbook of Biomass Downdraft Gasifier Engine Systems." Technical report, DOE, Solar Energy Research Institute, SERI, Colorado, US, 1988.

Reimert, R., & G. Schaub. *Gas production, Chapter 4: Gas production from coal, wood, and other solid feedstocks.* Ullmann's encyclopedia of industrial chemistry. Wiley-VCH, 2003, 7 Edition.

Rentizelas, A., S. Karellas, E. Kakaras, & I. Tatsiopoulos. "Comparative techno-economic analysis of ORC and gasification for bioenergy applications." *Energy Conversion and Management* 50: (2009a) 674–681.

Rentizelas, A.A., I.P. Tatsiopoulos, & A. Tolis. "An optimization model for multi-biomass tri-generation energy supply." *Biomass and Bioenergy* 33: (2009b) 223–233.

———. "An optimization model for multi-biomass tri-generation energy supply." *Biomass and Bioenergy* 33: (2009c) 223–233.

Rentizelas, A.A., A.J. Tolis, & I.P Tatsiopoulos. "Logistics issues of biomass: The storage problem and the multi-biomass supply chain." *Renewable and Sustainable Energy Reviews*

13: (2009d) 887–894.

Rhodes, C., S.A. Riddel, J. West, B.P. Williams, & G.J. Hutchings. "The low-temperature hydrolysis of carbonyl sulfide and carbon disulfide: a review." *Catalysis Today* 443–464.

Robinson, P.J., & W.L. Luyben. "Simple Dynamic Gasifier Model that Runs in Aspen Dynamics." *Industrial and Engineering Chemistry Research* 47: (2008) 7784–7792.

Rodrigues, M., A. Water, & A.P.C. Faaij. "Performance evaluation of atmospheric biomass integrated gasifier combined cycle systems under different strategies for the use of low calorific gases." *Energy Conversion and Management* 48: (2007) 1289–1301.

Rosillo-Calle, F., P. De Groot, S. L. Hemstock, & J. Woods. *The Biomass Assessment Handbook. Bioenergy for a Sustainable Environment.* London, UK: Earthscan, 2007.

Rubin, Edward S., Chao Chen, & Anand B. Rao. "Cost and performance of fossil fuel power plants with CO2 capture and storage." *Energy Policy* 35, no. 9: (2007) 4444–4454. `http://www.sciencedirect.com/science/article/B6V2W-4NKB231-1/2/f3f775fd22ce46b994005d5f228eb015`.

Ruggiero, M., & G. Manfrida. "An equilibrium model for biomass gasification processes." *Renewable energy* 16: (1999) 1106–1109.

Sadhukhan, J., Y. Zhao, M. Leach, N.P. Brandon, & N. Shah. "Energy Integration and Analysis of Solid Oxide Fuel Cell Based Microcombined Heat and Power Systems and Other Renewable Systems Using Biomass Waste Derived Gas." *Industrial and Engineering Chemistry Research* 49: (2010) 11,506–11,516.

Sahoo, B.B., N. Sahoo, & U.K. Saha. "Effect of engine parameters and type of gaseous fuel on the performance of dual-fuel gas diesel engines-A critical review." *Renewable and Sustainable Energy Reviews* 13: (2009) 1151–1184.

Sami, M., K. Annamalai, & M. Wooldridge. "Co-firing of coal and biomass fuel blends." *Progess in Energy and Combustion Science* 27: (2001) 171–214.

Santandreu, E., & P. Santandreu. *Manual de finanzas.* Barcelona, Spain: Ediciones Gestión 2000, 2000.

Senelwa, K., & R.E.H. Sims. "Opportunities for small scale biomass-electricity systems in Kenya." *Biomass and Bioenergy* 17: (1999) 239–255.

Serpagli, A., G.P. Nagori, G. Amoriggi, & C. Calvosa. "The use of cassava wastes to produce energy: outcomes of a feasibility study implemented in Ghana." Technical report, International Fund for Agricultural Development (IFAD), Rome, Italy, 2010.

Sharma, A.K. "Experimental study on 75 kW_{th} downdraft (biomass) gasifier system." *Renewable Energy* 34: (2009) 1726–1733.

Sharma, S.D., M. Dolan, D. Park, L. Morpeth, A. Ilyushechkin, K. McLennan, D.J. Harris, & K.V. Thambimuthu. "A critical review of syngas cleaning technologies - fundamental limitations and practical problems." *Powder Technology* 180: (2008) 115–121.

Sheth, P.N., & B.V. Babu. "Experimental studies of producer gas generation from wood waste in a downdraft biomass gasifier." *Bioresource Technology* 100: (2009) 3127–3133.

Siemons, R.V. "Identifying a role for biomass gasification in rural electrification in developing countries: the economic perspective." *Biomass and Bioenergy* 20: (2001) 271–285.

Silva, D., & T. Nakata. "Optimization of decentralized energy systems using biomass resources for rural electrification in developing countries." *Energy Policy* 37: (2008) 3096–3108.

———. "Multi-objective assessment of rural electrification in remote areas with poverty considerations." *Energy Policy* 37: (2009) 3096–3108.

Silveira, S. *Bioenergy - Realizing the potential.* Oxford, UK: Elsevier, 2005, 1st Edition.

Sims, R.E.H. *Bioenergy Options for a Cleaner Environment in Developed and Developing Countries.* Oxford, UK: Elsevier, 2004, 1st Edition.

Song, W. J., L. H. Tang, X. D. Zhu, Y. Q. Wu, Y. Q. Rong, Z. B. Zhu, & S. Koyama. "Fusibility and flow properties of coal ash and slag." *Fuel* 88, no. 2: (2009) 297–304.

Sridhar, G., P.J. Paul, & H.S. Mukunda. "Biomass derived producer gas as a reciprocating engine fuel-an experimental analysis." *Biomass and Bioenergy* 21: (2001) 61–72.

Stahl, K., & M. Neergaard. "IGCC power plant for biomass utilisation, Varnamo, Sweden." *Biomass & Bioenergy* 15, no. 3: (1998) 205–211.

Stassen, H.E. "Small-Scale Biomass Gasifiers for Heat and Power: A Global Review." World Bank Technical Paper, Energy Series 296, United Nations Development Programme, The Word Bank, Washington D.C., 1995.

Strachan, N., & H. Dowlatabadi. "Distributed generation and distribution utilities." *Energy Policy* 30: (2002) 649–661.

Sultana, A., A. Kumar, & D. Harfield. "Development of agri-pellet production cost and optimum size." *Bioresource Technology* 101: (2010) 5609–5621.

Sutton, D., B. Kelleher, & J.R.H. Ross. "Review of literature on catalysts for biomass gasification." *Fuel Processing Technology* 73: (2001) 155–173.

Thiers, S., B. Aoun, & B. Peuportier. "Experimental characterization, modeling and simulation of a wood pellet micro-combined heat and power unit used as a heat source for a residential building." *Energy and Buildings* 42: (2010) 896–903.

Thumann, A., & D.P. Mehta. *Handbook of Energy Engineering.* The Fairmont Press, Inc. and CRC Press (Taylor & Francis Group, 2008, 6th Edition.

Tillman, D.A. "Biomass cofiring: the technology, the experience, the combustion consequences." *Biomass and Bioenergy* 19: (2000) 365–384.

Tilman, D., J. Hill, & C. Lehman. "Carbon-Negative Biofuels from Low-Input High-Diversity Grassland Biomass." *Science* 314: (2006) 1598–1600.

Toonssen, R., N. Woudstra, & A.H.M. Verkooijen. "Decentralized generation of electricity from biomass with proton exchange membrane fuel cell." *Journal of Power Sources* 194: (2009) 456–466.

Turban, E., J.E. Aronson, & T.P. Liang. *Decision Support Systems and Intelligent Systems.* New Jersey, USA: Pearson Prentice Hall, 2005, 7th Edition.

Turton, R., R.C. Bailie, W.B. Whiting, & J.A. Shaeiwitz. *Analysis, Synthesis and Design of Chemical Processes.* Prentice Hall PTR, 1998, 3rd Edition 2009.

Ubalua, A.O. "Cassava wastes: tretment options and value addition alternatives." *African Journal of Biotechnology* 6, no. 18: (2007) 2065–2073.

Ulrich, G. D., & P. T. Vasudevan. *Chemical Engineering Process Design and Economics. A pratical guide.* Sheridan Books, Process Publishing, 2004.

Uma, R., T.C. Kandpal, & V.V.N. Kishore. "Emissions characteristics of an electricity generation system in diesel alone and dual fuel modes." *Biomass and Bioenergy* 27: (2004) 195–203.

Urban, F., R. M. J. Benders, & H. C. Moll. "Modelling energy systems for developing countries." *Energy Policy* 35: (2007) 3473–3482.

US, Energy Department. "Energy efficiency and renewable energy: biomass program." Technical report, US Department of Energy, 2010.

Uslu, A., A.P.C. Faaij, & P.C.A. Bergman. "Pre-treatment technologies, and their effect on international bioenergy supply chain logistics. Techno-economic evaluation of torrefaction, fast pyrolysis and pelletisation." *Energy* 33: (2008) 1206–1223.

Usón, S. "Modelo cinético-químico del gasificador." Technical report, Centro de Investigación de Rendimiento de Centrales Eléctricas, CIRCE, 2001.

Usón, S., A. Valero, L. Correas, & A. Martínez. "Co-Gasification of Coal and Biomass in an IGCC Power Plant: Gasifier Modeling." *Int.J. Thermodynamics* 7: (2004) 165–172.

Valero, A., & S. Usón. "Oxy-co-gasification of coal and biomass in an integrated gasification combined cycle (IGCC) power plant." *Energy* 31, no. 10-11: (2006) 1643–1655.

Van Belle, J.F., M. Temmerman, & Y. Schenkel. "Three level procurement of forest residues for power plant." *Biomass and Bioenergy* 24: (2003) 401–409.

Van Den Broek, R., A. Faaij, & A. Van Wijk. "Biomass combustion for power generation." *Biomass and Bioenergy* 11, no. 4: (1996) 271–281.

Van Dyken, S., B.H. Bakken, & H.I. Skjelbred. "Linear mixed-integer models for biomass supply chains with transport, storage and processing." *Energy* 35: (2010) 1338–1350.

Van Ruijven, B., F. Urban, R.M.J. Benders, H.C. Moll, J.P. Van der Sluijs, B. De Vries, & D.P. Van Vuuren. "Modeling Energy and Development: An Evaluation of Models and Concepts." *World Development* 36, no. 12: (2008) 2801–2821.

Verbong, G., W. Christiaens, R. Raven, & A. Balkema. "Strategic niche management in an unstable regime: biomass gasification in India." *Environmental Science and Policy* 13: (2010) 272–281.

van Vliet, P.P.R., Faaij A.P.C., & W.C. Turkenburg. "Fischer-Tropsch diesel production in a well-to-wheel perspective: a carbon, energy flow and cost analysis." *Energy Conversion and Management* 50: (2009) 855–876.

Wang, L., W. Shen, H. Xie, J. Neelamkavil, & A. Pardasani. "Collaborative conceptual design - state of the art and future trends." *Computer-Aided Design* 34: (2002) 981–996.

Wang, L., C.L. Weller, D.D. Jones, & M.A. Hanna. "Contemporary issues in thermal gasification of biomass and its application to electricity and fuel production." *Biomass and Bioenergy* 32: (2008) 573–581.

Wang, Y., & C.M. Kinoshita. "Kinetic model of biomass gasification." *Solar Energy* 51: (1993) 19–25.

Wang, Y., P. H. Qiu, S. H. Wu, & Z. Z. Li. "Performance of an Integrated Gasification Combined Cycle System with Different System Integration Options." *Energy & Fuels* 24: (2010) 1925–1930.

Watson, G.H. "Methanation Catalysts." Report number ictis/tr09, International Energy Agency (IEA) Coal Research, London, 1980.

Wells, G.L., & L.M. Rose. *The art of chemical process design*, Vol. 1-2 of *Computer-aided chemical engineering*. Elsevier, Amsterdam, 1986.

Wen, C.Y., & T.Z. Chaung. "Entrainment Coal Gasification Modelling." *Industrial and Engineering Chemistry Process Design and Development* 18: (1973) 684–695.

Wender, I. "Reactions of synthesis gas." *Fuel Processing Technology* , no. 48: (1996) 189–297.

Wu, H., Y. Yu, & K. Yip. "Bioslurry as a Fuel 1. Viability of a Bioslurry-Based Bioenergy Supply Chain for Mallee Biomass in Western Australia." *Energy and Fuels* 24: (2010) 5652–5659.

Yu, Y., J. Bartle, C.Z. Li, & H. Wu. "Mallee Biomass as a Key Bioenergy Source in Western Australia: Importance of Biomass Supply Chain." *Energy and Fuels* 23: (2009) 3290–3299.

Yuehong, Z., W. Hao, & X. Zhihong. "Conceptual design and simulation study of a co-gasification technology." *Energy Conversion and Management* 47: (2006) 1416–1428.

Zainal, Z.A., A. Rifau, G.A. Quadir, & K.N. Seetharamu. "Experimental investigation of a downdraft biomass gasifier." *Biomass and Bioenergy* 23: (2002) 283–289.

Zeng, X., Y. Ma, & L. Ma. "Utilization of straw in biomass energy in China." *Renewable and Sustainable Energy Reviews* 11: (2007) 976–987.

Zhao, Y. H., W. Hao, & Z. H. Xu. "Conceptual design and simulation study of a co-gasification technology." *Energy Conversion and Management* 47, no. 11-12: (2006) 1416–1428.

Zhu, Yunhua. *Evaluation of gas turbine and gasifier-based power generation system*. Ph.D. thesis, 2004.